Editors:
Jon Børre Ørbæk, Kim Holmén, Roland Neuber, Hans Petter Plag,
Bernard Lefauconnier, Guido de Prisco and Hajime Ito

The Changing Physical Environment

PROCEEDINGS FROM THE SIXTH NY-ÅLESUND INTERNATIONAL SCIENTIFIC SEMINAR

Polar Environmental Centre, Tromsø, Norway, 8-10 October 2002

Norsk Polarinstitutt
INTERNRAPPORT
Nr. 10, Tromsø 2002

Norsk Polarinstitutt

Editors
Jon Børre Ørbæk, Kim Holmén, Roland Neuber, Hans Petter Plag,
Bernard Lefauconnier, Guido de Prisco and Hajime Ito

The Changing Physical Environment

PROCEEDINGS FROM THE SIXTH NY-ÅLESUND INTERNATIONAL SCIENTIFIC SEMINAR

Polar Environmental Centre, Tromsø, Norway, 8-10 October 2002

Norsk Polarinstitutt 2002

Address:

Norwegian Polar Institute
Polar Environmental Centre
N-9296 Tromsø
Norway

Technical editors: Jon Børre Ørbæk, Gunn Sissel Jaklin, Anne Kibsgaard and Trond Svenøe
Cover design: Jan Roald
Cover photo: Jon Børre Ørbæk, Norwegian Polar Institute
Printed: Norwegian Polar Institute, October 2002
ISBN: 82-7666-192-0

Sixth Ny-Ålesund International Scientific Seminar
"The Changing Physical Environment"
Polar Environmental Centre, Tromsø, Norway,
8-10 October 2002

CONTENTS

Sixth Ny-Ålesund International Scientific Seminar
"The Changing Physical Environment"
Polar Environmental Centre, Tromsø, Norway,
8-10 October 2002

Scientific Programme Committee
Jon Børre Ørbæk (chairman), Kim Holmén, Roland Neuber, Hans Peter Plag, Bernard Lefauconnier, Guido de Prisco, Hajime Ito

Local Organizing Committee
Anne Kibsgaard, Trond Svenøe, Gunn Sissel Jaklin, Marit Raak-Pettersen, Jan Erling Haugland, Jon Børre Ørbæk

Seminar Sponsors
This Sixth Ny-Ålesund International Scientific Seminar is sponsored by the Norwegian Polar Institute, the Norwegian Research Council (project 155661/700) and the European Commission IHP-programme (contract HPRI-CT-1999-00057).

Organizers
The seminar is hosted by the Norwegian Polar Institute (NPI) and organized in collaboration with the Ny-Ålesund Science Managers Committee (NySMAC) and the Ny-Ålesund Large Scale Facility programme.

Introduction

Photo: Jørgen Hinkler

Initiated by the Ny-Ålesund Science Managers Committee (NySMAC), the Ny-Ålesund International Scientific Seminars aim at facilitating more exchange and collaboration between the scientists involved in research activities in the Ny-Ålesund area.

During the past decade or so, Ny-Ålesund has developed into a well recognized international research and monitoring facility in the European Arctic. More than 10 different nations have now established permanent research and monitoring activities at the site, and scientists from more than 20 nations perform field research campaigns at the research stations or in the nearby pristine environment during all times of the year.

Ny-Ålesund has since 1996 been recognized by the European Commission (EC) as a "Large Scale Facility"/"Major Research Infrastructure", and the EC 5th Framework Programme (Improving Human Potential) still contributes significantly to the transnational research mobility and exchange under the programmes for the "Ny-Ålesund Large Scale Facility for Arctic Environmental Research". As owner and operator of the general infrastructure on behalf of the Norwegian state, and host of all the permanent research stations on long term contracts, Kings Bay Company has a specific responsibility in developing a sustainable research site which maintains the pristine environment and the conditions for international top quality Arctic environmental research.

The Ny-Ålesund research community is large, multidisciplinary and international. The large amount of new data that is gathered by the individual scientists and monitoring programmes in Ny-Ålesund represent an impressive bank of state-of-the-art knowledge about the Arctic environment and environmental change. The opportunities for multidisciplinary exchange within contemporary fields including climate change, ozone/UV-radiation and long range transport of pollutants are unique at the site, involving marine and terrestrial biologists, atmospheric physicists and chemists, scientists within geodesy and glaciology, geomorphology and others. The Ny-Ålesund Seminars significantly contribute to the increased communication and collaboration across both disciplinary and national borders.

The first Ny-Ålesund Scientific Seminar was hosted by Alfred Wegener Institute (AWI) in Potsdam, Germany, in May 1995, involving all fields of sciences. The second seminar gave emphasis to the biological sciences and was hosted by the Natural Environment Research Council (NERC) in Cambridge, UK, in February 1996. The third seminar in April 1997 was devoted to the atmospheric research in Ny-Ålesund and was hosted by the Norwegian Institute of Air Research (NILU) at Kjeller, Norway. The fourth seminar was hosted by the Italian National Research Council (CNR) in Ravello, Italy, in March 1998, focussing on the broad field of "Arctic and Global Change". The fifth seminar

was organized by the National Institute of Polar Research (NIPR) in Tokyo, Japan, in February 2000 as part of the 2nd International Symposium on Environmental Research in the Arctic, inviting also a broader international community on Arctic research.

This Sixth Ny-Ålesund International Scientific Seminar is hosted by the Norwegian Polar Institute (NPI) in Tromsø, Norway, during the period 8-10 in October 2002, and organized in collaboration with NySMAC and the Ny-Ålesund Large Scale Facility programme. It is devoted to "Physical Environment Research" in Ny-Ålesund, involving contributions from the cryospheric, atmospheric, solarterrestrial, solid earth and marine environments. A few ecosystem effect studies on environmental change are also presented at the seminar. The seminar is co-sponsored by the Norwegian Polar Institute, the Norwegian Research Council (project 155661/700) and the European Com-mission IHP-programme (contract HPRI-CT-1999-00057).

The seminar programme represents a cross-section of the activities at the site, but it does not include the complete set of contemporary physical environment research in Ny-Ålesund. Most of the contributions belong to the atmospheric and cryospheric environment, more specifically from the fields of Arctic aerosols, long range transport of pollutants, air quality, glacier monitoring and mass balance measurement, hydrological processes and energy balance studies. There are relatively few contributions from the fields of Solar-Terrestrial, Solid Earth and Marine environments, and an important goal for future seminars is to attract also these important fields for multidisciplinary scientific dialogue. Noteworthy is that a comprehensive set of contemporary marine multi-disciplinary research projects in Ny-Ålesund will be presented at the "Kongsfjorden Ecosystem Workshop II" in Poland 7-10 November 2002. The set of 4-page extended abstracts of each paper/ poster presented at the seminar is published in these conference proceedings. The 10-15 highest quality papers will subse-quently be selected and invited by the scientific programme committee to publish coherently in a special issue of the peer-reviewed journal "Physics and Chemistry of the Earth".

A major objective of the seminar is to create new ideas and identify new research needs at the site through the discussions at the meeting. This is also the first step in new research proposals for the national and European research councils. The third day of the seminar is dedicated to workshops on instrumental techniques and observational needs concerning research into the Atmospheric, Cryospheric, Solar-Terrestrial, Solid Earth and Marine environments. All participants at the seminar are invited to contribute to these important activities. At the time this introduction is written, participants are invited to specific workshops concerning the "Corbel Clean Base Project", the "Tethered Balloon Initiative", the "CALIPSO/Climate Ground Validation Initiative" and the "Ny-Ålesund Large Scale Facility Workshop".

On behalf of the Scientific Programme Committee,

Jon Børre Ørbæk,

25 September 2002

Sixth Ny-Ålesund International Scientific Seminar
"The Changing Physical Environment"
Polar Environmental Centre, Tromsø, Norway,
8-10 October 2002

PROGRAMME

Monday 7 October 2002

19.00 - 22.00 Welcome and registration: Reception at the Polar Environmental Centre.

Tuesday 8 October 2002

09.00 - 10.05 Welcome and Introductory Review Talks

Chair: Jon Børre Ørbæk

09.00 - 09.25 *Welcome and presentation of seminar programme*
Prof. Olav Orheim, Director, Norwegian Polar Institute
Prof. Guido di Prisco, Chairman of NySMAC
Dr. Jon Børre Ørbæk, Conference Coordinator

09.25 - 09.45 *Perspectives from Kings Bay on the international collaboration and future development of Ny-Ålesund.* Monica Kristensen Solås, Director, Kings Bay AS, Ny-Ålesund. Invited introductory review talk

09.45 - 10.05 *Coordination and integration of biological research in Ny-Ålesund in the framework of the new Marine Laboratory.* Guido di Prisco, Chairman of NySMAC, Institute of Protein Biochemistry, CNR, Naples, Italy. Invited introductory review talk

10.05 - 15.25 Atmospheric and Solar-Terrestrial Environment

10.05 - 10.25 *Climate trends in the European Arctic during the last 100 years.* Inger Hanssen-Bauer, Norwegian Meteorological Institute, Oslo, Norway. Invited speaker

10.25 - 10.40 *An atmospheric transport climatology for Ny-Ålesund using clustered trajectories.* Eva Kristina Eneroth et al., Stockholm University (MISU), Stockholm, Sweden. Oral presentation

10.40 - 11.00 *Coffee break*

Chair: Kim Holmen

11.00 - 11.15 *Variation of atmospheric constituents and their climatic impact in the Arctic - Preliminary report of "Arctic Airborne Measurement Program 2002 (AAMP02)".* Takashi Yamanouchi et al., National Institute of Polar Research, Japan. Oral presentation

11.15 - 11.30 *One year of particle size distribution and aerosol chemical composition measurements at the Zeppelin station, Svalbard, March 2000-March 2001.* J. Umegård et al. (presented by Johan Ström), Institute for Applied Environmental Research, Air-Pollution Laboratory, Stockholm University, Sweden. Oral presentation

11.30 - 11.45 *Size distribution of aerosols and snow particles in different type airmasses.* Makoto Wada et al., National Institute of Polar Research, Japan. Oral presentation

11.45 - 12.00 *A polar cloud analysis using ground-based Micro-pulse Lidar data.* Masataka Shiobara et al., National Institute of Polar Research, Japan. Oral presentation

12.00 - 12.15 *The Zeppelin Station – an overview of NILU's research activities and some results.* Chris Lunder et al., NILU, Kjeller, Norway. Oral presentation

12.15 - 12.30 *Lead-210 concentration in the air at Mt. Zeppelin, Ny-Ålesund, Svalbard.* Jussi Paatero et al., Finnish Meteorological Institute, Air Quality Research, Helsinki, Finland. Oral presentation

12.30 - 13.30 *Lunch*

Chair: Takashi Yamanouchi

13.30 - 13.45 *Study of the exchange of reactive gases between the snowpack and the atmosphere at Ny-Ålesund.* Florent Dominé et al., CNRS, Glaciology Laboratory, France. Oral presentation

13.45 - 13.50 *Long range transport of pollutants – evidences from rainfall chemistry Hornsund, Svalbard.* Piotr Glowacki and Wieslawa E. Krawczyk, Institute of Geophysics, Polish Academy of Sciences. Warszawa, Poland. Poster presentation

13.50 - 13.55 *Trace element distribution in size separated aerosols from Ny-Ålesund during the ASTAR 2000 campaign.* M. Kriews et al., Alfred Wegener Institute for Polar and Marine Research. Poster presentation

13.55 - 14.00 *Comparing methane data from Ny-Ålesund with results from a regional transport model (MATCH).* Ine-Therese Pedersen et al., Norwegian Institute for Air Research, Tromsø, Norway. Poster presentation

14.00 - 14.05 *Tropospheric water vapour observations by ground-based lidar.* Michael Gerding et al. (presented by R. Neuber), Alfred Wegener Institute, Research Unit Potsdam, Germany. Poster presentation

14.05 - 14.10 *The enrichment of particular bromated (BrO_3^-) in the boundary layer of the winter and spring Arctic.* Keiichiro Hara et al., Nagoya University, Solar Terrestrial Environment Laboratory, Japan. Poster presentation

14.10 - 14.15 *Occurrence and optical properties of tropospheric aerosols.* Christoph Ritter et al. (presented by R. Neuber), Alfred Wegener Institute for Polar and Marine Research, Potsdam, Germany. Poster presentation

14.15 - 14.20 *Characteristics of different solid PSC particles observed by lidar in Ny-Ålesund.* Marion Müller et al. (presented by R. Neuber), Alfred Wegner Institute for Polar and Marine Research, Potsdam, Germany. Poster presentation

14.20 - 14.25 *European Network for Arctic-Alpine Multidisciplinary Environmental Research – ENVINET*: *Coordination and harmonisation of research, facilities and services among environmental research infrastructures in Europe.* Jon Børre Ørbæk, Norwegian Polar Institute, Tromsø, Norway. Poster presentation

14.25 - 14.45 *Coffee Break*

Chair: Roland Neuber

14.45 - 15.05 *Trends in surface UV radiation in Polar regions.* Arne Dahlback, Department of Physics, University of Oslo, Norway. Invited speaker

15.05 - 15.25 *The Arctic Ozone Layer.* Markus Rex (presented by Ralph Lehman), Alfred Wegener Institute for Polar and Marine Research, Germany. Invited speaker

15.25 - 16.15 Changing Environment & Ecosystem Effects I

15.25 - 15.45 *Effects of persistent organic pollutants (POPs) on Arctic seabirds and marine mammals.* Geir Wing Gabrielsen, Norwegian Polar Institute, Tromsø, Norway. Invited speaker

15.45 - 16.00 *Modelling spatial co-variation of plant species and temperature using GIS and remote sensed data.* T. Brossard et al. (presented by Lennart Nilsen), Laboratoire ThéMA, CNRS, Université de Franche-Comté, Besançon, France. Oral presentation

16.00 - 16.15 *Enhanced UV radiation ands its implications for seaweeds from Spitsbergen.* Christian Wiencke et al., Alfred Wegener Institute, Bremerhaven, Germany. Oral presentation

16.15-18.00 Poster Session

18.30 *Visit to POLARIA, Visitors centre on polar regions*

Wednesday 9 October 2002

09.00-09.40 Introductory Review Talks

Chair: Richard Hodgkins

09.00 - 09.20 *The Ny-Ålesund LSF programme 1996-2002: Experiences from 7 years of European Mobility and Research Exchange in Ny-Ålesund. New opportunities and plans for the FP6.* Jon Børre Ørbæk, Norwegian Polar Institute, Tromsø, Norway.

09.20 - 09.40 *Integrating the physical environment research in Ny-Ålesund.* Hans Peter Plag, Norwegian Mapping Authority, Hønefoss, Norway.

09.40 - 14.40 Cryospheric Environment

09.40 - 10.00 *The next large surge in Kongsfjorden.* Bernard Lefauconnier, IPEV/IFRTP, Brest, France. Invited speaker

10.00 - 10.15 *Calving intensity of Spitsbergen glaciers.* Jacek Jania, University of Silesia, Department of Geomorphology, Poland. Oral presentation

10.15 - 10.30 *Ice cores from Svalbard – useful archives of past climate and pollution history.* Elisabeth Isaksson et al., Norwegian Polar Institute, Tromsø, Norway. Oral presentation

10.30 - 10.45 *Re-calculation of the mass balance record for Midre Lovénbreen and Austre Brøggerbreen, Svalbard.* Jack Kohler et al., Norwegian Polar Institute, Tromsø, Norway. Oral presentation

10.45 - 11.05 *Coffee break*

Chair: Elisabeth Isaksson

11.05 - 11.25 *Proglacial surface sediment characteristics: Spatial variation at Midre Lovénbreen, Svalbard.* Richard Hodgkins et al., Department of Geography, University of London, UK. Invited speaker

11.25 - 11.40 *Accuracy of GPS for glacier monitoring under special conditions in high arctic.* Manfred Stober et al., Hochschule für Technik, Stuttgart, Germany. Oral presentation

11.40 - 11.55 *Changes of geometry and dynamics of NW Spitsbergen glaciers based on the ground GPS survey and remote sensing.* Jacek Jania et al., University of Silesia, Department of Geomorphology, Poland. Oral presentation

11.55 - 12.10 *Glacier monitoring and detection of superimposed ice on Kongsvegen, Svalbard, using SAR satellite imagery.* Max König et al., Norwegian Polar Institute, Tromsø, Norway. Oral presentation

12.10 - 12.15 *Regional patterns of meteorological variables in the Kongsfjorden area, Svalbard.* Friedrich Obleitner and Jack Kohler (presented by J. Kohler), Innsbruck University, Austria. Poster presentation

12.15 - 13.15 *Lunch*

Chair: Bernard Lefauconnier

13.15 - 13.30 *Runoff in Svalbard.* Lars-Evan Pettersson, Norwegian Water Resources and Energy Directorate. Oslo, Norway. Oral presentation

13.30 - 13.45 *Chemical denudation rates in the Bayelva catchment (Svalbard) in September – October of 2000.* Wieslawa Ewa Krawczyk et al., University of Silesia, Poland. Oral presentation

13.45 - 14.00 *Sea ice surface reflectance and under- ice irradiance in Kongsfjorden, Svalbard.* Jan-Gunnar Winther et al., Norwegian Polar Institute, Tromsø, Norway. Oral presentation

14.00 - 14.15 *Observations of superimposed ice formation at melt-onset on fast ice on Kongsfjorden, Svalbard.* M. Nikolaus et al., Alfred Wegener Institute for Polar and Marine Research, Bremerhaven, Germany. Oral presentation

14.15 - 14.30 *Detection of spatial, temporal, and spectral surface changes in the Ny-Ålesund area 79 N, Svalbard, using a low cost multispectral camera in combination with spectroradiometer measurements.* Jørgen Hinkler et al., University of Copenhagen, Denmark. Oral presentation

14.30 - 14.35 *Radiation and physical characteristics of tundra and landfast ice snow cower, by the example of Barentsburg region and Greenfjord.* Boris V. Ivanov et al., Arctic and Antarctic Research Institute, Saint-Petersburg, Russia. Poster presentation

14.35 - 14.40 *Study of the river and glacier hydrology of the western Spitsbergen.* E. Chevnina, Arctic and Antarctic Research Institute, Saint-Petersburg, Russia. Poster presentation

14.40 - 15.00 *Coffee break*

15.00 - 16.35 Solid Earth & Marine Environment

Chair: Hans Peter Plag

15.00 - 15.20 *Kongsfjord geochemistry: Initial Results.* Tracy Shimmield et al., Scottish Association for Marine Science, Dunstaffnage Marine Laboratory, Oban, Scotland. Invited speaker

15.20 - 15.35 *Oceanographic processes in the inner Kongsfjord (Svalbard): multidisciplinary results from 2000-2001 campaigns.* R. Delfanti et al. (presented by S. Aliani), Marine Environment Research Centre, La Spezia, Italy. Oral presentation

15.35 - 15.50 *Stability of VLBI and GPS reference points at Ny-Ålesund.* Christoph Steinforth et al., University of Bonn, Geodetic Institute, Germany. Oral presentation

15.50 - 16.05 *Micro-movements on permafrost ground with regard to stability of geodetic reference points.* H-J. Kümpel and Marcus Fabian, Leibniz-Institute for Applied Geosciences, Hannover, Germany. Oral presentation

16.05 - 16.20 *Results from the 2000 GPS campaign for the measurement of the reference point for the VLBI antenna in Ny-Ålesund.* M. Negusini et al., Istituto di Radioastronomia del CNR, Sezione di Matera, Italy. Oral presentation

16.20 - 16.35 *Validation and use of a new diffusive sampler for ozone monitoring in polar troposphere.* Franco De Santis et al., CNR, Institute on Atmospheric Pollution, Rome, Italy. Oral presentation

16.35 - 17.25 Changing Environment & Ecosystem Effects II

Chair: Jon Børre Ørbæk

16.35 - 16.50 *Extremophilic fungi in coastal Arctic environment.* Nina Gunde-Cimerman et al., University of Ljubljana, Biotechnial Faculty, Slovenia, Invited speaker

16.50 - 16.05 *Diversity of cyanobacteria and eukaryotic micro-algae in subglacial soil (Ny-Ålesund, Svalbard).* Josef Elster et al., Institute of Botany, Academy of the Czech Republic, Czech Republic. Oral presentation

17.10 - 17.25 *Nitrogen in terrestrial arctic systems; Soil pools, plant growth, and environmental change.* Davey Jones et al. (presented by John Farrar), Institute of Environmental Science, University of Wales, Bangor, UK. Oral presentation

17.25 - 19.00 Poster Session

19.30 *Conference dinner*

Thursday 10 October 2002

09.00 - 09.20 Introductory Review Talk

09.00 - 09.20 *Public participation in climate change knowledge production. An assessment of communication models.* Joana Diaz Pont, Catalan Institute of Technology, Granada, Spain.

0920 - 12.30 Workshops, Thematic Sessions

09.20 - 09.30 *Introduction to workshop sessions; Plans and deliverables*. Jon B. Ørbæk, Norwegian Polar Institute, Tromsø, Norway.

09.30 - 12.30 Working groups

12.30 - 13.30 *Lunch*

13.30 - 14.30 Plenary session; Reports from working groups

14.30 - 15.00 Final remarks, end of conference

Workshops and sessions open to participants

(registrations will be done at the seminar)

Workshops on instrumental techniques and observational needs concerning the

1. Atmospheric environment, troposphere and stratosphere
2. Cryospheric environment, snow and ice
3. Solar-terrestrial environment, solar radiation and surface properties
4. Solid earth and marine environment, soil processes, land form, ocean circulation
5. Changing environment and ecosystem effects, key parameters

Specific workshop initiatives

Corbel Clean Base Initiative:
Chaired by Franck Delbart / Florent Dominé

Tethered Balloon Initiative:
Chaired by Franck Delbart/François Dulac

CALIPSO/Climate Ground Validation Initative:
Chaired by Kim Holmén

Ny-Ålesund Large Scale Facility Workshop:
Chaired by Jon Børre Ørbæk

Sixth Ny-Ålesund International Scientific Seminar
"The Changing Physical Environment"
Polar Environmental Centre, Tromsø, Norway,
8-10 October 2002

Introductory Review Talks

Guido **di Prisco** (Chairman of NySMAC): Coordination and integration of biological research in Ny-Ålesund in the framework of the new marine laboratory.

Jon Børre **Ørbæk**: The Ny-Ålesund Large Scale Facility Program 1996-2002: Experiences from 7 years of European Research and Mobility Exchange in Ny-Ålesund

Joana **Diaz Pont**: Public participation in climate change knowledge production. An assessment of communication models.

Coordination and integration of biological research in Ny-Ålesund, in the framework of the new Marine Laboratory

Guido di Prisco

Institute of Protein Biochemistry, CNR, Naples, Italy

A few years ago, the Ny-Ålesund Science Managers Committe (NySMAC) appointed an international Marine Systems Working Group, consisting of representatives of Norway, Italy, Japan and Germany. The tasks of the Group, open to other NySMAC representatives with interest in marine environmental research, are centered on discussing, initiating and coordinating marine research initiatives in waters surrounding Svalbard, including Kongsfjorden.

Several initiatives have been taken in this framework. In one of these, plans have been developed in collaboration with Kings Bay AS for establishing a new Arctic Marine Biology Laboratory in Ny-Ålesund, Svalbard. All participants of the WG have taken part in the development process. Each institution (AWI, CNR, NIPR, NP) has invested funds in a multinational rental consortium for this international project. Additionally committed partners are UNIS (Longyearbyen, Norway) and NSF (USA).

The building of the new Marine Biology Laboratory (a unique structure in the Arctic) is of paramount importance for scientific development. It will become a focal point of research in Ny-Ålesund, ensuring a boost effect due to allowing a wide range of studies *in situ* on vertebrates and invertebrates, and entailing a strong development of marine science in several disciplines all year long.

During a recent workshop in Poland, Kongsfjorden was selected as one of the "Biodiversity Flagship Sites in Europe". Ample coordination of research in this scenario has been initiated during a Kongsfjord Ecosystem Workshops, which took place in Longyearbyen in 2000. Two comprehensive papers on the physical and biological Kongsfjord system have been recently published in Polar Research, with exceptionally large authorship, assembling the contribution of many countries (the article on the biological aspects has 28 authors). A second Kongsfjord Ecosystem Workshop will be held at the Hel Biological Station (Sopot, Poland) in November 2002. Papers resulting from this workshop are expected to be published in Oceanology. These papers will be focussed on specific topics, which can be pursued in more detail than in the two overview papers.

The preparation of proposals, involving Kongsfjorden, to be submitted to the 6th EU Framework Programme, is under way. The proposals will include a strong laboratory research component with emphasis on ecological physiology and adaptations. Much of the research, which is also (at least in part) an outcome of the European Network for Arctic-Alpine Multidisciplinary Environmental Research (ENVINET), is expected to be performed in the new Marine Laboratory in Ny-Ålesund.

Thus, the role of the Marine Laboratory in the coordination and integration of multinational and multidisciplinary research collaborative efforts appears clearly.

The Ny-Ålesund Large Scale Facility Program 1996-2002: Experiences from 7 years of European Research and Mobility Exchange in Ny-Ålesund

Jon Børre Ørbæk

Norwegian Polar Institute, Polar Environmental Centre, N-9296 Tromsø, Norway. E-mail: jonbo@npolar.no, Phone/fax: +47 79 02 26 21 / 26 04

Introduction

Located at the high latitude of 78°55'N, 11°56'E, Ny-Ålesund is one of the world's northernmost human settlements. The research site represents a *unique European platform for international Arctic environmental research* with its mild climate, easy accessibility and well-developed infrastructure with highly specialised research facilities. The multitude of research projects and observation programs, advanced laboratories and instruments from a large number of disciplines, represent a unique opportunity for multidisciplinary dialogue and collaboration within environmental research such as climate change, ozone/uv-radiation, long-range transportation of pollutants, ecology and ocean-atmosphere interactions. The human impacts on the surrounding environment are kept at a low level, and the ecosystems are largely intact.

Ny-Ålesund is owned and run by the Norwegian state-owned company Kings Bay (KB), which provides the local general infrastructure. Norwegian authorities have designated Ny-Ålesund as centre for environmental research at Svalbard, and other activities must pay due consideration to the needs and demands of the research. The aim is to maintain and elaborate Ny-Ålesund as an *internationally recognised environmental research and monitoring facility in the European Arctic.* Ny-Ålesund now hosts research stations for Norway, Germany, UK, Japan, Italy, France, South Korea, and Sweden and the Netherlands have permanent activities and installations there too. Most of the buildings are rented by the various research institutes on long-term contracts (10-20 years) from Kings Bay.

The Ny-Ålesund Large Scale Facility

Since 1996 Ny-Ålesund has status as a European Major Research Infrastructure (previously called Large Scale Facility – LSF). It has been supported by the European Commission under the "Access to Research Infrastructures" activity of the 4th Framework *Training and Mobility of Researchers* (TMR) and the 5th Framework *Improving Human Potential* (IHP) programmes. The Ny-Ålesund LSF is run as a consortium between Norwegian Polar Institute (NP), Norwegian Institute of Air Research (NILU), Norwegian Mapping Authority (NMA), Alfred Wegener Institute (AWI), Natural Environment Research Council (NERC) and Kings Bay (KB), the Norwegian Polar Institute being the co-ordinator of the programme. The main aim is to increase the international collaboration at and among the stations in Ny-Ålesund and improve the ability of young European scientists to perform Arctic environmental research at the site, thus benefiting from the international Arctic research community there.

The support schemes for Research Infrastructures (RI's) of the European Commission framework programmes emphasises the importance of state-of-the-art research infrastructures to enable European scientists to operate at the forefront of their research. A "Major RI" is rear in Europe, provides world class essential services for conducting top quality research, has high investment costs and is able to provide adequate scientific, technical and logistic support to external, particularly first time users.

Transnational access and mobility of European young scientists

The main objective of the activity is to sponsor new opportunities for European research teams to obtain access to the major research infrastructures and services they require to conduct their research, irrespective of their nationality or the location (in the Member States or Associated States) of the infrastructures. European researchers can apply for grants from the Ny-Ålesund LSF to cover travel and subsistence costs for up to 2 months of field campaigns or instrument/laboratory work at the relevant LSF research installations. The opportunities are announced twice a year in Nature as well as on the programs web-pages at: http://www.npolar.no/nyaa-lsf. If supported, the new European scientists will access all the scientific, technical, logistical and engineering support that is normally provided to external users at the facilities.

The evaluation and selection of projects and research teams under the Ny-Ålesund LSF are based on scientific quality and a number of eligibility criteria set down by the European Commission. A selection panel with internal and independent external members perform an independent peer review of the proposals based on scientific merit and the interest of the Community. Main priority is always given to high quality proposals from transnational researchers that are new to the facilities. However, the complementary value, cross-disciplinary and cross-infrastructure collaboration and the European basis have also been emphasised, giving significant added value to the thematic activities present at the stations.

Broad European interest in Arctic research

Kings Bay provides accommodation for at present approximately 10.000 research days per year at the international research station of Ny-Ålesund. The Ny-Ålesund LSF research consortium contributes to more than 50% of the total research, whereas the fraction of research that are granted access through the Ny-Ålesund LSF programme represents between 5-10% of the total research at the sites. Keeping in mind that each research station primarily gives priority to their own internal/national users, the Ny-Ålesund LSF programme represents a significant fraction and stimulation of the transnational exchange at and among each research facility.

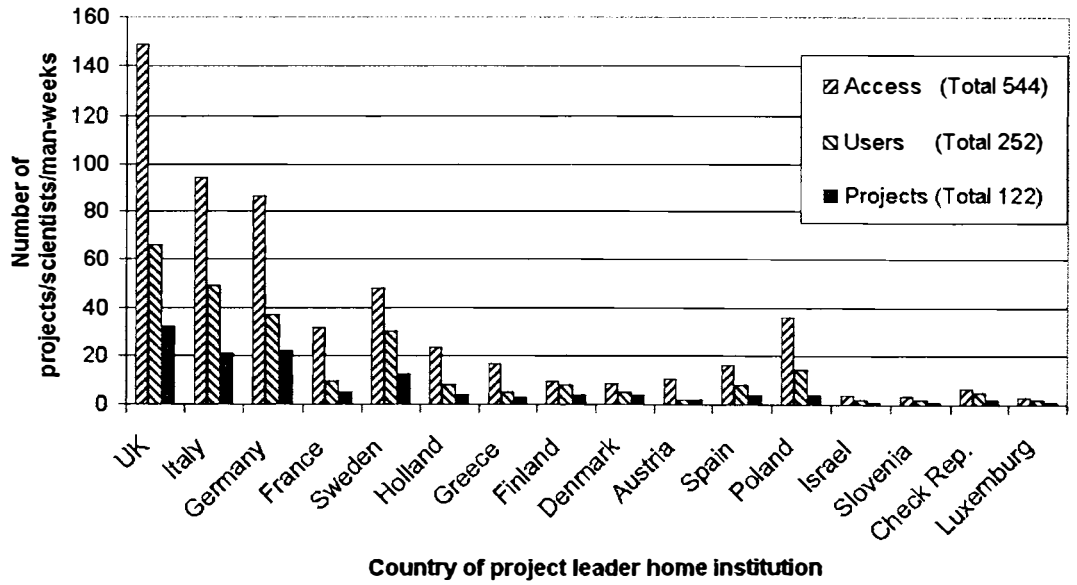

Figure 1: The nationality of the 122 European research projects granted access to the Ny-Ålesund Large Scale Facility during the period 1996 – 2002.

Since 1996, more than 250 individual scientists in more than 120 research projects have benefited from the travel grants given under the Ny-Ålesund LSF, representing almost 4000 research days at the site. The visiting scientists have originated from more than 20 Member States or Associated States of the European Union. Figure 1 presents the user statistics for the whole period 1996-2002 under 3 different EC-contracts. It shows the European distribution of the total set of projects, scientists and research days, limited to the country of project leader home institution. Research teams from the UK, Italy, Germany are the most numerous under this activity, but the figure illustrate that the Ny-Ålesund LSF has been able to attract interest from a broad European scientific user community.

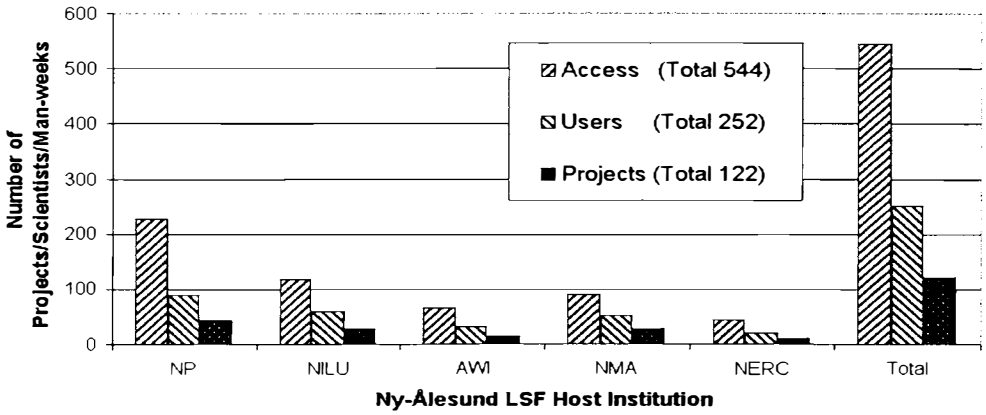

Figure 2: The host distribution of the 122 European projects granted access to the Ny-Ålesund Large Scale Facility during the period 1996 – 2002

The research projects as distributed over the various host stations in the consortium, reflect the initial distribution of access in the contract, the scientific field of interest of the research proposals, the scientific priorities given at each station and the fact that the access is limited to transnational research collaboration. Norwegian scientists have not benefited (not been eligible) from the program except for one small project. Figure 2 shows how the total number of projects is shared by the different host facilities.

Scientific highlights and priorities

The projects given access to the facilities under the Ny-Ålesund LSF program during the whole period 1996-2002 were distributed as is shown in table 1. Several of these projects benefited from the coordinated support by two or three of the installations at the facility. Some of the projects were single season field campaigns while others involved the installation of advanced research equipment at the facilities that were operated over several months by the station personnel.

The Ny-Ålesund LSF significantly benefits from the new European Network for Arctic Alpine Multidisciplinary Environmental Research – ENVINET (HPRI-CT-1999-40009), funded as a Research Infrastructure Network under the IHP-program and coordinated also by the Norwegian Polar Institute. The network has created several new research initiatives, management and logistical contacts for the Ny-Ålesund LSF to other high quality environmental research facilities in Europe. An important aim of ENVINET is to create new connections and give access to research groups that can introduce new methods and research activities at our facilities.

43 Research Projects		**Sverdrup Station (NP)**
13 Biology	Marine	Biodiversity, marine birds, benthic ecology, seals, microbial processes, primary production, ecotoxicoloty/radionucleides, costal zone ecology, climate change effects,
11 Biology	Terrestr./Freshw.	Barnacle geese, Arctic plants, Bentic freshwater ecology, camouflage strategies, Arctic fox, Long Range Transport of Pollutants, climate variability effects, genetic diversity,
8 Geophysics	Glaciology/Hydr.	Mass balance, Radar, Snow hydrology, Glacial sediments and nutrient transport, calving intensity, 3d-radar surveys,
6 Geophysics	Radiation./Heat	Active layer, radiation balance/energy budget, spectral reflectance, snow cover albedo
5 Geoph./Bio	UVB-effects	Marine phyto-plankton, freshwater zoo-plankton, terrestrial plants, freshwater microbial communities
28 Research Projects		**Zeppelin Station (NILU/NP)**
13 Atm. Chem.	Pollutants	Aerosols, VOCs, organic halogens, sulphate sources, heavy metals, acid and nitrogen deposition, POPs, PBT-compounds, mercury,
8 Atm.Chemist.	Trace Gases	Carbon cycle, Carbon monoxide isotops, aerosol formation, methane, DOAS-techniques,
5 Atm.Chemist.	Surface Fluxes	Surface O3, Tropospheric O3, CO2 flux, inorganic C, organic C, chemical denudation rates,
2 Atm.Physics	Circulation	Atmospheric transport studies
13 Research Projects		**Koldewey Station (AWI)**
5 Atm.Chemist.	Ozone	Tropospheric O3, Total O3
7 Atm.Physics	Clouds/Aerosols	Cirrus, PSCs, Boundary layer meteorology, Tropospheric profiling, Arctic Aerosols
1 Biology	Terrestrial	Soil arthropods
28 Research Projects		**Geodetic Observatory (NMA)**
13 Geodesy	VLBI/GPS	Improvement of geodetic reference frames, ground movements, active fault monitoring
5 Geodesy	PRARE, gravity	Geodynamics, Tracking and calibration of ERS, absolute gravity measurements
9 Geophysics	Geod.Techn.	GPS/Atmospheric water vapour, GPS/ionosphere effects, Sea level, Tides/tide gauge, ice-cap changes
1 Social Science	Communication	Communication for environmental awareness (all stations)
10 Research Projects		**Harland Station (NERC)**
9 Biology	Terrestrial	Soil biomass, arctic plants, microhabitats, inorganic carbon cycle, Barnacle gees, UV-effects on plants, genetic diversity of collembolans, physiology of pants and algae, Soil nitrogen dynamics, soil biodiversity,
1 Biology	Marine	Extremophilic fungi in coastal environments,

Table 1: Research projects carried out under the Ny-Ålesund LSF during the period 1996-2002.

Future opportunities and acknowledgements

The current 5th framework IHP-access contract terminates in February 2003. However, the mobility of European young researchers and the support for RI's are significantly strengthened and subject to high priority at the European level in the 6th framework program, identified as one of the cornerstones in structuring the European Research Area. On the basis of our broad European user community and documented quality of research and infrastructure, Ny-Ålesund should have good opportunities to still benefit from the European support for several years. This will contribute to the further development of this unique site as an internationally recognised high quality environmental research station in the European Arctic.

The Ny-Ålesund Large Scale Facility has been funded under the European Community TMR and IHP-programs, Contracts: ERB FMGE CT95 0065 & HPRI-CT-1999-00057.

Public participation in climate change knowledge production. An assessment of communication models.

Joana Diaz Pont
Environmental communication researcher, Catalan Institute of Technology, Ciutat de Granada, 131, 08018 Barcelona, email: joana@ictonline.es, phone: +34 93 4858585

Public understanding of and public participation in science

Research has shown that public environmental behaviour is influenced by many factors (both internal and external to the individual) and especially by cultural infrastructures. The definition of environmental problems is culturally based and many actors are involved in this process. The media, the educators, policy-makers or scientists and experts are enrolled in setting the agenda of the environmental debate and they all play a decisive role in determining social behaviour towards sustainability.

Sustainable behaviour is a chain of processes of perception, attitude, conduct and action. There is no simple mechanism for previewing (or modifying) social behaviour from perception. In other words, we can perceive climate change (a quite "invisible" issue for the public) as an environmental problem thank to the information transmitted through the media or facilitated by credible scientific sources. This perception might make us aware of facts such as rising sea level in pacific islands or rapid glacier retreat. But this awareness will not necessarily drive a different behaviour concerning for example the reduction of CO2 emissions through the use of public transport instead of the private vehicle. Information received by the audience raises awareness but it does not necessarily involve the public in the identification and implementation of a joint solution.

Public involvement in environmental problem solving goes beyond perception and awareness and it is a matter of many actors. On their side the media contribute to making environmental problems visible to the public. They contribute to setting the environmental agenda but they cannot be made accountable for social behaviour. Sustainable behaviour is the result of the interaction between the media, the audience, sources of information and the different actors of the problem.

Structured and systematic interaction of the audience with the information they receive and with the sources can influence the contents of this information. Such interaction generates a different knowledge that holds not only the vision of policy makers and scientists (primary producers of knowledge) but also that of the public in their capacity as citizens and consumers. The phenomenon of interaction of the public in information contents, and thus their participation in knowledge construction, has been studied in the field of public understanding of science and technology and especially in the environmental field. This phenomenon, known as public participation, is in a broad sense the compromise and involvement in decision and policy making processes of actors who are not only professional experts and scientist but also a wider range of social actors (such as NGO representatives, local communities, interest groups, social movements or citizens)

Participation has promoted or facilitated public debate on questions of science and technology that could not be detached from the social and cultural values of citizens. This is the case of the debate on genetic engineering and genetically modified organisms (GMOs) or, going back to the first applications of public participation in environmental debate, the NIMBY effect (Not In My BackYard). Recently, there have been experiences of public participation in the debate on climate change, a complex problem due to its invisibility for the citizen and to the scientific burden it carries.

The growing importance given to public understanding of science and technology starts in the 60s with the questioning of technocracy that sees social development as being dependent only on scientific and technologic knowledge, underestimating social conflict and democratic debate. At that moment more importance began to be given to the fact that more and better-informed public would understand the benefits and results of research and development. This view is known as the *deficit model* of public understanding. According to this model scientists are knowledgeable experts and the public are (to varying degrees) ignorant lay people. There needs to be improved communication from expert knowledge to the public.

But the really democratic challenge is the involvement of the public in the deliberative process. This is the base of the *democratic model* of public participation in science. It considers the active role of the public in the process of scientific and technologic development and even in the scientific process of knowledge construction although this might be questioned by scientists who fear a loss of rigor in their data and results.

As Durant (99) puts it "where the deficit model privileges scientists and emphasises one-way communication from experts to lay people, the democratic model seeks to establish a relationship of equality between scientists and non-scientists and emphasises dialogue between experts and lay people as a precondition for the satisfactory resolution of disagreements. Where the deficit model privileges scientific over other forms of expertise, the democratic model recognises the existence of multiple (and occasionally conflicting) forms of expertise, and seeks to accommodate them all through open, constructive public debate. Where the deficit model sees formal knowledge as the key to the relationship between science and the public, the democratic model sees a wider range of factors, including knowledge, values, and relationships of power and trust, as having an important part to play."

Public participation in climate change knowledge production

The understanding of climate change knowledge production on which the present paper builds is based on the data collected through interviews to climate change scientists and participant observation during their fieldwork at the Ny-Ålesund International Arctic Environmental Research Station (July-August 2001, 16 climate change research projects studied. 27 interviews) Content analysis of communication materials published by these researchers has also been used as well as further research and documentation on their subjects of study and the link to communication and public participation.

During interviews and participant observation at the arctic research station scientists' methods and motivations were studied as a way to seek a link with public understanding and participation. Although researchers are mainly motivated by science, it is a relevant fact that they have increasing interests beyond research itself: one third of scientists interviewed stated that elements such as communication or implementation of results were taken into account when designing their research.

Their personal preferences are also relevant since they give an idea of how scientists can balance the requirements of their work with their personal skills or preferences. More than 60% of researchers would like to perform science beyond knowledge production, either through communication (37%), implementation (13%), or a combination of all (13%). The scenario showed that there is a changing pattern in the stereotype that sees science and technology restricted by its own characteristics to a closed world formed by experts –experts that are seen as very specialised in their field of work and that maintain little or no contact with other disciplines. Although this might still be true for a good number of experts, we saw that implementation of research results is increasingly beyond science. Our scenario showed some

potential areas of work for public participation Scientists view public participation coming mainly from society and public institutions. They are very concerned about the real possibilities and use of this participation in their research. In science, the process of knowledge construction is regulated by the scientific method. Scientists are suspicious about involving others in their method, fearing a loss of rigor in their data, analysis, or results, which are subject to peer review and other types of assessment. This distrust became apparent during interviews with half of the scientists accepting public involvement only in the design phase, and 25% of them not accepting it at all.

Despite of this, examples of direct contributions of the public to the process of knowledge production could be identified where public involvement resulted in better design and better understanding. On the one hand, research design was improved in the sense of being closer to public needs while at the same time being relevant for scientific purposes. On the other hand, there was an improvement in understanding of the research final uses and possible applications for society. Both scientists and the public obtained a benefit from their co-operation.

In most cases, mechanisms of participation in knowledge construction on climate change are promoted by social networks or public institutions. We have been unable to identify initiatives coming from the private sector. Scientists interviewed view companies as clients instead of partners. The mechanisms are mainly bottom-up initiatives where the social network has found ways to get to science and work together. The co-operation takes various forms and different levels of maturity depending on the final implementation level of research results: more public involvement at local level; on the subsystem of study: more involvement in biospheric, hidrospheric and criospheric studies, and less in atmospheric studies; and on the experience and accumulated knowledge of the network as well as their capability to build efficient mechanisms of information and knowledge exchange. It is of special interest the co-operation between entomologist societies or ornithologists and climate change scientists, between fishing communities and marine biologists or even between mountain hikers and glaciologists.

The science-society mechanisms identified and studied follow a regular pattern concerning its effectiveness in terms of communication:

- Social networks share a common understanding of climate change as an environmental problem. This understanding has been facilitated by a common identity and shared knowledge.
- The linkage to science has been built upon the idea of joint construction of climate change knowledge.
- In more mature mechanisms there is a formalisation of the means of co-operation.
- When these mechanisms are functioning they are proved to become powerful communication tools. They can also become governance systems used for policy making.
- These mechanisms define a new kind of communication professional that plays a triple role in communication, education and participation.

Changing communication models: the role of new communication actors

Environmental communication cannot be a lineal process of information transmission from the sources to the audience. Lineal communication limits the real capacity of the public to change their behaviour towards sustainable action. Effective environmental communication for sustainable decision making is an information-action cycle. Information is used not just as a tool to improve quality of what is known, but to serve to the specific objectives of an actor that can take multiple forms (a journalist, an NGO, a company, a scientist, etc). The actor modifies the contents of information to make it useful for his/her final purposes. Information is not merely

representing external data. Instead, it is enriching the knowledge of the actor, thus guiding and facilitating action.

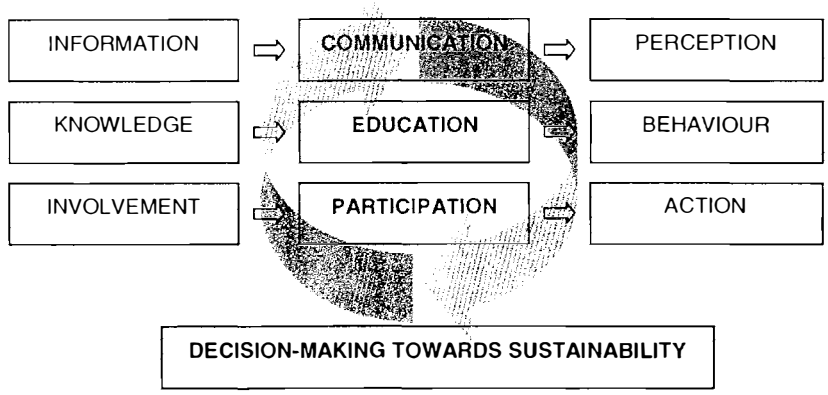

This systemic model of environmental communication defines what we call *New Communication Actors* (NCA). NCAs emerge when communication involves action-information. When dealing with another type of information the main actors are, in general, mass media. There, information is modified and enriched by the actor through interaction with external data. The final user is not involved in the definition of the contents, or at least not to the extent of being able to decide what contents have to be released. On the contrary, action-information is based on interactivity between supply and demand of information.

NCAs include the mass media (when they work in high interaction with the final users) and other professionals from the various sectors of society that hold a stake in environmental problems and produce and/or demand information for decision-making: public institutions, companies, non-governmental organisations, scientists and experts, and, of course, the public.
NCAs co-operate actively in the process of environmental communication. They can be producers, transmitters and receptors. There is a tacit co-responsibility between NCAs to build together the means by which decision-making is made compatible with sustainable development: the media can be both delivering and retrieving information; society can be both learning from and educating the experts; scientists are providing knowledge that is built upon the experience of the public. There is an intricate interdependency between NCAs that results in a joint construction of knowledge.

References

Bell, A. 1994. *Climate and opinion: public and media discourse on the global environment. Discourse and Society*, 5(1):33-64.
CEIA, 1998. *Un nou model de comunicació ambiental per a Europa.* EEA
Fischer, Frank, 1993. *Bürger, Experten un Politik nach dem Mimby-Prinzip: ein Plädoyer für die participatorische Policy-Analyse*, Politische Vierteljahresschrift, 34(24), 451-470
Jasanoff, Sheila, 1990. *The Fifth Branch.* Harvard University Press, Cambridge MA
Joss, Simon, Durant, J. (editors) 1995, *Public Participation in science; the role of consensus conferences in Europe.* Science Museum, Londres.
Latour, Bruno, 1987. *Science in Action.* Harvard University Press, Cambridge, MA
Tabara, D. 1993. "Mitjans de comunicació i medi ambient" (the media and the environment). *Perspectiva Social,* 81-95.
Ungar, S. 1994. Social Scares and Global Warming: Beyond the Rio Convention, Society and Natural resources, V8 pp.443-456

Sixth Ny-Ålesund International Scientific Seminar
"The Changing Physical Environment"
Polar Environmental Centre, Tromsø, Norway,
8-10 October 2002

Session: Atmospheric and Solar-Terrestrial Environment

Inger **Hanssen-Bauer**: Climate trends in the European Arctic during the last 100 years.

Eva Kristina **Eneroth** et al.: An atmospheric transport climatology for Ny-Ålesund using clustered trajectories.

Takashi **Yamanouchi** et al.: Variation of atmospheric constituents and their climatic impact in the Arctic - Preliminary report of "Arctic Airborne Measurement Program 2002 (AAMP02)".

J. **Umegård** et al.: One year of particle size distribution and aerosol chemical composition measurements at the Zeppelin station, Svalbard, March 2000-March 2001.

Makoto **Wada** et al.: Size distribution of aerosols and snow particles in different type airmasses.

Masataka **Shiobara** et al: A polar cloud analysis using ground-based Micro-pulse lidar data.

Chris **Lunder** et al.: The Zeppelin Station – an overview of NILU's research activities and some results.

Jussi **Paatero** et al.: Lead-210 concentration in the air at Mt. Zeppelin, Ny-Ålesund, Svalbard.

Florent **Dominé** et al.: Study of the exchange of reactive gases between the snowpack and the atmosphere at Ny-Ålesund.

Piotr **Glowacki** and Wieslawa E. Krawczyk: Long range transport of pollutants – evidences from rainfall chemistry Hornsund, Svalbard.

M. **Kriews** et al.: Trace element distribution in size separated aerosols from Ny-Ålesund during the ASTAR 2000 campaign.

Ine-Therese **Pedersen** et al.: Comparing methane data from Ny-Ålesund with results from a regional transport model (MATCH).

Michael **Gerding** et al.; Tropospheric water vapour observations by ground-based lidar.

Keiichiro **Hara** et al.: The enrichment of particular bromated (BrO_3) in the boundary layer of the winter and spring Arctic.

Christoph **Ritter** et al.: Occurrence and optical properties of tropospheric aerosols

Marion **Müller** et al.: Characteristics of different solid PSC particles observed by lidar in Ny-Ålesund.

Jon Børre **Ørbæk**: European Network for Arctic-Alpine Multidisciplinary Environmental Research – ENVINET: Coordination and harmonisation of research, facilities and services among environmental research infrastructures in Europe.

Arne **Dahlback**: Trends in surface UV radiation in Polar regions

Markus **Rex**: The Arctic Ozone Layer.

Climate trends in the European Arctic the last 100 years

Inger Hanssen-Bauer

Norwegian Meteorological Institute, P.O.Box 43 - Blindern, 0313 Oslo, Norway. E-mail: i.hanssen-bauer@met.no

1. Introduction

Global surface temperatures have increased by 0.6 °C during the 20th century (IPCC, 2001). While the temperature increase during the earlier decades of the century mainly seem to be explainable by natural variability (e.g. variation in solar radiation and volcano activity), antropogenic increase of the atmospheric concentrations of greenhouse-gases is at least partly responsible for the warming during the later decades. Most simulations by global climate models indicate that the Arctic areas are especially exposed to climate change caused by increased greenhouse effect (e.g. Kattenberg et al. 1996). It is therefore crucial to monitor long-term variations of various climate elements in the Arctic. The present paper, will focus on results from recent analyses of climate data from the European sector of the Arctic. Both trends through the whole century and trends during specific sub-periods will be addressed. Most of the results refer to previously published analyses. Some of these are based upon the NARP (Nordic Arctic Research Program) dataset, which is available at *http://projects.dnmi.no/~narp*. This dataset includes stations in Greenland, Iceland, Faroe Islands Svalbard and Jan Mayen.

2. Temperature

The mean annual temperature in the European Arctic has thus undergone large variations during the 20th century. Analyses of the temperature series in the NARP dataset show for most stations a positive trend up to the late 1930s, a negative trend from the 1930s to the 1960s, and from the late 1960s the temperature has increased at all stations except for Nuuk at Western Greenland (Førland et al, 2002). At all stations, the warmest two decades on an annual basis were the 1930s and the 1950s.

The increase in the global mean temperature during the 20th century (~0.6°C) is highly significant (IPCC 2001). At average, the warming has been even larger at high latitudes. However, at the stations in the NARP data set, the trend in annual mean temperature (1910-1999) is not statistically significant at any station. Not even for the station with the highest trend rate (Svalbard Airport, trend ~1.4 °C/century) is the rate statistically significant. This is partly due to the large year-to-year variations in temperatures in the Arctic, and the resulting low "signal-to-noise" ratio. Even though climate models indicate substantial greenhouse induced warming in the Arctic, the low "signal-to-noise" ratio implies that it is not evident that the first significant "greenhouse signal" will be found in this region. But the non-significant trends during 1910-1999 are also due to that the temperature in the European Arctic has experienced another pattern than the global and Northern Hemisphere temperatures. According to the latest IPCC-report (Folland & Karl 2001), the global mean temperatures increased rather steadily from the end of the 19th century up to around 1945, followed by a period with rather constant temperature level up to 1975. After 1975 the global temperature has increased, and this increase is more than twice the rate experienced during 1910-1945. For the globe as a whole, and even for Northern Europe, the present temperature level is significantly higher than the level from the 1930s (Parker and Horton 1999). Also in the European Arctic there has been two periods with strong warming, but the warming rate was higher and more significant in the first than in the latter warming period. At most stations in the region, the present temperature level is still lower than during the 1930s and 1950s.

It may be concluded that there are different geographical signatures on the two periods with positive temperature trends: While the warming during the recent decades has been of a more "global character", the warming up to the 1940s was especially strong at high northern latitudes, and especially in the Atlantic sector. It is still not fully understood what triggered this warming (Fu et al. 1999), which often is referred to as the "early 20th century warming".

3. Precipitation

Annual precipitation has increased in both the Svalbard region and at the Faeroe Islands during the last 7-8 decades. Because of the harsh weather conditions, sparse station network, missing data and several relocations it is complicated to establish long-term homogenized precipitation series from Svalbard and Greenland. Førland et al. (2002) present linear trends for a selection of the most reliable long-term series from the European Arctic. All stations have experienced an increase in annual precipitation, and at most of the stations the increase is statistical significant at the 5% level. At Svalbard Airport and Bjørnøya the increase is equivalent to more than 25% per century. Also for Jan Mayen and stations in Iceland, Faeroe Islands and Greenland an increase in annual precipitation exceeding 10-15% is indicated. At Jan Mayen and Torshavn, most of the increase in annual precipitation happened before 1960, while the increase at the other stations is more evenly distributed throughout the 20th century. The relative precipitation increase at Svalbard and the Faeroe Islands is considerably higher than the similar increases on the Fennoscandian mainland (Tuomenvirta et al. 2001), and also higher than the "average high latitude increase" estimated by Hulme (1995).

It should be stressed that reliable measurements of precipitation are difficult to obtain at Arctic stations. The combination of dry snow and open tundra results in considerable drifting snow, even at moderate wind-speeds. Drifting/blowing snow often occurs in combination with snowfall, and complicates precipitation measurements. On the other hand, the harsh weather conditions in the Arctic dramatically increase the catch deficiency of precipitation gauges. Based on field measurements at Spitsbergen, Førland and Hanssen-Bauer (2000) deduced correction factors for the aerodynamic catch deficiency in the Norwegian precipitation gauge. As a rough estimate it was suggested that for a «normal» year, the "true" precipitation would be about 50% higher than the measured precipitation. The gauge undercatch is especially large for solid precipitation. A positive trend in the annual temperature might lead to a reduced gauge undercatch, and thus a false positive trend for precipitation (Førland and Hanssen-Bauer 2000). The potential for such artificial trends is at maximum in areas with strong winds and where a large percentage of the annual precipitation is solid, as e.g. in the Euopean Arctic.

4. Sea ice

According to the estimate of Vinje (2001a), the sea ice extent in the Nordic Seas in April has been reduced by 33% from 1864 to 1998. The reduction has, however not been linear. Observations from areas located at the very margin of Arctic sea ice revealed a significant multiyear changes in its spreading. During the 20th century one may define four stages in the development of sea ice. These are two stages of ice expansion (1900-1918 and 1938-1968) and two stages of ice cover reduction (1918-1938 and 1968-1999), expressed at the background of secular Arctic ice area decrease (Zakharov, 2002). Generalizations of data on instrumental sea ice observations from satellites beginning from 1978, confirm a noticeable decrease of its extent for the last two decades (e.g. Chapmen and Walsh, 1993; Johannessen et al., 1995, 1999; Cavalieri et al., 1997; Parkinson et al., 1999). However, Parkinson (2000) finds that recent trends vary considerably by region.

Deser et al. (2000) show that the dominant mode of Northern Hemisphere winter sea ice variability is an antiphase fluctuation between the Labrador and Greenland/Barents seas. The time series of this mode has a high winter-to-winter autocorrelation. It is dominated by decadal-

scale variations and a longer downward trend, which consists of diminishing ice cover east of Greenland and increasing ice cover west of Greenland. This is associated with anomalies in sea level pressure and air temperature that closely resemble those associated with the North Atlantic Oscillation (NAO).

5. Atmospheric circulation indicies

Both the North Atlantic Oscillation (NAO) and the Arctic Oscillation (AO) winter indices showed strong positive trends from 1976 to 2000. The positive temperature trend in most of the European Arctic and the negative trend at western Greenland may thus partly be explained by this. During the earlier period of temperature increase, however, there was a negative trend in the winter NAOI and an insignificant trend in the AOI. A more detailed analysis of the connection between the air temperature at Svalbard Airport and atmospheric circulation (Hanssen-Bauer and Førland 1998) revealed that the temperature increase at Svalbard from the 1960s to the 1990s to a large degree may be explained by an increase in the average strength of winds from south and west, and thus increased transport of warm airmasses to Spitsbergen. Similar variations in circulation, however, account for only 1/3 of the observed temperature increase at Svalbard from 1912 to the 1930s and the temperature decrease from the 1930s to the 1960s. One possible reason for this may be that the warming in the first part of the 20th century has been caused by changes in ocean circulation and sea surface temperatures (Fu et al. 1999). Hanssen-Bauer and Førland (1998) concluded that in addition to atmospheric circulation, other factors like sea surface temperature, sea ice extent, cloudiness etc. are needed to model long-term temperature variations in the Arctic. The observed long-term variations in precipitation on the west coast of Spitsbergen since 1912, may be explained mainly by variations in the average atmospheric circulation conditions (Hanssen-Bauer and Førland 1998). The main reason for the close relationship between circulation and precipitation, is that the precipitation at West-Spitsbergen is strongly influenced by orographic effects.

6. Conclusions

Analyses of climate series from the European Arctic show major inter-annual and inter-decadal variability, but no statistically significant long-term trend in annual mean temperature during the 20th century in this region. Although the temperature increased significantly from the 1960s to 2000 in large parts of the area, the present temperature level is still slightly lower than it was during the 1930s. The temperature increase at Svalbard from the 1960s to the 1990s may to a large degree be attributed to a large-scale variation in atmospheric circulation indices, but this is not the case for the temperature increase from 1912 to the 1930s and the temperature decrease from the 1930s to the 1960s. The Arctic temperatures are also influenced by factors like sea surface temperatures, sea ice extent and cloudiness.

In large parts of the European Arctic, annual precipitation has increased substantially during the last century. Both in the Svalbard region, and at stations in the Faeroe Islands, Iceland and Greenland, a long-term increase equivalent to more than 15% per century has been observed. At Svalbard Airport and Bjørnøya the increase exceeds 25%. The observed long-term variations in precipitation on the west coast of Svalbard since 1912 may to a large degree be explained by variations in the average atmospheric circulation conditions. However, increasing temperatures during the later decades lead to a reduced fraction of solid precipitation, and consequently an increased catch efficiency of precipitation gauges. This increased gauge catch efficiency for the precipitation gauges implies that parts of the observed positive precipitation trend during the latest decades is fictitious.

The recent warming is also evident over the central Arctic Ocean. This is accompanied by a general downward tendency in Northern Hemisphere sea ice extent since 1979 and apparent

thinning of the multiyear ice cover. Observed regional decadal scale variability in the sea-ice extent can be related to a variation in indices of the NAO/AO. However, the long-term negative trend is not connected to these indices.

References

Cavalieri, D.J., P. Gloersen, C.L. Parkinson, J.C. Comiso and H.J. Zwally, 1997: Observed hemispheric asymmetry in global sea ice changes, *Science*, 278, 1104-1106.

Chapman, W.L. and J.E. Walsh, 1993: Recent variations of sea ice and air temperature in high latitudes, *Bull. Amer. Meteorol. Soc.*, 74, 33-47.

Deser, C., J.E. Walsh and M.S. Timlin, 2000: Arctic sea ice variability in the context of recent atmospheric circulation trends, *J. Climate*, 13, 617-633.

Folland, C. & T.R. Karl, 2001: Observed Climate Variability and Change. In: IPCC (International Panel on Climate Change), 2001: Climate Change 2001: The Scientific Basis. Contribution of Working Group I to the Third Assessment Report of IPCC. Available at *www.ipcc.ch*

Fu,C., H.F.Diaz, D.Dong and O.Fletcher, 1999: Changes in Atmospheric Circulation over the Northern Hemisphere Oceans associated with the Rapid Warming of the 1920s. International Journal of Climatology, 19,581-606

Førland, E.J. and I.Hanssen-Bauer, 2000: Increased Precipitation in the Norwegian Arctic: True or False. Climatic Change, 46, 485-509

Førland, E.J., I. Hanssen-Bauer, T. Jónsson, P. Nordli, O.E. Tveito, and E.V. Laursen, 2002: Twentieth-century variations in temperature and precipitation in the Nordic Arctic. *Polar Record*, 203-210

Hanssen-Bauer, I. and E.J.Førland, 1998: Long-term Trends in Precipitation and Temperature in the Norwegian Arctic: Can they be explained by Changes in the Atmospheric Circulation Patterns. Climate Research, 10, 143-1 53

Hulme, M.: Estimating Global Changes in Precipitation. Weather 50 (2), 34-42

IPCC (International Panel on Climate Change), 2001: Climate Change 2001: The Scientific Basis. Contribution of Working Group I to the Third Assessment Report of IPCC (Available at www.ipcc.ch)

Johannessen, O. M., E. Shalina, and M. Miles, 1999: Satellite evidence for an Arctic Sea ice cover in transformation, *Science,* 286, 1937-1939.

Johannessen, O. M., M. Miles, and E. Bjorgo, 1995: The Arctic's shrinking sea ice. *Nature,* 376, 126-127.

Kattenberg, A., G.V. Gruza, J. Jouzel, T.R. Karl, L.A. Ogallo and D.E. Parker, 1996: Observed Climate Variability and Change. In: Houghton, J.T., L.G. Meira Filho, B.A.Callander, N.Harris, A. Kattenberg and K. Maskell (Eds.), Climate Change 1995 - The Science of Climate Change. Cambridge University Press. 289-357.

Parker, D.E.and E.B.Horton, 1999: Global and Regional Climate in 1998. Weather 54(6), 173-184.

Parkinson, C.L., 2000: Recent trend reversals in Arctic sea ice extents: Possible connections to the North Atlantic Oscillation, *Polar Geography*, 24, 1-12.

Thomson,D.W.J. and J.M.Wallace, 1998: The Arctic Oscillation Signature in the Wintertime Geopotential Height and Temperature Fields. Geophysical Research Letters, Vol.25, No.9, 1297-1300

Tuomenvirta, H., H. Alexandersson, A. Drebs, P. Frich, P.Ø. Nordli, 2001: Trends in Nordic and Arctic Temperature Extremes and Ranges. Journal of Climate. 13, 977 - 990.

Vinje, T., 2001a: Anomalies and trends of sea ice and atmospheric circulation in the Nordic Seas during the period 1864-1998, *J.Climate*, 14, 255-267.

Zakharov, V.F., 2002: Inter-decade changes of sea-ice conditions of the Arctic Seas in the last century. *In: Shaping and dynamics of recent Arctic climate. Ed. Alekseev G.V.* St.-Petersburg, Gidrometeoizdat, (in press).

An atmospheric transport climatology for Ny-Ålesund – using clustered trajectories

Kristina Eneroth[1], Ine-Therese Pedersen[1,2], Erik Kjellström[1], Kim Holmén[1]

[1] Department of Meteorology, Stockholm University (MISU), S-106 91 Stockholm, Sweden.
E-mail: Kristina.Eneroth@misu.su.se
[2] Norwegian Institute for Air Research (NILU), N-9296 Tromsö, Norway.
E-mail: Ine-Therese.Pedersen@nilu.no

1. Introduction

Previous studies (e.g. Halter and Peterson, 1981; Halter and Harris, 1983; Higuchi and Daggupaty, 1985) have demonstrated a relationship between the CO_2 variability at Arctic monitoring stations and variations in the synoptic-scale atmospheric circulation. Their results are in agreement with the idea that air reaching the Arctic is not well-mixed and thus retains memory of the spatial distribution of the local and regional sources and sinks of CO_2. In this paper we establish a climatology of long-range transport to Ny-Ålesund, Svalbard through an analysis of three-dimensional 5-day back-trajectories. The trajectories are classified into distinct transport patterns through the use of cluster analysis. We use this climatology to investigate if there is a consistent relationship between anomalous CO_2 concentration values and trajectories of air parcels arriving at Ny-Ålesund.

2. Trajectory model and cluster analysis

The three-dimensional model of McGrath (1989) is used to calculate 5-day back-trajectories for the period 1997-2000. The model uses input wind fields taken from the European Centre for Medium-Range Weather Forecasts (ECMWF). The trajectories are classified into distinct transport patterns through the use of cluster analysis. We chose to use the Ward's minimum variance technique (Romesburg, 1984) for the classification. The cluster variables are points along the trajectories (i.e. latitude and longitude) at one-hour intervals. The cluster procedure is performed separately for yearly and monthly sets of trajectories arriving twice daily (00 and 12 UTC) at 950, 850 and 750 hPa respectively to examine both year-to-year and month-to-month variability in flow characteristics. To decide how many trajectory clusters to produce we looked at the total within-cluster variance as a function of number of clusters (Eneroth, 2002).

3. Results

3.1 Climatology

To summarize and study the variability in atmospheric transport through the year we cluster all trajectories for the year 1998. We find that seven clusters for the total data set is sufficient to describe the major flow patterns to Ny-Ålesund. Figure 1 shows cluster-membership plots of trajectories arriving at 850 hPa. The dominating transport regime during 1998 is air originating from the Arctic Basin (cluster 5). The two northerly flow patterns (clusters 4 and 6) together represent 29% of the trajectories during 1998. Cluster 7 occurs 17% of the time, describing atmospheric transport from Europe and Russia. Cluster 3 accounts for 12% of the data, representing transport from the Ob-region and Northern Siberia. The westerly clusters differ in trajectory length (i.e. wind speed), cluster 1 originates from the northern North Atlantic whereas cluster 2 represents trajectories from the east coast of North America and the Atlantic.

We find that the transport patterns to Ny-Ålesund differ from month to month (i.e. the clusters are unevenly distributed between the months). For instance, cluster 2, representing westerly transport, occurs only sporadically during the summer period. Whereas, on the other

hand cluster 7, representing southeasterly transport from Europe and Russia, is the dominating one during July and August. Table 1 shows the distribution of trajectories in the clusters for each month during 1998.

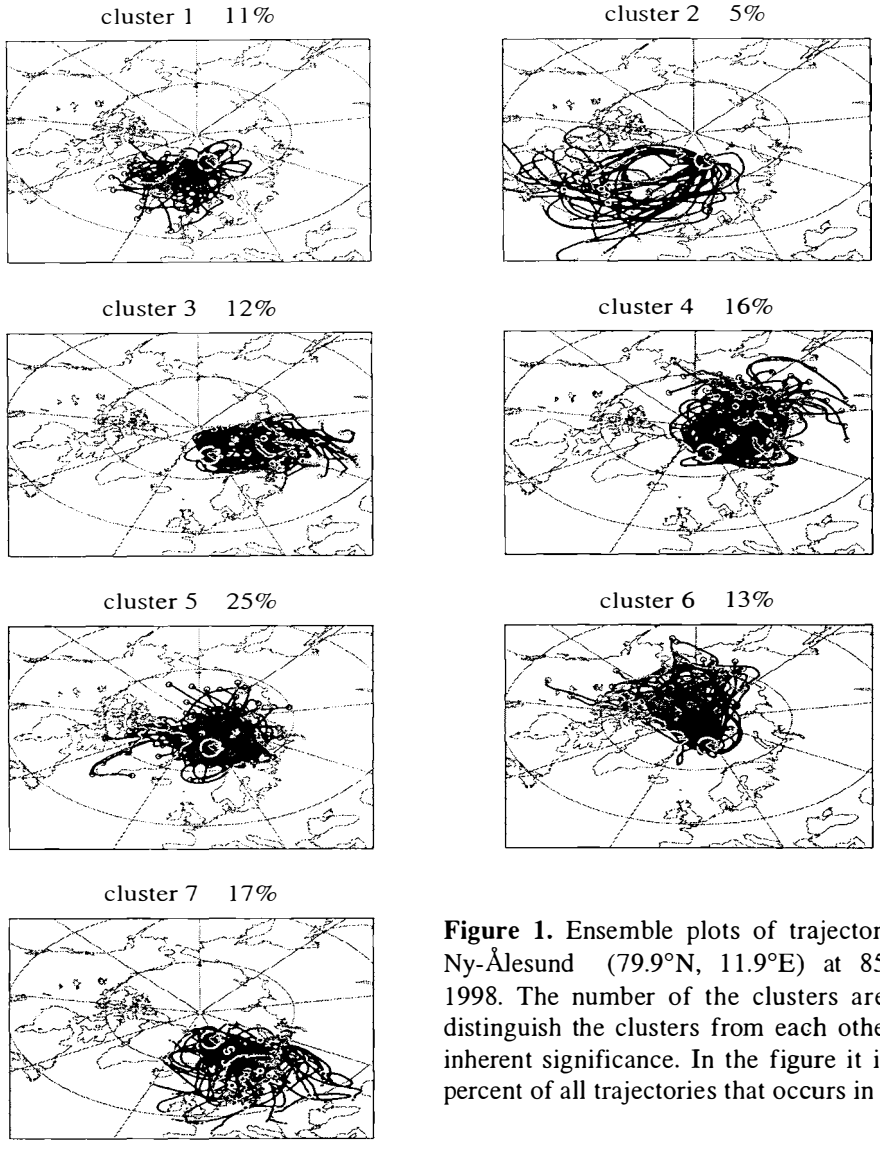

Figure 1. Ensemble plots of trajectories arriving at Ny-Ålesund (79.9°N, 11.9°E) at 850 hPa during 1998. The number of the clusters are only used to distinguish the clusters from each other and have no inherent significance. In the figure it is indicated the percent of all trajectories that occurs in that cluster.

Table 1. Number of trajectories in the clusters obtained with Ward's method for 5-day back-trajectories arriving at Ny-Ålesund (79.9°N, 11.9°E) at 850 hPa for each month 1998.

Cluster no	Jan	Feb	Mar	Apr	May	Jun	Jul	Aug	Sep	Oct	Nov	Dec	Tot
1	6	0	5	3	13	5	4	15	6	9	7	6	79
2	0	0	13	5	2	0	0	1	3	0	9	7	40
3	22	7	10	8	9	2	9	6	2	5	1	6	87
4	11	8	8	15	6	6	9	3	12	17	9	10	114
5	4	24	10	22	23	24	7	11	18	13	18	12	186
6	12	12	2	5	5	15	10	0	12	4	5	15	97
7	7	4	14	2	4	8	23	26	7	14	11	6	126

Note that this climatology is only valid for 1998. Cluster analysis performed on monthly data sets containing trajectories from the four-year period 1997-2000, shows a large variability in atmospheric circulation from year to year.

3.2 Short-term variability in CO_2 and atmospheric transport

Continuos measurements of atmospheric CO_2 concentration have been performed at Ny-Ålesund (79.9°N, 11.9°E) since late 1988 (see Fig. 2). The monitoring station is located 474 m above sea level at Mt. Zeppelin, a mountain ridge with steep rocky slopes and glaciers on all sides. The measurement program is described in detail in Holmén et al. (1995).

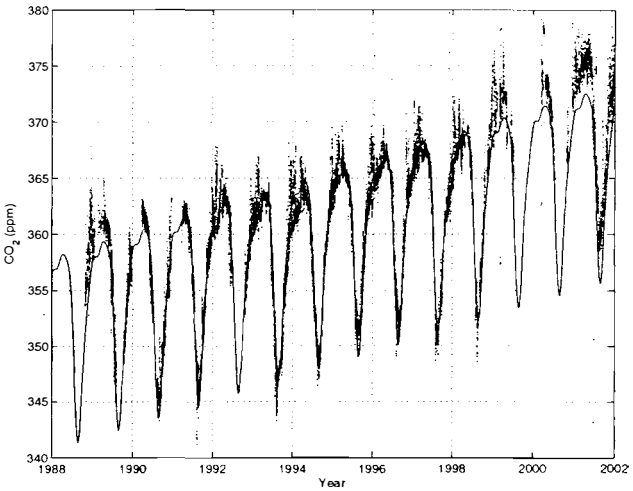

Figure 2. Time-series of atmospheric CO_2 mixing ratio at Mt. Zeppelin, Ny-Ålesund (79.9°N, 11.9°E) during 1988-2002. The black dots are instantaneous measurements and the black curve is the smooth annual variation and long-term trend obtained by fitting a linearly increasing harmonic function through the data.

To determine the short-term anomalies and facilitate the comparison between CO_2 and transport variability, the annual cycle and the long-term trend are removed from the CO_2 record. The anomalies are calculated as the difference between the instantaneous measurements and the harmonic function shown in Fig. 2. In addition to observed CO_2 anomalies, we also calculate anomalies based on simulated CO_2 mixing ratios at Ny-Ålesund. The simulations are performed with a three-dimensional transport model, MATCH (Robertson et al., 1999), which in the present setup uses meteorological parameters from the ECMWF with a 1°x1° horizontal resolution at six-hour intervals. CO_2 surface fluxes from the terrestrial biosphere and the oceans are included as well as man-made emissions (Kjellström et al., 2002). The calculated CO_2 anomalies during 1998 are shown in Figure 3.

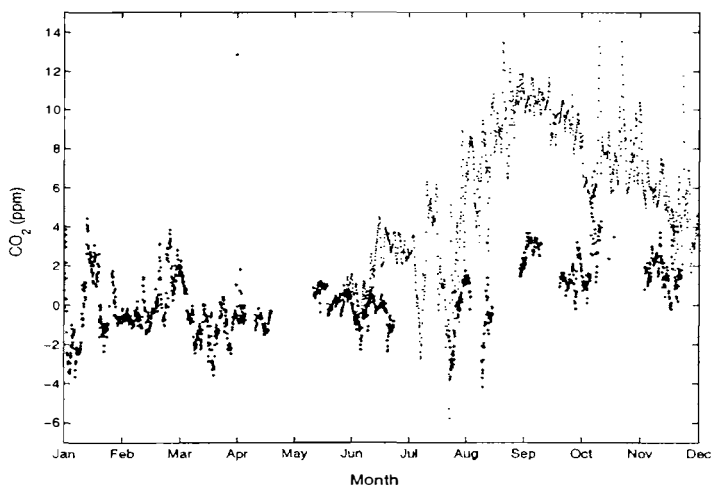

Figure 3. CO_2 anomalies calculated from CO_2 measurements (large dots) and model simulations (small dots) at Ny-Ålesund (79.9°N, 11.9°E) during 1998.

We find some relationship between transport patterns and short-term CO_2 variability. Large positive anomalies during winter are often associated with transport from Europe and Russia (cluster 2) consistent with earlier findings by Lejenäs and Holmén (1995). On the other hand, during summer the same transport pattern result in negative anomalies, reflecting CO_2 uptake by the terrestrial biosphere. However, often we see no conclusive linkage between fluctuations in CO_2 and variations in the atmospheric circulation.

4. Conclusions and discussion

In this study a climatology for Ny-Ålesund is established. The identified transport patterns are used to examine the relationship between variability in atmospheric circulation and CO_2 in Ny-Ålesund during 1998. We find that the CO_2 observations are influenced by synoptic scale atmospheric flow patterns. However, some of the day-to-day variability can not be explained solely based on our climatology. Possible the 5-day duration of the trajectories is not enough to identify distant sink and source regions. Also the trajectory calculations are associated with uncertainties. Furthermore, Eneroth (2002) demonstrated the importance of consider the vertical transport when interpreting CO_2 mixing ratios. Therefore, in a future study, we will also take into account the altitude of the trajectories in the clustering process. Interannual variability in transport patterns will also be explored systematically. This will further aid in the interpretation of the CO_2 measurements at Mt. Zeppelin.

5. Acknowledgments

We thank Ray McGrath at the Irish Meteorological Service for providing the trajectory model. We also thank the Norwegian Polar Institute and the Norwegian Institute for Air Research for a fruitful cooperation. The CO_2 monitoring at Mt. Zeppelin station, Ny-Ålesund is supported by the Swedish Environmental Protection Agency.

6. References

Eneroth K. 2002: Inter-annual and seasonal variations in transport to a measuring site in western Siberia, and their impact on the observed atmospheric CO_2 mixing ratio. *Report CM-98,* May 2002. Department of Meteorology, Stockholm University.

Halter B. C. & Peterson J. T. 1981: On the variability of atmospheric carbon dioxide concentration at Barrow, Alaska during summer. *Atmos. Environ. 15,* 479-488.

Halter B. C. & Harris J. M. 1983: On the variability of atmospheric carbon dioxide concentration at Barrow, Alaska during winter. *J. Geophys. Res. 88*, 6858-6874.

Higuchi K. & Daggupaty S. M. 1985: On variability of atmospheric CO_2 at station Alert. *Atmos. Environ. 19*, 2039-2044.

Holmén K., Engardt M. & Odh S.-Å. 1995: The carbon dioxide measurement program at the Department of Meteorology at Stockholm University. *Report CM-84*, March 1995. Department of Meteorology, Stockholm University.

Kjellström E., Holmén K., Eneroth K., & Engardt M. 2002: Summertime Siberian CO_2 simulations with the regional transport model MATCH: A feasibility study of carbon uptake calculations from EUROSIB data. Tellus, 54B, in press.

McGrath, R. 1989: Trajectory models and their use in the Irish Meteorological Service. Irish Meteorological Service, Glasnevin Hill, Dublin, *International Memorandum No. 112/89*, 12pp.

Lejenäs H. & Holmén K. 1996: Characteristics of the large-scale circulation during episodes with high and low concentrations of carbon dioxide and air pollutants at an Arctic monitoring site in winter. *Atmos. Environ. 30,* 3045-3057.

Robertson L., Langner J. & Engardt M. 1999: An Eulerian limited-area atmospheric transport model. *J. Appl. Meteor. 388*, 190-210.

Romesburg, H. C. 1984: *Cluster analysis for Researchers.* Lifetime Learning Publications, 334pp.

Variations of atmospheric constituents and their climatic impact in the Arctic - Preliminary report of "Arctic Airborne Measurement Program 2002 (AAMP 02)"-

Takashi Yamanouchi, Makoto Wada, Masataka Shiobara
National Institute of Polar Research, Tokyo 173-8515, Japan. yamanou@pmg.nipr.ac.jp
and Andreas Herber
Alfred-Wegener Institute for Polar and Marine Research, Bremerhaven, Germany. aherber@awi-bremerhaven.de

Introduction

The Arctic Airborne Measurement Program 2002 (AAMP 02) campaign was carried out in March 2002 by NIPR under the cooperation with AWI together with several other institutions, as one of the sub program of "Variations of atmospheric constituents and their climatic impact in the Arctic" (Special Scientific Research Program, No. 11208201). The research objectives of AAMP 02 were to elucidate 1) spatial distribution, long-range transport and transformation of greenhouse gases and aerosols, related to stratosphere –troposphere exchange and polar vortex; 2) optical properties of aerosols, especially of stratosphere and upper troposphere, and their radiative forcing on the earth-atmosphere system; 3) structure of atmospheric disturbance especially of polar low. An instrumented jet plane, Gulfstream II (G-II), was used and flown from Nagoya, Japan through Barrow (71°N, 157° W), Alaska to Longyearbyen (78° N, 15° E), Svalbard, crossing the Arctic Ocean at 12 ~ 13 km height, and three local flights over the Greenland Sea around Svalbard. During the campaign, intensive surface operations were also conducted at Ny-Ålesund (79° N, 12° E), Svalbard. Airborne measurements are also to be compared with surface observations at Barrow by NOAA/CMDL and SAGE-III satellite measurements by NASA. This airborne campaign was a follow on of AAMP 98 with similar operation and ASTAR 2000 (Arctic Study of Tropospheric Aerosol and Radiation; specially focused on Arctic haze).

Recent research projects in the Arctic

The following specific research has been conducted during the current year related to the project, "Variations of atmospheric constituents and their climatic impact in the Arctic".

(1) Long term observations of greenhouse gases: At the Rabben observatory in Ny-Ålesund scientific station, Svalbard, long term air sampling for greenhouse gases and stable isotope analysis, and continuous measurements of surface ozone and meteorology have been continued (Morimoto et al., 2001). We also accumulated data concerning exchange of carbon dioxide between ocean and atmosphere, in collaboration with the oceanographic group (eg. CONVECTION; Hashida et al, 2001).

(2) Aerosol and cloud observations: Measurements of aerosol number concentrations, optical depth, vertical distributions, composition and precursor gases (Hara et al., 2002); and observations of precipitable water, cloud liquid water, ice water amount and precipitated snow particles, have been continued at Ny-Ålesund to determine the relationship between aerosols, clouds and precipitation (Wada and Igarashi, 1998). Doppler radar observation are also conducted at Bear Island.

(3) ASTAR 2000: Coordinated airborne and ground-based observations of aerosols and radiation were carried out in the Svalbard area through March and April, 2000 (Yamanouchi and Herber, 2001). A German aircraft Polar 4 (Dornier 228) was used to measure vertical distributions of aerosols and radiation, while remote sensing and sampling were conducted on ground. In addition, SAGE-II satellite observations were compared, and the radiative forcing of aerosols over a wide area

was evaluated by incorporating the observational results into an Arctic regional climate model (HIRHAM).
(4) AAMP 98: Similar campaign as AAMP 02 of airborne observation using jet plane (G-II) was carried out in March 1998 with long range stratosphere flights over the Arctic Ocean and local profiling flights in the vicinity of Svalbard (Shiobara et al., 1999).

AAMP 02 observations

Airborne observations

A trans-Arctic airborne observation was conducted in 5-14 March 2002. Flight schedule, total in 49.2 hrs, was as follows: March 5, Nagoya, Japan - Petropavlovsk, Russia, 3.8hr; Petropavlovbsk - Anchorage, USA, 4.7hrs. March 6, Anchorage - Barrow, USA, 3.3hrs including profile observation flight; Barrow - North Pole - Longyearbyen, Svalbard, Norway, 5.5hrs. March 7, Local profile flight in the vicinity of Ny-Ålesund: 3 hrs. March 10, Local profile flight in Norwegian Sea and in the vicinity of Ny-Ålesund: 4.9 hrs. March 11, Local flight for the polar low in Norwegian Sea: 4.4 hrs. March 12, Longyearbyen - North Pole - Barrow: 4.9hrs. March 13, Barrow - Anchorage: 3.3hrs including profile flight. March 14, Anchorage - Petropavlovsk: 4.5hrs; Petropavlovsk - Nagoya: 4.3hrs.

The plane, G-II, was equipped with CO_2 and ozone analyzer, gas sampling systems (for CO_2, CH_4, N_2O, CO, SF_6, O_2/N_2 and the isotope; for COS), aerosol filter sampler and impactor, aerosol particle counter, nephelometer, absorption photometer, PMS particle probes, sunphotometer, dew point meter and drop sonde system.

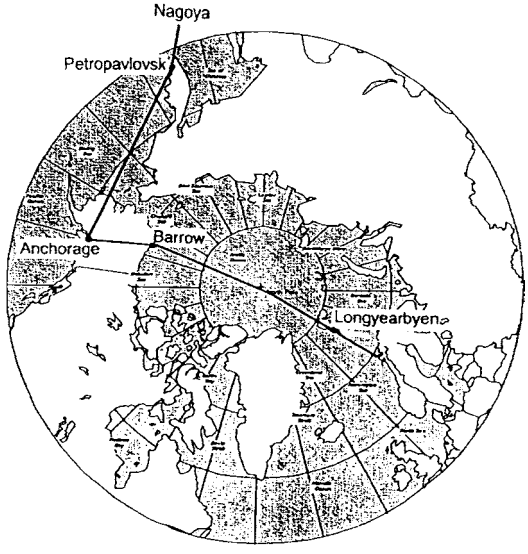

Fig.1 Flight route of AAMP02. Nagoya – Peteropavlovsk – Anchorage – Barrow – (North Pole) – Longyearbyen; Vicinity of Svalbard.

Ground based observations

The airborne measurements were complemented by comprehensive ground-based measurements st Ny-Ålesund. At NIPR Rabben Station, air sampling for greenhouse gases, continuous measurements of surface ozone and aerosol particles, remote sensing by sky radiometer, microwave radiometer, micro-pulse lidar and radar were made; at AWI Koldewey Station, sunphotometer, lidar and FTIR remote sensing together with balloon launchings were made.

Preliminary results

Atmospheric condition in the Arctic during the outward flight was rather special. From 250 hPa

height field, polar vortex was shifted to European side, and the center was around the north of Greenland. Drop sonde profile shows that, along the route, in the Alaskan side tropopause was very high around 250 to 300 hPa and flight route was out of polar vortex (mid-latitude airmass), while in the European side tropopause became low, close to 400 hPa and route was in the core of polar vortex (Fig. 2).

This atmospheric condition affects greenhouse gases, and different vertical profiles are seen at Anchorage, Barrow and Longyearbyen. Vertical profiles of ozone and CO_2 show different tendency from the troposphere to the stratosphere; ozone profile shows a distinct change at the tropopause, however, CO_2 profile shows a gradual change from upper troposphere to the stratosphere and no distinct change at the tropopause. Increase of CO_2 concentration in the lower stratosphere (around 12 km) during March 1998 and 2002 was about 6 - 8 ppmv.

Aerosol samplings were performed by filter sampler and impactor. Ionic components were analyzed with ionchromatography, and chemical components with electron microscope. Optical parameters will be calculated with the aid of particle number concentrations and compared with scattering and absorption measurements.

From sunphotometer measurements, optical depth of the stratosphereic aerosols shows a good agreement in wide area of flight, around 0.004 to 0.005 at 500 nm from the height range 11 – 12 km. Also an extremely good agreement of extinction profile with SAGE-III satellite measurement was found between 3 to 15 km height at 72° N, off Barrow.

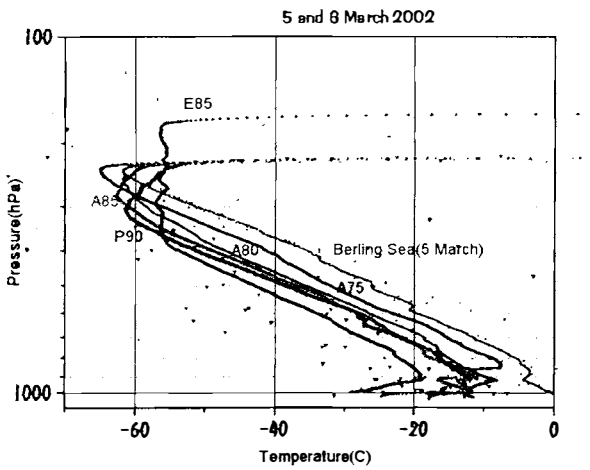

Fig. 2 Temperature profiles from drop sonde measurements along the flight route at Bering Sea, Alaskan side, 75° N, 80° N, 85° N, Pole, 85° N in the European side, on 5 – 6 March 2002.

References

Hara, K., Osada, K., Matsunaga, K., Sakai, T., Iwasaka, Y. & Furuya, K. 2002: Concentration trends and mixing states of particulate oxalate in Arctic boundary layer in winter/spring. *J. Geophys. Res., 107*, in press.

Hashida, G., Aoki, S., Morimoto, S., Nakaoka, S., Watai, T., Yoshimura, S., Nakazawa, T. & Yamanouchi, T. 2001: Temporal and spatial variations of surface oceanic CO2 in the Greenland Sea and the Barents Sea. *Extended Abstracts, 6th International Carbon Dioxide Conference, October 1-5, 2001, Sendai, Japan*, 639-640.

Morimoto, S., Aoki, S. & Yamanouchi, T. 2001: Temporal variations of atmospheric CO2 concentration and carbon isotope ratio in Ny-Alesund, Svalbard. "Environmental Research in the Arctic 2000", *Mem. Natl. Inst. Polar Res., Spec. Issue, 54*, 71-80.

Shiobara, M., Fujii, Y., Morimoto, S., Asuma, Y., Yamagata, S., Sugawara, S., Inomata, Y., Watanabe, M. & Machida, T. 1999: An overview and preliminary results from the Arctic Airborne Measurement Program 1998 campaign. *Polar Meteorol. Glaciol., 13*, 99-110.

Wada, M. & Igarashi, M. 1998: Atmosheric observations of liquid water in cloud and of chemical species in aerosols and gases near the ground and in fallen snow at Svalbard, Arctic. *Atmos. Res., 46*, 383-389.

Yamanouchi, T. & Herber, A. 2001: Plan of Arctic field campaign ASTAR2000 (Arctic Study of Tropospheric Aerosol and Radiation). "Environmental Research in the Arctic 2000", *Mem. Natl. Inst. Polar Res., Spec. Issue*, *54*, 101-106.

One year of particle size distribution and aerosol chemical composition measurements at the Zeppelin Station, Svalbard, March 2000-March 2001

J. Umegård[1], J. Ström[1], K. Tørseth[2], P. Tunved[1], H.-C. Hansson[1], K. Holmén[3], A. Herber[4], G. König-Langlo[4]

[1]Institute for Applied Environmental Research, Air-Pollution Laboratory, Stockholm University, SE-106 91 Stockholm.
[2]Norwegian Institute for Air Research
[3]Department of Meteorology, Stockholm University
[4]Alfred Wegener Institute Foundation for Polar and Marine Research.

Introduction

One of the most basic and important properties to characterize an aerosol is the size distribution. From several locations around the world there are observations available of aerosol size distributions that extend many years back in time and which contribute to new understanding about the aerosol life cycle. In the Arctic region however, aerosol size distributions have been observed only as part of singular experiments.

In middle of March 2000 a DMPS (Differential Mobility Particle Sizer) system was implemented at the Zeppelin station. Here we report on findings from the first year of operation covering the period March 2000 to April 2001. We present the full annual cycle of size distributions based on observations made every second minute as well as the integral particle number, and calculated aerosol surface and volume densities.

Experiment

The measurement site is situated at 78°58' N and 11°53' E on the Zeppelin Mountain in the Ny Ålesund community on Svalbard. The Zeppelin station is 474 m above sea level and an ideal location for atmospheric monitoring. For more information about the station we refer to: http://www.nilu.no/niluweb/services/zeppelin/. The DMPS system is a custom built Hauke type Differential Mobility Analyzer (DMA) coupled to a TSI 3760 Condensation Particle Counter (CPC). This system uses a closed loop sheath air circulation as described in (Jokinen and Mäkela, 1997). The aerosol sample flow is 1.5 L min^{-1}, while the sheath airflow is set to 5.5 L min^{-1}. This yields a rather broad transfer function, but improves counting statistics during periods of low aerosol loading. The mobility distribution measured by the DMA instrument is inverted to a number distribution assuming a Fuchs charge distribution. From 28 October 2000 and onwards the size range is 20 nm to 630 nm in diameter. Prior to that date the range is 22 nm to 500 nm in diameter. One size distribution is provided every second minute. A second CPC, model TSI3010, is used for measuring the total particle number density for particles larger than 10 nm in diameter. This instrument yields some information about the population of particles between 10 and 20nm by differentiating between the CPC3010 and the DMPS-system. During periods void of particles smaller than 20 nm the CPC3010 is used to check the consistency of the integrated number density from the inverted size distribution given by the DMPS-system.

Observations and Discussion

The anthropogenic influence on air composition in the Arctic show a very strong seasonal variation with a pronounced maximum in late winter early spring and a minimum in the summer months. The reason for this difference by season is due to the position of the Polar front and the associated circulation pattern. In summer, the Polar front is located north of the main source regions and serve as an effective scrubber for many pollutants.

The seasonal difference is also clearly depicted in the aerosol size distribution observed at the Zeppelin station. Figures 1a-c present the monthly means for March, June, September and December of number, surface, and aerosol volume-density distributions, respectively. In terms of number distribution the summer month dominates with a main mode in the Aitken size range around 30 nm. The spring month shows less integral number of particles and the dominant particle size is found in the accumulation mode size range around 150 nm. Although a minor Aitken mode around 40 nm is also suggested in the distribution. The fall moth presents even less particles, but the distribution is broader and the mode is found around 80 nm. The winter month show the least particles and with a very small contribution of particles smaller than 70 nm.

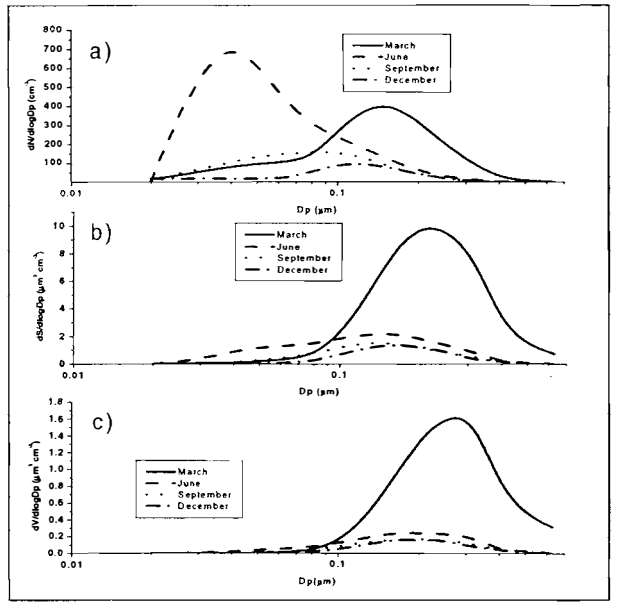

Figure 1. Monthly average distributions for March, June, September, and December. Number density a), surface density b), and volume density c).

The differences between the seasons are obvious in the number distribution as seen in Figure 1a, but in the other two moments the month of March stands out considerably (Figures 1b and 1c). At times the aerosol loading in the Arctic during springtime becomes large enough to significantly reduce visibility, which is the well-known Arctic Haze phenomenon. Due to the rather narrow accumulation mode in spring and winter the difference between surface and volume distributions are not so large. Compared to the spring, the other three seasons are not so different, which is especially true for the fall and winter period.

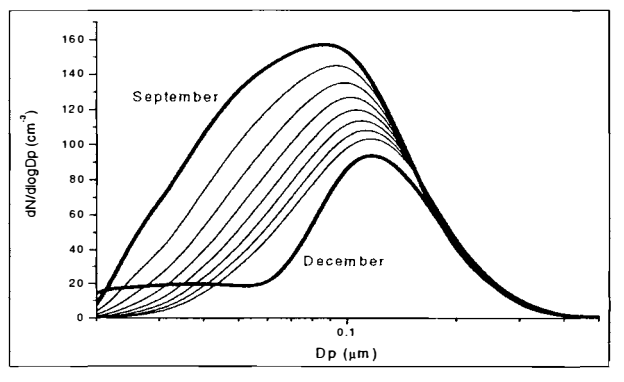

Figure 2 The thick lines show the monthly mean size distributions for September and December. The thin lines represent the calculated change in the aerosol size distribution due to coagulation for each 2 weeks of simulated time. The model was initialized wit the September distribution.

To study how the distribution evolves over time, the hourly average distributions were normalized to their maximum value in each distribution. This way variability simply due to changes in the total number density is removed and the evolution of the shape of the distribution can be followed. The result are not presented but are briefly discussed below. The first part of the year is characterized by a fairly stable location of the maximum or main mode, but around day 150 (29 May) into the year a sudden change from one regime to the other takes place over only a few days. The maximum shifts from the accumulation mode range to the Aitken mode range. The maximum essentially remains in the Aitken mode, typically around 30 nm, until about day 250 (6

September), but the distribution is not as stable as earlier in the year. By day 250 the maximum recovers to a size typically just below 100 nm, but the appearance remain variable. By day 300 (26 October) the variability relaxes and the maximum gradually moves towards larger diameters back to the same location as in the beginning of the year.

Low precipitation rate together with a dark and stable atmosphere in winter, give the aerosol time to age and grow. From about day 300, when the station is in darkness through the whole day, the main mode shifts from about 100 nm diameter to about 160 nm. This shift in size between fall and winter can almost entirely be explained by coagulation. Figure 2 hows a simulation made with a simple model, where the September distribution was used as the initial distribution and the aerosol then let to age in the model. For each 2 weeks of simulated time a distribution is plotted together with the mean distribution for December. Clearly coagulation explains well the evolution of the aerosol during the fall and early winter when growth by condensation and new particle formation is essentially shut off

That sunlight may play a very important role for the seasonal variation of the aerosol in the Arctic is well illustrated in Figure 3 Here a 7-day running mean of the integral number density from the DMPS system is plotted as function of the year together with the 7-day running mean insolation (measured using a CM11 pyranometer). On a seasonal scale, an increase in the aerosol number density is seen during the arctic spring when the light returns after the polar night. The opposite is true for the fall period when a decrease in sunlight is followed by a decrease in particle number density. During the illuminated period of the year the number density shows large variations, which is characteristic for the polar summer. Kawamura et al., (1996) reported enhanced particle concentrations just after polar sunrise at Alert, Canada, which was attributed to photochemical reactions.

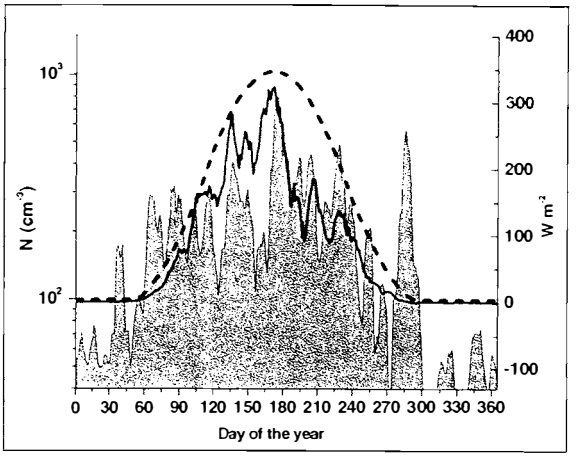

Figure 3 Particle number density as a 7-day running mean gray area (note that data is plotted on a logarithmic scale), and the incoming solar radiation as a 7-day running mean (solid line) and ideal distribution (dashed line).

A closer look at the time series in Figure 3shows that the peak particle number densities are systematically higher during the second half of the polar summer. The somewhat surprising observation is that this enhancement in number density corresponds in time with a relative reduction of the insolation compared to an ideal curve. A reduction in insolation is simply the result of increased cloudiness. Clouds may enhance particle production near the edges of the cloud due to the increased radiative flux by the reflecting clouds. It is not probable that this mechanism is strong enough to affect the entire boundary layer and to influence the daily average number. Clouds may also enhance new particle formation by removing aerosol surface area through scavenging accumulation mode particles (Pruppacher and Jaenicke, 1995). The strong reduction of sulfate mass observed during the summer would be in supported of this mechanism.

However, if preexisting surface area were the controlling parameter for the observed enhancement in particle number densities we would expect an anti-correlation between these two parameters. An analysis show that the relation between number density and aerosol surface are is different for different seasons, but always positive. That is, the number density and surface areas covariates.

A decrease in insolations or increase in cloudiness which coincide with the increased particle number density may be indicative of a change in air mass properties. To investigate this, three-dimensional backwards trajectories where calculated. However, the analysis here gave no strong support for any particular type of air mass being responsible for the enhance particle number density. Bigg (2000) discuss the role of snow on the ground in modulating the emissions from the soil of aerosol precursors from decomposition of organic matter. The process requires liquid water, which means that the strongest contribution would be when the snow cover is melting. A parameter describing the surface conditions is the reflectance. The amount of radiation that is measured from the surface is of course dependent on the amount that is received from above, but it should be possible to distinguish from situations with or without snow cover on the ground. The observed reflectance is plotted in Figure 4atogether with the particle number density as in Figure 3(but on a linear scale).

Clearly the retreating snow cover very well marks the onset of enhanced particle number densities. The change in ambient conditions is also seen in the temperature record presented in Figure 4. The days surrounding day 173 marks the change from sub zero temperatures to a period when the temperature remains steadily above the freezing point. This period lasts until approximately day 250 to 260 when the temperature again move steadily below the freezing point. It is difficult to imagine that the little non-ocean area surrounding the sampling site could generate such large impact on the aerosol measurements from the release of additional precursor gases from the soil.

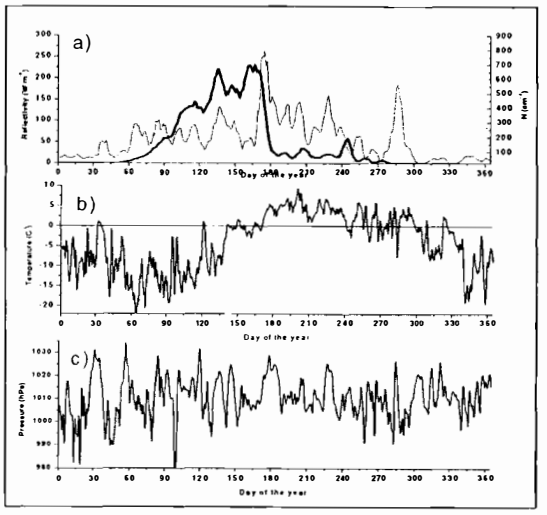

Figure 4 Radiation reflected from the ground presented as a 7-day running mean (thick line) and the particle number density presented as a 7-day running mean a), surface temperature b) and surface pressure c).

The seasonal variation in temperature above and below the freezing point and the melting of the snow in the summer of course occurs elsewhere in the Arctic as well. A potential source region that would fit in time is the Siberian Tundra. Over a very large region the transition from sub zero temperature occurs around the end of May beginning of June. The only currently measured parameter at the Zeppelin station that could be a tracer for such emissions and transport is ammonia. This data shows that the summer months are not the months with the largest amounts of ammonia in the particles but it is the period of the year where there is a noticeable covariation between this species and in particle number density.

Future experiments will be designed to test this hypothesis.

References

Bigg, E.K., 2001. The aerosol in a boreal forest in spring. Tellus 53B, 510-519.

Clement, C.F., Pirjola, L., dal Maso, M., Mäkelä, J.M., Kulmala, M., 2001. Analysis of particle formation bursts observed in Finland. Aerosol Sci., 32, 217-236.

Jokinen, V., Mäkelä, J.M., 1997. Closed-loop arrangement with critical orifice for DMA sheath/excess flow system. J. Aerosol Sci. 28, Issue 4, 643-648.

Kawamura, K., Kasukabe, H., Barrie, L., 1996. Source and reaction pathways of dicarboxylic acids and dicarbonyls in Arctic aerosols: one year of observations. Atmos. Environ., .30 (10/11), 1709-1722.

Pruppacher, H.R., Jaenicke, R., 1995. The processing of water vapor and aerosols by atmospheric clouds, a global estimate. Atmos. Res. 38, 282-295.

Size distributions of aerosol and snow particle in different type airmasses

Makoto Wada*, Hiroyuki Konishi+, Shinji Morimoto* and Takashi Yamanouchi*
*:National Institute of Polar Research, Itabashi-ku, Tokyo, Japan. Email: wada@pmg.nipr.ac.jp, phone +81-3-3962-5580
+:Osaka Kyoiku University, Osaka, Japan. Email: konishi@cc.osaka-kyoiku.ac.jp

1. Introduction

Our group started observations of a precipitation rate, a size distribution of precipitation particles and a size distribution of aerosols larger than 0.3um at Ny-Aalesund, Svalbard in 1998. The observations have several purposes, such as research for seasonal and annual variation of precipitation in a region where measurements of snow precipitation are severe because of drifting snow (wada et al., 1996). One of other purposes is a research for basic formation mechanism of cloud and precipitation with aerosol, cloud nuclei and ice forming nuclei.

Discussions about role of aerosols in cloud are prosperously in climate research field recently(e.g. IPCC, 1990). Observations of aerosol size distribution and species have been carried out at ground and in the atmosphere using aircraft(e.g. Curry, 2001). Observations of cloud condensation nuclei and cloud particles have been also actively in the world(e.g. Raes et al., 2000). Some results(e.g. Hobbs, 1993) show good relations between number density of cloud condensation nuclei and cloud particles. But a relation of number density between aerosol particles and cloud particles is not clear or no relation is reported. Distributions of aerosols and snow particles in a special day are reported and processes forming the size distributions are discussed in this paper. Many meteorological and chemical observations are conducted in other sites of Ny-Aalesund. We are happy if you will analyze your data of same day with comparing to our data.

2. Instruments

Precipitation Occurrence Sensor System(POSS) made by Andrew Inc., Canada can measure precipitation rate and size distributions of precipitation. The POSS is a low power, X-band, bi-static doppler radar with a scattering angle defined by the axis of transmitter and receiver(Sheppard, 1990). A dual frequency microwave radiometer with 23.8GHz and 31.4GHz by Radiometric Co., U.S.A. can measure precipitable water and column liquid water in the atmosphere. The Dasibi Ozone Monitor measures surface ozone

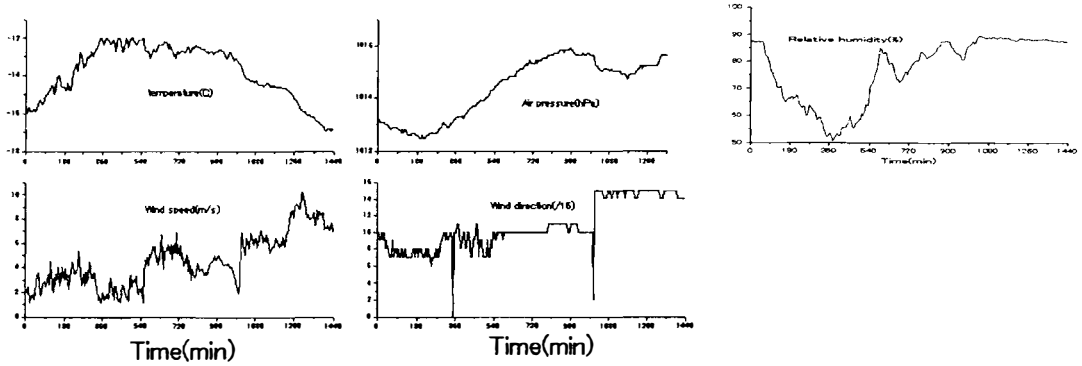

Fig. 1: Basic meteorological data of air temperature, wind speed, , air pressure and wind direction and relative humidity on 9 March 1998.

concentration(Yamanouchi, 1996). Optical particle counter(OPC) by Rion Inc., Japan measures

number densities of aerosols which are larger than 0.3um, 0.5um, 1um, 3um and 5um. A vertical pointing radar records radar echo intensities in the atmosphere. Precipitation rate can also be estimated using the echo intensities. The vertical pointing radar is a X-band pulse radar. Basic meteorological instruments, recording air temperature, relative humidity, atmospheric pressure, wind speed and wind direction, are also installed there.

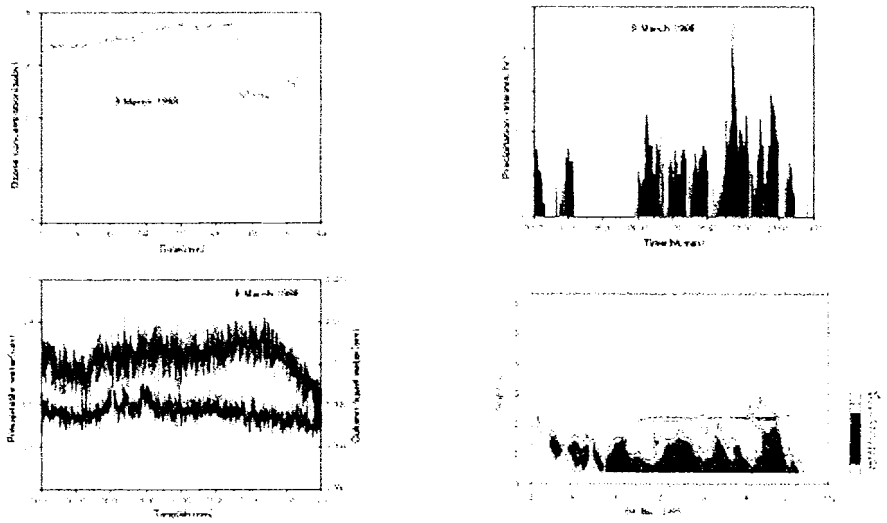

Fig. 2: Ozone concentration, precipitation rate by POSS, precipitable water and column liquid water by dual microwave radiometer and radar echo on 9 March.

Weather charts from Deutscher Wetterdienst and NOAA satellite quicklook images from Dundee University, U.K. are used for examining synoptic condition.

3. Observations and results

A cloud region accompanied by a cyclone came from south went over Svalbard on 9 March 1998. Details of this cloud over sea were reported by Asuma et al.(2002). Basic meteorological data at Ny-Aalesund on 9 March are shown in Fig. 1. Precipitation rate from POSS, radar echo image, precipitable water, column liquid water and surface ozone concentration are also shown in Fig. 2. Viewing from NOAA satellite image Ny-Aalesund was being sometimes covered over by cloud around 03UTC on 9 March. The cloud region passed over Ny-Aalesund between two satellite images at 17:06UTC on 9 March and 2:53UTC on 10 March from west to east. The wind direction and wind speed of basic meteorological data at just before 18:00UTC changes rapidly. Temperature, relative humidity and pressure data also changed at the time.

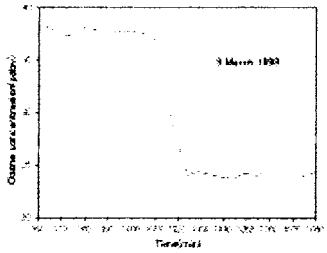

Fig. 3: Ozone concentration from 16:00 to 18:00 on 9 March.

Ozone concentration data, moreover, shows a big depression. But other data, precipitation rate, radar echo, precipitable water and column liquid water show no remarkable change at the time.

Although some items such as precipitable water did not change, items of basic meteorological data suggests a change of airmass at just before 18:00UTC. Especially big depression of ozone concentration supports the difference of airmasses before and after the time. Figure 3 shows an enlarged graph of ozone concentration. The big depression, about 13ppm, occurred between 16:49UTC(1009) and 17:04UTC(1024). Since it is thought that two different airmasses covered over Ny-Aalesund before and after the above period, size distributions of snow particles by POSS and of aerosols by OPC are investigated between 16:30UTC and 17:12UTC, when includes the above period. Figure 4 shows the both size distributions. The size distributions of snow particles show that snow particles after 16:52UTC are relatively larger than those before 16:51UTC. The size distributions of aerosols show that aerosol particles after 16:52UTC are more than those before 16:52UTC and the tendency is stronger in large size than in small size.

4. Discussion

Surface wind direction changed from SW to NNW at 16:50UTC as shown in Fig. 2. A

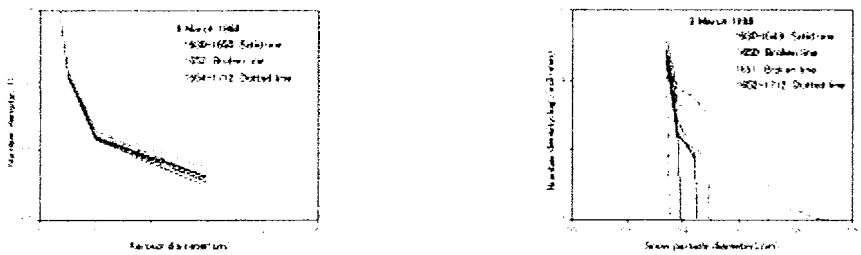

Fig. 4: Size distribution of aerosols and snow particles.

southerly wind generally conveys a warm air to Ny-Aalesund and a northerly wind conveys a cold air there. But air temperature change was not strong, only 2 degrees decrease from -12C to -14C. Average precipitable water did not change between 16:00UTC and 18:00UTC, though many noisy fluctuations were found in the data. This results would suggest that two airmasses did not connect directly with a strong cyclone which conveys a warm air from mid latitude. An airmass before 16:50 is named as a 1st airmass and an airmass after 16:50 is named as a 2nd airmass.

Snow particles less than 0.5 mm only were formed in the 1st airmass and ones bigger than 0.5 mm were found in the 2nd airmass only. The 1st airmass contained less aerosol concentration than the 2nd one. The fact is found strongly in large size aerosols. A size distribution of snow particles is related to many processes such as vertical motion, condensation/sublimation process from water vapour to cloud/ice particles, aerosol concentration and so on in a developing stage of precipitation. Downward motion affects a size distribution not only of snow particles, but also of aerosols, for example collision and coalescence processes between different size particles by gravitational falling, a washout process of aerosols by precipitating particles and so on in a developed stage.

Since the precipitation rate in the two airmasses did not show a big difference, the difference of size distributions of aerosol would be occurred in a developing stage. Collision and coalescence processes in a developed stage would not be important as precipitation rate was weak, less than 0.5 mm/hr. The size distributions of snow particles and aerosols would be brought up in a forming stage of cloud and/or a developing stage from cloud to snow.

5. Summary

Analyzing the observation data on 9 March 1998 obtained at Ny-Aalesund, we found two type of airmasses in which size distributions of snow particles were different. It is found that the size distributions of aerosols was also different in the two airmasses. Cloud formation or precipitating processes in the two different airmasses would contribute to the two types of size distributions of snow particles and aerosols.

References

Asuma Y., Fukuda, Y., Kikuchi, K., Shiobara, M., Wada, M. and Moore G.W.K., 2002: Airborne measurements of a polar low over the Norwegian Sea(in Japanese). *Antarctic Record, 46 1A*, in printing.

Curry, J.A., 2001: Introduction to special section: FIRE Arctic Clouds Experiment. *J. Geophy. Res., D14, 106,* 14985-14987.

Hobbs P.V., 1993: Aerosol-cloud interactions. In Aerosol-cloud-climate interactions. Edited by P.V. Hobbs. *Academic Press*, 33-73.

IPCC, 1990: Climate change. Edited by Houghton J.T., Jenkins G.J. and Ephraums J.J., *Cambridge Univ. Press,* 364p.

Raes, F., Bates, T., McGovern, F. and Liedekerke, M.V., 2000: The 2nd aerosol characterization experiment(ACE-2): general overview and main results. *Tellus, 52B,* 111-125.

Sheppard, B. E., 1990: Measurement of raindrop size distributions using small doppler radar. *J. Atmospheric and Oceanic Tech., 7,* 255-268.

Wada, M., Konishi, H. and Yamanouchi T., 1996: Variation of monthly precipitation and frequency of radar echo existence at some altitudes in Ny-Aalesund, Svalbard, Arctic. *Mem. Natl Inst. Polar Res. Spec Issue, 51*, 239-246.

Yamanouchi, T., Aoki, S., Morimoto, S. and Wada, M., 1996: Report on atmospheric science observations at Ny-Aalesund, Svalbard. *Proc. Int. Symp. Env. Res. in the Arctic*, 153-163.

A polar cloud analysis using ground-based Micro-pulse Lidar data

Masataka Shiobara, Masanori Yabuki & Hiroshi Kobayashi

National Institute of Polar Research, Tokyo 173-8515, Japan.
E-mail: shio@nipr.ac.jp, phone +81 3-3962-4740
Center for Environmental Remote Sensing, Chiba University, Chiba 263-8522, Japan.
E-mail: yabuki@ceres.cr.chiba-u.ac.jp, phone +81 43-290-3852
Department of Ecosocial System Engineering, Yamanashi University, Japan
E-mail: koba@js.yamanashi.ac.jp, phone +81 55-220-8341

In order to acquire long-term data sets of back-scatter profiles of clouds and aerosols in polar regions, we started Micro-pulse Lidar (MPL) measurements at Ny-Alesund, Svalbard in March 1998 and at Syowa Station, Antarctica in January 2001. Fine structures of clouds and their temporal change were observed by MPLs with a 30-m range resolution and a 1-min time average. Statistical features of the cloud base height were investigated from the Arctic and Antarctic measurements. These results from preliminary analysis for limited cloud climatology based on the MPL data from Ny-Alesund and Syowa will be shown in this paper.

Introduction

Clouds play an important role in radiation balance of the global climate system. Especially climatology of cloud physical parameters such as the cloud optical thickness, cloud base and top heights, cloud appearance and amount is essential for climate research. However, it is generally known that detection of polar clouds is difficult from satellite-borne passive sensors. Also ground-based observations of clouds are spatially limited particularly in the polar regions, and sometimes the reliability is not enough. Therefore cloud observations using active sensors like lidars and radars are needed.

The National Institute of Polar Research (NIPR) promotes atmospheric research in both Arctic and Antarctic regions. In the Arctic, NIPR has started an international program for aerosol-cloud-radiation studies based at Ny-Alesund (78° 56' N, 11° 52' E, 40m a.s.l.), Svalbard. For ground-based remote-sensing and in-situ measurements, NIPR has placed cloud and aerosol observation systems, including a Micro-pulse Lidar (MPL), at the Rabben Observatory, a Japanese research base in Ny-Alesund. Also in Antarctica, the MPL measurement at Syowa Station (69° 00' S , 39° 35' E, 30m a.s.l.) started in January 2001 as part of the 42nd Japanese Antarctic Research Expedition (JARE 42) activity. Based on preliminary analysis of the MPL data, the performance of MPLs for cloud measurements and statistical features of polar clouds from Arctic and Antarctic measurements will be shown and discussed in this paper.

Measurements

Micro-pulse Lidar (MPL) is an eye-safe maintenance-free lidar system that has been originally developed by Spinhirne (1993) in order to acquire long-term datasets of backscatter profiles of aerosols and clouds. MPLs with the same concept and design as the Spinhirne's original are commercially available from SESI, USA and employed for Arctic and Antarctic measurements in this study. MPLs use a diode-pumped Nd:YLF laser of which wavelength is 523 nm. The telescope of MPL for laser transmission and return signal receiver is declined at 45 degrees (but 34 deg until December 2001 in Ny-Alesund) from zenith and looking up through a glass window of the observatory building. The full-time basis measurement is acquired with a 30-m range resolution and a 1-min averaging interval for normal operations. Data from Ny-Alesund are transferred by ftp via Internet, and the status of measurements is monitored in Japan. Although the measurement at Ny-Alesund started in 1998, the data have not been acquired very much due to its hardware troubles. Real time data from the Antarctic MPL is not available because the Internet is not always accessible to Syowa Station and the data line via satellite is still narrow between Japan and Antarctica.

Results and discussion

Fine structure of ice clouds

Figure 1 shows a time series plot of the range-corrected backscatter signal from ice clouds observed at Syowa Station on 19 January 2001. On that day, it was almost overcast by cirrus and cirrostratus clouds. The MPL detected not only the cloud base but also the cloud top since clouds were optically thin. Temperatures at the cloud top and base were -40℃and –25℃, respectively. Relative humidity measured by radiosondes was saturated for ice in the cloud layer, but extremely low in the lower troposphere under the cloud base. The result in the figure shows that ice crystals growing and falling in the cloud layer vanished at the cloud base by evaporation. Falling speed of ice crystals was estimated to be around 1 m/s from the slope of many bright lines in the cloud layer. This speed suggests the existence of large snow crystals to be formed from small ice crystals in the cloud.

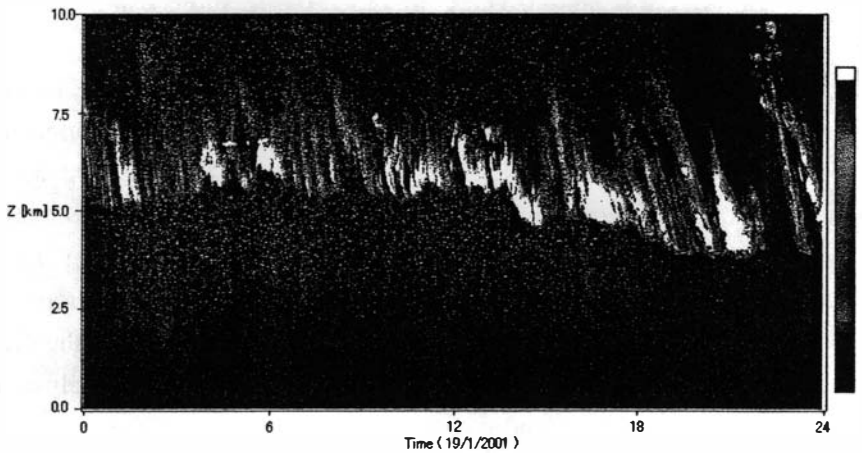

Fig. 1. An example of fine structure measurements of clouds. Time series of backscatter signals are plotted for 19 January 2001 at Syowa Station, Antarctica.

Statistics of cloud base hight

The SESI MPL data acquisition software includes the cloud base height (CBH) analysis with Campbell's algorithm (Campbell et al., 2002) in real time basis and records CBHs as well as backscatter signal. Figure 2 shows the monthly frequency of the CBH appearance in July – December 1999 (left panel) and in March – July 2002 (right panel). Though it may be difficult to discuss on the CBH climatology from these limited statistics, general features can be seen as follows: Low clouds in the Arctic boundary layer with CBHs below 2km are dominant in summer and early autumn. Clear sky days are not expected in this season. On the other hand, frequency of clear sky days is relatively high and higher clouds are rather dominant in late autumn to spring.

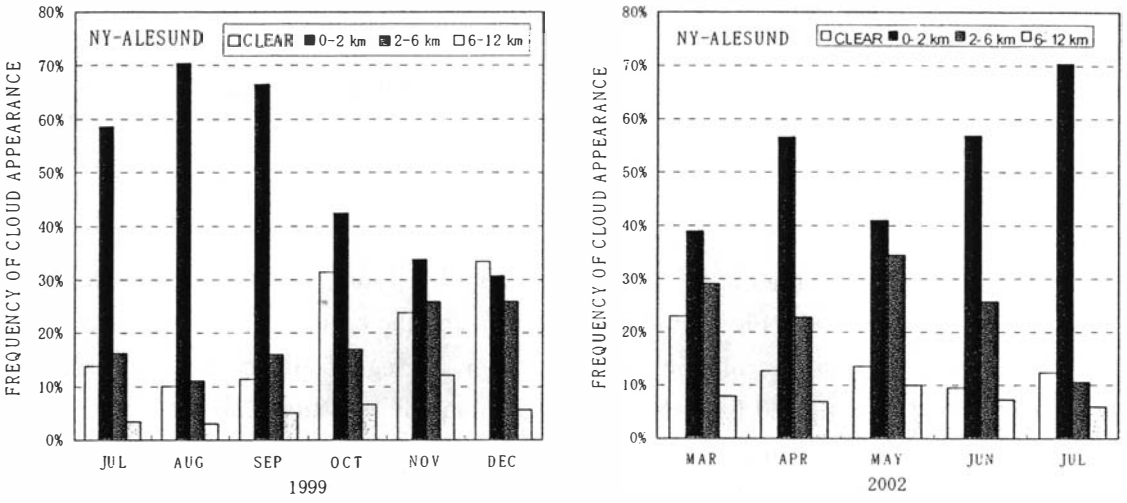

Fig.2. Monthly statistics of frequency of cloud appearance with CBH of 0-2 km, 2-6 km, and 6-12 km height at Ny-Alesund in July – December 1999 (left) and March – July 2002 (right).

Classification of thin/thick clouds

Penetration of laser beam through clouds is diagnosed by analyzing return signals. Figure 3 shows an example of classification of thin and thick clouds over Syowa Station based on the penetration analysis. In this classification, "thin" or "thick" means whether the laser has passed through the cloud layer or not. From the figure, it can be seen that thin clouds at high altitude, i.e., cirrus like clouds are rather dominant in winter. On the other hand, in summer thin clouds are likely to appear in low altitude. Generally speaking, the laser cannot penetrate clouds when the cloud optical thickness is larger than about 2. However, more precise and exact analysis of laser penetration is needed for quantitative discussion on the cloud optical thickness. Also the multiple scattering effect of laser in clouds should be taken into account.

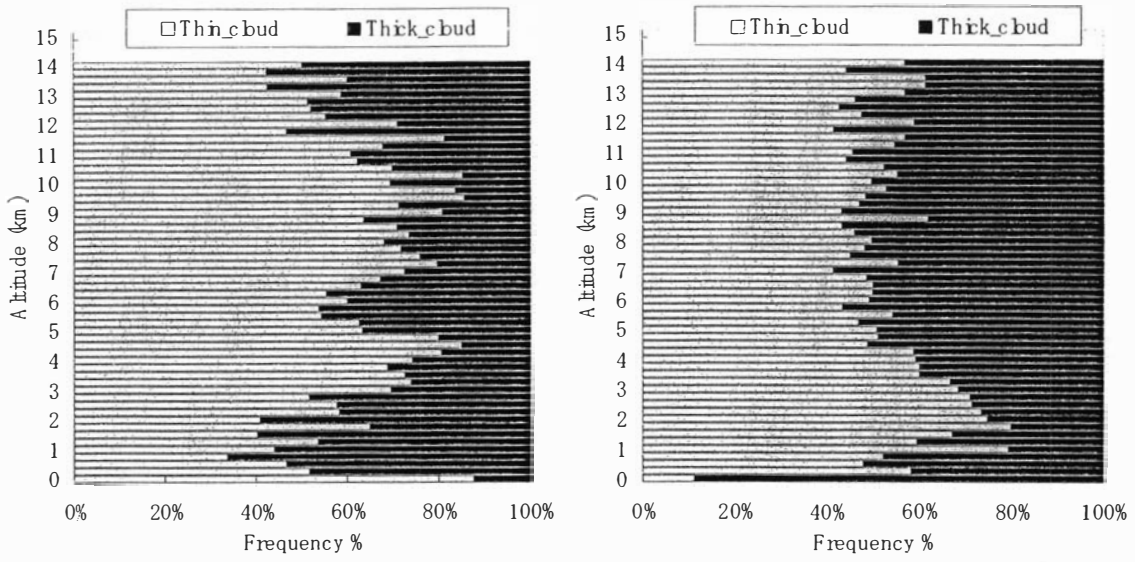

Fig. 3. Classification of relatively thin and thick clouds by examining penetration of lidar signals for July 2001(left panel) and December 2001(right panel) at Syowa Station, Antarctica.

Summary

MPL measurements started at Ny-Alesund, Svalbard in March 1998 and at Syowa Station, Antarctica in January 2001. Fine structures of clouds and their temporal change were observed by MPL with a 30-m range resolution and a 1-min time average. Statistical features of the cloud base height were investigated from the Arctic and Antarctic measurements. Results from MPL measurements at Ny-Alesund, Svalbard showed seasonal variation of cloud appearance and cloud base height. Long-term data sets from the MPL measurements will contribute to the polar cloud climatology for climate research.

Acknowledgments

Helpful advices and technical support for MPL measurements were provided by J.D. Spinhirne and his colleagues at NASA/GSFC. Operations of MPL at Ny-Alesund were helped by Are Baecklund of Norwegian Polar Institute. The Antarctic MPL measurement was supported by JARE 42.

References

Campbell, J.R., D.L. Hlavka, E.J. Welton, C.J. Flynn, D.D. Turner, J.D. Spinhirne, V.S. Scott, III, and I.H. Hwang (2002): Full-time, eye-safe cloud and aerosol lidar observation at Atmospheric Radiation Measurement program sites: Instruments and data Processing. *J. Atmos. Oceanic Tech.*, 19, 431-442.

Shiobara, M., 2000: Arctic cloud and aerosol observations using a Micro-pulse Lidar in Svalbard. *Proc. 1st Int'l Workshop on Spaceborne Cloud Profiling Radar, Tsukuba, Japan, 24-26 January 2000,* 179-182.

Spinhirne, J.D., 1993: Micro pulse lidar. *IEEE Trans. Geosci. Remote Sens.*, 31, 48-55.

The Zeppelin Station – an overview of NILU's research activities and some results

Chris Lunder, Ove Hermansen, Norbert Schmidbauer, Torunn Berg, Stein Manø, Christian Dye, Martin Schlabach

Norwegian Institute for Air Research (NILU), P.O. Box 100, N-2027 Kjeller, Norway. E-mail: Chris.Lunder@nilu.no , phone + 47 63 89 80 00

Background

NILU is responsible for the scientific programmes at the Zeppelin Station and co-ordinating the scientific activities undertaken by NILU and other institutions, as well as a number of international research groups' campaigns. MISU (Department of Meteorology at Stockholm University) co-operates closely with NILU in developing the scientific activities and programmes at the station. The Zeppelin Station is owned and operated by Norwegian Polar Institute The monitoring and research programmes address several issues, such as: climate change, arctic stratospheric ozone layer depletion, global distribution of toxic pollutants, distribution of radioactive contaminants.
The Zeppelin activities contribute to regional, national and global monitoring networks such as European Monitoring and Evaluation Programme (EMEP), Network for detection of Stratospheric Change (NDSC), Global Atmospheric Watch (GAW) and Arctic Monitoring and Assessment Programme (AMAP)

Activities handled by NILU:

Greenhouse gases

NILU has for several years measured greenhouse gases at Zeppelin Station. Modern instruments as Gas Chromatograph (GC) and GC coupled with a mass spectre detector (GC-MS) monitor the most important greenhouse gases from hour to hour. These instruments measure methane, carbon mono oxide, ozone and industry related greenhouse gases containing fluorine, chlorine and bromine. Hydrocarbons and aldehydes are sampled and analysed at NILU.

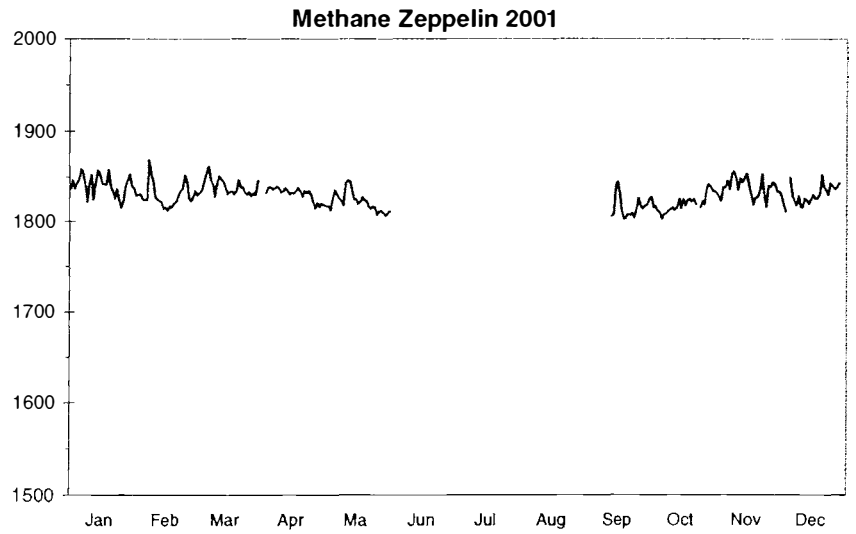

Figure 1: Plot of methane data - 2001.

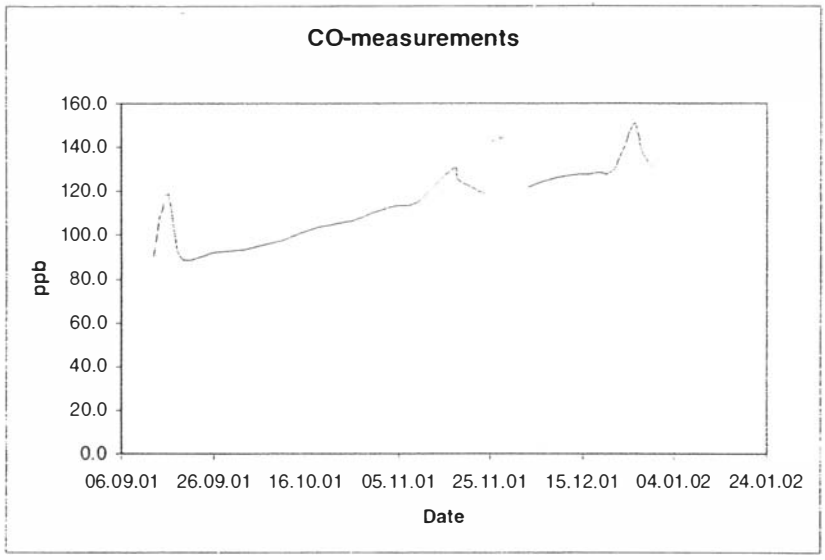

Figure 2: Plot of CO measurements late 2001, showing small episodes 16th Sep and 26th Des

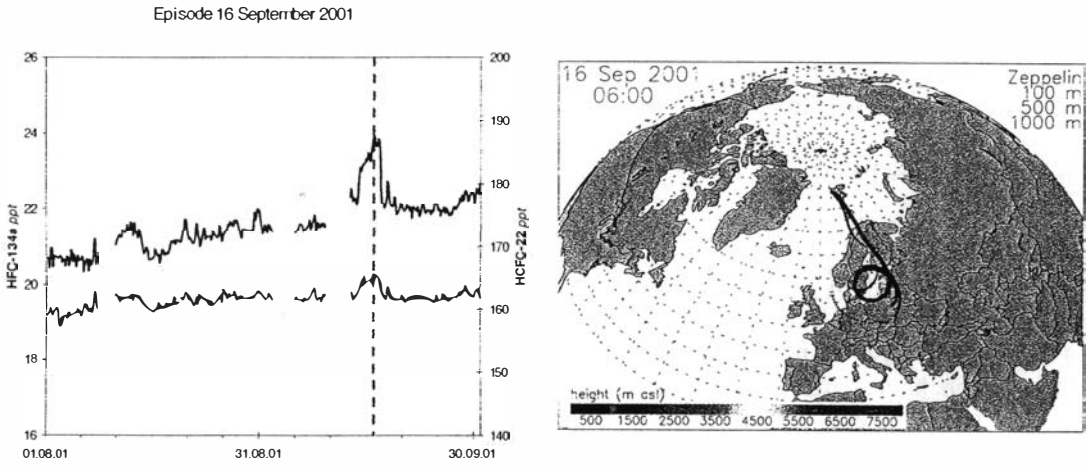

Figure 3: Measurements of HFC-134a and HFC-22 during an episode of polluted air transported from the continent 16 September 2001

POP's

For the last 20 years NILU has carried out research on persistent organic pollutants (POPs) and heavy metals in the Arctic; since 1993 this has been done on routine basis at Zeppelin Station. The results are reported to AMAP.

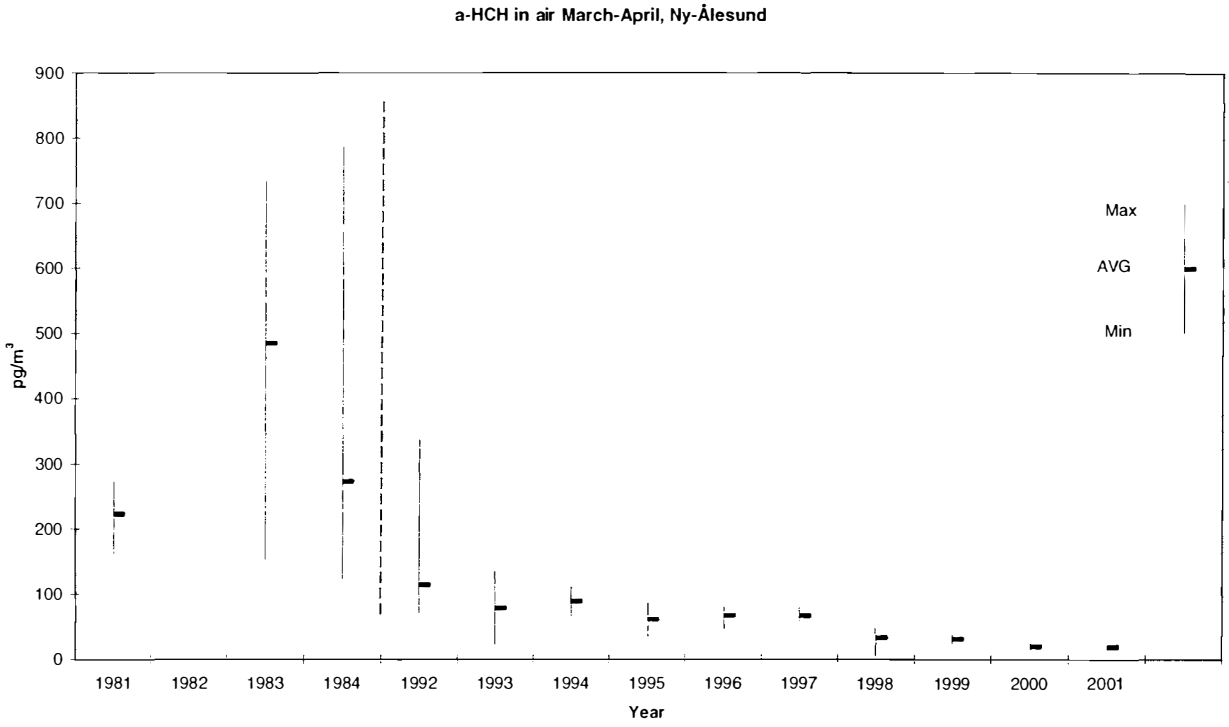

Figure 4: α-HCH in air (March – April) from 1981 – 2001 at Ny-Ålesund

Decrease in α-HCH concentration from early 80's until today is caused by replacement of use of technical HCH (65-70% α-HCH) to lindan (>99% γ-HCH) as pesticide.

Inorganic components in air and precipitation

Since 1974 NILU has measured concentrations of sulphur components in the air in Ny-Ålesund. Measurements of inorganic components in precipitations started in 1981. Today the measurements are included in the EMEP programme. SO_2, SO_4^{2-}, (NO_3^-+ HNO_3) and (NH_4^+ + NH_3) are measured in air and 10 parameters in precipitations.

Stratospheric ozone

NILU has instruments that measure ozone thickness and some of the chemical compounds destroying ozone. The instrument use optical methods to discern the attenuation of solar radiation through the atmosphere. The reduction of the ozone layer is a concern mainly because ozone shelters the Earth's surface from harmful ultraviolet (UV) radiation, which is also measured at ground level.

Heavy metals

With a mercury monitor gas phase mercury is observed during the year and results are reported to AMAP. Other heavy metals as As, Cd, Co, Cr, Cu, Pb, Mn, Ni, V, Z are trapped on filters.

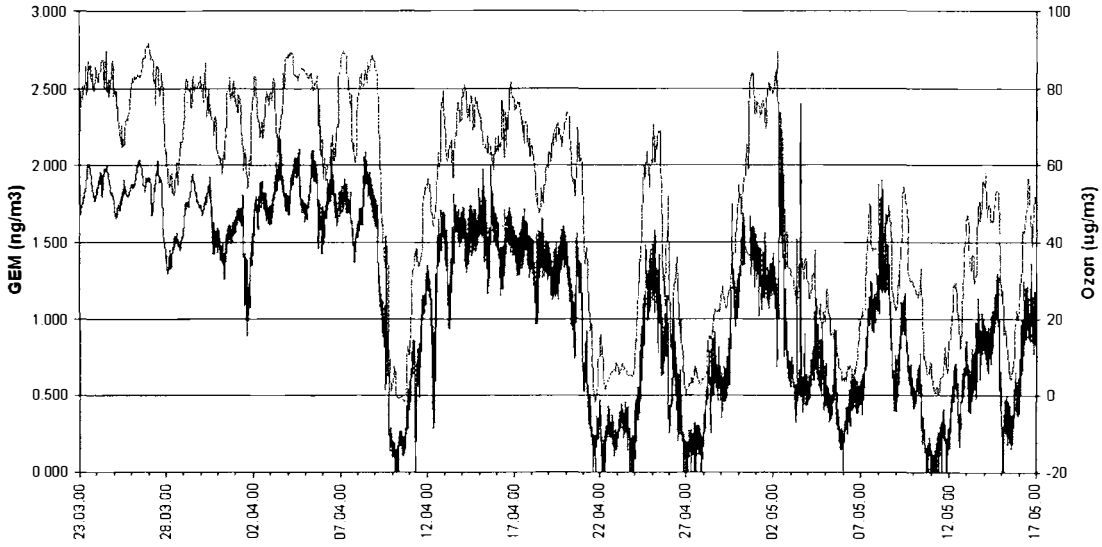

Figure 5: Mercury and ozon (ground level, 474 m.a.s.l) concentration at Zeppelin Station spring 2000

During spring of 2000 there were several episodic depletions in mercury vapour concentrations correlating well with the depletions of surface ozone, during the three-month period following polar sunrise. Highly variable concentrations of the mercury vapour and ozone concentrations are seen following polar sunrise, with a pronounced tendency towards unusually low concentrations.

Activities handled by MISU:

CO_2

MISU maintains a continuous infrared CO_2 instrument on Zeppelin Mountain. The continuous data are enhanced by weekly flask sampling programmes in co-operation with other institutions. The flask data give CO_2, ^{13}C, ^{18}O, CH_4 and CO data.

Particles

MISU has several instruments at Zeppelin Station which measure particles in the atmosphere. Aerosol particles tend to reflect light and can therefore alter Earth's radiation balance. The optical particle counter (OPC) operated by MISU gives the concentration of aerosol particles and, combined with data from the nephelometer, clues to the particles' age and origin. Size distribution is acquired from a differential mobility analyser (DMA).

Other international institutes / projects:

Radon-isotope

University of Heidelberg in co-operation with MISU has for some years used a monitor to measure the radon^{222} isotope.

Lead isotope

Finnish Meteorological Institute (FMI) has for almost the last 2 years sampled Pb-isotopes on filters.

Black carbon

Inst. for Nuclear Technology - Radiation Protection, Greece has for almost the last 2 years sampled black carbon using a Aethalometer.

LEAD-210 CONCENTRATION IN THE AIR AT Mt. ZEPPELIN, NY-ÅLESUND, SVALBARD

Jussi Paatero[1], Juha Hatakka[1], Kim Holmén[2] and Yrjö Viisanen[1]

1. Finnish Meteorological Institute, Air Quality Research
Sahaajankatu 20E, FIN-00810 Helsinki, Finland, e-mail: Jussi.Paatero@fmi.fi

2. Department of Meteorology, Stockholm University
S-106 91 Stockholm, Sweden, e-mail: Kim@misu.su.se

Introduction

During the past three decades, there has been increasing interest in the presence of airborne pollutants in the Arctic region. However, the interpretation of the results has suffered from the lack of data concerning the atmospheric and coupled oceanic/atmospheric transport processes in the area. In this project we have measured concentration of lead-210 (^{210}Pb) in the air at Ny-Ålesund, Svalbard. The data on atmospheric ^{210}Pb can be used as a tracer to help to identify natural, e.g. due to the North Atlantic Oscillation (NAO), and anthropogenic variations in the transport behaviour of air masses and thus also air pollutants in the Arctic region.

Lead-210 is formed in the atmosphere from the radioactive noble gas radon-222 (^{222}Rn) emanating from the Earth's crust. 99 % of the airborne ^{222}Rn originates from land and only 1 % from the sea (Baskaran et al. 1993). Owing to the long half-life (22 years) of ^{210}Pb, its removal from the atmosphere is governed by the different scavenging processes affecting the aerosol particles carrying it rather than radioactive decay. Based on the activity ratio of ^{210}Pb and its progeny, mean aerosol residence times of one to two weeks have been obtained (Mattsson 1975; Papastefanou & Bondietti 1991).

Preiss et al. (1996) have reviewed the publications of ^{210}Pb activity concentrations in the air. High ^{210}Pb concentrations are found in continental air masses. Lead-210 has been used as a tracer for particle-bound sulphate because they are both secondary aerosols, i.e. produced in the atmosphere from their gaseous precursors ^{222}Rn and SO_2, respectively (Turekian et al. 1983; Mattsson et al. 1993).

Recently it was discovered that the several-year oscillation of the ^{210}Pb activity concentrations in the air in Southern Finland is connected to the state of the northeastern part of the Atlantic Ocean. Low ^{210}Pb activity concentrations are associated with the more frequent arrival of maritime air masses in Finland. On the other hand, high ^{210}Pb concentrations are associated with the more frequent presence of continental air masses. Higher amounts of warm and saline water in the North Atlantic Ocean are closely connected to enhanced cyclonic activity and low ^{210}Pb air concentrations in Finland (Mattsson et al. 1996a; Paatero et al. 1998; Paatero et al. 2000).

Materials and methods

The sampling site was at Mt. Zeppelin Global Atmosphere Watch (GAW) station, Ny-Ålesund, (78°58´ N, 11°53´ E), on the west coast of Spitsbergen, the largest island in the Svalbard archipelago (NILU 2002; WMO 2002). The station is located 474 m above sea level.

High-volume aerosol particle samples were collected onto glass fibre filters (Munktell MGA). The sampler is made of stainless steel. The flow rate is ca. 120 m^3/h and it is measured with a pressure difference gauge over a throat. Three samples per week were collected with filter changes on Mondays, Wednesdays, and Fridays. The sampling programme was started in December 2000. One out of 25 filters is left unexposed and is used as a field blank sample.

Lead-210 activity concentration results of two stations in Finland were used for comparison. Nurmijärvi (60°30'N, 24°39'E, h = 105 m above sea level [a.s.l.]) is in southern Finland 40 km north of the Baltic sea coast. Sodankylä (67°22'N, 26°39'E, h = 178 m a.s.l.) is in central part of northern Finland.

The exposed filters together with field blanks were assayed for lead-210 six months after the sampling with an automatic alpha/beta analyser (Mattsson et al., 1996a). The measurement is based on the alpha counting of the in-grown daughter nuclide polonium-210. Background samples (unexposed filters) and reference samples (^{242}Pu, ^{90}Sr and ^{55}Fe) are measured daily.

Results and discussion

The observed ^{210}Pb activity concentrations at Mt. Zeppelin, Ny-Ålesund, Svalbard vary between 11 and 620 µBq/m³ (Fig. 1). A Japanese research group observed ^{210}Pb activity concentrations ranging from 83 to 1204 µBq/m³ and an average concentration of 325 µBq/m³ at Ny-Ålesund in February-March 1995 (Suzuki et al. 1996), in agreement with this study. They also reported aerosol residence times ranging from 26 to 78 days based on the ^{210}Po/^{210}Pb activity ratio. These values are much higher compared to studies made in USA and Finland, where the residence times have usually been one to two weeks (Mattsson 1975; Papastefanou & Bondietti 1991; Balkanski et al. 1993). Samuelsson et al. (1986) reported an average concentration of 75 µBq/m³ in July-September 1980 between the 75th and 83rd latitude north and between Greenland and Frans Josef Land.

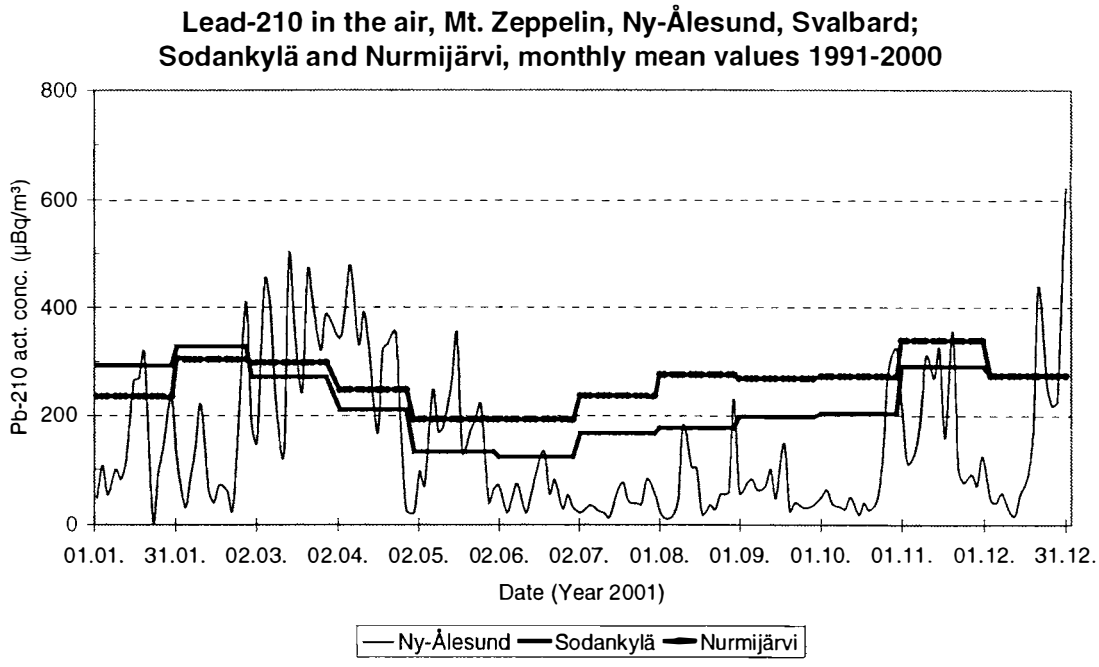

Figure 1. ^{210}Pb activity concentration (µBq/m³) in the air at Mt. Zeppelin GAW station, Ny-Ålesund, Svalbard in 2001 and monthly mean values at Nurmijärvi and Sodankylä, Finland 1991-2000.

The lowest ^{210}Pb concentrations are found in summer both at Svalbard and in Finland. The concentrations are lower at Svalbard than in Finland because Svalbard is further away from the source regions of ^{210}Pb, i.e. continental areas. The highest concentrations occur in March...April at Svalbard. This differs from the seasonal behaviour of ^{210}Pb in Finland, where the highest concentrations are usually observed in February...March. This one month difference between Svalbard and Finland may be related to the strength of solar radiation and its capability to cause vertical mixing of the air. However, the results from Finland are 10-year averages, but individual years, especially winters, can differ considerably from an "average year". In Finland the wintertime ^{210}Pb activity concentrations seem to follow more or less the North Atlantic Oscillation (more westerly winds bringing more frequently maritime air masses with a low ^{210}Pb concentration or more easterly winds bringing more frequently continental air masses with a high ^{210}Pb concentration) (Paatero et al. 2000). Earlier it has been shown that in winter the air masses coming from Arctic regions to northern Finland contain relatively high amounts of ^{210}Pb (Paatero & Hatakka 2000). This was attributed to the small amount of precipitation, reduced air chemistry and stagnant mixing conditions in the troposphere during the Arctic night. These factors increase the aerosol residence time and thus the accumulation of ^{210}Pb into the air.

The 25, 50, and 75 % percentiles of the ^{210}Pb activity concentrations at Mt. Zeppelin are 42, 83, and 220 μBq/m³ (Fig. 2). The values are clearly lower than at Sodankylä with corresponding values of 100, 170, and 270 μBq/m³. The arithmetic mean concentrations in 2001 were 144 and 245 μBq/m³ at Mt. Zeppelin and Sodankylä, respectively.

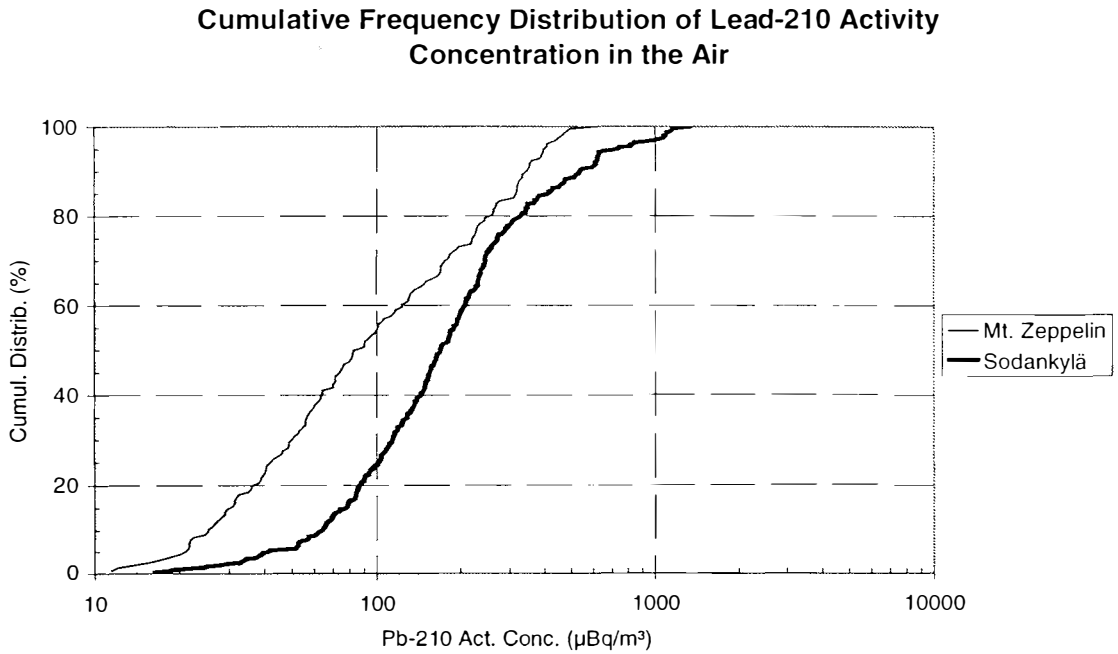

Figure 2. Cumulative frequency distribution of ^{210}Pb activity concentrations at Mt. Zeppelin, Svalbard and Sodankylä, northern Finland in 2001.

The future work will include the comparison of the ^{210}Pb observations to e.g. sulphate, black carbon and aerosol particle concentrations and studies on the relation between ^{210}Pb and various meteorological parameters.

Acknowledgements

The authors would like to thank the Norwegian Polar Institute and the Norwegian Institute for Air Reasearch for a pleasant cooperation. We are also indebted to Kings Bay AS for logistical support. The financial support of the Ny-Ålesund LSF Project, European Community – Access to Research Infrastructure action of the Improving Human Potential Programme is gratefully acknowledged.

References

Baskaran, M., Coleman, C.H. & Santschi, P.H. 1993. Atmospheric Depositional Fluxes of ^{7}Be and ^{210}Pb at Galveston and College Station, Texas. *Journal of Geophysical Research* 98(D11), 20555-20571.

Mattsson, R. 1975. *Measurements of ^{210}Pb, ^{210}Bi and ^{210}Po in Urban and Rural Air in Finland. Finnish Meteorological Institute Contributions No. 81.* Finnish Meteorological Institute.

Mattsson, R., Hatakka, J., Paatero, J. & Reissell, A. 1993. The variations and trends of the particle-bound sulphur in the ground level air in Finland during the last 30 years. *Report Series in Aerosol Science No. 23.* Pp. 159-165. Helsinki: Finnish Association for Aerosol Research.

Mattsson, R., Hatakka, J. & Paatero, J. 1996a. Analysis of Long-term Air Quality Trends and Variations in Northern Europe. In Kulmala, M. and Wagner, P.E. (Eds.). *Nucleation and Atmospheric Aerosols 1996.* Pp. 695-698. Oxford: Elsevier.

Mattsson, R., Paatero, J. & Hatakka, J. 1996b. Automatic alpha/beta analyser for air filter samples - absolute determination of radon progeny by pseudo-coincidence techniques. *Radiation Protection Dosimetry* 63(2), 133-139.

NILU 2002. *http://www.nilu.no/niluweb/services/zeppelin.*

Paatero, J. & Hatakka, J. 2000. Source Areas of Airborne ^{7}Be and ^{210}Pb Measured in Northern Finland. *Health Physics* 79(6), 691-696.

Paatero, J., Hatakka, J., Mattsson, R., Aaltonen, V. & Viisanen,Y. 2000. Long-term Variations of Lead-210 Concentrations in Ground-Level Air in Finland: Effects of the North-Atlantic Oscillation. In Midgley, P. M., Reuther, M. & Williams, M. (Eds.), *Transport and Chemical Transformation in the Troposphere: Proceedings of the EUROTRAC-2 Symposium 2000.* Pp. 322-324. Berlin: Springer-Verlag. CD-ROM.

Paatero, J., Hatakka, J., Mattsson, R. & Viisanen, Y. 1998. Analysis of daily ^{210}Pb air concentration in Finland, 1967-1996. *Radiation Protection Dosimetry* 77(3), 191-198.

Papastefanou, C. & Bondietti, E.A. 1991. Mean Residence Times of Atmospheric Aerosols in the Boundary Layer as Determined from ^{210}Bi/^{210}Pb Activity Ratios. *Journal of Aerosol Science* 22(7), 927-931.

Preiss, N., Mélières, M.-A. & Pourchet, M. 1996. A compilation of data on lead 210 concentration in surface air and fluxes at the air-surface and water-sediment interfaces. *Journal of Geophysical Research* 101(D22), 28847-28862.

Samuelsson, C., Hallstadius, L., Persson, B., Hedvall, R., Holm, E. & Forkman, B. 1986. ^{222}Rn and ^{210}Pb in the Arctic Summer Air. *Journal of Environmental Radioactivity* 3, 35-54.

Suzuki, T., Nakayama, N., Igarashi, M., Kamiyama, K. & Watanabe, O. 1996. Concentrations of 210Pb and 210Po in the atmosphere of Ny-Ålesund. Svalbard. *Memoirs of National Institute of Polar Research No. 51.* Pp. 233-237. Tokyo: National Institute of Polar Research.

Turekian, K.K., Benninger, L.K. and Dion, E.P. 1983. ^{7}Be and ^{210}Pb total deposition fluxes at New Haven, Connecticut and Bermuda. *Journal of Geophysical Research* 88, 5411-5415.

WMO 2002. *http://www.wmo.ch.*

Study of the exchange of reactive gases between the snowpack and the atmosphere at Ny-Ålesund

Florent Dominé, Jean Luc Jaffrezo, Stephan Houdier, Christophe Ferrari,

Michel Legrand

CNRS, Glaciology Laboratory (LGGE), BP 96, 38402 St Martin d'Hères cedex, France. E-mail: florent@lgge.obs.ujf-grenoble.fr , Phone: (33) 476 82 42 69

The snowpack: a multiphase photochemical reactor

Recent field campaigns in the Arctic and Antarctic have revealed the considerable impact of the snowpack on the chemistry of the lower troposphere (Dominé and Shepson, 2002). Beside the episodical complete destruction of ozone in coastal areas that was documented over a decade ago (Barrie et al., 1988), these new campaigns have shown that the presence of the snowpack resulted in:

- Concentrations of nitrogen oxides NO_x (= NO + NO_2) enhanced by over an order of magnitude (Honrath et al, 2002).
- Concentrations of HONO enhanced by about an order of magnitude (Zhou et al., 2001).
- Concentrations of OH radicals enhanced by about an order of magnitude (Mauldin et al., 2001).
- Increased concentrations of light aldehydes HCHO and CH_3CHO (Grannas et al., 2002).
- Reduced concentrations of elemental mercury (Steffen at al., 2002).

One of the driving forces for these perturbations appears to be the photolysis of the nitrate ion, NO_3^-, contained in snow (Figure 1). Photolysis products include OH, HONO and O_3. HONO is itself readily photolyzed into OH and NO. Thus OH and O_3 produced in the snowpack can oxidize organic compounds contained in the snow, and that can be either adsorbed, dissolved, or in the form of atmospheric aerosols deposited on the surface of snow crystals. It is currently though that aldehydes emitted by the snowpack are in part produced by such in-snowpack oxidation.

The snowpack can therefore be considered as a multiphase photochemical reactor. Nitrate photochemistry is but one example of the

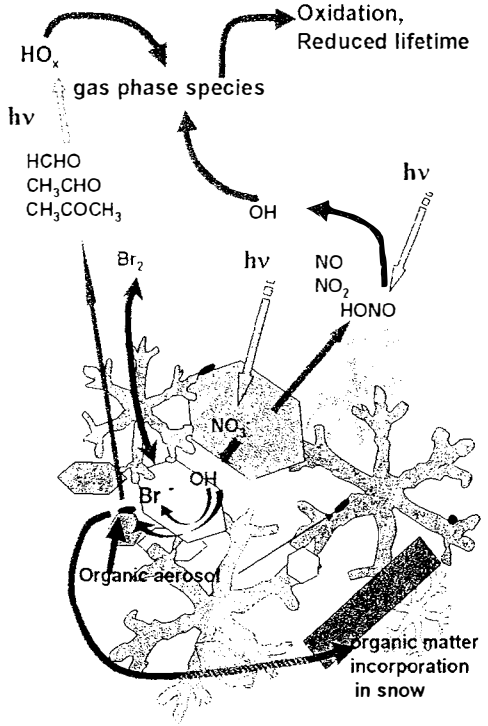

NO_3^- + hν → NO_2^- + $O(^3P)$
+ hν → NO_2 + O^-
O^- + H^+ → OH
NO_2^- + H^+ → HONO
NO_2^- + hν → NO + O^-
$O(^3P)$ + O_2 → O_3
$O(^3P)$, OH, O_3 + DOM → carbonyl compounds

Figure 1. *Effects of the photolysis of the nitrate ion, NO_3^-, contained in snow. Photolysis products, and especially OH, can lead to the oxidation of various compounds contained in snow.*

numerous reactions that can take place there. Photolyzable bromine, in the form of Br_2 or BrCl, can also be produced (Foster et al., 2001) and initiate ozone destruction episodes. However, at present, it is difficult to model snowpack processes, and their effect of the composition of the lower atmosphere, because the individual processes taking place have not been clearly identified.

Elementary processes taking place in the snowpack.

A mixture of physical and chemical processes can *a priori* be invoked to explain the chemical impact of the snowpack (Figure 2). The snowpack is a dynamic medium where exchanges of water vapor and of trace gases continuously take place between snow layers and with the atmosphere (Dominé and Shepson, 2002). These exchanges are driven by wind circulation through the snowpack, and by the temperature gradient that almost always exist in the snowpack, and which cause gradients of water vapor pressure that generate fluxes.

Water vapor gradients also cause the sublimation of snow crystals in warmer snow layers, and the condensation of water vapor onto existing crystals in colder layers. These sublimation/condensation cycles, that cause changes in the sizes and shapes of snow crystals, are regrouped under the term 'snow metamorphism'. Numerous gases, such as HCl, HNO_3 and possibly HCHO (Thibert and Dominé 1998; Perrier et al., 2002), are dissolved in the ice volume and are entrained by these water vapor movements during snow metamorphism, leading to their sublimation and co-condensation. Thus, quantifying snow metamorphism is needed to quantify the exchange of solutes between snow layers and with the atmosphere.

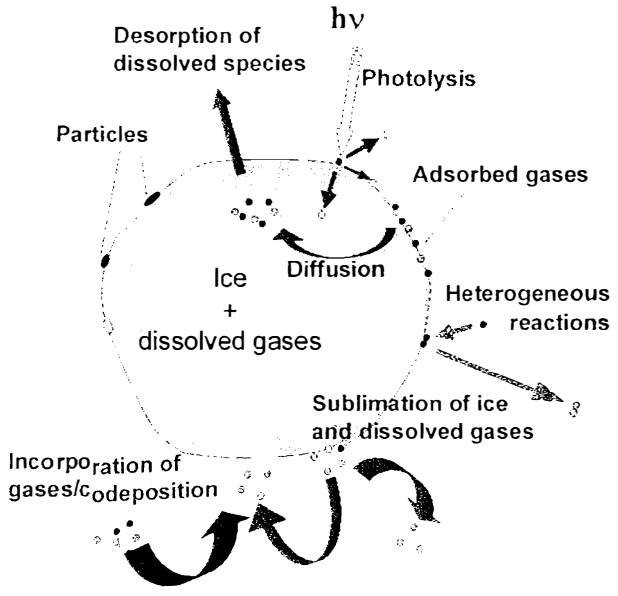

Figure 2. *Physical and chemical processes taking place in the snowpack*

Trace gases can also be adsorbed onto the surface of snow crystals. Quantifying adsorbed gases requires the knowledge of (i) the adsorption isotherms of the trace gas of interest on ice and (ii) the measurement of the specific surface area (SSA) of the snow sample of interest. The SSA is the surface area of snow accessible to gases, per mass unit of snow, and is often expressed in cm^2/g (Dominé et al., 2002). Gases that can adsorb onto ice surfaces include hydrophilic molecules, that have a strong dipole moment, such as alcohols, organic acids, and aldehydes (Sokolov and Abbatt, 2002) and also hydrophobic molecules with a low vapor pressure, such as pesticides, that can be cryopumped by the snowpack (Wania et al., 1998).

Heterogeneous reactions can also be catalyzed by ice surfaces. For example, the reaction sequence (1) to (2), that can initiate the formation of photolyzable bromine, has been shown to be rapid on ice (Oum et al., 1998; Huff and Abbatt, 2002).

$$O_3 + Br^- + H^+ \rightarrow HOBr + O_2 \qquad (1)$$

$$HOBr + Br^- + H^+ \rightarrow Br_2 + H_2O \quad (2)$$

Other processes such as solid phase diffusion in and out of ice crystals can also take place in the snow pack, and lead to the sequestration/release of trace gases that can be produced in the snowpack. For example, it has been suggested that the emission of formaldehyde by the snowpack could have a contribution from HCHO diffusing out of snow crystals (Perrier et al., 2002).

The snowpack is thus a complex medium that can accommodate numerous processes, resulting in complex modifications of the composition of the lower polar atmosphere. Moreover, snowpack chemistry also modifies snow composition, and complicates ice core interpretation (Legrand and Mayewski, 1997). Understanding these modifications is a current major challenge of atmospheric chemistry, that has implications for paleoclimate studies. Along with laboratory measurements and modeling studies, carefully planned field campaigns are necessary to perform the observations needed to elucidate the processes involved. It is crucial that such campaigns be performed in a pristine environment, far from local pollution sources, for the observations to be more readily interpretable and to have a general bearing.

Use of the Corbel clean base near Ny-Ålesund

Integrated measurement campaigns are needed to shed light on air-snow interactions. Campaigns should be focused on specific topics whose definition should be discussed in detail. In all cases, both air and snow chemistry, chemical fluxes, light intensity above and in the snow, micrometeorology parameters, and snowpack physics should be investigated to allow a quantitative interpretation of results and their modeling. Possible campaign topics include :

- The processing of organic matter in the snowpack. Organic compounds are lost by snow, presumably by snowpack photochemistry. Recent evidence suggest that aldehydes and ketones are some of the products of this chemistry, but neither the nature of the organic precursors nor the details of the chemical pathways and reaction products are elucidated. Understanding the recycling of organics by the snowpack, and therefore the extend to which pristine areas can be affected by anthropogenic pollution, requires detailed chemical measurements and organic speciation.
- The fate of hydrophobic organic chemicals (HOCs) in the snowpack. HOCs in general and pesticides in particular have a large impact on the Arctic biosphere and their processing by the snowpack deserves careful studies. This topic can be considered as a sub-topic of the previous one, but its biological implications require specific analytical tools that warrant a focused campaign.
- Processing of reactive nitrogen species by the snowpack. NO_3^- is now known to be photochemically processed in the snowpack, and to lead to the production and release of NO_x, HONO and OH. However, the species that cause the NO_3^- in snow and ice have not be clearly identified, and the interactions between organic nitrates, ice, and other reactive nitrogen species deserve further studies. Ice core data indicate that the preservation of the nitrate signal in ice (and therefore the reactivity of nitrate) depends on overall snow chemistry (Thibert and Dominé, 1998), and interactions between nitrate and other ionic species in snow must also be investigated.

The Corbel base, about 5 km upfjord from Ny-Ålesund, appears well suited for such integrated campaigns, provided that a clean energy source is provided. Solar panels, wind turbines and fuel cells can be envisaged. Air pollution by the village is a possibility, but pollution episodes can be detected and the corresponding data filtered out.

References

Barrie, L.A., Bottenheim, J.W., Schnell, P.J., Crutzen, P.J. and Rasmussen, R.A. 1988. Ozone destruction and photochemical reactions at polar sunrise in the lower Arctic atmosphere, *Nature, 334*, 138-141.

Dominé, F. and Shepson, P.B. 2002. Air-snow interactions and atmospheric chemistry. *Science, 297,* 1506-1510.

Dominé, F., Cabanes, A. and Legagneux, L. 2002. Structure, microphysics, and surface area of the Arctic snowpack near Alert during ALERT 2000. *Atmos. Environ. 36*, 2753-2765.

Foster, K., R. Plastridge, J. Bottenheim, P. Shepson, B. Finlayson-Pitts and C. W. Spicer 2001. First Tropospheric Measurements of Br_2 and BrCl and Their Role in Surface Ozone Destruction at Polar Sunrise, *Science, 291,* 471-474.

Grannas, A.M., Shepson, P.B., Guimbaud, C., Sumner, A.L., Albert, M., Simpson, W., Dominé, F., Boudries, H., Bottenheim, J.W., Beine, H.J., Honrath, R., Zhou, X. 2002. A study of carbonyl compounds and photochemistry in the arctic atmospheric boundary layer. *Atmos. Environ. 36*,.2733-2742.

Honrath, R., Peterson, M. C., Lu, Y., Dibb, J. E., Arsenault, M. A., Cullen, N. J., and Steffen, K. 2002. Vertical fluxes of nitrogen oxides above the snowpack at Summit, Greenland. *Atmos. Environ. 36*,.2629-2640.

Huff, A.K. and Abbatt, J.P.D. 2002. Kinetics and product yields in the heterogeneous reactions of HOBr with ice surfaces containing NaBr and NaCl. *J. Phys. Chem. A, 106*, 5279-5287.

Legrand, M., and Mayewski, P. 1997. Glaciochemistry of polar ice cores: a review. *Rev. Geophys. 35*, 219-243.

Mauldin, R.L., Eisele, F., Tanner, D.J., Kosciuch, E., Shetter, R., Lefer, B., Hall, S.R., Nowak, J.B., Buhr, M., Chen, G., Wang, P. and Davis, D. 2001. Measurements of OH, H_2SO_4, and MSA at the South Pole during ISCAT. *Geophys. Res. Lett. 28*, 3629-3632.

Oum, K. W., Lakin, M. J., et Finlayson-Pitts, B. J. 1998. Bromine activation in the troposphere by the dark reaction of O_3 with seawater ice, *Geophys. Res. Lett., 25*, 3923-3926,

Perrier, S., Houdier, S., Dominé, F., Cabanes, A., Legagneux, L., Sumner, A.L., Shepson, P.B. 2002. Formaldehyde in Arctic snow. Incorporation into ice particles and evolution in the snowpack. *Atmos. Environ. 36,*.2695-2705.

Steffen, A., Schroeder, W., Bottenheim, J., Narayan, J. and Fuentes J.D. 2002. Atmospheric mercury concentrations: measurements and profiles near snow and ice surfaces in the Canadian Arctic during Alert 2000. *Atmos. Environ. 36*, 2653-2661.

Sokolov, O. and Abbatt, J.P.D. 2002. Adsorption to ice of n-alcohols, acetic acid, and hexanal. *J. Phys. Chem. A, 106*, 775-782.

Thibert, E., and Dominé, F. 1998. Thermodynamics and kinetics of the solid solution of HNO_3 in ice. *J. Phys. Chem. B. 102,* 4432-4439.

Wania, F., J.T. Hoff, C.Q. Jia, D. Mackay 1998. The effects of snow and ice on the environmental behaviour of hydrophobic organic chemicals. *Environ. Pollut. 102*, 25-41.

Zhou, X., Beine, H.J., Honrath, R.E., Fuentes, J.D., Simpson, W., Shepson, P.B., 2001. Snowpack photochemical production of HONO: a major source of OH in the Arctic boundary layer in spring time. *Geophys. Res. Lett.*, 28, 4087-4090.

Long Range Transport of Pollutants – Evidences From Rainfall Chemistry in Hornsund (Svalbard)

Piotr Głowacki & Wiesława Ewa Krawczyk

Institute of Geophysics, Polish Academy of Sciences, 01-452 Warszawa, Ks. Janusza 64, Poland, E-mail: glowacki@igf.edu.pl, phone +48 22 6915890

Faculty of Earth Sciences, University of Silesia, 41-200 Sosnowiec, Będzińska 60, Poland, E-mail: wkraw@us.edu.pl, phone +48 32 2918901

Introduction

Data on the chemistry of atmospheric precipitation in Svalbard are scarce. Most of the research has been conducted on snow chemistry (e.g. Semb et al. 1984, Arkhipov et al. 1990, Arkhipov et al. 1992, Głowacki & Pulina 2000) or glacier ice chemistry (e.g. Motoyama et al. 2000).

At the Polish Polar Station in Hornsund research on precipitation chemistry was started in 1988, within the environmental programme. Earlier data on pH of rainfall in this region are coming from the seventies, Pulina (1975) reporting seven rainfall events with pH<4 in August and September of 1972.

Before the summer of 2000 investigations covered only measurements of precipitation pH, specific electric conductivity (SpC) and chloride concentrations by argentometric method.

Preliminary elaboration of results covered the expedition years 1993/94 and 1998/99 (Burzyk et al. 2002). The polar summer seasons of 1993 and 1998 were amongst the warmest known in the entire Arctic and it was found that pH of rainfall during summer seasons was lower than pH of winter precipitation. The first comprehensive chemical analyses of summer rainfall were made in 2000, and discussed in relation to atmospheric circulation patterns by Krawczyk et al. 2002, Głowacki et al. 2002.

Methods

Precipitation samples are collected using polypropylene funnels with areas of 0.25 m^2, situated at the height of 2 meters above the ground in the Fugleberget catchment about 500 meters NE from Polish Polar Station (77°00.386'N 15°33.178'E). Samples are retained in polythene bottles, both funnels and bottles being washed with distilled water between precipitation events. Each rainfall and snowfall is collected individually. Measurements are made when precipitation is exceeding 0.5 mm (w.e). Immediately after sampling measurements of pH (with Elmetron CP-315 pH-meter) and specific electric conductivity (with Elmetron CC-318 conductivity meter) are made. Sub-samples are filtered on 0.45 μm membrane filters in a filtering system and transported to Poland.

In laboratories at the Faculty of Earth Sciences, University of Silesia, Sosnowiec samples are analysed for anions (Cl^-, NO_3^-, SO_4^{2-}) by ion chromatography on Metrohm IC 761 and for cations (Ca^{2+}, Mg^{2+}, Na^+ and K^+) with a Solaar M6 atomic absorption spectrometer. Before cation analysis samples are acidified with HNO_3.

The meteorological situation at Hornsund

The Polish Polar Station has been operating continuously since 1978. Its data show an increasing trend in annual precipitation totals. This increase is mainly due to increase during the summer month (June-September) totals of rainfall, which have ranged from totals of 84.4 mm in

1998 to 386.1 mm in 1994. Winter precipitation totals (October – May), although very variable, (minimum 135 mm in 2001, maximum 350 mm in 1995) show no secular trends.
This increasing trend in total annual precipitation is accompanied by an increasing trend in mean monthly air temperature in September. In the years 1990-2000 only once (in 1994) was this temperature below 0°C. As a result the polar summer period has become longer and more precipitation falls as rain, directly influencing polar environmental conditions.

The summer of 2000 was the longest one in the period, 1978-2001 (Table 1). During its 149 days (May 29 to October 24) mean daily temperature was 3.2°C and total precipitation amounted to 321.7 mm; the highest rainfall was 26.7 mm, on August 2. Aggregate wind speeds were also highest for the period, 1978-2001.

Table 1. Meteorological characteristics of polar summer periods in Hornsund

	Period	Duration	Mean diurnal temperature (°C)		
	(dates)	(days)	Mean	Max.	Min.
Mean	02.06-29.09	119	3.2	7.9	-1.6
Maximum	29.05-24.10	149	4.2	10.8	0.8
Minimum	10.06-30.08	82	2.5	6.1	-4.2

	Degree - Days		Wind speed (m/s)		Precipitation	Sunshine
	(PDD+)	(NDD-)	Mean	Totals	(mm) w.e.	(hours)
Mean	385.7	-6.1	4.2	500.7	200.9	511.4
Maximum	527.2	0.0	5.5	650.7	384.3	705.4
Minimum	298.2	-20.5	2.8	360.9	60.0	256.0

Chemical composition of rainfall

Measurements of precipitation pH, started in 1989, show a trend to a slight increase in mean precipitation-weighted pH (Figure 1), but of the twelve years only three had pH>5. In other years precipitation was notably acid, with pH<5. The summer of 2000 was marked by a very low mean precipitation pH of 4.70, rain with pH<5 comprising nearly 49% of all precipitation.

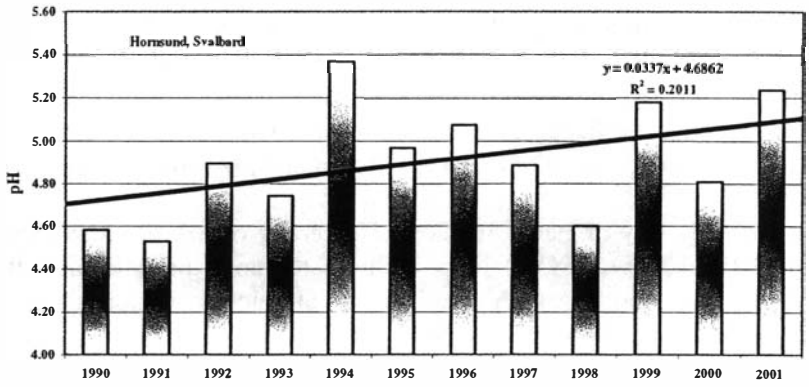

Figure 1. Mean pH of polar summer rainfall in the period 1990-2001.

Mean concentrations of ions in the two polar summers of 2000 and 2001 were distinctly different (Table 2). Ions of sea-salt origin (Cl^- and Na^+) prevail, as is typical for a station located on the sea shore. Sulphate concentrations were in 2000 nearly two times greater than in 2001. In 2001 there were higher concentrations of nitrate, in 2000 a few rainfall events were without nitrates.

Table 2. Mean (volume weighted) cation and anion concentrations in Hornsund rainfall (in mg/l)

summer	n	Ca^{2+}	Mg^{2+}	Na^+	K^+	SO_4^{2-}	NO_3^-	Cl^-
2000	18	0.24	0.32	2.70	0.14	1.00	0.07	4.76
2001	12	0.21	0.08	0.91	0.07	0.52	0.36	1.55

n - number of samples analysed

In 2000 total dissolved solids (TDS) concentrations were higher due to greater amounts of the marine component (sea salt). This can be explained by meteorological conditions, which were very windy. The other components in TDS concentrations were of crustal and anthropogenic origin (Figure 2).

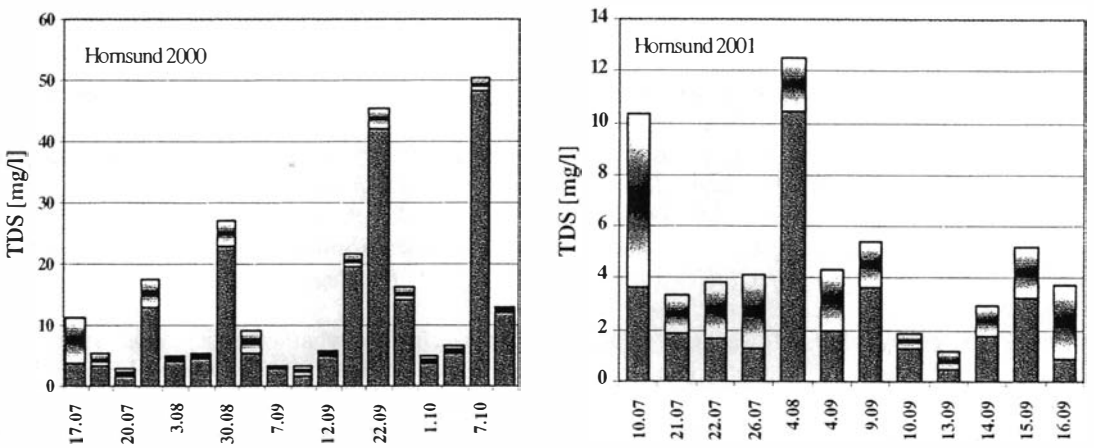

Figure 2. Total dissolved solids (TDS) concentration in Hornsund rainfall in the summers of 2000 and 2001; lower bar – marine components; upper bar – crustal and anthropogenic components.

Plot of estimated solute loads delivered from the atmosphere in the Hornsund region shows that chloride and sodium are dominant (Figure 3). In the summer of 2000 the total sulphate load was 321.6 kg/km^2. Non-sea-salt (nss)-sulphates comprised 42% of all sulphates. The estimated load of this pollutant was 138.5 kg/km^2.

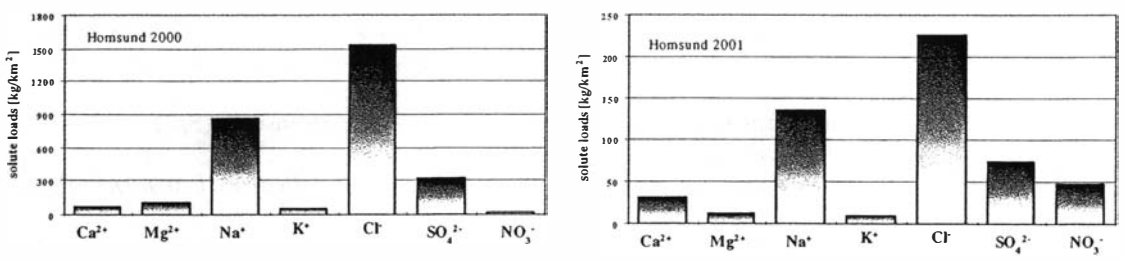

Figure 3. Estimated solute loads transported from the atmosphere in summers of 2000 and 2001.

Evidences of long range transport of pollutants - conclusions

Acid rain is falling in Hornsund, with a mean pH mostly below 5.20. In the summer of 2000 nearly 64% of rainfall with pH<5 occurred with a C-8 circulation, i.e. advection of air masses from S+SW and cyclonic situation (Niedźwiedź 1993). The lowest pH and the highest concentrations of nss-sulfate and nss-chloride (possibly originating from HCl) occurred in September 2000. Synoptic maps for this period show that air masses were moving from S+SW directions, transporting air containing higher concentrations of SO_2, NO_x and HCl.

The total load of nss-sulphur deposited on the ground was 46.2 kgS/km^2, nearly 1.5 times more than the yearly load of sulphur deposited in the Arctic nearly 20 years ago (as shown in AMAP data).

Acknowledgments

Rainfall samples were collected during 23rd and 24th Spitsbergen Expedition of Institute of Geophysics, Polish Academy of Sciences. This work was supported by the European Union - Access to Research Infrastructure, Action of the Improving Human Potential Programme (LSF grant) and Faculty of Earth Sciences (BW-21/2001).

References

AMAP, 1998. AMAP Assessment Report: Arctic Pollution Issues. *Arctic Monitoring and Assessment Programme (AMAP)*, Oslo, Norway, 859 pp.

Arkhipov, S.M., Evseev, A.B. & Vostokova, T.A. 1990. Preobrazovaniye geokhimicheskih kharakteristik snezhnogo pokrova wperiod ablacyi. *Materialy Glyatsiologicheskih Issledovaniy. 70*, 95-101

Arkhipov, S.M., Moskalevsky, M., Glazovsky, A., Mayevski, P. & Whitlow, S. 1992. Snow cover geochemistry on the Kongsvegen glacier and Amundsenisen (Spitsbergen). *Proceedings of the 2nd International Symposium of Glacier Caves and Karst in Polar Regions. Międzygórze-Velka Morava, Sosnowiec*, 7-20.

Burzyk, M., Burzyk, J. & Głowacki, P. 2002. Comparative chemical characteristics of precipitation in the Hornsund region (SW Spitsbergen) in the years 1993-1994 and 1998-1999. *Polish Polar Research, 22(3-4),* 233-247.

Głowacki, P., Krawczyk, W. E. & Niedźwiedź, T. 2002. Precipitation in Hornsund (SW Spitsbergen) in Summers of 2000 and 2001 – its chemistry and influence of atmospheric circulation. In G.G. Matishov & G.A. Tarasov (eds.): *International Conference Proceedings Collection – The complex investigations of the Spitsbergen Nature.* Russian Academy of Sciences, Kola Science Centre, 112-116.

Głowacki, P. & Pulina, M. 2000. The physico-chemical properties of the snow cover of Spitsbergen (Svalbard) based on investigations during the winter season 1990/1991. *Polish Polar Research, 21(2),* 65-88.

Krawczyk, W. E., Głowacki, P. & Niedźwiedź, T. 2002: Charakterystyka chemiczna opadów atmosferycznych w rejonie Hornsundu (SW Spitsbergen) latem 2000 r. na tle cyrkulacji atmosferycznych. In A. Kostrzewski & G. Rachlewicz (eds.): *Polish Polar Studies.* 187-202.

Motoyama, H., Kamiyanma, K., Igarashi, M., Nishio, F. & Watanabe O. 2000. Distribution of chemical constituents in superimposed ice from Austre Broggerbreen, Spitsbergen. *Geografiska Annaler, 82A (1),* 33-38

Niedźwiedź, T. 1993. The main factors forming the climate of the Hornsund (Spitsbergen). *Zeszyty Naukowe UJ Kraków, Prace Geograficzne 94*, 49-63.

Pulina, M. 1975: Preliminary studies on denudation in SW Spitsbergen. *Bulletin de l'Academie Polonaise de Sciences 22(2),* 83-99.

Semb, A., Brekkan, R. & Joranger, E. 1984: Major ions in Spitsbergen snow samples. *Geophysical Research Letters, 11*, 5, 445-448.

Trace element distribution in size separated aerosols from Ny Alesund during the ASTAR 2000 campaign

M. Kriews, A. Herber, C. Lüdke*, E. Hoffmann*, J. Skole*

Alfred-Wegener-Institute for Polar- and Marine Research P.O. Box 120161, D-27515 Bremerhaven, FRG, E-mail: mkriews@awi-bremerhaven.de, phone: ++4947148311420

*Institute for Spectrochemistry and applied Spectroscopy, Albert-Einstein-Straße 9, D - 12489 Berlin, FRG, E-mail: luedke @isas-berlin.de, phone: ++493063923554

Introduction

The influence on climate, ecosystems and human health by atmospheric particles is undoubted but measurements to quantify the emissions from natural and anthropogenic sources as well as the transport and deposition behaviour in polar regions are still incomplete. To study these processes in combination with remote sensing techniques like LIDAR, Sunphotometer, Nepheleometer, it is necessary to analyse different properties of aerosols like size distribution, chemical composition, isotope ratios etc. because suche data enter into global modelling.
During the ASTAR campaign in March/April 2000 ground based aerosol sampling was performed by two different sampling systems, which were installed on top of the roof at the Japanese station Rabben 8 m above ground level.
Results will be presented fror trace element analyses carried out by solution ICP-MS and ETV-ICP-MS. In addition data from electron microscopy measurements will be presented to have information about morphology and composition of main constituents.

Experimental

Aerosol sampling with an eight stage cascade impactor

Size classified aerosol sampling was carried out during special events 24 hourly by an eight stage impactor with a size range from 0.35-16.5 µm on grapite targets for subsequent multielement analysis by ETV-ICP-MS [Lüdke et al. 1999]. In addition SEM/EDXA studies were carried out to characterize the morphology of the aerosol particles and to get informations about the major components. The pump rate for the eight stage impactor was 2.2 m^3/h.
Aerosol characterisation was carried out for typical tracer elements by ETV-ICP-MS: (mineral dust: Mn, Fe, Co and anthropogenic sources: Pb, Ni, Sb, Pt, Cd, Ag and Tl).

Aerosol sampling with a single stage impactor

Size classified aerosol sampling was performed by a flow rate of 35 m^3/h on precleaned silicon oil covered cellulose filters. With this setup the cut off diameter is at 2 µm. The sampling time was between 24 and 48 hours depending on the atmospheric aerosol particle load. Element analyses were carried out after a wet oxidative digestion for the aerosol particles under clean room conditions (U.S. class 100) by solution ICP-MS [Kriews and Schrems 1998].
Characterisation of aerosol samples was performed for 49 isotopes by ICP-MS. Typical tracer elements for mineral dust are Al, Ca Co, Fe, K, REE (Rare Earth Elements), Th and U. Na, Mg, Sr and Rb present sea salt sources. Anthropogenic sources are characterised by Ag, Cd, Cr, Cu, Ni, Pb, S, Tl and Zn.

Results

Morphological and main component determination by SEM/EDXA

Typical aerosol particles from anthropogenic sources, sea salt as well as from mineral dust and ammonium sulphate are exemplarily shown in figure 1.

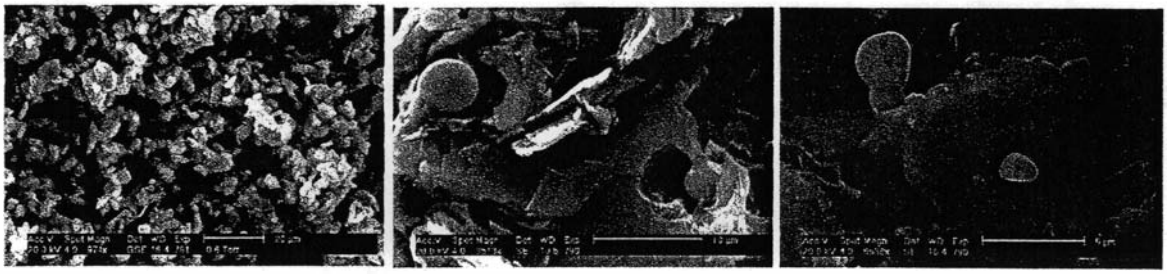

Figure 1: SEM photographs of typical aerosol particles collected on graphite targets: left: sea salt and mineral dust particles for impactor 10 on stage 3.45 µm, center: typical anthropogenic particles from high temperature combustion processes for impactor 4 on stage 3.45 µm, right: two ammonium sulphate particles for impactor 4 on stage 0.35 µm.

ETV-ICP-MS results

Fe size distributions (tracer for mineral dust) and Pb size distributions (tracer for anthropogenic sources) are exemplarily shown for two different atmospheric situations in figure 2. Impactor 4 represents an enriched aerosol, while impactor 10 shows the distribution for a background aerosol.

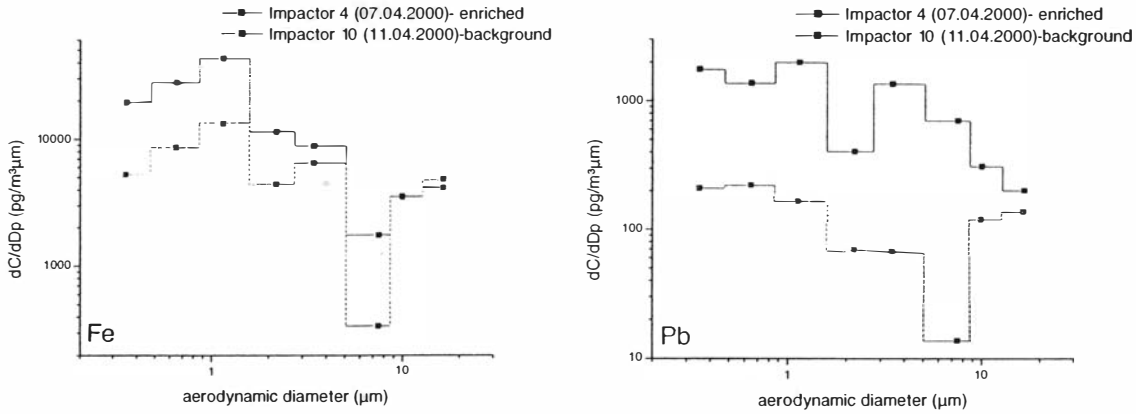

Figure 2: Fe and Pb size distribution for an enriched and a background aerosol

ICP-MS results

Size distribution and time series for some typical tracer elements (Al as a tracer for mineral dust, Na as a tracer for sea salt and Pb as a tracers for anthropogenic sources are exemplarilly shown in figure 3 a-c. Comparable results were measured for Ca Co, Fe, K, REE (Rare Earth Elements), Th and U (mineral dust), Mg, Sr and Rb (sea salt) and for Ag, Cd, Cr, Cu, Ni, S, Tl and Zn (anthropogenic sources).

During the Haze event on March 23rd all anthropogenic elements and mineral dust elements are enriched up to factor of 30 in comparison to a background situation on March 19th. This is in a good agreement with the evaluation of 120 hours backward trajectories, which have shown that the air masses arryving Ny Alesund on March 23rd were coming from the European continent. The concentration ratio between a Haze event and a backgroung situation is shown in figure 4.

Ground based measurements performed with a Nephelometer and an Optical Particel Counter at Rabben as well as DMPS data from Zeppelin mountain have shown a high aerosol concentration at 10th of April. This is in not a Haze event. The high aerosol load is due to aerosol particles originated from sea salt.

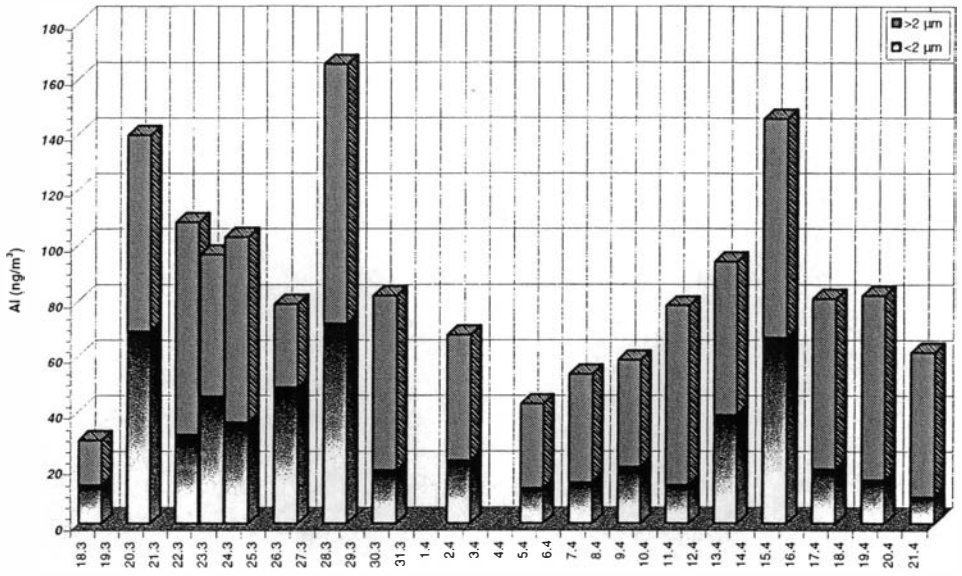

Figure 3 a: Al concentration for fine and coarse particles during ASTAR 2000

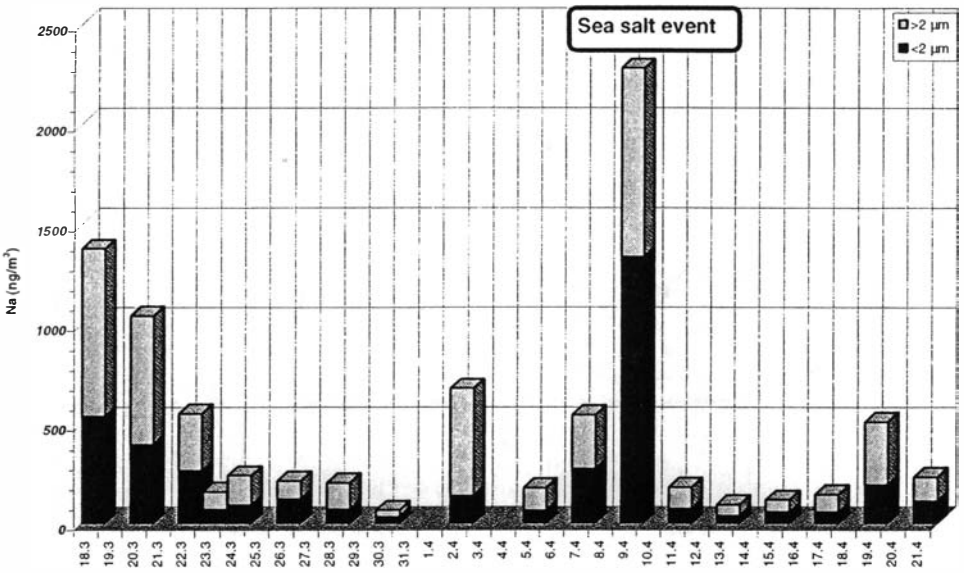

Figure 3 b: Na concentration for fine and coarse particles during ASTAR 2000

Summary and Outlook

* Concentrations of mineral dust and anthropogenic components are a factor 3-30 higher during Haze events than in background situations in spring time.
* This is in a good agreement with data from remote sensing methods (Lidar, Sunphotometer).
* Measurements with the eight stage impactor show higher element concentrations for mineral dust and anthropogenic elements as well as different size distributions.
* Further investigations have to be done to connect the chemical remeote sensing data.
* Future campaigns (spring 2004) will be used also for measurements of aerosol concentration with improved systems.

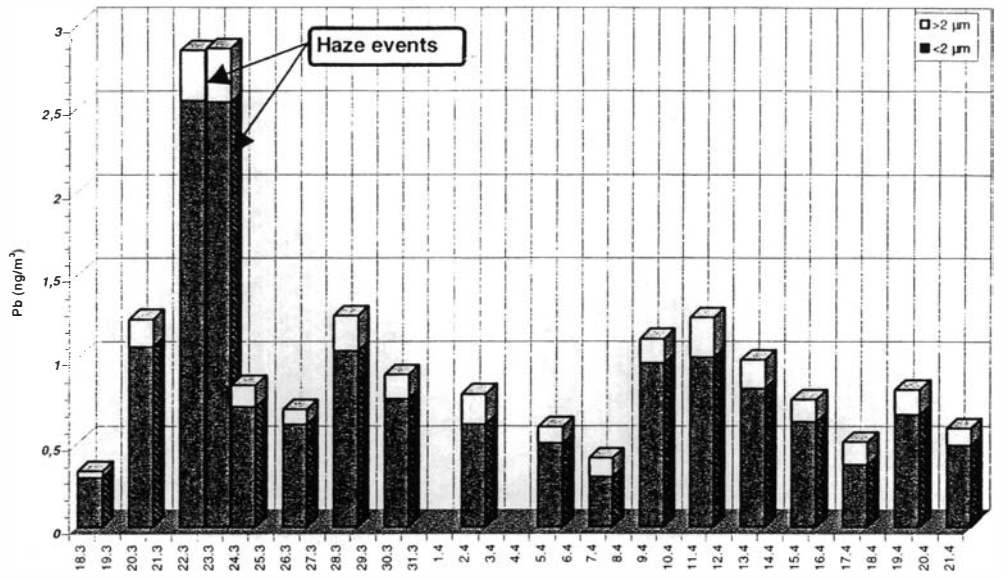

Figure 3 c: Pb concentration for fine and coarse particles during ASTAR 2000

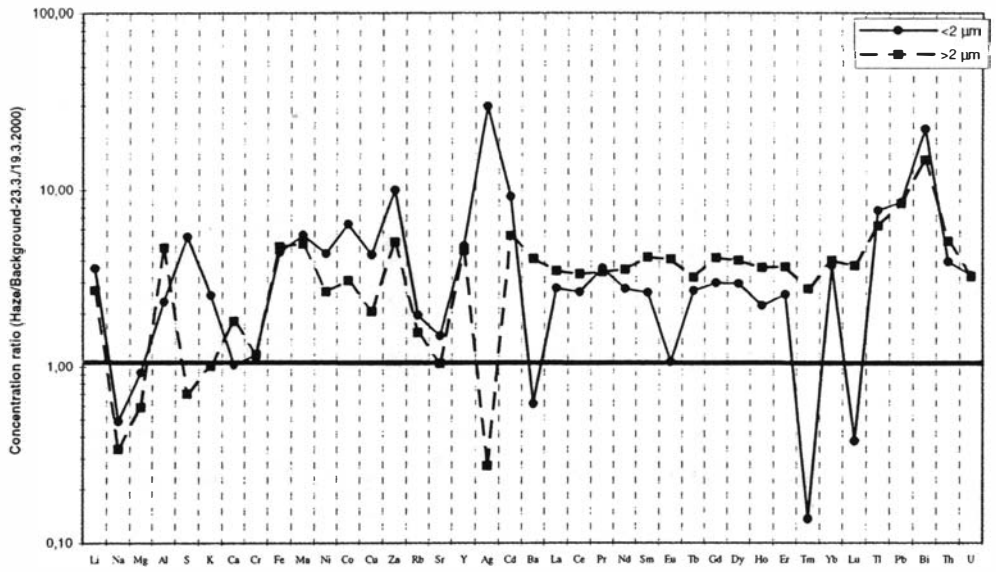

Figure 4: Element concentration ratios between a Haze event (23.3.2000) and a backgound aerosol (19.3.2000).

References

Kriews, M. and Schrems, O. (1998): Aerosol sampling depending on precipitation at Spitsbergen, Journal of Aerosol Science, Vol 29, Suppl. 1, pp. S685-S686.

Lüdke, C., Hoffmann, E., Skole, J. and Kriews, M., (1999): Determination of trace metals in size fractionated particles from arctic air by electrothermal vaporization inductively coupled plasma mass spectrometry, Journal of Analytical Atomic Spectrometry, Vol. 11, 1685-1690.

Comparing methane data from Ny-Ålesund with results from a regional transport model (MATCH)

Ine-Therese Pedersen[1,2], Kristina Eneroth[1], Erik Kjellström[1],
Ove Hermansen[2], Kim Holmén[1]

[1] Department of Meteorology, Stockholm University (MISU), S-106 91 Stockholm, Sweden.
E-mail: Kristina.Eneroth@misu.su.se
[2] Norwegian Institute for Air Research (NILU), N-9296 Tromsø, Norway.
E-mail: Ine-Therese.Pedersen@nilu.no

Introduction

Methane is an important greenhouse gas and a key molecule in tropospheric photochemistry. The global burden of atmospheric methane has risen dramatically since the preindustrial era, and recent measurements show global CH_4 mixing ratios continuing to rise although the rate of increase has slowed over the past decade (Dlugokencky et al., 2001). The effect of methane transport source/sinks regions has been investigated on several stations in the CMDL network. At Mauna Loa Observatory (MLO) on Hawaii, Harris et al. (1992) concluded that changes in the methane record are linked to perturbations of the flow regime and not exclusively depended on source/sink characteristics. In the Arctic, north of the polar front, winter meteorology is somewhat stagnant, with few storms and little precipitation to mix and clean the atmosphere (Raatz, 1991). Furthermore, the polar front limits how midlatitude surface sources can influence tracer fields in the Arctic. At the Barrow (BRW) station in Alaska analysis of the in situ methane measurements and trajectories during winter showed that pollution measured there often is emitted within the Arctic basin and transported close to ground to the site (Harris et al., 2000). In this project the in situ methane measurements from the Zeppelin station in Ny-Ålesund, Svalbard (ZEP) are studied by comparing continuous gas chromatograph data and flask data to simulated methane concentrations from an atmospheric transport model. The model is used to investigate the distribution and transport of methane in and out of the Arctic region.

Methods

Model

For this study a 3-dimensional Eulerian transport model MATCH (Multiple-scale Atmospheric Transport and Chemistry modelling system) is used (Robertson et al., 1999). The meteorological fields (wind, temperature and pressure) are taken from the European Centre for Medium range Weather Forecasts, ECMWF, available every 6 hours. The chosen domain covers most of the Arctic (Figure 1). Emission and boundary conditions for methane are taken from a global tracer transport model developed at "Centre for Atmospheric Science" in Cambridge, U.K, on 5° x 5° resolution (Warwick et al, 2002). The boundary fields are read for every 30 hours. These and the ECMWF data are both interpolated to the rotated grid used in the model domain and then linearly interpolated in time to one-hour resolution. The horizontal resolution is 1°x 1°. The vertical resolution is the same as in the input meteorological fields i.e. 31 levels unequally distributed from the surface to 10 hPa.

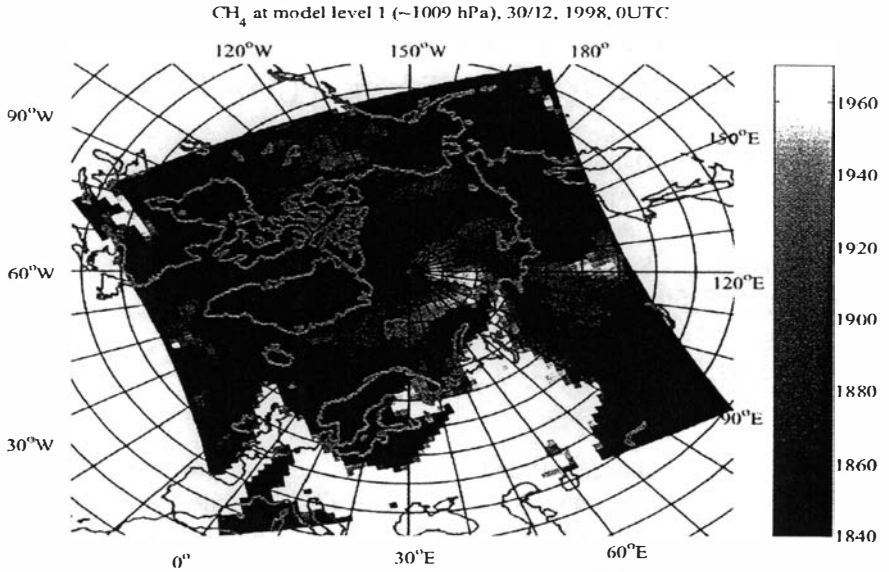

Figure 1 Model methane-mixing ratio in ppb for the Arctic region on 30th December 1998 at 00 UTC

Instrument and data description

The sampling site is at Zeppelin station on Mt. Zeppelin at 474 m above sea level near Ny-Ålesund, (78°58´ N, 11°53´ E), on the west-coast of Spitsbergen. The in situ methane measurement system at Zeppelin consists of a custom-built sampling system, a Carlo Erba gas chromatograph (GC) with flame ionisation detection (FID) and a 1 ml sample loop. The measurement system alternates between ambient air and standard gas, three air-samples between every standard sample. A sample is measured every 15 min giving 96 chromatograms per day (Zellweger et al., 2001). The instrument has been working for periods from 1997-2001, with a long break when the new station at Mt. Zeppelin was built between June 1999 and March 2000. Other gaps in the record are due to system malfunctions. The chromatograms have been integrated with a MATLAB program, but much of the data collected are noisy. The standard values are interpolated and the ratio of the ambient peak area to the standard peak area is multiplied by the value of the CH_4 mixing ratio assigned to the reference gas.

The Zeppelin station is a part of the CMDL cooperative Air Sampling Network (Dlugokencky et al., 1994). At least once a week flask samples are collected using a portable pumping unit. Two flasks are connected in series, flushed with air, and then pressurized to 1.2 - 1.5 times ambient pressure. All samples are analysed at NOAA CMDL in Boulder, Colorado by a GC/FID (http://www.cmdl.noaa.gov/).

Results and discussion

The retrievable methane data at Zeppelin Station from 1998 are plotted in Figure 2 together with flask data (circles). The observed mixing ratio varies roughly between 1700 ppb and 1950 ppb, with a mean around 1850 ppb. In October the flask data and the measured data correlate well and the 5 different times where flask samples are taken are within the domain measured with the gas chromatograph. Also in November the flask data corresponds approximately to the mean data from the continuous instrument. But in December only two of the flask samples show a value close to the continuous measurement. In the period between the 9th and the 21st of December the quality of the chromatograms are poor and it is hard to distinguish any median value. On the 30th of December the flask sample is 40 ppb to 50 ppb lower than the mean chromatogram. Figure 3 shows December

1998 flask data compared with methane values for Zeppelin calculated by the MATCH model. Before the 9th and after the 21st the simulated time-series show good agreement with the raw data, except that from the 25th to the 31st there is an underestimation by the model. Even so both show an increase from the 25th leading to the maximum on the 30th at 00 UTC. With an increase in concentration at approximately the same time for CH_4 estimated and CH_4 modelled, it is clear that the mixing ratio is more dependent, as expected, on transport than on local sources. The 5-day back-trajectory arriving at Zeppelin the 30th show that the air is coming from Siberia (Figure 4). Hence the constituents could have been released at the Siberian gasfields and then transported to Ny-Ålesund. This transport is also shown in the model where elevated mixing ratios can be tracked back to Siberia during the days preceding the 30th of December. This result is consistent with the interpretation of CO_2 data by Engardt et al. (1999). The underestimation by the model in the period could be due to weaknesses in the emission estimates from Siberian. This needs to be studied further.

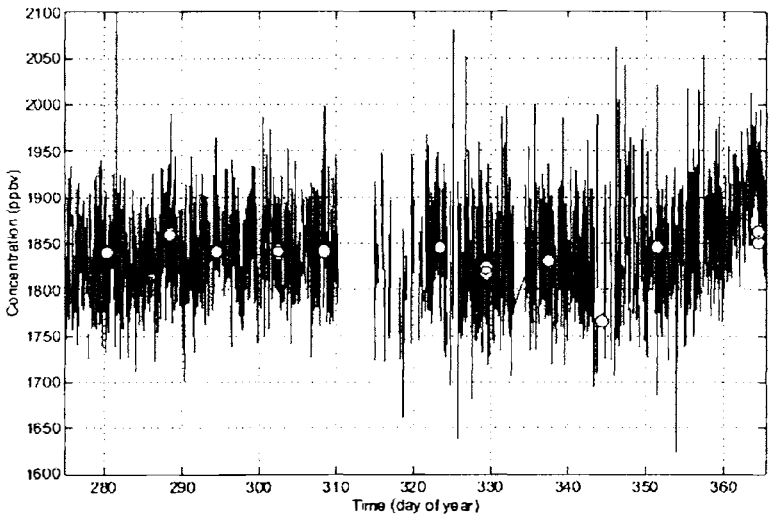

Figure 2 Methane concentration from Zeppelin Station 1998 from the gas chromatograph and flask samples (circles)

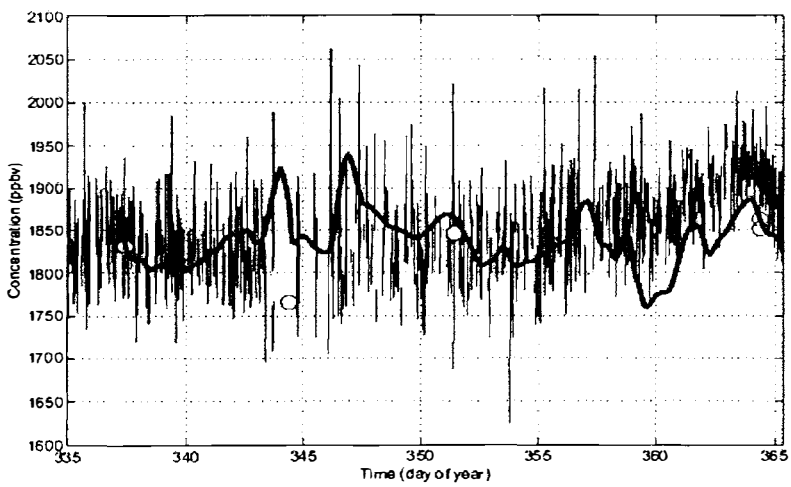

Figure 3 Methane from continuous measurements (thin line) and flask samples (circles) compared with model calculations (thick line) in December 1998 at Zeppelin Station.

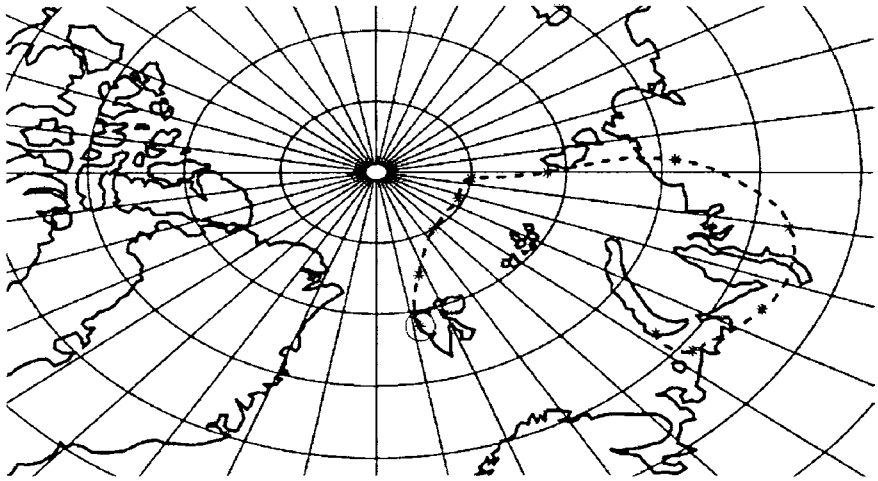

Figure 4 5-day back-trajectories arriving at Mt. Zeppelin the 30th December 1998 at 0950 UTC

Conclusions

A 3-dimensional transport model has been used to investigate the distribution and transport of methane in the Arctic region. A model time-series for December 1998 at Zeppelin station, Ny-Ålesund, have been compared with continuous measurements from a gas chromatogram and weekly flask samples. During some periods we find some relationship between these parameters and also strong indications that long-range transport is important for the methane concentration measured at the site. Work is currently done to improve the quality of the gas chromatograms at the station; hence longer periods can be used in future studies with the model.

References

Dlugokencky, E.J., Steele, L.P., Lang, P.M. and Masarie, K.A., 1994. The growth rate and distribution of atmospheric methane. *J. Geophys. Res. 99*: 17,021-17,043

Dlugokencky, E.J., Walter, B.P., Masarie, K.A., Lang, P.M. and Kasischke, E.S., 2001. Measurements of an anomalous global methane increase during 1998. *Geophys. Res. Letters 28:499-502*

Engardt, M., Holmén, K., 1999. Model simulations of anthropogenic-CO_2 transport to an Arctic monitoring station during winter. *Tellus 51B*: 194-209

Harris, J.M., Tans, P.P, Dlugokencky, E.J., Masarie, K.A., Lang, P.M, Whittlestone, S. and Steele, L.P., 1992. Variations in atmospheric methane at Mauna Loa Observatory related to long-range transport. *J.Geophys. Res. 97*: 6003-3010

Harris, J.M., Dlugokencky, E.J., Oltmans, S.J., Tans, P.P., Conway, T.J., Novelli, P.C. and Thoning, K.W., 2000. An interpretation of trace gas correlations during Barrow, Alaska, winter dark periods, 1986-1997. *J.Geophys. Res. 105:* 17267-17278

Raatz, W.E., 1991. The climatology and meteorology of Arctic air pollution. *Pollution of the Arctic Atmosphere*, edited by J.W.T. Sturges, *pp. 13-42*, Elsvier Sci., New York.

Robertson, L., Langner, J. and Engardt, M., 1999. An Eulerian Limited-Aewa Atmospheric Transport Model. *J. Appl. Meteo. 38*:190-210

Warwick, N.J., Bekki, S., Law, K. S., Nisbet, E.G. and Phyle, J.A., 2002. The impact of meteorology on the interannual growth rate of atmospheric methane. *In press.*

Zellweger, C., Buchmann, B., Klausen, J. and Hofer, P., 2001. System and performance audit for surface ozone, carbon monoxide and methane. *EMPA WCC- report 01/3*

Tropospheric water vapour observations by ground-based lidar

Michael Gerding, Christoph Ritter, and Roland Neuber

Alfred Wegener Institute for Polar and Marine Research, Research Department Potsdam, D-14473 Potsdam, Germany, mgerding@awi-potsdam.de

Abstract: Ground-based lidars can provide continuous observations of tropospheric humidity profiles using the Raman-scattering of light by water vapour and nitrogen molecules. Profiles obtained since the beginning of year 2000 at the Koldewey Station (Ny-Ålesund, Spitsbergen) will be presented. Under nighttime conditions the observations cover a range from about 200 m altitude up to the upper troposphere, while daylight limits the observations to the lower troposphere, depending on water vapour content of the atmosphere. Lidar soundings are limited to clear-sky and high-cloud conditions. The usage of additional, weather-independent methods like radiosonde or GPS-based observations will be discussed. Simultaneous observations of humidity and aerosol extinction during the advection of aerosol rich air masses from the Kara Sea show some delay of the extinction increase compared with humidity increase. By another case study, the influence of the mean wind direction and the orography on the water vapour concentration near the ground and in the free troposphere will be discussed. E.g. during wintertime often a humidity inversion up to about 1.5 km altitude with drier air near the ground has been found, if wind comes from the south-east. Such local effects and small-scale structures observed by stationary lidar mostly cannot be resolved by satellite soundings or atmospheric models used e.g. for meteorological analyses or regional climate investigations.

Introduction

Water vapour causes about two third of the natural greenhouse effect of the Earth's atmosphere and is for this reason the most important greenhouse gas. Several climate models show that an increase in atmospheric humidity by 12-25 % will have the same global mean radiative effect than doubling the CO_2 concentration (Harries 1997). But in contrast to the homogenous distribution of the long-lived carbon dioxide is the water vapour distribution highly variable in space and time. Additionally, beside its (direct) radiative effect water vapour acts indirectly by interaction with aerosols, clouds, and precipitation (Hegg et al. 1996; Ramanathan et al. 2001). This indirect effect of surface cooling provides one of the largest uncertainties in the understanding of the radiative balance of the Earth's atmosphere (IPCC 2001).

To improve the understanding of the role of water vapour in the atmosphere, extensive water vapour soundings with high spatiotemporal resolution are necessary. Up to know, radiosondes provide the most valuable humidity data set, e.g. for numerical weather prediction (NWP) models. But today's standard radiosondes are of limited accuracy under the dry and cold conditions (Elliot & Gaffen 1991; Miloshevich et al. 2001) typical for the Arctic. Process studies of the hydrological cycle and aerosol-water vapour interaction require time series of humidity profiles, typically not performed by free ascending radiosondes. But this continuous water vapour soundings can be provided by optical lidar.

Water vapour observations by detection of the Raman-scattering of laser light have been described first by Melfi et al. (1969). A short laser pulse is emitted into the atmosphere. Besides elastic Rayleigh scattering with the air molecules, inelastic Raman scattering occurs, producing light with a wavelength shift characteristic for the scattering molecule. Water vapour Raman lidars detect the light backscattered by nitrogen and water vapour molecules. The ratio of the photons scattered by water vapour and nitrogen is proportional to the water vapour mass mixing

ratio. Water vapour lidars dispread past the end of the 80ies, when more powerful laser system elude the problems of small Raman backscatter cross sections (e.g. Whiteman et al. 1992).
The Koldewey Aerosol Raman Lidar (KARL) at Ny-Ålesund (78.9°N, 11.9°E) was build up in the end of the 90ies (Schumacher et al. 2001) and started regular water vapour sounding in the beginning of year 2000. It emits light at three different wavelengths (UV, vis, IR), and detects the backscattered light at seven different wavelengths from different height regimes in the troposphere and lower stratosphere. Table 1 summarises the system parameters. The KARL water vapour channels cover an altitude range between about 200 m and 6 km at nighttime conditions, while daylight limits the range to the lower troposphere, depending on water vapour content and skylight conditions. Typically, integration times of 30-60 minutes, altitude resolutions of 60 m and additional running averages of 180 m to 300 m are applied for water vapour profiles. The resolution in time can be increased for time series.

Laser			
emitted wavelength [nm]	1064.2	532.1	354.7
pulse energy [mJ]	180	80	70
pulse length [ns]	6-8	5-7	5-6
repetition rate [s^{-1}]	30	30	30
Detection/ Telescope	***small***		***large***
diameter [mm]	110		300
focal length	445		1200
aperture diameter [mm]	1		1
field of view [mrad]	2.2		0.8
detected wavelength [nm]	660.5, 607.3, 532.1		1064.2, 607.3, 532.1, 407.5, 386.7, 354.7

Table 1: System parameters of the Koldewey Aerosol Raman Lidar (KARL)

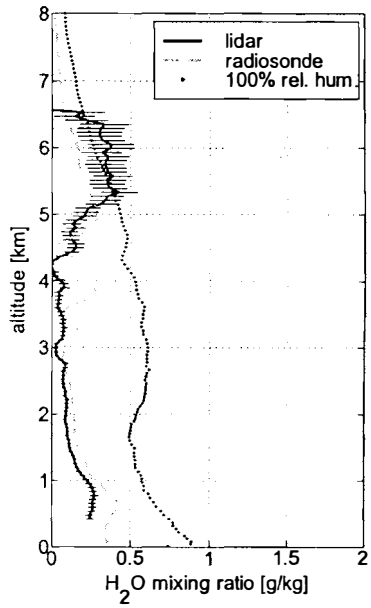

Figure 1: Water vapour profile from January 17, 2002

Figure 1 gives an example for a water vapour profile observed by lidar compared with the regular radiosonde. It was observed on January 17, 2002 between 14:04 and 15:01 UT. The water vapour mixing ratio was found below 0.5 g/kg in all altitudes, even in the lower and middle troposphere. In the upper troposphere the mixing ratio increased, providing small supersaturation between 5.3 and 6.5 km altitude. The regular radiosonde launched at 11 UT measured a smaller, but probably underestimated humidity. Simultaneous to the lidar sounding a balloon-borne SnowWhite frostpoint hygrometer was launched, observing also a supersaturated layer in about 6 km altitude (M. Fujiwara, private communication).

Observations on November 11, 2001

On November 11, 2001 the KARL has been operational during the whole day for aerosol and humidity soundings, with only minor gaps for system maintenance. The time evolution of observed parameters is displayed in Figure 2 (left and right, respectively). The left part of Figure 2 shows a maximum in water vapour mixing ratio slightly above 1 km altitude. The maximum humidity changes during the day between about 0.5 and 0.75 g/kg. The vertical extension of the humid layer as well as the gradient at the top vary strongly. After about 12 UT the water vapour concentration between 1.5 and 3 km altitude increased. The right part of Figure 2 displays the aerosol extinction coefficient for 532 nm wavelength (see Ritter et al., this

issue). A nearly aerosol free troposphere until about 12 UT is obvious from the figure. Between 15 UT and 17 UT a small but vertical expanding cloud appears above the station, affecting also the water vapour soundings. The aerosol extinction coefficient rises past 17 UT in the same altitude range as the expanded humid layer. While the humidity decreases again in the late evening of November 11, this can not be stated from the aerosol soundings.

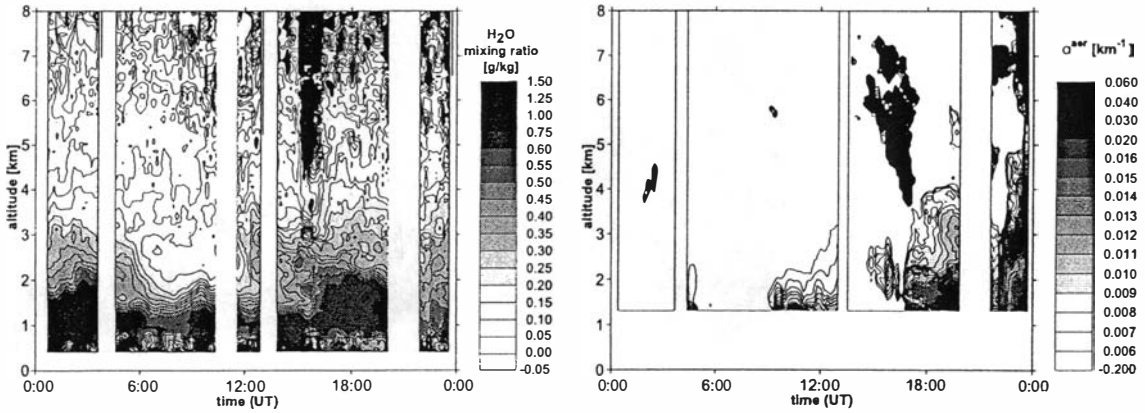

Figure 2: Water vapour mixing ratio (left) and aerosol extinction at 532 nm (right) on November 11, 2001 as observed by KARL.

Continuous records of meteorological parameters at 2 m and 10 m exhibit a decrease in temperature by about 5 K simultaneous with the water vapour increase below 3 km altitude after 12 UT (not shown here). During the whole day the pressure was rising by about 16 hPa. Despite there may be some different evolution between the temperature at ground and in the free troposphere, it seems likely that the relative humidity between 1 and 3 km rises past noon. Stationary lidar observations do not allow to separate between changes in the sounded air and advection of air masses with different properties. But the phase differences between the changes in humidity and aerosol extinction give reason for the assumption of growing aerosol particles during the increasing humidity. Of course, further analyses e.g. of the backscattered UV and IR light is necessary to prove this scenario. Trajectory calculations from European Centre for Medium Range Weather Forecast (ECMWF) analyses reveal a change in air mass origin from the Arctic Ocean to the Kara Sea during the day (not shown here).

Observations on February 28, 2002

During February 28, 2002 lidar soundings with the KARL have been performed throughout the whole day. But the humidity profiles between about 6 UT and 16 UT have been omitted in Figure 3 (left), because they are strongly affected by daylight. Figure 3 (left) shows a nearly homogenous humid layer up to 2 km altitude above the station. The mixing ratio amounts up to about 1.5 g/kg. Above 2.3 km the humidity decrease strongly, reaching less than 0.1 g/kg at 4 km altitude. The layer remains about unchanged during the first six hours of the day. Also past 16 UT the maximum of water vapour mixing ratio was about 1.5 g/kg around 1.5 km, with the upper ledge of the humid layer still near 2.5 km altitude. But now also a distinct lower ledge has been formed, with a dry boundary layer below 1 km altitude.

Meteorological ground data reveal a fast change in wind direction at 12:30 UT, succeeded by a decrease in 2 m relative humidity (Figure 3, right). The westerly wind past 4 UT comes from the direction of the Arctic Ocean, while the south-easterly wind of the afternoon has passed the mountain- and glacier-covered Spitsbergen inland. Before 4 UT the wind velocity was found very small (below 2 m/s), increasing later (not shown here).

Global weather analyses show no significant mesoscale change in wind direction because of transient weather systems. Trajectories reveal about the same path of air parcels throughout the day. The regular pressure data from Koldewey Station confirm only small changes of the air

pressure. Therefore, the wind field seem to be affected by local phenomena like e.g. air-sea interaction and orography. In turn, the lidar data show that the regional orography and the different surface conditions above the ocean and the inland are able to affect the humidity profile in the boundary layer above Ny-Ålesund. Local wind speed influences the contribution of the surface parameters to the boundary layer humidity (cp. before 3 UT).

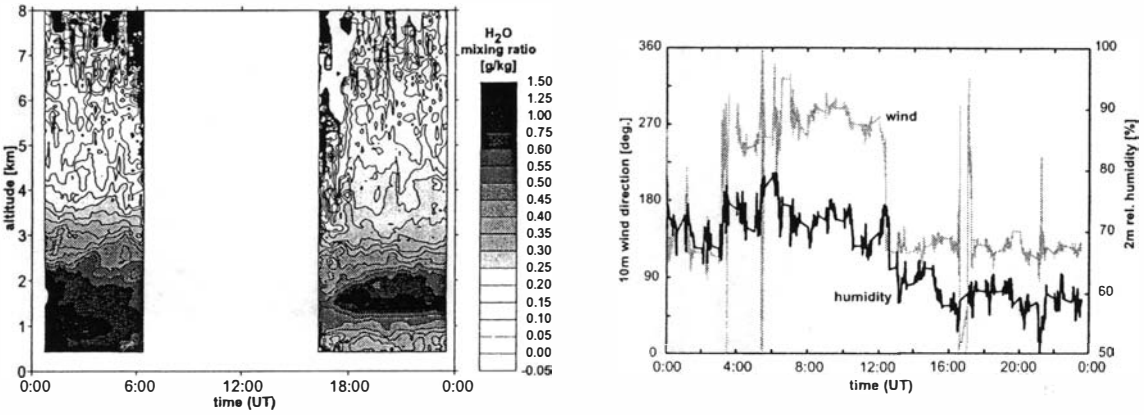

Figure 3: Water vapour mixing ratio observed by KARL (left) and wind and relative humidity from the meteorological station on February 28, 2002.

Summary

The Koldewey Aerosol Raman Lidar KARL provides atmospheric humidity data since the beginning of year 2000 in a combination of regular and intense campaign soundings. During dark conditions the profiles cover large parts of the troposphere nearly from the ground up to about 6 km altitude. The multi-wavelength detection system allows the retrieval of aerosol parameters in the UV-vis-IR range simultaneous and in a common volume with the water vapour soundings. This enables the investigation of aerosol-humidity interaction as an important parameter in the radiative budget of the Earth's atmosphere. The possible influx of local orography and surface conditions on the boundary layer humidity has been demonstrated.

References

Elliot, W. P. & Gaffen, D J. 1991: On the utility of radiosonde humidity archives for climate studies, *Bulletin of the American Meteorological Society, 72*, 1507-1520.

Harries, J. E. 1997: Atmospheric radiation and atmospheric humidity, *Quarterly Journal of the Royal Meteorological Society, 123*, 2173-2186.

Hegg, D. A., Hobbs, P. V., Gasso, S., Nance, J. D. & Rangno, A. L. 1996: Aerosol measurements in the Arctic relevant to direct and indirect radiative forcing, *Journal of Geophysical Research, 101*, 23349-23363.

IPCC 2001: *Intergovernmental Panel on Climate Change. Third Assessment Report: Climate Change 2001. WG I: The Scientific Basis, Summary for Policymakers*, Geneva, Switzerland.

Melfi, S. H., Lawrence, J. D. jr. & McCormick, M. P. 1969: Observation of Raman scattering by water vapor in the atmosphere, *Applied Physics Letters, 15*, 295-297.

Miloshevich, L. M., Vömel, H., Paukkunen, A., Heymsfield, A. J. & Oltmanns, S. J. 2001: Characterization and correction of relative humidity measurements from Vaisala RS80-A radiosondes at cold temperatures, *Journal of Atmospheric and Oceanic Technology, 18*, 135-156.

Ramanathan, V., Crutzen, P. J., Kiehl, J. T. & Rosenfeld, D. 2001: Aerosols, climate, and the hydrological cycle, *Science, 294*, 2119-2124.

Schumacher, R., Neuber, R., Herber, A., Rairoux, P. & Schrems, O. 2001: Extinction profiles measured with a Raman lidar in the Arctic troposphere. In: A. Dabas, L. Loth, and J. Pelon (eds.), *Advances in Laser Remote Sensing, International Laser and Radar Conference 2000.*

Whiteman, D. N., Melfi, S. H. & Ferrare R. A. 1992: Raman lidar system for the measurement of water vapor and aerosols in the Earth's atmopshere, *Applied Optics, 31*, 3068-3082.

The enrichment of particulate bromate (BrO_3^-) in the boundary layer of the winter and spring Arctic

Keiichiro Hara[1 (now at 2)], Kazuo Osada[1], Chiharu Nishita[1], Shinji Morimoto[2], Shuji Aoki[3], Gen Hashida[2], Katsuji Matsunaga[1], Yasunobu Iwasaka[1], and Takashi Yamanouchi[2]

1: Nagoya University, Solar Terrestrial Environment Laboratory

2: National Institute Polar Research

3: Tohoku University, Center for atmospheric and oceanic studies

Introduction: Atmospheric bromine species play important roles in atmospheric chemistry in troposphere. In particular, bromine catalytic system causes low O_3 concentration during the polar sunrise in both Arctic and Antarctica. This catalytic system involves bromine atom and bromine monoxide, as follows;

(R1) $Br + O_3 \rightarrow BrO + O_2$

(R2) $2\,BrO \rightarrow 2\,Br + O_2$.

The origins of the key species and their precursors leading to surface O_3 depletion (SOD) are believed to be the heterogeneous reactions in sea-salt particles and sea-salts on sea-ice and snow packs [McConnell *et al.*, 1992; Sumner *et al.*, 1999; Foster *et al.*, 2001; Hara *et al.*, 2002]. In addition to the SOD, particulate bromate (BrO_3^-) was recently found in the boundary layer of winter/spring Arctic [Hara *et al.*, 2002a]. Particulate BrO_3^- can be formed via the following heterogeneous reactions;

(R3) $Br^- + O_3 \rightarrow OBr^- + O_2$

(R4) $OBr^- + O_3 \rightarrow Br^- + 2O_2$

(R5) $OBr^- + O_3 \rightarrow BrO_2^- + O_2$

(R6) $HOBr + O_3 \rightarrow BrO_2^- + O_2 + H^+$

(R7) $HOBr \leftrightarrow H^+ + BrO^-$

(R8) $2BrO + H_2O \rightarrow BrO^- + BrO_2^- + 2H^+$

(R9) $BrO_2^- + O_3 \rightarrow BrO_3^-$

(R10) $BrO_2^- + CO_3^- \rightarrow BrO_2 + CO_3^{2-}$

(R11) $2BrO_2 \leftrightarrow Br_2O_4$

(R12) $Br_2O_4 + OH^- \rightarrow BrO_3^- + BrO_2^- + H^+$

(R13) $HBrO_3\,(g) \rightarrow H+ + BrO_3^-$.

Although Br^-, HOBr, BrO and $HBrO_3$ are identified as possible precursors of BrO_3^- (R3~R13), suggested the largest contribution of BrO in BrO_3^- formation was suggested owing to quite larger reaction velocity of R8 ($K=4.9\times10^9\ M^{-1}\ S^{-1}$ at 293 K) [Hara *et al.*, 2002]. However, the contribution of $HBrO_3$ (g) is still unknown. Despite less information of photolysis rate of BrO_3^- as far as we know, photochemical decomposition of BrO_3^- can lead to form reactive halogen species (e.g., Br_2 and BrO) bromine radicals (e.g., BrO and BrO_3) in aqueous phase [Zuo and Katsumura, 1998]. As BrO_3^- formation and decomposition have close relationship to other atmospheric reactive bromine species, some contribution of BrO_3^- to atmospheric bromine cycle is expected in the boundaly later of winter/sprig Arctic. The present study will focus on variation of BrO_3^- concentration from winter until polar sunrise.

Sample and analysis: Sampling of atmospheric aerosol particles and acidic gases were carried out at Ny-Ålesund, Svalbard (78°55'N, 11°56'E) from early-January until the end of April in 2000. Non-size-segregated aerosol particles and acidic gases were collected using filter holder (NILU) with 47 mm Teflon membrane filter with 1.0 μm pore size (PTFE, Advantec) in series of 2-stage alkaline (1 wt% Na_2CO_3 + glycerol) impregnated filters for one day (January~March) and half day (April). Filter holder was set outside and supported downward facing in weather shields at a height of 5 m from snow surface because of collection of the atmospheric samples under ambient temperature, and because of the reduction of volatilization of thermally unstable species such as ammonium nitrate. After sampling, each filter was kept into polypropylene 15 ml centrifuge vial with airtight cap, immediately, in order to prevent from contamination during the sample storage. Sample vials were packed in polyethylene bags and were kept at about –20 °C in a freezer until chemical analysis in Japan. After extraction by ultra pure water (Milli-Q water, 18.3 MΩ), each constituent was determined with ion chromatography. **Results and Discussion:** As shown in Figure 1, particulate BrO_3^- concentration ranged from below-determination-limit (BDL; 0.01 nmol m^{-3}) to 0.3 nmol m^{-3}. Mean BrO_3^- concentration was about 0.02 nmol m^{-3} before local polar sunrise (LPS: DOY=61.5), whereas about 0.01 nmol m^{-3} after LPS. However, background BrO_3^- concentration (not including several BrO_3^- peaks) after LPS showed mostly BDL. This obvious contrast of mean BrO_3^- concentration strongly suggests preferential photolysis of BrO_3^- and its precursors such as BrO and HOBr after LPS. Two high g_Br concentration events were observed in DOY= 99.3~102.6 and

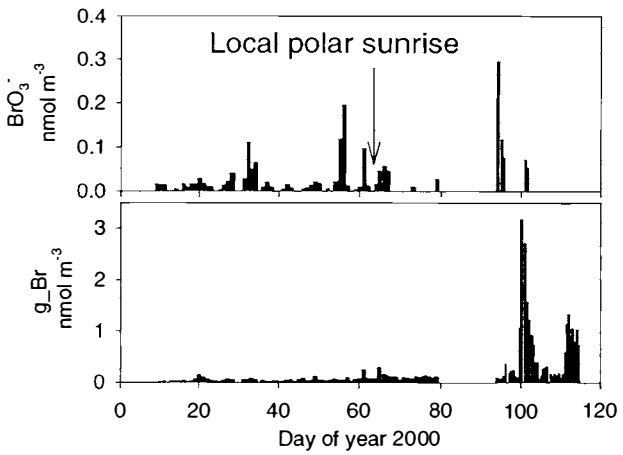

Figure 1. Variarions of the concentration BrO_3^- and gaseous inorganic bromine species (g_Br).

110.9~114.7 under the SOD conditions in Ny-Ålesund. Although high BrO_3^- concentration events were often observed, obvious increase of g_Br (HX, HOX, XNO_2, XY, X_2, $XONO_2$ and XNO; X or Y = Cl or Br) was not obtained in high BrO_3^- concentration. In order to know the origin of BrO_3^- rich air mass, backward trajectories were calculated. Typical examples of the backward trajectory [NOAA; Hysplit 4] were shown in Figure 2. Each BrO_3^- rich air mass was transported from the Arctic Ocean covered with sea-ice (Fig. 2a). Although the end points in each 4-day backward trajectory were distributed in different geographical locations (Figure 2a), vertical transport from either upper boundary layer (UBL) or lower free troposphere (LFT) over the Arctic Ocean covered with sea-ice was obtained as common trend (Figure 2b~d). In particular, air mass with the highest BrO_3^- enrichment on 3~4 April (DOY=93.6~94.3) originated in the LFT (~3000m) of the Arctic Ocean. Lower sea-salt (Na^+) concentration and higher O_3 concentration in DOY=93.6~94.3 support this trajectory result. In other periods (1~4 February, DOY=31.5=34.1; 5~8 March, DOY = 63.8~67.1), BrO_3^--rich air masses were also transported from the LFT and UBL (~2300m). Although, in the present study, direct evidence of vertical transport of BrO_3^- rich air mass is only backward trajectory, obvious vertical mixing was not observed in background BrO_3^- concentration level (~0.02 nmol m^{-3}). Thus, enrichment of BrO_3^- and its precursors is expected to be in LFT and UBL in the winter/spring Arctic troposphere.

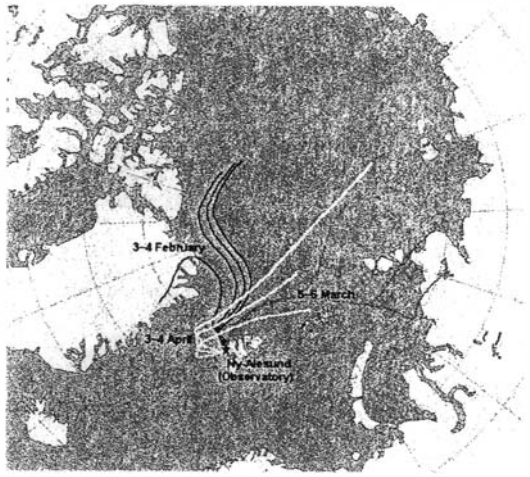

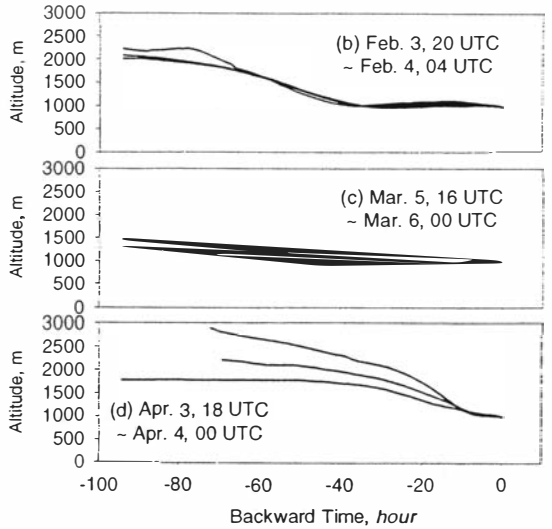

Figure 2. Backward trajectory during the periods with higher BrO_3^- concentrations. (a) Geographical location (black line, 3~4 February; gray line, 5~6 March; white line, 3~4 April), and height features (b) on 3~4 February, (c) on 5~6 March and (d) on 3~4 April.

The BrO_3^- enrichment in the UBL and LFT might strongly relate to the BrO_3^- formation through the heterogeneous reactions (R3~R12) during the transport, and to the vertical profiles of BrO_3^- precursors such as BrO. As mentioned above, the heterogeneous reactions of BrO may make a significant contribution to BrO_3^- formation. Tropospheric BrO profile in the Arctic winter (February) and spring suggested higher BrO concentration in the UBL ~ LFT (2~4 km) [McElroy *et al.*, 1999; Fitzenberger *et al.*, 2000]. In addition, vertical gradient of bromine activation from aerosols was suggested to lead to high mixing ratio of reactive species such as BrO at the UBL [von Glasow and Sander, 2001; Hara *et*

al., 2002c]. If this higher BrO concentration in UBL and LFT is a typical BrO profile in the winter/spring Arctic troposphere, higher BrO concentration may cause BrO_3^- formation in the UBL and LFT in the winter/spring Arctic during the transport.

Acknowledgement: The authors are grateful to Y. Fujitani, the staff members of Kings Bay Kull Company for help of sampling at Ny-Ålesund. This study was supported by the Ministry of Education, Arts, Science and Culture, Japan (No. 09041104 and 11208201) and Resarch Fellowship of the Japan Society for the Promotion of Science for Young Scientists.

References

Fitzenberger *et al.*, First profile measurements of tropospheric BrO, ***Geophys. Res. Lett., 27***, 2921-2924, 2000.

Foster *et al.*, The role of Br_2 and BrCl in surface ozone destruction at polar sunrise, ***Science, 291***, 471-474, 2001.

Hara *et al.*, Atmospheric inorganic chlorine and bromine species in Arctic boundary layer of the winter/spring, ***J. Geophys. Res.,*** in press., 2002a

Hara *et al.*, Vertical features of sea-salt modification in the boundary layer of spring Arctic during the ASTAR 2000 campaign, ***Tellus, 54, 361-376, 2002***2002b

McConnell *et al.*, Photochemical bromine production implicated in Arctic boundary-layer ozone depletion, ***Nature, 355***, 150-152, 1992.

McElroy *et al.*, Evidence for bromine monoxide in the free troposphere during the Arctic polar sunrise, ***Nature, 397***, 338-341, 1999.

Sumner *et al.*, Snowpack production of formaldehyde and its effect on the Arctic troposphere, ***Nature, 398***, 230-233, 1999.

von Glasow and Sander, Variation of sea-salt aerosol pH with relative humidity, ***Geophys. Res. Lett., 28,*** 247-250, 2001.

Zuo and Katsumura, Formation of hydrated electron and $BrO_3^{\bullet}$ radical from laser photolysis of BrO_3^- aqueous solution, ***J. Chem. Soc. Faraday Trans., 94***, 3577-3580, 1998.

Occurrence and Optical Properties of Tropospheric Aerosol

Christoph Ritter, Roland Neuber, Michael Gerding

Alfred Wegener Institute for Polar and Marine Research, Research Department Potsdam,
D-14473 Potsdam, Germany, critter@awi-potsdam.de

Introduction and Motivation

The main purpose of the tropospheric aerosol project is the examination of the optical properties of aerosols, mainly using the Koldewey Aerosol Raman Lidar (KARL), to constrain their still unknown impact on climate modelation. Especially we are interested in Arctic Haze. However, in spite of extended observing sessions this year's spring from mid February to mid May only in the lowest 3km of the troposphere pronounced Arctic Haze events have been recorded whose backscatter-signal monotonically decreased with height. On the other hand, frequently cirrus clouds have been seen in our data. Apart from these clouds the higher troposphere generally appeared considerably clear. For this discussion some typical days with characteristic Lidar signals have been selected.

Technical Description

All Lidar data have been recorded with KARL. In this article focus is laid to the 532nm laser wavelength which can be recorded in the original, linear state of polarisation of the Nd:YAG laser, as well as linear perpendicular to it. Moreover another Rayleigh backscatter-signal at 1064nm and a 607nm line of Nitrogen Raman backscatter have been obtained. The KARL consists of two different telescopes which look at the laser beam at slightly different angles. A larger mirror of 30cm diameter serves for detecting the long range and lacks any incomplete overlapp above some 1200m height, a smaller 10cm mirror is adjusted such as to record the lower troposphere and delivers useful data above approximately 400m. More details about the KARL might be found in Gerding et al., 2002.

The elastic backscatter (Rayleigh) profiles have been evaluated according to Klett (Klett, 1981 and Klett, 1985). Thereby a Lidar Ratio (LR:= extinction / backscatter of the aerosols) of 40 has been assumed. The solutions depend only slightly on this value, however. Independently aerosol extinction was derived from the inelastic Raman backscatter at 607nm using Ansmann's formula (Ansmann et al., 1992).
Recall that the Raman evaluation depends on the derivative of a small signal and is therefore severely effected by noise. Thus, we restrict ourselves of processing data obtained under night-time conditions (minimal sky-glow background) with a sufficient long temporal smoothing. Finally, the extinction profiles have been further smoothed in normal (not in Fourier) space, because different SNR (Signal to noise ratio) and, maybe, physical conditions of absorbers should lead to a power spectrum that depends on height. Synthesized profiles of extinction- and backscatter coefficients have been generated by merging the two telescopes' solutions in the height interval between 2km and 5km, where both the small and the large mirror should have seen the same unbiassed signal with a sufficient SNR.
The small 10cm telescope cannot record the infrared 1064nm line and hence results in this colour only are plotted above 1200m.

Observations and Results

Two different phenomena of backscatter-signal have been derived this spring: First of all a surface layer which generally does not vary noticeably in time and, second, cirrus clouds. We

will discuss the results for some typical days who shall give a general idea of backscatter- and extinction coefficients recorded by KARL.
On March 5th a clear, stratified and with height monotonically decreasing surface-layer was visible the whole day. Assuming a Lidar Ratio of 40 the layer has an optical depth of 0.1 at 532nm wavelength.
Apart from this feature the morning seemed very clear, judged from the 532nm light in the laser's polarisation, but in the afternoon an extended structure of increased backscatter formed (Figure1).
Our Lidar-data suggest that this cloud does show a slightly distinct physical nature compared to the surface layer: Figure 2 shows the ratio of the polarisation states of the aerosol backscatter coefficient. The state of polarisation perpendicular to the laser is divided by the one parallel to it. According to Mie's theory spherical particles do not alter the polarisation of a light beam. Hence this quotient is a measure of the deviation of the particles' shape from sphericity. It is evident from Figure 2 that the surface layer (SL) below 3km height does only show a slight increase of backscattering in the perpendicular polarised light. Therefore these particles are more spherical. Contrary, in the cloud the backscatter of this perpendicular state of polarisation exceeds the parallel state by a factor 10 to 100.

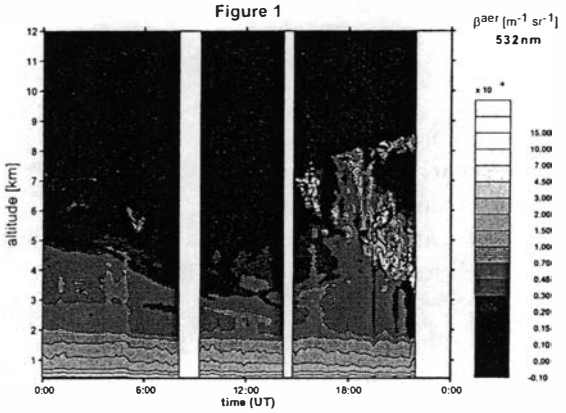

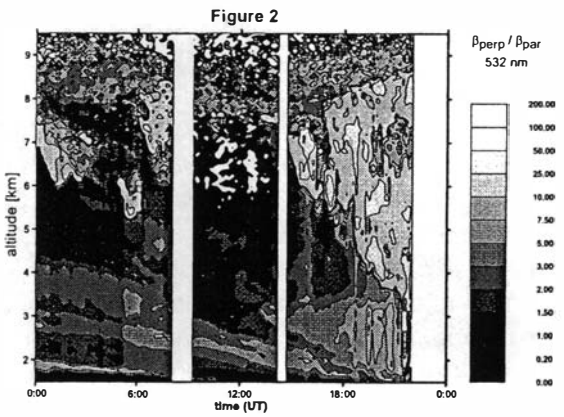

March 5th: backscatter coefficient in laser polarisation *and ratio perpendicular divided by parallel*

An idea of the particles size might give Figure 3: There the ratio of backscattering in 1064nm wavelength divided by the backscattering at 532nm is plotted. Again, the highest values are only found in the cloud, not in the SL. The interaction between light and matter depends on the size of the particles compared to the wavelength: A higher interaction at longer wavelength is characteristic for larger particles.
It might be worth to mention that even in the morning between 0UT and 6UT as well in the perpendicular polarised as in the 1064nm light between 5km and 7.5km some activity is visible, which is only inconspicuous in parallel backscatter (Fig. 1).
The optical depth in 532nm is presented in Figure 4. The higher boundary of the SL was arbitrarily set to 3km height, according to Figure 1. An optical depth of 0.1 still might be considered as a clear atmosphere, but this value depends on the LR. In the cloud the optical depth is one order of magnitude higher and more variable in time.
Therefore we conclude that this day two different backscattering layers are effective. First, the in time only slowly variable surface layer, containing smaller and more spherical particles. And second the dynamical cloud formed by larger, non-spherical particles giving rise to a strong backscatter signal.
Taking into account these attributes, the cloud seems to be most probably an ice-cirrus.
General appearance of our Lidar profiles was very similar for March 6th and 7th, hence we will not repeat all the details here for brevity. On March 6th the SL only was confined to the lowest

2km of the troposphere with an optical depth of 0.13 at 532nm at an LR of 40 (This corresponds to 0.26 at an Lidar Ratio of 80). A persistent cloud layer between 4km and 8km height was visible with an optical thickness 20 times larger than that of the surface layer.
On March 7th the SL covered the lowest 2.5 km with an optical depth around 0.16 (LR=40).

Figure 3

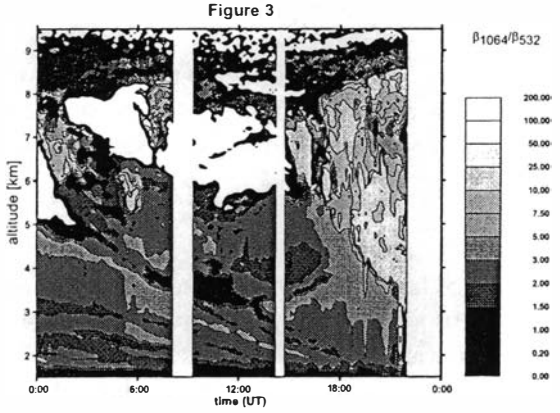

March 5th: ratio backscatter coefficient at 1064nm / 532nm

Figure 4

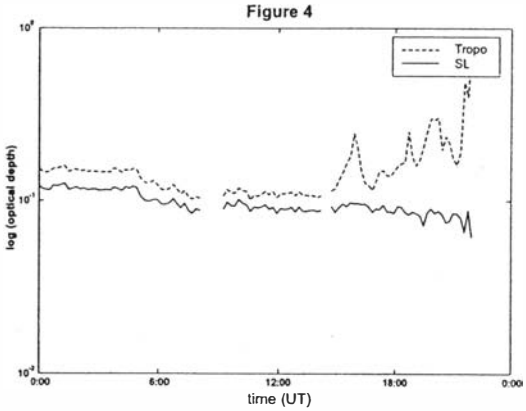

optical depth of surface layer(SL) and cloud

Mighty cloud layers between 4km and 8km height also were visible on March 8th and 9th. However, the optical depth seemed to be so high that one of the lidar's primary assumptions of single scattering surely was violated. Therefore we do not discuss these days further and just remark that a surface layer below 2km seemed to be present again.
After two days of completely cloudy skies (inappropriate weather conditions for a Lidar), March 12th gave an opportunity for a short observation with the sun being some 18 degree below the horizon. (This means astronomical darkness). Only a stable aerosol layer was visible (Figure 5). This nearly time-independent condition allowed us to compare the results of the Rayleigh evaluation of Klett's algorithm with the extinction derived from the Raman wavelength.
According to Figure 6, the Klett solution only marches the extinction coefficient calculated from the Raman-line, if a considerable high Lidar Ratio of 60 is applied. This result is remarkable for it disagrees with the low Lidar Ratios of approx. 15 for cirrus and 25 for sea-salt particles, but coincides flawlessly with anthropogenic pollutants or mineral dust. The latter one seems to be very unlikely in March of course. Hence we must take into account the possibility, that this material is of non-natural origin. Total optical depth sums up to 0.3 in the troposphere

Figure 5

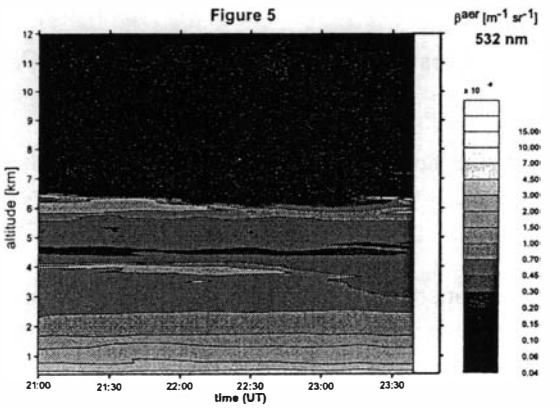

backscatter coefficient at 532nm

Figure 6

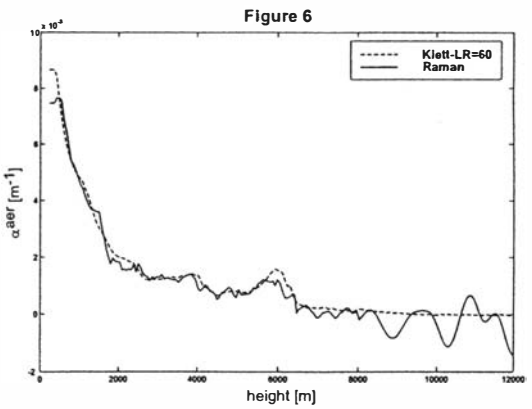

extinction profile: Klett (LR=60) versus Raman method

at 532nm at the stated LR; above 3km height the optical depth decreases to 0.09. Generally we found highest aerosol loading in the lowest troposphere.
This might be of interest for the influence on the climate is determined by the heigth of the highest layer of aerosols according to Quijano et al. (2000).

This finding of a persistent and hardly time-variable aerosol layer confined to the lowest 3km is not fully consistent to the results of the ASTAR campaign in 2000 at first glance (Schumacher, 2001).
That year aerosol contamination was more variable and spread all heights up to 7km. However, it should be stressed that for this work also days with cirrus occurence have been selected. Moreover all days since March 1st were characterized by very slow (around 2m/sec) wind from changing, but predominantly southern directions.

Summary and Conclusion

This March we have frequently seen a persistent surface layer of increased backscatter signal. It seems to consist of small, spherical particles which absorb light very effectively, with a Lidar Ratio around 60. The total optical depth of this layer was measured to be some 0.3 at green light. Above this layer, between 4km and 8km height, cirrus clouds consisting of strong depolarising particles are common. Apart from these the middle and high troposphere showed up to be generally very clear.
In the future we want to pay attention especially to the lowest troposphere (planetary boundary layer). Therefore we intent to correct all of the various channels of KARL by their geometrical compression. Moreover, we want to include sun- and star photometer measurements to our Lidar data. Due to the clear importance of the lowest 2km we support the installation of another photometer at the Zeppelin mountain. Comparing its results to the data obtained at the Koldewey station, an estimation of the ground layer also should be possible.

References

Ansmann, A.; Wandinger, U.; Riebesell, M. & Weitkamp, C. 1992: Independent measurements of extinction and backscatter profiles in cirrus clouds by using a combined Raman elastic-backscatter Lidar *Applied Optics* 31, 7113-7131 (1992)

Gerding, M; Ritter, C. & Neuber, R. 2002: Tropospheric water vapor observations by ground-based lidar *this edition*

Klett, J. D. 1981: Stable analytical inversion solution for processing lidar returns. *Applied Optics* 20, 211-220

Klett, J.D. 1985: Lidar inversions with variable backscatter/extinction values. *Applied Optics* 24, 1638-1648

Quijano, A. L.; Sokolik, I. N.; Toon, O. B. 2000: Radiative heating rates and direct radiative forcing by mineral dust in cloudy atmospheric conditions. *Journal of Geophysical Research* 105, 12207-12219

Schumacher, R. 2001: Measurements of optical properties for tropospheric aerosols in the arctic. *Reports on Polar and Marine Research by Alfred-Wegener-Institute*, Potsdam Dissertation (in German language)

Characteristics of different solid PSC particles observed by lidar in Ny-Ålesund

Marion Müller [1], Roland Neuber [1] and Stefan Fueglistaler [2]

(1) Alfred Wegener Institute for Polar and Marine Research, Telegrafenberg A43, D-14473 Potsdam, Germany. E-mail: mmueller@awi-potsdam.de, phone + 49 331 2882166

(2) Institute for Atmospheric and Climate Science, ETH Zürich, Hoenggerberg HPP, CH- 8093 Zürich, Switzerland. E-mail: stefanf@atmos.umnw.ethz.ch, phone + 41 633 40 63

Abstract

Stratospheric lidar observations from Ny-Ålesund are presented, revealing different characteristics in backscatter ratio and depolarisation of solid polar stratospheric clouds (PSCs). The focus is drawn to PSC type I a with strong depolarisation, which is analysed in terms of lidar parameters and further examined using T-matrix calculations. It is found that the strong depolarisation seem to be linked to a high non-sphericity of the PSC particles.

Introduction

Polar stratospheric clouds (PSCs) play a crucial role for the stratospheric ozone layer in the polar regions (*Solomon, 1999, and references therein*). Their various forms of appearance - e.g. the state of aggregation and size of their particles- have a decisive influence on the amount of activated chlorine leading to ozone destruction.

At the NDSC primary station Ny-Ålesund, Spitsbergen (79°N, 12°E), lidar measurements of polar stratospheric clouds have been performed since 1991/1992. Liquid (spherical) and solid (non-spherical) PSC particles are identified by their depolarisation signal. Both liquid and solid as well as mixed-phase clouds are commonly observed in Ny-Ålesund. While liquid cloud particles have a larger direct effect due to high activation rates (*Ravishankara and Hanson, 1996*), solid particles can have serious consequences via sedimentation and thus denitrification (*Waibel et al., 1999; Fahey et al., 2001*). Accordingly, the effect of solid PSCs on ozone loss strongly depends on the particle size. From the long-term Ny-Ålesund lidar dataset, solid PSCs with different particle properties can be distinguished. Noteworthy is the occurrence of solid PSCs with an exceptional high depolarisation that has been observed in some cases. These strongly depolarising PSCs are analysed in terms of their occurrence frequency, lidar parameters and context to other solid PSC particles, e.g. PSC type I a 'enhanced'. The measurements are further investigated using T-matrix calculations to retrieve information on size, number density and shape of the cloud particles.

Observations

If the according stratospheric temperatures conditions are met, solid PSCs are frequently observed by the Ny-Ålesund lidar system. Even if the *PSC type II* (consisting of water ice) has never been detected, the observations of the solid *PSC type I a* show a large variability in terms of the measured parameters, as shown in the examples of Figure 1.

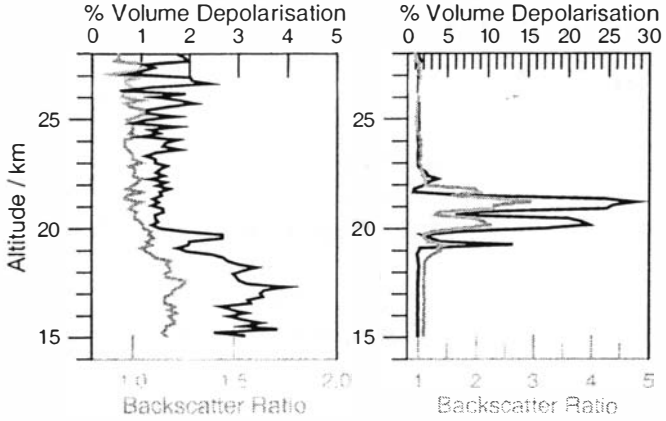

Fig.1: Backscatter Ratio (*grey line*) and volume depolarisation (*black line*) of different solid PSC observations. *left:* common PSC I a on January 31, 2000, 10-min-integration at 08:11 UTC. *right*: PSC I a with strong depolarisation on January 25, 2000, 10-min-integration at 01:04 UTC.

The events of solid PSC occurrence can be classified in different categories according to their backscatter ratio and volume depolarisation (Fig.2). While the common *PSC I a* reveal low backscatter ratio around R = 1.3 and a volume depolarisation up to δ_{VOL} = 10-15 %, the *PSC I a enhanced* generate a higher backscatter ratio of up to around R = 8 as well as a higher volume depolarisation. Nevertheless, some events are outstanding of this classification. They are described as *PSC I a with strong depolarisation*, which are characterised by a backscatter ratio up to R = 2-3 and a very high volume depolarisation up to δ_{VOL} = 35-40 %.

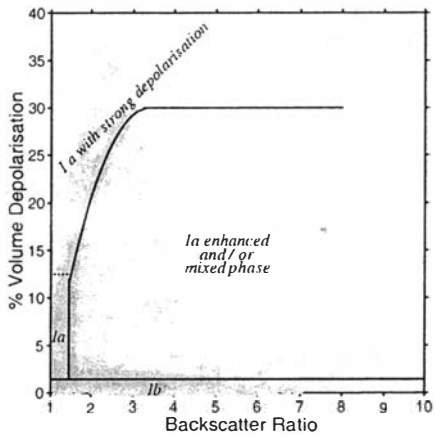

Fig. 2: All Ny-Ålesund PSC measurements at λ = 532nm since winter 1994/1995. Each datapoint represents a PSC signal in a 10-min-datafile with a vertical resolution of Δz = 150m (from 1997 onwards) or 250m (before 1997).

Within the large dataset of stratospheric lidar, two main episodes of these *PSC I a with strong depolarisation* occurred: December 21-23, 1995, and January 25-27, 2000. Concerning the aerosol depolarisation (Fig.3), these PSC particles seem to present an upper limit to the *PSC type I a enhanced* which is characterised by a higher backscatter ratio.

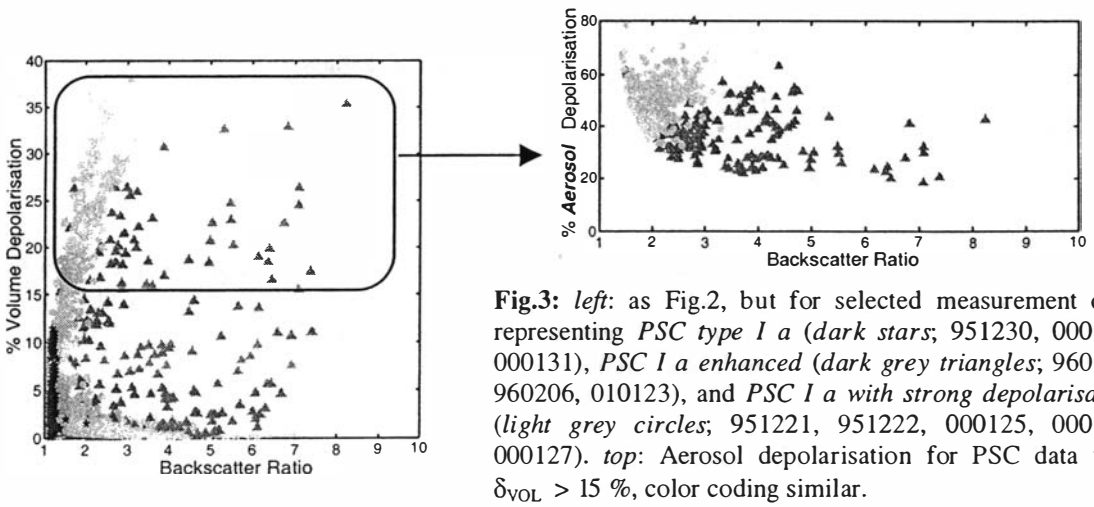

Fig.3: *left*: as Fig.2, but for selected measurement days representing *PSC type I a* (*dark stars*; 951230, 000129, 000131), *PSC I a enhanced* (*dark grey triangles*; 960105, 960206, 010123), and *PSC I a with strong depolarisation* (*light grey circles*; 951221, 951222, 000125, 000126, 000127). *top*: Aerosol depolarisation for PSC data with δ_{VOL} > 15 %, color coding similar.

It is imaginable that the strong depolarisation is linked either to the size, the number, the shape or the composition of the particles. The measured multi-wavelength lidar parameters allow a first estimation, as the color ratio $C_{532/353} = (R_{532} - 1 / R_{353} - 1)$ gives an indication of the particle size. For particles with $r >> \lambda$, the color ratio $C_{532/353}$ is expected to approach the normalized value 1. In this context, Fig.4 shows that for the strong depolarising PSC events the solid particles are the larger, the stronger their depolarisation.

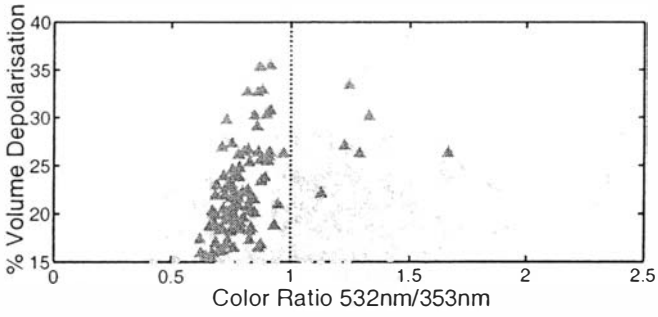

Fig.4: Volume depolarisation (δ_{VOL} >15 %) and color ratio $C_{532/353}$ of the *PSC I a with strong depolarisation* (*light grey circles*) and the *PSC I a enhanced* (*dark grey triangles*).

T-Matrix Results and Discussion

To retrieve further information on the particle size as well as on number density and particle shape, the measurements are further investigated using the T-matrix methode.

T-matrix calculations were performed based on the two used lidar wavelengths 532nm and 353nm. Different amounts of HNO_3 bound in the particles were assumed, and the resulting possibilities for particle radius and number density were retrieved for different aspect ratios (AR). Finally, the theoretical results were combined with the detected lidar parameters.

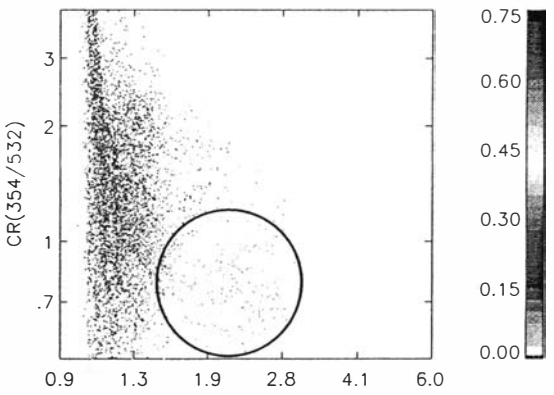

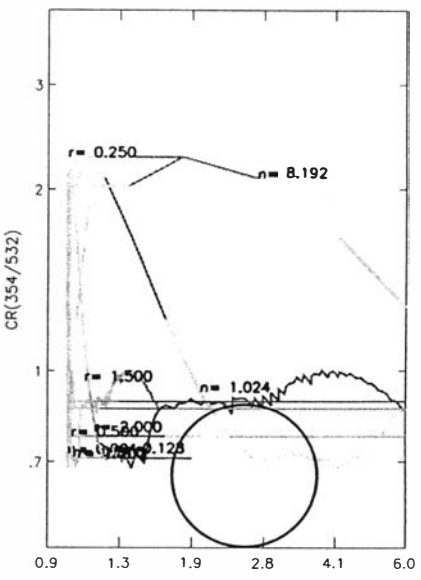

Fig.5: *top*: Color ratio $C_{353/532} = (R_{353} - 1 / R_{532} - 1)$ versus backscatter ratio for the examples of PSC I a with strong depolarisation. The grey scale marks aerosol depolarisation, and the highest depolarisation is found in the region within the circle. *right:* Result of T-matrix calculations for aspect ratio AR = 0.65. Again, the circle marks the region that best represents the measurements of *PSC I a with strong depolarisation*.

For the presented case study of different solid PSCs, the combination of lidar backscatter ratio, depolarisation and color ratio with the T-matrix calculations reveals that the particle size of the different PSC groups is rather similar. Differences seem to occur in the shape of the particles.

While the particles of the *common PSC type I a* are nearly spherical, the particles of *PSC type I a enhanced* are best simulated with an aspect ratio of AR = 0.85. The *PSCs I a with strong depolarisation* are best presented by the T-matrix simulations with an aspect ratio of AR = 0.65 or 0.75 (Fig.5). The strong depolarisation thus seems to be linked to a high non-sphericity of the particles. The considerations are limited by the fact that the T-matrix calculation is based on spheroids which describe only a limited prototype for NAT particles and cannot reproduce the full range of observations.
The difference in sphericity of the particles may be caused by a different growth process of the particles which is related to the temperature history and the amount of the available HNO_3 and H_2O. Trajectory calculations also have been performed (not shown here), but no remarkable differences in the PSC temperature histories can be found. The possible involvement of non-resolved leewave temperature fluctuations can not be excluded.

Summary

Solid PSCs with different backscatter and depolarisation characteristics have been observed by lidar in Ny-Ålesund. The PSC I a with strong depolarisation are of special interest because of the possibility that they are composed of large particles leading to denitrification.
While the detected lidar parameters allow only a rough estimation of the particle size, theoretical models like T-matrix calculations help interpreting the lidar observations in terms of particles size, number density and shape of the particles. It is found that the strong depolarisation of the PSCs is rather caused by high non-sphericity than by increased size of the particles. The T-matrix calculations fit the observations of PSC I a with high depolarisation best at an aspect ratio of AR = 0.65. Still there are limits to the described method, as the particles in the T-matrix model are represented by spheroids.
Temperature trajectories did not reveal a different temperature history for different depolarisation behaviour, but as the trajectories are based on synoptic scale analyses they might miss mesoscale effects of e.g. mountain gravity waves. Although T-matrix calculations broaden the conclusions following from lidar observations, the microphysical reason for the large depolarisation and thus the non-sphericity of the particles could not be found on the basis of lidar data and temperature trajectories.

References

Fahey, D.W., et al. 2001: The detection of large HNO_3-containing particles in the winter Arctic stratosphere. *Science 291*, 1026-1031

Ravishankara, A.R. & Hanson D. R. 1996: Differences in the reactivity of type I polar stratospheric clouds depending in their phase. *Journal of Geophysical Research 101*, 3885-3890

Solomon, S. 1999: Stratospheric ozone depletion: a review of concepts and history. *Reviews of Geophysics 37*, 275-316

Waibel, A.E., Peter T., Carslaw K. S., Oelhaf H., Wetzel G., Crutzen P. J., Pöschl U., Tsias A., Reimer E. & Fischer H. 1999: Arctic ozone loss due to denitrification. *Science 283*, 2064-2069

European Network for Arctic-Alpine Multidisciplinary Environmental Research – ENVINET: Coordination and harmonisation of research, facilities and services among environmental research infrastructures in Europe.

Jon Børre Ørbæk

Norwegian Polar Institute, Polar Environmental Centre, N-9296 Tromsø, Norway. E-mail: jonbo@npolar.no, phone/fax: +47 79 02 26 21/26 04

Introduction

ENVINET is an *Infrastructure Co-operation Network* focussing on multidisciplinary environmental research in Europe. The network brings together operators and users of marine, terrestrial and atmospheric research infrastructures for the main purpose of fostering new cross-discipline and cross-infrastructure collaboration among the partners in order to improve the research and monitoring programs and the basic understanding of processes involved in environmental change.

The network is funded under the action "Enhancing Access to Research Infrastructures" of the "Human Potential Programme" (IHP) of the European Community (EC) 5th framework program. The duration is May 2000- April 2003. The Norwegian Polar Institute is the responsible co-ordinator of the network and hosts the secretariat. ENVINET involves representatives from 17 European research infrastructures and 3 international organisations. The members come from Norway, Sweden, Denmark, Finland, United Kingdom, Ireland, Germany, Italy, France, Austria and Belgium. Table 1 shows the current list of the members and research stations of ENVINET.

The participating research infrastructures are located along a latitudinal gradient from the European Alps to the Arctic. They cover a broad range of environmental sciences within atmospheric physics, atmospheric chemistry, marine- and terrestrial biology. The network address environmental change under the following fields:

- Climate change and ecosystem response,
- Ozone, UV-radiation and biological effects,
- Long range transport of pollutants and eco-toxicology.
- Biodiversity

Purpose and Objectives

ENVINET shall contribute to improve the quality and the quantity of the European environmental research in order to increase the understanding of processes involved in environmental changes and to monitor such changes. An important goal of the new collaboration is related to the improvement and harmonisation of data sets, analyses tools and measurement protocols, quality assurance and instruments. The general purpose is to spread good practice and make observations and data inter-comparable across the sites. Working groups elaborate on specific scientific and technical projects related to the documentation of research projects and infrastructure, the management of the research infrastructures and the harmonisation and improvement of observations, data and methods.

Research Infrastructure	Participating Organisation	Responsible Scientist
Sverdrup Research Station, Ny-Ålesund LSF	Norwegian Polar Institute, Norway	Jon Børre Ørbæk
Kristineberg Marine Research Station	University of Gøteborg, Sweden	Odd Lindahl
Bergen Marine Food Chain Res. Infrastructure	Universitetet i Bergen, Norway	Dag Aksnes
Dunstaffnage Marine Laboratory	The Scott. Ass. For Marine Science, Scotland	Graham Shimmield
Zackenberg Field Station	Dansk Polarcenter, Denmark	Morten Rasch
Abisko Scientific Research Station	Royal Swedish Academy of Sciences, Sweden	Terry Callaghan
Station Alpine du Lautaret / Chalet Lab.	Univ.Joseph Fourier – Grenoble, France	Serge Aubert
Harland Arctic Station, Ny-Ålesund LSF	Natural Environment Res. Council, England	Liz Morris
Alomar Observatory	Andøya Rocket Range, Norway	Michael Gausa
High Alpine Research Station of Jungfraujoch	Belgian Inst. Of Space Aeronomy, Belgium	Martine de Maziere
Kiruna Observatory	Swedish Inst. Of space Physics, Sweden	Kerstin Stebel
Koldewey Station, Ny-Ålesund LSF	Alfred Wegener Institute, Germany	Roland Neuber
Sodankylae Observatory	Finish Meteorological Institute, Finland	Esko Kyrö
Sonnblick Observatory	Vienna Univ. of Technology, Austria	Hans Puxbaum
Mace Head Field Station	National Univ. of Ireland, Galway, Irland	S. G. Jennings
Arctic Station Dirigibile Italia, Ny-Ålesund	Conciglio Nazionale delle Ricerche, Italy	Roberto Azzolini
Zeppelin Air Monitoring Station, Ny-Ålesund LSF	Norwegian Institute of air research, Norway	Roland Kallenborn
IASC	Internat. Arctic Science Committee, Norway	Odd Rogne
AMAP	Arctic Monit. And Assessment Prog., Norway	Lars-Otto Reiersen
SCANNET	Scan Tran Network, Sweden	Margaretha Johansson

Table 1: Current member list of ENVINET Research Infrastructures and member organisations.

Technical Tasks

In order to create a forum for scientific and technical collaboration and exchange between the infrastructures and between the infrastructures and their users, the network established 3 working groups (Marine, Terrestrial and Atmospheric). The groups are elaborating on a number of technical tasks related to the identification of the needs for harmonization of methodology, protocols, instruments, data-formats, "representativeness" and "complementarity" at and among the research infrastructures. Some tasks aim at facilitating better exchange of information and communication between the participating research infrastructures and between the infrastructures and their users, by documenting the basic infrastructure and services at the different sites as well as the previous and existing research projects. A station managers forum is established as a tool for the infrastructure operators for the spreading of best practice and information exchange between the inhomogeneous set of member infrastructures.

The following list presents the set of technical tasks that are currently elaborated in multidisciplinary working groups under ENVINET:

- Site Specific Information online search engine: Searchable database tool with documentation of basic infrastructure characteristics.
- Project Database online search engine: Searchable database tool with documentation of previous and current research and monitoring projects.
- Station Managers Forum: Site Management at the ENVINET Research Infrastructures
- Guidelines for use of meteorological/climatological data within ENVINET
- Long Range Transport of Pollutants and Boundary Layer Exch. in Arctic Alpine Regions
- Ozone/UV-rad. and effects; Harmonisation of data, projects and instrum. at ENVINET sites
- Meta Database of climatic data and biological measurements at the ENVINET sites
- Routines for collection of marine environmental data at the ENVINET sites
- Chemistry in and Above Snow: Documentation and recommendation of coord. Measurem.
- Harmonisation and intercomparison of stratospheric aerosols remote sensing measurem.

Station Managers Forum

The main idea of the Station Manager Forum is to identify the common practices of operation among the research infrastructures and to discuss how they are handled at the different stations. The project will produce a report/manual with a list of good advices, ideas and best practices for station management at the ENVINET-sites, with the main aim of improving the quality of services and infrastructure by spreading information among the infrastructure operators. The station managers are the ones responsible for practical management of the field stations. Although each station is unique, there are a lot of issues relating to the management of the stations that are common. The stations cover very different science issues, and the operation of the stations are practised very differently. Some stations are only manned during the field season, other stations are manned year round. Some stations are managed by scientists, others are not. Important questions that are addressed are related to station marketing, application forms for scientists visiting the stations, registration of projects (project databases), procedures for registration of disturbances or manipulations carried out by research projects, facilitating cross-disciplinary cooperation between scientists visiting the stations, procedures for handling scientists wishes at the stations, general services to the user community.

Online Search Engines: Site Information and Project Database Tools

For the purpose of improving the exchange of information and coordination among the research sites, ENVINET has established 2 online search engines for basic information about sites and research projects. The tasks and objectives of this project are:

- To establish a database to hold general information about ENVINET associated research facilities, the ENVINET Site Specific Information (SSI) database, and to make the content of this database available on the Internet.
- To adapt the AMAP Project Directory (PD) system to also hold ENVINET project descriptions, the ENVINET Project Directory. The Project Directories are implemented as an online database system. The ENVINET PD comprises as a subset of the records within the main AMAP PD database system. Both the AMAP PD and ENVINET PD web interfaces can be used to register new project descriptions (or update existing registrations) and to search/query the database content.
- To establishing appropriate linkages between the ENVINET Site Specific Information database and the ENVINET Project Directory.

The deliverables of these efforts are a fully functioning SSI online database at http://www.amap.no/envinet/queryform1.cfm and the PD online database http://pusnes.grida.no/amap/amappd/index.asp?org=2. The SSI online database presents all the participating infrastructures in a coherent way, and a high number of projects are registered in the

PD online database. These tools are identified as a very useful and important fundament for the further co-ordination and collaboration among the sites, which may contribute to increasing the access of new scientific user communities to the stations.

Relevance for the Ny-Ålesund Research Community

ENVINET has established new links between the Ny-Ålesund research facilities and similar research infrastructures at lower latitudes in Europe. The framework of collaboration and coordination follows the strategies for a more coherent policy on research infrastructures under the European Research Area. The support for research infrastructures and networking is further emphasised in the upcoming 6th framework programme (FP6) of the EC under the scheme for Integrated Infrastructure Initiatives (I3's). The Norwegian Polar Institute has received new mandate from the ENVINET consortium to prepare a new proposal for FP6 building on the experiences that have been acquired during the first contract.

The new collaboration and work under ENVINET is believed to be useful for the research infrastructures and the EC in several ways. ENVINET has contributed to the establishment of:

- Improved communication and coordination tools between environmental research infrastructures in Europe.
- New links between the disciplinary boundaries bringing together operators, managers and scientists at different research sites and different research disciplines
- New opportunities and ideas for coordinated and complementary studies along ENVINET-transects, the generation of new collaboration and exchange of research groups
- The ENVINET Technical Tasks with potential for improved quality and new multidisciplinary research collaboration
- The Station Managers Forum: A tool for improved site management, coordination and exchange of information and good practices among the sites
- The ENVINET Site Information Search Engine: A planning and coordination tool for infrastructure operators, research managers and scientists at the sites
- The ENVINET Project Directory Search Engine: A planning and coordination tool for research managers and scientists at the sites
- The ENVINET web-service and list-server: A tool for dissemination of information and new opportunities
- New collaboration, new research groups visits at new sites through the coherent use of the EC/IHP access and networking contracts
- A number of new and planned proposals for EC and national funding programs

References / Further Information:

- ENVINET Home Site: HTTP://WWW.NPOLAR.NO/ENVINET
- ENVINET Site Information Search Engine:
  HTTP://WWW.AMAP.NO/ENVINET/QUERIFORM1.CFM
- ENVINET Project Directory Search Engine
  HTTP://PUSNES.GRIDA.NO/AMAP/AMAPPD/INDEX.ASP?ORG=2
- ENVINET International Conference:
  "Arctic-Alpine Ecosystems and People in a Changing Environment":
  HTTP://WWW.NPOLAR.NO/ARCTICALPINE2003
- ENVINET Email List Server: envinet@npolar.no, envinet.all@npolar.no, envinet.atm@npolar.no, envinet.terr@npolar.no, envinet.mar@npolar.no

Trends in surface UV radiation in polar regions

Arne Dahlback, University of Oslo, Norway

The Norwegian UV monitoring network was established in 1995 and one of the instruments is located at Ny-Ålesund, Spitzbergen. The instruments measure UV radiation in 5 channels and they also provide quantitative information about total ozone, cloud-effects and surface albedo. Results from the measurements will be presented and the influence of clouds, ozone and surface albedo on surface UV will be discussed. A decline in total ozone has been observed in the Arctic over the last two decades by satellites as well as ground-based instruments. Unfortunately, time series of surface UV radiation from high quality instruments at high northern latitudes are too short for trend estimates. Time series and trend estimates of surface UV radiation for the period 1979-2000 based on satellite measurements and radiative transfer calculations will be presented.

The Arctic Ozone Layer

Markus Rex, Alfred Wegener Institute for Polar and Marine Research

The vertical distribution of stratospheric ozone has been measured with ozonesondes in Ny-Alesund for over ten years. These measurements are part of the international ozonesonde network and are used to study the processes that impact the abundance of ozone over the Arctic during winter. The total ozone levels in the Arctic are very variable. Changes on time scales of days, a seasonal cycle and a strong year to year variability all interplay. Particularly in spring the total ozone column in the Arctic is characterized by a pronounced variation from year to year and long term changes. The attribution of observed changes to anthropogenic activities and any projections into the future require a good understanding and quantification of the different mechanisms that drive the observed variability.

In Arctic winter chemical reactions involving breakdown products of manmade chlorofluorocarbons and halons can lead to the removal of large amounts of ozone in the stratospheric polar vortex. Simultaneously large amounts of ozone are supplied to the Arctic vortex by transport related processes, which are natural but may be modified by anthropogenic climate change. Both, chemistry and transport, are very variable from year to year. Their respective impacts depend on variable meteorological parameters during the winter and the chemical loss and dynamical supply of ozone anticorrelate because in the polar stratosphere low temperatures indicate less transport and favour chemical loss. This situation complicates the detection of chemically induced ozone loss, its precise quantification and any assessment of its impact on the total column abundance of ozone. Over recent years a number of approaches have been developed to distinguish between the impact of chemistry and transport on the variability of the Arctic total ozone column and a ten-year climatology of chemical ozone losses and dynamical supply of ozone to the Arctic has been compiled. Local chemical ozone loss rates as measured with the lagrangian approach "Match", the overall degree of chemical loss over the winter and the overall amount of dynamical supply during the winter are presented for the past decade. The variability and long term changes of these individual processes are discussed and related to long term changes in the meteorology of the Arctic stratosphere over the last 35 years. Model calculations are used to assess our current understanding of the various mechanisms. Implications for the future evolution of the Arctic ozone layer are discussed and our current ability to predict future levels of Arctic ozone are assessed.

Sixth Ny-Ålesund International Scientific Seminar
"The Changing Physical Environment"
Polar Environmental Centre, Tromsø, Norway,
8-10 October 2002

Session: Changing Environment & Ecosystem Effects I

T. **Brossard** et al.: Modelling spatial co-variation of plant species and temperature using GIS and remote sensed data.

Christian **Wiencke** et al.: Enhanced UV radiation ands its implications for seaweeds from Spitsbergen.

Modelling spatial co-variation of plant species and temperature using GIS and remote sensed data

Brossard, T.(1) , Joly, D.(2) , Nilsen, L. (3) and Elvebakk, A. (4)

(1-2) Laboratoire ThéMA, CNRS & Université de Franche-Comté, Besançon, France
E-mail: thierry.brossard@univ-fcomte.fr (1) daniel.joly@univ-fcomte.fr (2) Phone: 333 81 66 54 01 Fax : 333 81 66 54 00

(3-4) Department of Biology, University of Tromsø, N-9037 Norway
E-mail: lennart@ibg.uit.no (3) arve@ibg.uit.no (4) Phone: 47 77 64 63 14 (3) +47 77 64 44 36 (4) Fax: 47 77 64 63 33

Introduction

In the Arctic most plant species are at their physiological tolerance limit (Junttila & Robberecht, 1993). Only a few species are able to grow in the climatologically most extreme habitats of the polar deserts. As summer temperature on Svalbard is low, it represents a strong ecological constraint and is one of the most important factors determining plant distribution (Robberecht & Junttila, 1993). Hence, significant changes in the plant cover are to be expected if climatic conditions, due to global change, continue to get warmer (Chapin & al. 1997; Reynolds & Leadley, 1992).
Predicting effects of climate change is in fact one of the major scientific challanges, as indices of a global warming trend has become more obvious (Maxwell, 1992). However, a global conclusion of temperature increase is not sufficient to establish the consequences of this phenomenon. Hence, the impact of climate change may vary according to geographic position and local conditions of a given area (McGraw & Fetcher, 1992). Thus, it is important to know how this global change will modify the temperature distribution at meso-scale (Nilsen et al. 1999).

With this aim in view, a method which links spatial analysis and the resources of remote sensed data and ground observations archived into a GIS was elaborated. The objectives were to establish spatial relationship between plants, defined in term of a Thermophily Index (TI) and temperature distribution.

Methods.

Species occurring in the Arctic can be divided according to their total distribution pattern. Four categories can be distinguished according to their temperature preferences: strongly, distinctly, moderately, and weakly thermophilous species. The 6, 5, 4 and 3°C July temperature isotherms broadly define these four groups, respectively. Many vascular plants and the vast majority of lichens and bryophytes in the study area show total distribution patterns apparently not restricted by low temperatures, and these are not included among the indicator species. A few species that are incompletely known phytogeographically are also omitted. An extensive systematic sampling of plant relevés covering the study area was made within quadrates of 1 x 1 km. A total of 166 units were studied. TI is calculated for each quadrate. The TI value is calculated based on the thermophily value, and frequency and quantity of each thermophilous species.

Temperatures were recorded by means of 37 temperature loggers distributed in the Kongsfjorden area. Their sensors were positioned at 20 cm above the ground surface. They

recorded temperatures once every 20 minutes from the 20th of July 2000 to the 10th of July 2001. Only a data set covering 104 days from the 20th of July 2000 to the end of October 2000 is used in the present study.

Two categories of data are to be considered and stored in the GIS. The first basic information source is a digital elevation model (DEM) previously established by the Norwegian Polar Institute at 100 x 100 m resolution. It was resampled to 50 m x 50 m resolution. From this primary data layer, many additional significant sub-layers are calculated, such as: gradient, aspect, topographic rugosity, theoretical solar energy balance, length of the slopes, distance to the closest crest line, distance to the closest channel.

The second basic information source in the GIS is a Landsat Thematic Mapper (TM) image. The original resolution of 30 x 30 m was reduced to 50 x 50 m to match and overlay the DEM. A land cover map was produced by means of an automatic classification of the TM image. According the well known formula; NDVI= (TM4-TM3)/(Tm4+TM3)), NDVI values were calculated for the study area. Two sub-layers were derived from the classified TM image: (a) distance to the seashore, (b) distance to the closest glacier. In the final modelling procedure, a total of 11 different GIS layers were considered as factors used to explain the temperature distribution.

The statistical correlations between temperature measurements and variables describing the environment conditions are systematically analysed for recognizing the most significant combination of factors establishing the spatial model of the temperature variation. The statistical tests were performed at both micro- and meso-scale (Brossard et al., 2000).

As temperature data were recorded at punctual locations scattered along transects in the study area, an interpolation technique was applied to produce a continuous data layer of temperature distribution at a 50 m resolution. The interpolation procedure involves calculating temperature values at each pixel, and producing a temperature surface with a high accuracy, covering the whole area. The calculations were made both for the daily maximum and minimum temperature of the complete observation period (104 days).

For a single interpolation, the modelling takes place in three steps following Fury & Joly, (1995). (a) First, the analysis of variation at meso-scale consists in a polynomial regression at the third degree, which combines two regressors: latitude and longitude, at the 37 measurement stations. (b) Secondly, the 11 sub-layers stored in the GIS are used as explanatory variables in a multiple regression model to describe temperature variation at the micro-scale. (c) At the third stage of the procedure, the regression model is used as cartographic operators.

The same procedure is applied for the 104 maximums and the 104 minimums of the whole observation period for obtaining 208 maps of temperature at 50 x 50 m resolution.

Finally, the temperature maps was resampled at a 1x1 km resolution in order to correspond to the observed botanical units. Areas that are covered by both botanical data and the modelled temperature data layers include 93 quadrats within four areas: Blomstrandøya, Dyrevika, Ossian Sarsfjellet and the northern strandflat of the Brøggerhalvøya peninsula.

Results.

West to east gradient

There is a strong gradient in measured daily maximum temperatures from the west to the east on. Kvadehuken (close to the open sea in the west) is characterised by a polar maritime climate with a smooth variation of temperatures and a high frequency of values close to 5°C until mid-September and close to 2 to 3°C until the end of October. Only a few of the daily maximum recordings fall below zero. Ossian Sarsfjellet is characterised by a high frequency of temperatures up to 10°C as far as mid-October. This easternmost and mid-continental part of the study area represents great temperature variability from day to day.

Observation period (July to October)

The correlation coefficient was calculated for the TI values and the average maximum temperature (103 values) during the observation period (July to October), reaching r = 0.67. TI values were correlated with average temperature for the four months (July-October), giving correlation coefficients of 0.64, 0.65, 0.56 and 0.57 respectively.

Calculating a temperature surface by regression

Knowing the mathematical relationship between the TI and temperature makes it possible to calculate a "regressed temperature" with a high accuracy for every 1 x 1 km quadrat where the TI values have been calculated. Thus it is possible to extrapolate and calculate temperature values for large areas outside the areas where temperature loggers have been placed, such as Kapp Guissez and the south facing slopes of Brøgger halvøya, using the regression formula: T= 4.8 + (0.34 x TI). T= temperature (°C), TI= Thermophily index.

The comparison between the obtained theoretical temperature values and the observed-interpolated values shows the places where the model works or fails. **Strong negative residues** appear on the southern part of Ossian Sarsfjellet, mainly in two quadrates. They correspond to places where the summer 2000 average temperatures are lower than what the TI values suggest. There, a perfect equivalence between the TI and temperature would be obtained with a high interpolated temperature (respectively 7,5°C and 6,7°C). This strong difference may result from the particular situation of the spot where plants grow: a narrow stripe of fertilised soil along the feet of a bird cliff. Summer 2000 temperature recordings did not reflect this micro-local particularity of climate. On the contrary, **strong positive residues** mark places where interpolated temperatures are high with regard to a low TI value. This concerns three quadrates at the Blomstrandøya Island where, a perfect equivalence between the TI and temperature would be obtained with a low observed-interpolated temperature (5,3°C, 5,5°C and 5,5°C).

Discussion

Corrleations between TI values and the temperature parameters selected here are much lower than in other papers, e.g. Karlsen & Elvebakk (1996) with r^2= 0.81 (data from 1991) and r^2=0.89 (1993) and Brosø & Elvebakk (2000), where r=0.94 and r^2=0.86 and 0.88. The reason for this is probably because this study focus on comparison between maximum and minimum values, and not on temperature sums, as the studies sited above.

Some distortions related to data gathering and processing oppose the two data sets that were used for comparison: (a) The TI reflects the average climate at a long-term time scale. Because the relevés were recorded at 1 x 1 km units, the index neglects the smaller mosaic between warm and cold places. (b) The interpolated temperature surface, restored at fine-

grained resolution (50 x 50 m) from punctual measurements, reflect the possibly great spatial variation of temperature due to strong local contrasts. As the measurements were recorded for only a single summer, the results partly reflect this time scale difference. In addition temperatures in September and October 2000 are higher than in a normal year. Mean daily temperatures at Ny-Ålesund are –0.3 °C and –5.7° C, for the two months, respectively (Førland et al. 1997).

The correlations between the TI and temperature values derived from the modelled temperature layers are systematically explored in order to recognise where this co-variation is verified or fails. The highest similarity of TI and the spatial distribution of temperature is given for:

- Daily maximum values
- July and August
- When temperature range is >8°C
- Quadrates belonging to the strandflat area

References

Brossard, T. Elvebakk, A. Joly, D., Nilsen, L.., 2000. Modelling Index of Thermophily by means of a multi-sources data base on Brøgger Peninsula (Svalbard). *Sixth Circumpolar Symposium on Remote Sensing of Polar Environment, 12th-14th June 2000, Yellowknife, Canada.*

Chapin, F. S., McFadden, J. P. & Hobbie, S. E. 1997. The role of arctic vegetation in ecosystem and global processes. In: Woodin, S. J. & Marquiss, M. (eds.) *Ecology of arctic environments*, Blacwell Science Ltd., Cambridge, 97-112.

Førland, E.J., I. Hanssen-Bauer & P.Ø. Nordli. 1997. Climate statistics and longterm series of temperature and precipitation at Svalbard and Jan Mayen. Det Norske Meterorologiske Institutt, Klima, Report 21797: 1- 72.

Karlsen, S. R. and Elvebakk, A. 1996. A botany based method for mapping local climate variation. Studiokylä, M-L. Development of Environmental Technology in the Barents Region. 68-76. Kemi, Studio Village.

Maxwell, B. 1992. Arctic climate: Potential for change under global warming. In: Chapin, F. S. e. al. (ed.), *Arctic Ecosystems in a Changing* Climate; an Ecophysiological Perspective, Academic Press, Inc, 11-34.

McGraw, J. B. & Fetcher, N. 1992. Response of tundra plant populations to climatic change. In: Chapin, F. S. e. al. (ed.), Arctic Ecosystems in a Changing Climate. An Ecophysiological Perspective, Academic Press, Inc, 359-376.

Reynolds, J. F. & Leadley 1992. Modelling the response of arctic plants to changing climate. In: Chapin, F. S. e. al. (ed.), Arctic Ecosystems in a Changing Climate. An Ecophysiological Perspective, pp. 413-438. Academic Press, Inc.

Robberecht, R. & Juntilla, O. 1992. The freezing response of an arctic cushion plant, *Saxifraga caespitosa* L.: Acclimatation, freezing tolerance and ice nucleation. *Annals of Botany*, 70: 129-135.

Enhanced UV radiation and its implications for seaweeds from Spitsbergen

Christian Wiencke, Dieter Hanelt, Kai Bischof, Helmut Tüg, Ulf Karsten* & Otto Schrems

Project Group Solar UV Radiation, Alfred Wegener Institute, D-27515 Bremerhaven, Germany. E-mail: cwiencke@awi-bremerhaven.de, phone +49 471 48311338, dhanelt@awi-bremerhaven.de, phone +49 4725 819239, kbischof@awi-bremerhaven.de, phone +49 471 48311417, htueg@awi-bremerhaven.de, phone +49 471 48311190, oschrems@awi-bremerhaven.de, phone +49 471 48311592

* Present address: Institute of Aquatic Ecology, University of Rostock, D-18057 Rostock, Germany, E-mail: ulf.karsten@biologie.uni-rostock.de, phone +49-381-4986090

Since the discovery of the ozone hole over Antarctica and the partial stratospheric ozone depletion in high northern latitudes there has been a strong interest in studying changes in ozone concentrations by atmospheric chemists, physicists and biologists. A direct effect of stratospheric ozone depletion is the increase in UVB radiation (UVBR) at the earth's surface. Because of its detrimental effect on many biological processes, enhanced UVBR represents a major threat to terrestrial and marine life. Within the project group "Solar UV radiation" at the Alfred Wegener Institute we investigate the changes of stratospheric ozone concentration, the transfer of UVR through the atmosphere and its effects on seaweeds. Seaweeds are ecologically important in coastal ecosystems and harbour a diverse fauna that directly feeds on these plants or uses these underwater forests as habitat or for recruitment of juveniles.

Our ozone measurements performed since the opening of the Koldewey-Station in Ny Ålesund indicate a substantial lowering of stratospheric ozone in the years 1995, 1996, 1997 and 2000 predominantly in the months March/April but also later in summer. The related increase of UVBR is clearly demonstrated by the so-called ozone index, i. e. the irradiance ratio of the wavelengths 300 and 320 nm. TOMS satellite and balloon-borne ozone data are negatively correlated with the ozone index. This indicates that UVBR at the earth's surface strictly depends on stratospheric ozone concentrations and that ozone concentrations can be estimated by measuring surface UVBR. The UVR penetration into the water strongly varies with the seasons. Directly after break up of sea ice the water of the Kongsfjord is very clear and UVBR decreases by only 20 % per meter corresponding to a 1 % depth of 20 m. Under these conditions the 1 % depth for UVAR is at 30 m. Later in the season water transparency decreases to about 50 % per meter due to the development of phytoplankton blooms and the inflow of turbid meltwater into the fjord. This results in a 1 % depth of 3-6 and 7-10 m for UVBR and UVAR, respectively.

One important target for UVR is algal photosynthesis. When seaweeds are transplanted from deeper waters to the surface followed by exposure to the full solar radiation (PAR+UVAR+UVBR), solar radiation depleted of UVBR (PAR+UVA) or to PAR (photosynthetically active radiation) only, photosynthesis is inhibited. Canopy species from the upper and mid sublittoral show photoinhibition at midday and a recovery of photosynthesis in the afternoon. Photoinhibition is induced mainly by PAR, additional UVAR and UVBR causes a delay in the recovery process in the afternoon and evening. This is shown e. g. in *Palmaria palmata* from the upper sublittoral. In contrast, the eulittoral *Fucus distichus* is almost insensitive to UVR, and in species from the lower sublittoral such as *Phycodrys rubens* even photodamage is evident as these species do not show any recovery of photosynthesis after high light stress. As one underlying mechanism degradation of the CO_2

fixing enzyme RubisCO has been demonstrated. In this context it should be noted that - in contrast to photosynthesis - respiration is generally not negatively affected in seaweeds by exposure to artificial UVR. Some species even show a stimulation of respiration after exposure to UVR.

UVBR also causes DNA damage predominantly by forming thymine dimers, which block replication and transcription of the genetic information and consequently impair cell function and division, and, thus, finally growth. On the other hand, light-dependent photolyase enzymes can repair the DNA. This repair is, however, considerably inhibited in the Arctic/cold temperate red algal species *Palmaria palmata*, *Coccotylus truncatus* and *Phycodrys rubens* by the prevailing low water temperatures on Spitsbergen, making these species susceptible to UVR stress.

Photosynthesis and other metabolic processes can also be inhibited indirectly by reactive oxygen species formed during exposure to high PAR and UVR. In order to prevent oxidative stress, plants have developed enzymatic antioxidant systems and specific scavengers mitigating or even preventing UVR induced oxidative stress. In macroalgae from the Kongsfjord these systems are particularly active in eulittoral and upper sublittoral species and show a very flexible response to the seasonal changes in radiation conditions.

Although UVR exposure clearly exhibits strong damaging effects, species from the upper sublittoral are able to acclimate to UVR. For example photosynthesis of the canopy species *Alaria esculenta*, *Laminaria saccharina* and *Saccorhiza dermatodea* considerably acclimates to the radiation climate in different water depths. When collected at various depths and exposed for 4 h to a simulated solar spectrum in the laboratory (including UVR, corresponding to the clear water conditions in spring in 1 m depth) recovery from high light stress is faster in individuals from shallow compared to individuals from deeper waters. In the ecologically important species *Alaria esculenta* photosynthesis acclimates to stressing radiation conditions within a few days only. Furthermore, the changes in radiation conditions over the course of the seasons are also reflected by changes in the UVR sensitivity of photosynthesis.

Beside the repair and protection mechanisms described above another physiological basis of acclimation may be the accumulation of UV-absorbing mycosporine-like amino acid compounds (MAAs), which are assumed to function as natural UV-sunscreens. A survey revealed that all red algae from the eulittoral/upper sublittoral from the Kongsfjord contain several MAAs. In contrast, deep-water red algae, as well as the Chlorophyceae and Phaeophyceae do not contain MAAs or exhibit only trace concentrations. The function of MAAs as potential UV-screening compounds is inferred from their absorption characteristics at wavelengths between 310 and 380 nm. Their content shows an inverse relationship to water depth. Transplantation and UV exclusion experiments with *Devaleraea ramentacea* have additionally shown that the treatment with PAR and PAR+UVA does not affect MAA concentrations, while the full solar spectrum leads to a strong accumulation of these compounds, especially of mycosporine-glycine and palythine, which mainly absorb in the UVB region. Similar results were obtained in *P. palmata*. The inhibition of photosynthesis is diminished even after exposure to the full solar spectrum, what is regarded as a result of the UV screening capacity of the MAAs. The results obtained show a significant capacity of MAAs to protect algae against UV stress and to adjust MAA synthesis to seasonally changing radiation conditions. In the brown algae, phlorotannins have been invoked as UVR screening compounds in particular in *Desmarestia aculeata,* a species exhibiting a remarkable UV tolerance of photosynthesis.

How are the effects of UVR on algal physiology expressed on the organism level? To answer this question, growth was measured in several key species from the Kongsfjord. Combined transplantation and UV exclusion experiments of upper and mid sublittoral species collected near Ny Ålesund to the water surface show a significant inhibition of growth due to UVR. Shade adapted species from the lower sublittoral such as *Phycodrys rubens* did not even survive. On the other hand, no UV-induced inhibition of growth was found in the

eulittoral *Fucus distichus* similar as for photosynthesis. This was confirmed also in laboratory studies.

The life-history stages most sensitive to UVR are the propagation units of brown algae, the zoospores, and depth distribution of these species reflects the light requirements of the unicellular stages. Zoospores suffer inhibition of photosynthesis, loss of germination capacity and DNA damage after exposure to a simulated sunlight spectrum including UVAR or UVAR+UVBR. In *Laminaria digitata*, loss of zoospore viability is the result of DNA damage and photodamage of the photosynthetic apparatus. Biologically weighted UVB doses in shallow waters are, however, too low to cause DNA damage in zoospores of the studied brown algae at Spitsbergen. Therefore, the observed decrease in germination capacity at depths down to 2 m may be related to a damage of the photosynthetic apparatus. Our results indicate that the upper distribution limit of the studied species is determined - beside ice abrasion – by the prevailing radiation regime. Changes in the zonation due to stratospheric ozone depletion and concomitant UVB increase may therefore be expected in species with UV sensitive microscopic developmental stages. This applies especially to seaweeds from the eulittoral and upper sublittoral. Species from very deep waters, however, are - although their macrothalli are extremely susceptible to UV stress - not affected due to the attenuation of UVR in the water column. UVR has certainly a greater influence in the outer part of the fjord compared to the inner part due to the high/low water transparencies in the different parts of the Kongsfjord. The UV effects will be most pronounced during the time right after sea ice break up, under conditions of clear waters, clear sky and low stratospheric ozone concentrations. Future studies on UV effects should focus not only on isolated physiological processes. Rather, growth, recruitment and UVR induced changes in community structure must be studied more intensively, especially during periods of clear water and high UVR.

References

Aguilera, J., Karsten, U., Lippert, H., Vögele, B., Philipp, E., Hanelt, D. & Wiencke, C. 1999: Effects of solar radiation on growth, photosynthesis and respiration of marine macroalgae from the Arctic. Mar. Ecol. Progr. Ser. 191, 109-119.

Aguilera, J., Dummermuth, A., Karsten, U., Schriek, R. & Wiencke, C. 2002: Enzymatic defences against photooxidative stress induced by ultraviolet radiation in Arctic marine macroalgae. Polar Biol. 25, 432-441

Aguilera, J., Bischof, K., Karsten, U., Hanelt, D., & Wiencke, C., 2002: Seasonal variation in ecophysiological patterns in macroalgae from an Arctic fjord. II. Pigment accumulation and biochemical defence systems against high light stress. Mar. Biol. 140, 1087-1095

Bischof, K., Hanelt, D., Tüg, H., Karsten, U., Brouwer, P. E. M. & Wiencke, C. 1998: Acclimation of brown algal photosynthesis to ultraviolet radiation in Arctic coastal waters (Spitsbergen, Norway). Polar Biol. 20, 388-395.

Bischof, K., Hanelt, D. & Wiencke, C. 1999: Acclimation of maximal quantum yield of photosynthesis in the brown alga *Alaria esculenta* under high light and UV radiation. Plant Biol. 1, 435-444.

Bischof, K., Hanelt, D. & Wiencke, C. 2000: UV-effects on photosynthesis and related enzyme reactions of marine macroalgae. Planta 211, 555-562.

Bischof, K., Hanelt, D. & Wiencke, C. 2001: UV-radiation and Arctic marine macroalgae. In D. Hessen (ed.): UV-radiation and arctic ecosystems. Springer, Berlin, Heidelberg, New York, 227-243

Bischof, K., Hanelt, D., Aguilera, J., Karsten, U., Vögele, B., Sawall, T. & Wiencke, C. 2002: Seasonal variation in ecophysiologiscal patterns in macroalgae from an Arctic fjord. I. Sensitivity of photosynthesis to ultraviolet radiation. Mar. Biol. 140. 1097-1106

Brouwer, P. E. M., Bischof, K., Hanelt, D. & Kromkamp, J. 2000: Photosynthesis of two Arctic macroalgae under different ambient radiation levels and their sensitivity to enhanced UV radiation. Polar Biol. 23, 257-264.

Groß, C., Tüg, H. & Schrems, O. 2001: Three years spectral resolved UV-measurements at Koldewey-Station (1997-1999). Mem. Natl. Inst. Polar Res, Special Issue 54, 113-123

Hanelt, D., Wiencke, C. & Nultsch, W. 1997: Influence of UV radiation on photosynthesis of Arctic macroalgae in the field. J. Photochem. Photobiol. B: Biology 38, 40-47.

Hanelt, D., Tüg, H., Bischof, K., Groß, C., Lippert, H., Sawall, T. & Wiencke, C., 2001: Light regime in an Arctic fjord: a study related to stratospheric ozone depletion as a basis for determination of UV effects on algal growth. Mar. Biol. 138, 649-658

Hop, H., Pearson, T., Hegseth, E.N., Kovacs, K.M., Wiencke, C., Kwasniewski, S.,Eiane, K., Mehlum, F., Gulliksen, B., Wlodarska-Kowalczuk, M., Lydersen, C.,Weslawski, J.M., Cochrane, S., Gabrielsen, G.W., Leakey, R., Lønne, O.J.,Zajaczkowski, M., Falk-Petersen, S., Kendall, M., Wängberg, S.Å., Bischof, K.,Voronkov, A.Y., Kovaltchouk, N.A., Wiktor, J., Poltermann, M., di Prisco, G., Papucci, C. & Gerland, S. 2002: The ecosystem of Kongsfjorden, Svalbard, Pol. Res. 21: 167-208

Karsten, U., Sawall, T., Hanelt, D., Bischof, K., Figueroa, F. L., Flores-Moya, A. & Wiencke, C. 1998: An inventory of UV-absorbing mycosporine-like amino acids in macroalgae from polar to warm-temperate regions. Bot. Mar. 41, 443-453.

Karsten, U. & Wiencke, C. 1999: Factors controlling the formation of UV-absorbing mycosporine-like amino acids in the marine red alga *Palmaria palmata* from Spitsbergen (Norway). J. Plant Physiol. 155, 407-415.

Karsten, U., Bischof, K., Hanelt, D., Tüg, H. & Wiencke, C. 1999: The effect of UV radiation on photosynthesis and UV-absorbing substances in the endemic Arctic macroalga *Develaraea ramentacea* (Rhodophyta). Physiol. Plant. 105, 58-66.

Karsten, U., Bischof, K. & Wiencke, C. 2001: Photosynthetic performance of Arctic macroalgae after transplantation from deep to shallow waters followed by exposure to natural solar radiation. Oecologia 127: 11-20

Michler, T., Aguilera, J., Hanelt, D, Bischof, K. & Wiencke, C. 2002: Long-term effects of ultraviolet radiation on growth and photosynthetic performance of polar and cold-temperate macroalgae. Mar. Biol. 140, 1117-1127

Svendsen, H., Beszczynska-Møller, A., Hagen, J.O., Lefauconnier, B., Tverberg, V.,Gerland, S., Ørbæk, J.B., Bischof, K., Papucci, C., Zajaczkowski, M., Azzolini, R.,Bruland, O., Wiencke, C., Winther, J.G. & Dallmann, W. 2002: The physical environment of Kongsfjorden-Krossfjorden, an Arctic fjord system in Svalbard. Pol. Res. 21, 133-166

Van de Poll, W. H., Eggert, E., Buma, A. G. J. & Breeman, A. 2002: Temperature dependence of UV radiation effects in Arctic and temperate isolates of three red macrophytes. Eur. J. Phycol. 37, 59-68

Wiencke, C., Gómez, I., Pakker, H., Flores-Moya, A., Altamirano, M., Hanelt, D. Bischof, K. & Figueroa, F. L. 2000: Impact of UV radiation on viability, photosynthetic characteristics and DNA of brown algal zoospores: implications for depth zonation. Mar. Ecol. Progr. Ser. 197, 217-229.

Sixth Ny-Ålesund International Scientific Seminar
"The Changing Physical Environment"
Polar Environmental Centre, Tromsø, Norway,
8-10 October 2002

Session: Cryospheric Environment

Bernard **Lefauconnier**: The next large surge in Kongsfjorden.

Jacek **Jania**: Calving intensity of Spitsbergen glaciers

Elisabeth **Isaksson** et al.: Ice cores from Svalbard – useful archives of past climate and pollution history.

Jack **Kohler** et al.: Re-calculation of the mass balance record for Midre Lovénbreen and Austre Brøggerbreen, Svalbard.

Richard **Hodgkins** et al.: Proglacial surface sediment characteristics: Spatial variation at Midre Lovénbreen, Svalbard.

Manfred **Stober** et al.: Accuracy of GPS for glacier monitoring under special conditions in high arctic.

Jacek **Jania** et al.: Changes of geometry and dynamics of NW Spitsbergen glaciers based on the ground GPS survey and remote sensing.

Max **König** et al.: Glacier monitoring and detection of superimposed ice on Kongsvegen, Svalbard, using SAR satellite imagery.

Friedrich **Obleitner** and Jack Kohler: Regional patterns of meteorological variables in the Kongsfjorden area, Svalbard.

Lars-Evan **Pettersson**: Runoff in Svalbard.

Wieslawa Ewa **Krawczyk** et al.: Chemical denudation rates in the Bayelva catchment (Svalbard) in September – October of 2000.

Jan-Gunnar **Winther** et al.: Sea ice surface reflectance and under- ice irradiance in Kongsfjorden, Svalbard.

M. **Nikolaus** et al.: Observations of superimposed ice formation at melt-onset on fast ice on Kongsfjorden, Svalbard.

Jørgen **Hinkler** et al.: Detection of spatial, temporal, and spectral surface changes in the Ny-Ålesund area 79 N, Svalbard, using a low cost multispectral camera in combination with spectroradiometer measurements.

Boris V. **Ivanov** et al.: Radiation and physical characteristics of tundra and landfast ice snow cower, by the example of Barentsburg region and Greenfjord.

E. **Chevnina**: Study of the river and glacier hydrology of the western Spitsbergen.

The next large surge in Kongsfjorden

Bernard Lefauconnier

IPEV
Present address: ADREA, Le Mollard, F-38700, Le Sappey en Chartreuse, France. E-mail: b.lefauconnier@wanadoo.fr, phone +33 (0)4 38 86 41 09.

As a first lecture relative to the cryospheric environment in the Kongsfjord, an overview of the past and present glaciations would have been appropriated. That has been already done during the Kongsfjord echo-system workshop held in Longyearbyen in November 2000 and published within a general paper by Svensen et al. (2002). Instead and with a smile, Jon Borre Orbaeck suggested the present title as an introduction of relevant information, some being not published yet, from the main ice fields dominating the fjord with more than 1000 km2. The aim of this presentation is to provide some help in the determination of future glaciological research.

Past glacier advances and surges of small cirque glaciers.

The Little Ice Age (LIA) is marked by a general glacial advance in Svalbard. In the Kongsfjord there is a high probability that the maximum advances of the small glaciers in the Southern coast occurred as surges. Morphological evidences exist for the Pedersenbreen. A. Brøggebreen, M and A. Lovénbreen probably surged also. Except the A. Brøggebreen, they still possess a small firn area and the slope of their longitudinal profile slowly increase. A surge is unlikely but possible and the impact will be limited.

Past glacier advances and surges of calving glaciers.

We must introduce some lines about the typology. The name of Kongsbreen refers to all the front from Conwaybreen, Kronebreen and Kongsvegen. Today with the present retreat, there are diverse ice-streams separated by mountains. At the head of the fjord, the main front is made by the coalescence of the Kongsvegen and the main branch of the Kronebreen (or South Kronebreen). Then, there is a small front located between Colethøgda and Ossian Sarsfjellet (Middle Kronebreen) and the last part of the Kronebreen flows to the Noth of Ossian Sars fjellet (North Kronebreen). The latter is presently splitting off from a common front with the Conwaybreen. The last calving glacier is the Blomstrandbreen glacier which has been for a long time ending on Blomstrandhalvøya and is now separated from this island by more than two kilometers. The following information about front positions and relative chronology are mainly from Liestøl (1988), Lefauconnier (1987), Hagen et al. (1993).

Blomstrandbreen (95 km2)

We do not know if the maximum extension of the Blomstrandbreen (several decades before 1861) is due to a surge. Since then, a continuous retreat has been only interupted by an about 600 meters of advance due to a surge of a tributary between 1960 and 1968. It is interesting to note nevertheless that on the Eastern side of Blomstrand as well as into the sea, two moraines reveal that there have been two large extension, the last one has possibly occurred after 1907. The calving, active since 1993 will soon be reduced again and because half of the glacier surface is located above 500 m a.s.l., the glacier may possess a suffisant accumulation area to (very slowly) eventually reconstruct an ice mass toward a new surge. But proper information are lacking both on mass balance and ice velocity.

Conwaybreen (56 km2)
The outern moraines (submarine and on land) of the maximum extension were built up before 1898. The morphology of the submarine moraine is comparable to some other known moraines deposed during a surge. This is an argument to think that possibly (not surely) the maximum extension of the Conwaybreen is due to a surge. The presence of an important second submarine moraine, 1700 m apart from the outern one, may indicate that a second advance occurred which may be linked to the 1948 advance, attested by aerial photography. The present retreat will slowly reduce the calving, the velocity will decrease and the front will be ending on land. We have no balance information for this glacier but half of its surface is is above 750 m a.s.l. thre accumulation area is probably large enough to lead, even with the present calving, a sligthy positive balance. Information about the ice velocity is necessary to indicate if the glacier is rebuilding an ice mass suffisant enough to initiate a new surge in the close future.

Kongsvegen. (100 km2)
The glacier has been pressed and narrowed by the large surge of Kronebreen (see below) just before 1869. It has also surged itself in 1948 or just before. The front advanced two kilometers. Frontal submarine moraines exist on both sides and the glacial deposits still dominate the South side of Ossian Sars landscape. At its top (Kongsvegpasset) the lowering of the ice was more than 40 meters. Since then, the glacier front retreats again but the mean annual mass balance has been very sligthly positive. A remarkable work (Melvold and Hagen) has shown that, due to a very slow ice motion (between 2 and 3 meters per year all over the basin), the glacier is rebuilding an ice mass toward a new surge.

Kronebreen (1000 km2).
Thanks to one artist in the crew of sir James Lamont (1876), we know that he largest surge in the fjord occurred around 1869. Due to the change in altitude through times of the top of the Isachsenfonna (see below) We believe that the surge was due to this basin. After the surge and until 1948, the front retreated by more than 4 km. After 1948, the retreat was of the same order of value. B. Lefauconnier (1987) has detected a submarine moraine about 800 meters out of the 1869 moraine. This submarine moraine may correspond to a remnant of a moraine deposit on the South shore partly recovered by sand. Analysis of micro-structure due to the cycle of freezing-thawing in this deposit, indicates a possible age long before or eventually at the beginning of the LIA.

The laboratory of glaciology in Grenoble has retrieved 16 shallow ice-cores (from five to 30 meters deep) over the three Isachsen, Holtedahl and Snefjellfonna. The japanes provided kindly a complementary core retrieved at the top of Snefjellfonna. Dated radioactive layers from Chernobyll accident (spring 1986) and thermo-nuclear tests conducted in Novalia Zemlya in 1961-1962 are detected and the following snow/ice accumulation since these event was computed. The method is described in Lefauconnier et al. The location of the cores are presented in the Figure 1. From the results an Equilibrium Line (EL) is suggested to be located between 600 and 650 m a.ls.l. The Accumulation area ratio (AAR) is then around 0.5 or 0.65 which in Svalbrd corresponds to a zero net balance.

To compare the change in elevation over a glacier by using different sources of information does not usually provide accurate results. An attempt is nevertheless made by using diverse sources. Geodetic work was carried out during the Isachsen expedition in 1906 and 1907 (Isachsen et al., 1912-1913 et 1914). The top of the Isachsenfonna was located at 850 m a.s.l. By comparison between the altitudes of diverse summits recorded by these expeditions and altitudes from the NP maps based on aerial photographs from 1966, a mean difference of

between+20 to +30 meters is noted. With an accuracy of ±5 we believe that in modern coordinates the mentionned elevation would have been of about 875 m. We introduce this elevation in the Table 1 together with the elevation at some points from NP maps based on aerial photographs from 1966 and from two GPS profiles conducted in 1996 and 1997. As expected, the data can only provide a rough information. The top of the Isachsenfonna reveals an important gain in elevation from 1906 to 1966. Since then, probably no change occurred. For other results we have to consider that small topographic effects can disturb the analysis by 5 to 10 meters but it is almost clear that below 800 m a.s.l over Isachsenfonna, exits a lowering of the glacier surface. Over Holtedahl-Snefjellfonna there is probably in average a sligth gain in elevation at the top and an almost steady surface as low as 525 meters.

1907 top of Isachsenf.	875									
1966 (aerial photos)	> 900	900	850	800	766	715	686	612		
1997 (Isachsenfonna)		897	850	800	750	700	650	622		
Change in elevation	**+25**	**-3**	**0**	**0**	**-16**	**-15**	**-36**	**+10**		
1966 (aerial photos)	1155	1142	1115	967	850	800	744	706	668	626
1996 (Holtedahlfonna)	1200	1150	1000	950	850	800	750	700	650	635
Change in elevation	**+45**	**+8**	**-15**	**-17**	**0**	**0**	**6**	**-6**	**-18**	**+9**

Table I. Difference (in meters) in elevation through time.

On both basins, such a result indicates that the net accumulation determined from ice-core is not confirmed, even if we take into account possible large sources of error. That means that the accumulation must be transfered down to the glacier due to high velocities. And that seems to be the case. By using satellite interferometry, Lefauconnier et al. (2001) have shown that a large part of the Isachsenfonna moves as a block at 20 cm per day over 20 km, and that the Snefjellfonna must be near stagnant, while below, the ice of the Holtedahlfonna is moving several cm per day and accelerate to 52 cm per day at 15 km to the front. At the front itself, a mean velocity of 2 m per day along the year has been recorded by different authors, sustaining an important calving of between 0.2 and 0.25 km3 per year (lefauconnier et al. 1994)

It is, nevertheless easy to note in the landscape, that the snow surface in the Snefjellfonna is high along the rock sides, the velocity there, is weak while below 650 m a.s.l., there is an increase in velocity. A future surge can affect this area. Moreover, the calving front retreat permanently and the buoyancy will reduce. The ice flow will slowly decrease as well as the negative balance flux. The glacier will lower its deficit in the higher basin and a new surge can occurred in a medium futur. The size of such a surge will be important, the front will move into the sea by several kilometers followed by a dramatic impact in the geo and eco-systems. To better forecast these possible events, new investigations are necessary as repeated GPS profiles over the three calving glaciers and/or other new and accurate remote sensing methods to survey their changes in elevation and velocity. In addition, the temperature regime of the glaciers is important, ice cores and drilling to the bedrock are required in accessible areas and at least on both Isachsen and Holtedahlfonna, where the glacier sole is though to be at the pressure melting point over large areas.

References

Hagen, J. O., Liestøl O., Roland E. & Jorgensen T. 1993. Glacier Atlas of Svalbard and jan Mayen. *Meddeleser 129*, Oslo 1993.

Isachsen G. & Hoel A. 1913. Résultats des campagnes scientifiques accomplies sur son yacth par Albert Ier de Monaco. Fascicule XLI, deuxième partie. Imprimerie de Monaco.

Lamont J. 1876. Yacthing in the Arctic seas. London 1976.

Lefauconnier B.1987. Fluctuations glaciaires dans le Kongsford, 79°N, Spitsberg, Svalbard. Analyse et conséquences. *Université Scientifique Technologique et médicale de Grenoble I, 25 Juin 1987. (unpublish thesis, in French).*

Lefauconnier B., Hagen J.O. & Rudant J.P.1994. Flow speed ans calving rate of Kongsbreen glacier using Spot images. *Second Circumpolar symposium on Remote sensing of Arctic Environnements. May 4-6, 1992, Tromsø, Norway, Polar research*, V 13, N 1, May 1994, 59-65.

Lefauconnier B., Massonnet D. and Anker G. 2001. Determination of ice flow velocity in Svalbard from ERS-1 interferometric observations. *Environmental Research in the Arctic 2000, Memoirs of National Institute of polar Research, special issue* 54, 279-290.

Liestøl O., 1988. The glaciers in the Kongsfjorden are, Spitsbergen, *Norsk geografisk tidskrift* 42, 231-238.

Melvold , K. & Hagen, J.O. 1998. Evolution of a surge-type glacier in its quiescent phase: Kongsvegen, Soitsbergen, 1964-1995. *J. Glaciol. 44,* 394-404.

Svensen H. and 14 authors. 2002. the physical environment of Kongsfjorden-Krossfjorden, an Arctic fjord system in Svalbard. *Polar Research 21 (1),* 133-166.

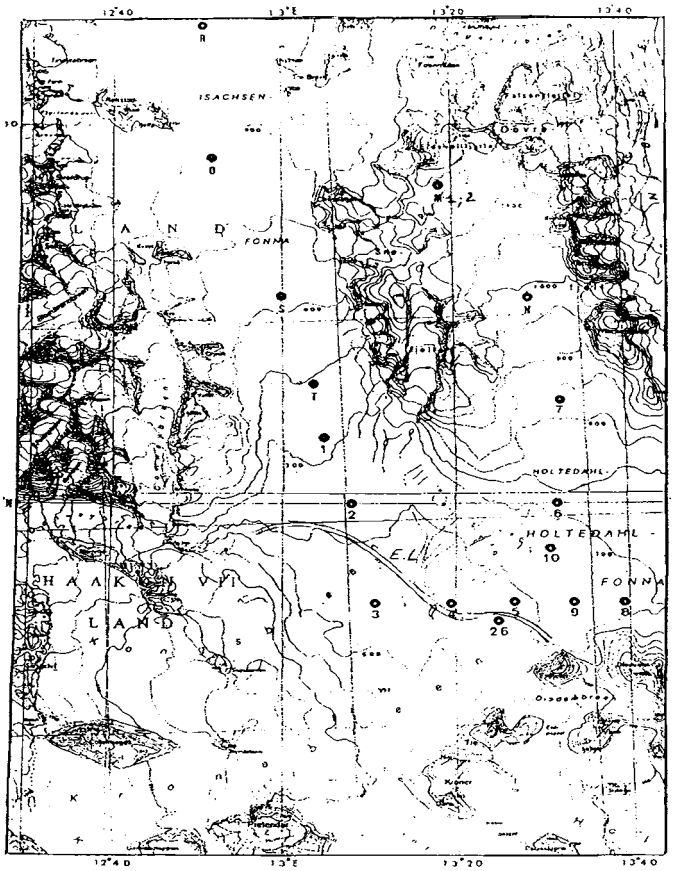

Figure 1. Localisation of Ice-cores over the Kronebree and of the computed equilibrium line (EL)

CALVING INTENSITY OF SPITSBERGEN GLACIERS

Jacek Jania

University of Silesia, Faculty of Earth Sciences, Department of Geomorphology, Sosnowiec, Poland
jjania@us.edu.pl; phone + 48 32 291 7086

Introduction

Tidewater glaciers are characteristic features of the Svalbard environment. They drain up to 63 per cent (23, 000 km^2) of the total area covered by glaciers on the archipelago. Retreat and thinning of tidewater glaciers are common and has been noted since beginning of the 20th century. Decrease of elevation is larger than only result of surface melting. It suggests a noteworthy contribution of calving to their total mass loss. Direct measurements of iceberg flux from glaciers are difficult, thus systematic studies of calving are very rare.

The aim of the paper is to estimate the importance of calving for the glacier mass balance and indication of factors influencing the process of breaking off of ice to the sea in Spitsbergen conditions.

Mass lost at the contact of the glacier front with the sea water is called *calving*. Mechanical breaking off of ice pieces and melting at the water/ice interface contributes to these processes. *Calving intensity* is the volumetric flux of iceberg from the front of a tidewater glacier in a time interval (day or year). *Calving speed* is defined as the calving flux divided by the area of the vertical terminus face (cross section). Thus, it is the difference between the ice flow velocity toward terminus and the rate of change of the glacier length (advance or retreat), expressed as linear rate in opposite direction to the glacier flow (Meier & Post, 1987).

The data problem

The first complex studies of tidewater glacier in Spitsbergen were conducted on Kongsvegen (ca. 102 km^2) in 1964/1965 (Voigt, 1979). Topographic mapping, survey of flow velocity and ice cliff position changes was done by use of terrestrial photogrammetry. This glacier has been in focus of number of research project, including measurements of mass balance, velocity and geometry changes during recent two decades (cf. Hagen et al., 1999). Unfortunately, Kongsvegen has only about 300 m wide partly active ice cliff. Very low calving rate is noted after retreat of glacier from the 1964 front position and squeezing of its frontal part by surge of the fast flowing neighbour – Kronebreen.

The longest series of data have been collected for Hansbreen (55 km^2) located in Hornsund, S Spitsbergen. The glacier has been systematically observed since 1982. Changes of its front position and surface velocity have been surveyed by means of the terrestrial photogrammetry. Electronic distance meters and the repeated precise GPS survey were employed recently (Jania, 1988; Vieli et al., 2002). Mass balance and glacier geometry changes have been also measured.

Data on other tidewater glaciers are sparse and limited. The majority of them are related to fluctuation of front and geometry changes in different time intervals. They cover glaciers in the Hornsund surrounding (Paierlbreen, Körberbreen, Hornbreen-Hambergbreen system), in SE Spitsbergen (Lefauconnier & Hagen, 1991) and in the NW Spitsbergen (Kronebreen, Åvasmarkbreen, Dahlbreen, Comfortlessbreen). There are also some data from the central part of the island (e.g. Fridtjovbreen). Shortage of data on glacier velocity causes drastic limitation of

wider studies on calving. Due to seasonal fluctuations of the glacier flow velocity, the SAR interferometric technique (InSAR) and the precise GPS survey done in short periods (cf. Jania et al. – this volume) are giving only haphazard information. They should be normalised to the mean annual velocities near glacier termini or to the flow rate in the active calving period. Unfortunately, the InSAR method could not be applied to summer periods due to lack of coherence of images.

Glacier flow velocity and calving rates

Studies on annual course of glacier velocity changes are unique. The complete year-round measurements were done only on Kongsvegen by the German expedition in 1964/1965 (Voigt, 1979). Not complete series are available for Hansbreen (Fig. 1). Spring months are the typical period of field measurements on large tidewater glaciers by snow mobiles. A chance for coherence of SAR images in interferometric survey of glacier velocities is also high for the same period. From the available data it was possible to estimate that values of velocities measured in March and April are in order of 85-90 per cent of mean annual flow rates of tidewater glaciers. Consequently, the InSAR data on glacier flow from spring months might be used with higher confidence for estimations of calving fluxes.

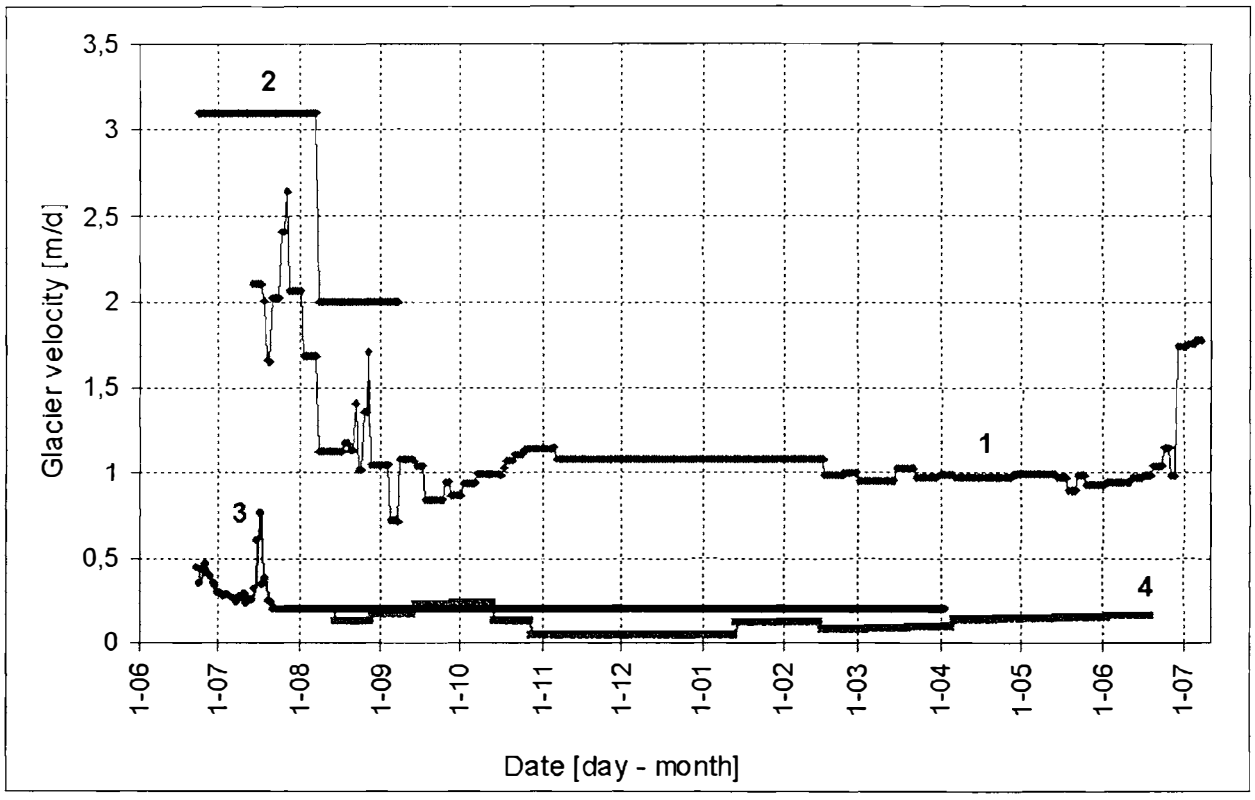

Fig. 1. Annual course of flow velocities of Kongsvegen-Kronebreen glacier system and Hansbreen. Data from different sources: 1 - Kongsvegen "Front Querprofile" 1964/1965 after Voigt (1979), 2 - Kronebreen P-2 profile 1986 (after Lafauconnier et al., 1994), 3 & 4 - Hansbreen (Vieli et al., 2002 and unpublished observations of J.Jania and D. Puczko & P. Glowacki, personal communication, March 2002).

The calving intensity of Hansbreen was calculated based upon direct measurements of velocity and front position changes (Jania, 1988; Vieli et al., 2002). It equals about 22 x 10^6 m^3 of

ice per year for period 1982-1984, while for the decade 1990-2000 was lower (c. 15 x 10^6 m^3 - 18.5 x 10^6 m^3). Data extracted from the excellent work of Voigt (1979) enable to estimate the calving flux from the Kongsvegen-Kronebreen glacier system as c. 172 x 10^6 m^3 of ice in year 1964/1965. Higher mean annual value (250 x 10^6 m^3 of ice) is suggested by Lefauconnier et al. (1994) for period 1983-1986. In contrast, calving rate from very narrow ice-cliff of Kongsvegen is very low: 5 x 10^6 m^3 (Hagen et al. 1999). New data were collected on Åvatsmarkbreen (80 km^2) recently. They made possible a crude estimation of the calving intensity as c. 3.3 x 10^6 m^3 of ice per year. Calving from the relatively narrow (1.5 km) ice cliff of Paierlbreen (105 km^2) in south Spitsbergen was very intensive during active phase of its surge in the second half of nineties. Surface velocity near terminus (higher than 500 m/yr) was inferred from the InSAR analysis of images from 10-11 April 1996 (Vieli, 2001). Hence, calving flux can be roughly estimated as greater than 95 x 10^6 m^3.

All the mentioned above values show wide variety of calving intensity of glaciers and their relation rather to the ice flow regime than to their size. Mass lost due to calving is significant for fast flowing surge-type glaciers and very low from slow glaciers (being probably in the quiescent state). It suggests that contribution of calving to the total annual mass loss of particular glaciers depend strongly from their dynamics.

Volume of ice lost to the sea expressed in the water equivalent and divided by the total area of glacier can be introduced to its mass balance. For Kongsvegen mass loss by calving is smaller than –0.05 m w.eq. (Hagen et al., 1999). Similar low value has been estimated for Åvatsmarkbreen –0.04 m w.eq., while for Hansbreen vary from –0.25 m w.eq. to –0.35 m w.eq. during last two decades. Lefauconnier et al. (1994) for Kronebreen have suggested a value of –0.25 m w.eq. The highest mass discharge by calving was estimated for Paierlbreen: -0.9 m w.eq. Consequently, calving is responsible for about 6-12 per cent of the total summer ablation (surface melting + calving) in cases of Kongsvegen and Åvatsmarkbreen, 20-25 per cent in Hansbreen and up to 45 per cent for Paierlbreen. For glaciers without direct mass balance measurements estimations were made using data from neighbour glaciers.

Factors influencing calving

A clear comprehensive physical model of calving for grounded tidewater glaciers has not been developed yet. Two kind of experimental models are proposed for explanation of the calving mechanism: (1) the calving intensity depends linearly from the sea depth at the glacier terminus and (2) higher glacier velocity produces the faster calving speed. It means, where (and when) sea is deeper calving flux should be higher (Meier & Post, 1987) and faster flowing tidewater glaciers calve more intense (Jania, 1988; Van der Veen, 1996). Both of them reflect factors determining calving. Importance of the sea depth is well known and it will not be considered here.

After beginning of summer melting, enhanced basal sliding appears causing acceleration of flow velocity towards front of tidewater glaciers. It generates the longitudinal stretching of its terminal part. High stretching rate induces frequent and deep crevassing of the frontal zone of glacier, thus facilitate calving. Open crevasses resulting in smaller bulk specific density of the frontal zone of tidewater glaciers. Detailed photogrammetric analysis of stereoscopic aerial photos of the Körberbreen frontal part (taken on 24 August 1961) was done. Crevasses occupied up to 50 per cent of the glacier area in the 1-km wide zone near the ice cliff. Depth of almost every crevasse was measured and the average value is 15 m. Volume of all crevasses was calculated (87.4 x 10^6 m^3). Assuming mean ice thickness of this part of glacier as 70-100 m, the most probable bulk density of this part of the glacier is about 0.85 – 0.87 g /cm^3, while 0.9 g/cm^3

is taken as representative for the glacier ice. Crevasses are wider and deeper more close to the terminus and the effective bulk density is decreasing in this. It reduces basal friction and enhances sliding.

A loop of the positive feedback of factors influencing calving can be suggested: (1) increase of glacier sliding velocity in time of summer melting → (2) stretching of the frontal zone → (3) fracturing → (4) decrease of the glacier bulk density → (5) increase of buoyancy → (6) reduction of basal friction → (7) further stretching → (8) widening of crevasses, etc. Fracturing of the frontal part of tidewater glacier make it ready for further breaking off of icebergs. In case of a surge events the whole tongues are badly crevassed.

InSAR studies on glacier velocity permitted to detect one more factor that seems to affects calving processes. Vertical displacement of frontal parts of glaciers of order of centimetres has been noted. They are results of tides. Amplitude of tides in Spitsbergen are low (1 – 1.5 m). Nevertheless, they affect buoyancy of frontal part of grounded glaciers. Regular tidal fluctuations of sea level could lead to fatigue glacier ice structure near terminus. Such factor is probably combined with the well-known glacier ice melting at its contact with sea water, even in negative temperatures (cf. Jania, 1988). Vieli (2001) stressed importance of concentrated melting of the Hansbreen ice cliff in zone of wave action and estimated summer melt rate at the waterline (1.06 m/day). The value is only slightly lower than observed average daily calving speed 1.37 m for this glacier. The melting at the waterline might act as triggering mechanism for mechanical calving.

In conclusion it is worth to stress importance of mass loss due to calving for fast flowing glaciers. Seasonal increase of calving intensity is related to summer acceleration of glacier flow. Periodic or episodic massive calving events are caused by surge of glaciers or reduce of back stress when glacier front is retreating from shallow water area to a deeper one as the case of Columbia Glacier, Alaska (Meier & Post, 1987). Combinations of both factors are possible. It is impossible to evaluate and understand of contemporary evolution of Spisbergen glaciers without quantitative studies and modelling of calving processes.

References

Hagen, J.O., Melvold, K., Eiken, T., Isaksson, E., Lefauconnier, B., 1999: Mass balance methods on Kongsvegen, Svalbard. Geografiska Annaler, 81A (4), 593-601.

Jania, J., 1988: Dynamiczne procesy glacjalne na południowym Spitsbergenie [Dynamic glacial processes in South Spitsbergen – summary]. Prace Naukowe Uniwersytetu Slaskiego, 955, Katowice, 258 pp.

Lefauconnier, B., Hagen, J.O., 1991: Surging and calving glaciers in Eastern Svalbard. Norsk Polarinstitutt Meddelelser, 116, 130 pp.

Lefauconnier, B., Hagen, J.O., Rudant J.P., 1994: Flow speed and calving rate of Kongsbreen glacier, Svalbard, using SPOT images. Polar Research, 13 (1), 59-65.

Meier, M.F., Post, A., 1987: Fast tidewater glaciers. Journal of Geophysical Research, 92 (B9), 9051-9058

Vieli, A., Jania, J., Blatter, H., Funk, M., 2002: Short-term velocity variations on Hansbreen, a tidewater glacier in Spitsbergen. Journal of Glaciology (submitted), 26 pp.

Van der Veen, C.J., 1996: Tidewater calving, Journal of Glaciology, 42(141), 375-385.

Vieli, A., 2001: On the dynamics of tidewater glaciers. Ph. D. Dissertation ETH No. 14100, Zurich,103 pp.

Voigt, U., 1979: Zur Blockbewegung der Gletscher. Geodatische und Geophysikalishe Veroffentlichungen, R. III, 44, 128 pp.

Ice cores from Svalbard - useful archives of past climate and pollution history

Elisabeth Isaksson[1], Mark Hermanson[2], Sheila Hicks[3], Makoto Igarashi[4], John Moore[5], Hideaki Motoyama[4],Veijo Pohjola[6], Rein Vaikmäe[7], Roderik S.W. van de Wal[8]

[1] Norwegian Polar Institute, Tromsø, Norway
e-mail: elli@npolar.no, phone: + 47 77 75 05 15

[2] University of Pennsylvania, Philadelphia, PA, USA

[3] Institute of Geosciences, University of Oulu, Oulu, Finland

[4] National Institute of Polar Research (NIPR), Tokyo, Japan

[5] Arctic Center, University of Lapland, Rovaniemi, Finland

[6] Department of Earth Sciences, Uppsala University, Uppsala, Sweden

[7] Institute of Geology at Tallinn Technical University, Tallinn, Estonia

[8] Institute for Marine and Atmospheric Research, Utrecht, The Netherlands

Introduction

Ice cores from the relatively low-lying ice caps in Svalbard have not been widely exploited in climatic studies due to uncertainties about the effect of melt water percolation. However, results from two recent Svalbard ice cores, at Lomonosovfonna and Austfonna (Fig. 1), have shown that with careful site selection, high-resolution sampling and multiple chemical analyses, it is possible to recover ice cores whose annual signals are preserved (*Pohjola, 2000*). These cores are estimated to cover the past 800 years and have been dated using a combination of known reference horizons and glacial modeling (*Isaksson et al., 2001;Watanabe et al., 2001).*

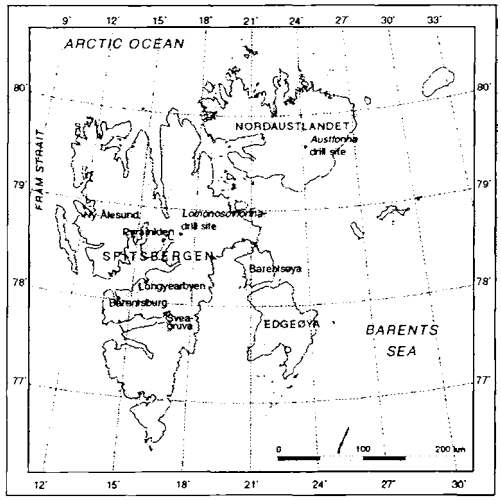

Figure 1. Map of Svalbard with the ice core locations on Lomonosovfonna and Austfonna.

Results and discussion

Climate reconstructions

The $\delta^{18}O$ data from both Lomonosovfonna and Austfonna ice cores suggest that the 20^{ieth} century was by far the warmest century during the past 800 years. This is also supported by the bore hole temperature record from Lomonosovfonna (*van de Wal et al., 2002*). We have been able to show that the Lomonosovfonna ice core correlates with other local climatic parameters such as air temperature, sea ice and sea surface temperature (SST), on a multi-year basis (*O'Dwyer et al., 2000; Isaksson et al., 2001*) since 1920. Because this time period has been the warmest period we expect the ice core records to be even less effected by percolating melt water prior to about 1920 and that the oxygen isotope record is then a reliable climatic indicator.

A comparison of the ice core and sea ice records from this period suggests that sea ice extent and Austfonna $\delta^{18}O$ are related over the past 400 years. This may reflect the position of the storm tracks and their direct influence on the relatively low altitude Austfonna. Lomonosovfonna may be less sensitive to such changes and primarily record atmospheric changes due to its higher elevation.

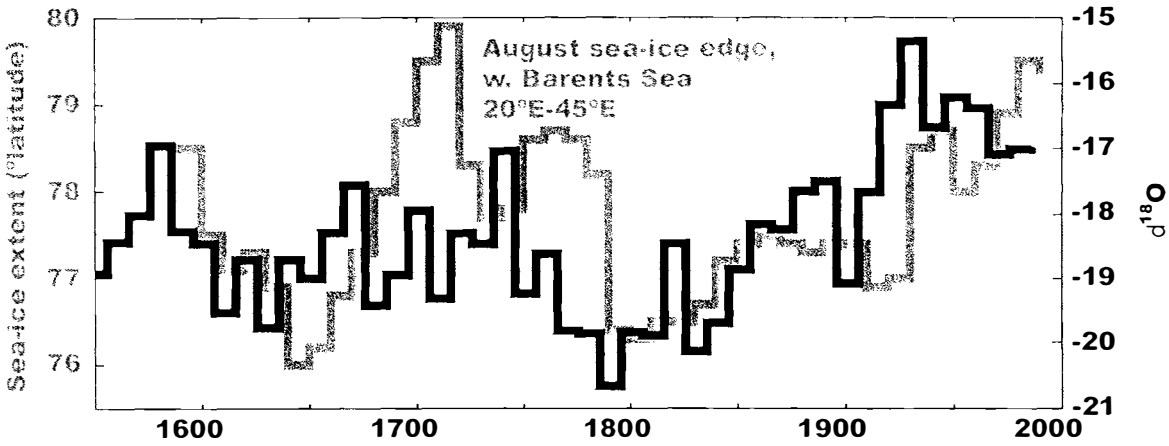

Figure 2. The decadal scale Austfonna $\delta^{18}O$ record (black) corresponds well to the August sea ice record (grey) from western Barents Sea, compiled with data from whaling ships (*Vinje, 2001*). This is suggesting that $\delta^{18}O$ in the precipitation is directly influenced by distance to moisture source in the Austfonna ice core (*from Isaksson et al., submitted*).

Pollution records

The anthropogenic influence on Svalbard environment is illustrated by increased levels of sulphate, nitrate, acidity (*Isaksson et al., 2000;Kekonen et al., 2002*). Also the organic contaminants, including legacy organochlorine compounds, current-use organophosphorus and triazine pesticides and herbicides (*Hermanson et al., unpublished*), and combustion byproducts such as naphthalene (*Vehviläinen et al., 2002)* (Fig. 3) and fly-ash (*Hicks et al., unpublished*) show a clear increase. There is a rapid increase of nitrate, legacy organic contaminants and fly-ash in the late 1940s. Then they remained high until late 1980s and decreased during the last 15 years, which is in agreement with the air measurements from Ny Ålesund. However, we observe a much earlier increase in non sea-salt sulphate concentrations beginning by 1850 and continuing to the 1980s, with some decrease in the most recent years (*Moore et al., submitted).* Polychlorinated biphenyls (PCB), a group of legacy organochlorine industrial compounds, show

a significant drop in surface layers (representing 1998 – 2000) at Lomonosovfonna relative to earlier years, with likely peaks in the 1960's. The exception is PCB congeners 8+5 (combined), which have low concentrations, but increase since the 1960's. Current-use organophosphorus compounds such as Diazinon, Fenitrothion, and methyl-Parathion, and a chloroacetanilide pesticide (Metolachlor), show growing concentrations in near surface layers at Austfonna (Fig. 4). Methoxychlor, a non-persistent organochlorine with a DDT-like structure, used since the mid-1930's, shows declining concentrations since the 1980's (Fig. 4). Triazine herbicides, including Pendimethalin and Hexazinone appear in the surface core segment at Austfonna, representing the 1990's, but do not appear earlier in significant quantities. Finally, also radioactive contamination can be obtained from the ice cores. Analysis of ^{137}Cs show one very distinct peak that we interpret the 1963 bomb test marker, also the Chernobyl event (1986) is visible (*Pinglot and others, 1999*).

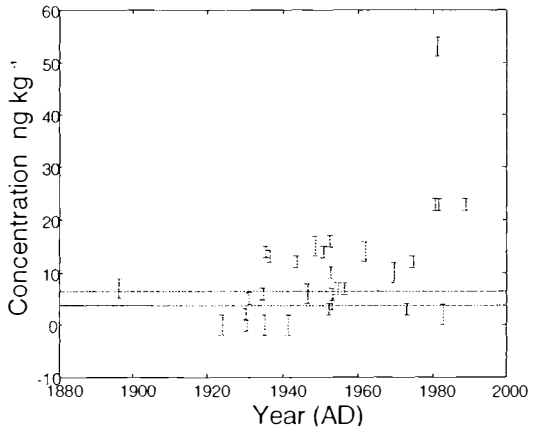

Figure 3. The naphtalene record (*from Vehviläinen et al. 2002*) from the Lomonosovfonna ice core.

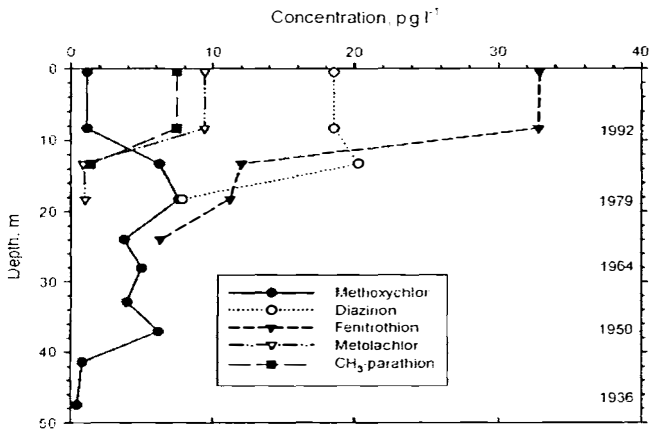

Figure 4. Profile of selected organophosphorus (OP) pesticides, with methoxychlor and metolachlor. The relative high concentrations of OP's in near surface layers suggest a current use and growing inputs of these compounds.

Conclusions

The distribution of species in these two Svalbard ice cores has probably been altered to some degree by melt but the records still provide information about major trends in atmospheric variability of both climate parameters and pollution history. The cores show organic contaminant profiles that reflect known production and use patterns in temperate climates. The presence of organophosphorus pesticides, many of which are still used and which are intended to dissociate once released into the environment, shows that the atmosphere is able to deliver these compounds to Svalbard before they decompose. Once these compounds are frozen in solid ice, which is reached at relatively shallow depths on Svalbard, the decomposition is likely impeded, and the compound may remain indefinitely.

References

Isaksson, E., Pohjola, V., Jauhiainen, T., Moore, J., Pinglot, J-F., Vaikmäe, R., van de Wal, R.S.W., Hagen, J-O., Ivask, J., Karlöf, L., Martma, T., Meijer, H.A.J., Mulvaney, R.,Thomassen, M.P.A. & Van den Broeke, M. 2001: A new ice core record from Lomonosovfonna, Svalbard: viewing the data between 1920-1997 in relation to present climate and environmental conditions. *Journal of Glaciology 47 (157),* 335-345.

Isaksson, E., Kohler, J., Moore, J., Pohjola, V., Igarashi, M., Karlöf, L., Martma, T., Meijer, H.A.J,. Motoyama, H. & van de Wal, R.S.W. Climate and sea ice variability around Svalbard - results from two ice cores. *Submitted to The Holocene.*

Kekonen, T., Moore, J. Mulvaney, R., Isaksson, E., Pohjola, V. & van de Wal, R.S.W. 2002: A 800 year record of nitrate from the Lomonosovfonna ice core, Svalbard. *Annals of Glaciology* 35, *in press.*

Moore, J., Kekonen, T., Mulvaney, R., Isaksson, E., Pohjola, V. & van de Wal, R.S.W. A Record of Sulphuric Acid Deposition in a Svalbard Ice Core Spanning the Industrial Revolution. *Submitted to Geophysical Research Letters.*

O'Dwyer, J., Isaksson, E., Vinje, T., Jauhiainen, T, Moore, J., Pohjola, V.,Vaikmäe, R. & van de Wal, R. 2000: Methanesulfonic acid from a Svalbard ice core as an indicator of ocean climate. *Geophysical Research Letters 27 (8),* 1159-1162.

Pinglot, J.F., Pourchet, M., Lefauconnier, B., Hagen, J.O., Isaksson, E., Vaikmäe, R. & Kamiyama, K. 1999: Investigations of temporal change of the accumulation in Svalbard glaciers deducted from nuclear tests and Chernobyl reference layers. *Polar Research 18(2),* 315-321.

Pohjola, V., Moore, J., Isaksson, E., Jauhiainen, T, van de Wal, R.S.W., Martma, T., Meijer, H.A.J. & Vaikmäe, R. 2002. Preservation of climatic signals in an ice field affected by periodical melt: a qualitative and quantitative study of the upper 36 m of an ice core from the summit of Lomonosovfonna, Svalbard. *Journal of Geophysical Research 107(D4),* 10.1029/2000JD000149.

Vehviläinen, J., Isaksson, E. & Moore, J. 2002: The record of polyaromatic hydrocarbons (PAH) in an ice core from Svalbard. *Annals of Glaciology* 35, *in press.*

Vinje T. 2001: Anomalies and trends of sea ice extent and atmospheric circulation in the Nordic Seas during the period 1864-1998. *Journal of Climate 14 (2),* 255-267.

Wal, v.d. R.S.W., Mulvaney, R., Isaksson, E., Moore, J., Pohjola, V. & Thomassen, M.P.A. 2002: Historical temperature reconstructions from temperature measurements in a medium-length bore hole on the Lomonosovfonna plateau, Svalbard. *Annals of Glaciology* 35, *in press.*

Watanabe, O, Motoyama, H. Igarashi, M., Kamiyama, K.,Matoba, S., Goto-Azuma, K., Narita, H. & Kameda, H. 2001: Studies on climatic and environmental changes during the last few hundred years using ice cores from various sites in Nordaustlandet, Svalbard. *Memoirs of National Institute of Polar Research Special Issue 54,* 227-242.

Re-calculation of the mass balance record for Midre Lovénbreen and Austre Brøggerbreen, Svalbard

Jack Kohler, Ola Brandt, Marzena Kaczmarska
Norwegian Polar Institute, Polar Environmental Centre, N-9296 Tromsø, Norway.
E-mail: jack@npolar.no

Introduction

Glacier mass balance is the amount of snow and ice lost or gained on a glacier. The annual net balance $\bar{b}_n$ is the sum of the summer balance $\bar{b}_s$ (roughly May-Sept., in the arctic) and the winter balance $\bar{b}_w$ (Sept.-May). Balance varies over the extent of the glacier, but on most glaciers there is a high degree of correlation between balance and elevation.

The typically quoted mass balances $\bar{b}_i$, where $i = n,s,w$ for net, summer, or winter, are areally-averaged quantities calculated from

$$\bar{b}_i = A^{-1} \int_A b_i(z) dA, \qquad (1)$$

where A is the glacier area, and $b_i(z)$ are the various balances as a function of elevation. NPI currently monitors mass balance on three glaciers, all near Ny-Ålesund: Austre Brøggerbreen, (1967-present), Midtre Lovénbreen (1968-present), and Kongsvegen, (1987-present). The first two are the longest continuous arctic glacier mass balance time-series.

The annual balances defined above reflect the loss or gain averaged for the glacier as a whole. From a climatic perspective, though, it is the balances as a function of elevation $b_i(z)$ that are more relevant, since they reflect more directly the regional-scale climate at a particular elevation band, as opposed to glacier-averaged balances, which by Equation 1 are influenced by the individual glacier's geometry.

While the Norwegian Polar Institute (NPI) has always measured mass balance as a function of elevation on the three study glaciers, these data have never been reported in the literature. In fact, for the two older series, these data were never recorded in any systematic way, prior to 1987. In this paper, we present a reconstructed time-series of net, winter and summer mass balance as a function of elevation for these two glaciers, Midre Lovénbreen (MLB) and Austre Brøggerbreen (BRG).

Methods

We use original stake data from archived field notebooks and maps at NP, graphs of balance as a function of elevation taken from old NP reports (NP Årbok 1967-1982), and in those cases where either were lacking, regression analysis of reconstructed elevation-dependent balances against reported net balances.

The specific winter balance b_w, that is, the winter balance at a particular point, is calculated from any of the following data: change in exposed stake height between and spring and the previous autumn; spring snow-depth sounding; snow depth measurements in snow pits located close to the stakes; or hand-contoured accumulation maps derived from snow soundings. Snow depth is transformed to water equivalent depth using the average of the particular years' snow densities, where reported. When density information is missing, we assume the long-term average value of 0.37 g/cm^3.

The specific summer balances b_s can only be calculated from the change in exposed stake lengths above the snow/firn/ice surface between autumn and the previous spring. Conversion to water equivalent is trickier than in the case of the winter balance since the density depends on the amount of each component (snow, ice, firn) that is melted. We assume that on stakes well below the equilibrium line altitude (EL), snow and ice (when appropriate) are melted, with the winter density used to determine the snowmelt and a density of 0.9 g/cm^3 used for the ice melted. For stakes above the ELA, or in general, for cases in which not all the snow is melted,

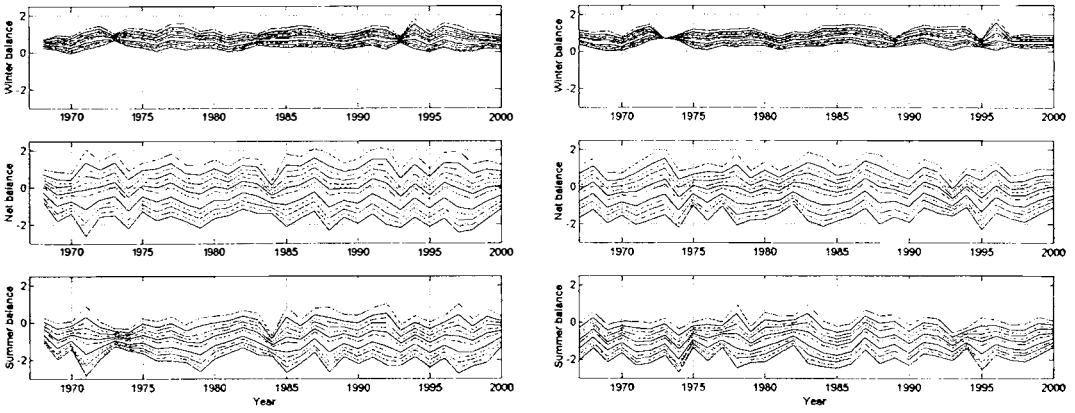

Figure 1. ***Winter, net and summer balances for each 50 m elevation interval from 700 (upper lines) - 0 (lower lines) m a.s.l. for MLB, (left) and BRG (right)***

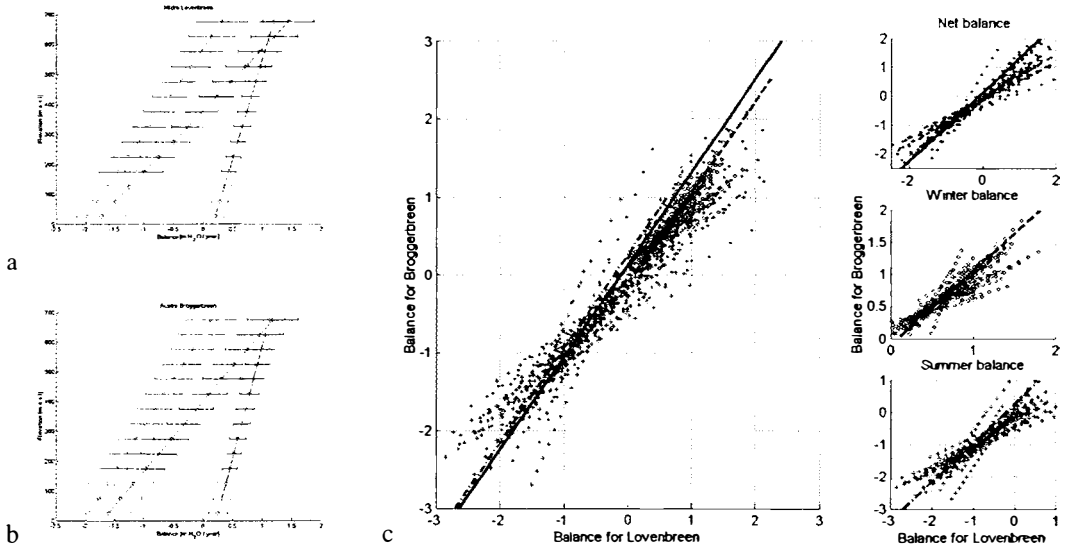

Figure 2 ***Mean of summer, net, and winter balances for (a) MLB and (b) BRG, as a function of elevation using all years up to 2000. (c) Balances as a function of elevation for MLB and BRG plotted against each other for all years, with separate balances in right hand plots (d-f), and best-fit lines.***

the snow remaining above the previous fall minimum is assumed to have a density of 0.55, a "typical" end of melt-season value, and the same value used for melted firn. We take no special account of superimposed ice or internal accumulation since these quantities have not been reported in any of the years prior to 1993.

Finally, the specific net balances are simply the difference between winter and the summer balance for each stake: $b_n = b_w + b_s$

Archived stake and sounding data are not available for some years. In such cases, the data are digitised from graphs of balance as a function of elevation presented in the NP Årbok series. For MLB, data for 1973-74, and 1976-77 are derived from the NP Årbok. The plots in the reports normally show the balance as a function of elevation. In some of the years, stakes are displayed, but in most cases only a hand-fit line is drawn. Similarly, BRG stake data for the years 1972-1974, 1976, and 1994 are missing and are digitized from figures in the old year books.

Balances as a function of elevation

Re-calculated balances as a function of elevation are then derived from a robust linear fit of the specific balances and their respective elevations. Robust fitting is less sensitive to data outliers compared to ordinary least-squares regression.

The choice of a straight-line fit is deliberate; while the usual practice of the earlier mass balance workers was to hand-fit a curved line to interpolate and extrapolate the specific balance measurements, we feel that there is no evidence to suggest that a curved relation is statistically preferable to a straight line. A variety of questions arise when using a curved line: what sort of relation to apply (piecewise, polynomial, spline); how to prevent the relation from doing unreasonable things in the regions of extrapolation; and what to do when the original specific balances are missing and we use the digitized hand-fit curves? The records from MLB and BRG suggests that winter balances are probably safely modelled using a linear relation. Summer balances are more variable; in particular years, there are discernable kinks or bends in the summer balance relation, usually at the lower elevations. However, a straight-line fit does not lead to appreciable errors for re-calculating the glacier mass balances $\bar{b}_i$ since most of the glacier's area is confined to the intermediate elevation bands, where the $b_i(z)$ are adequately described by a linear fit. And any errors in individual years are minimized when considering long-term averaged balances as function of elevation.

There are no archive data at all for MLB in 1986 and BRG in 1985-86. The $b_i(z)$ for these years must instead be reconstructed from a regression of the reported annual net balances from 1967-2000 against our re-calculated $b_i(z)$ for the years in which we have data.

We estimate errors by bootstrapping (Efron and Tibshirani, 1991). The bootstrap is made for each year and each balance term by randomly re-sampling 100 new populations from the original distribution of n specific balance measurements. Re-sampled populations with less than four unique data points are discarded since the robust fit requires a minimum of three data points. For each of the new 100 populations a robust fit is made, from which mean and standard deviation can be calculated at the desired elevation bands.

Results

Reconstructed net, winter and summer balances for MLB and BRG in 50 m wide elevation bands from 0-700 m asl are shown in Figure 1, and the balances for the two glaciers are compared with respect to each other in Figure 2. The balances in individual years are not always similar for the two glaciers; this is particularly true for the summer and net balances. Comparing the balances averaged over the entire measurements period (Figure 2a-b), however, shows that the mean balances for the two glaciers over the measurement period are similar. The mean winter balances are essentially the same, although there appears to be a slightly less negative (and thereby net) summer balance on MLB when compared to BRG at the higher elevations. Nevertheless, the difference is small and within the estimated error limits. This gives us some confidence in our reconstruction since the two glaciers are of similar size and orientation with respect to the local topography, and should therefore experience a similar microclimate.

This is underscored by comparing (Figure 3) the reconstructed $b_i(z)$ for MLB and BRG to those of Kongsvegen (KNG), a much larger, more exposed glacier lying to the east of Ny-Ålesund. KNG balances are decidedly more negative; this may be due to the fact that KNG is more exposed to the effect of wind, which both reduces the winter accumulation and increases the summer melt. In addition, KNG gets less shade from surrounding mountains than do MLB and BRG, so that the glacier surface is exposed to radiative melting for a greater part of the summer days.

As a final check, the reconstructed balances are used together with the distribution of area by elevation bands and Equation 1 to recalculate the balances $\bar{b}_i$. We present only results from MLB (Figure 4). The results show that the recalculated balances $\bar{b}_i$ are, for the most part, similar to those previously presented (e.g. LeFauconnierc and others, 1999), again within the error

limits. We therefore are reasonably confident that we have not distorted the balance data as far as the original stake measurements are concerned.

References

Efron, B. and R. Tibshirani, 1991. Statistical data analysis in the computer age. *Science*, 253, 390-395

Lefauconnier, B., Hagen, J-O, Ørbæk, J.B., Melvold, K., and Isaksson E., 1999. Glacier balance trends in the Kongsfjord area, western Spitsbergen, Svalbard, in relation to the climate. *Polar Research* 18(2), 307-313

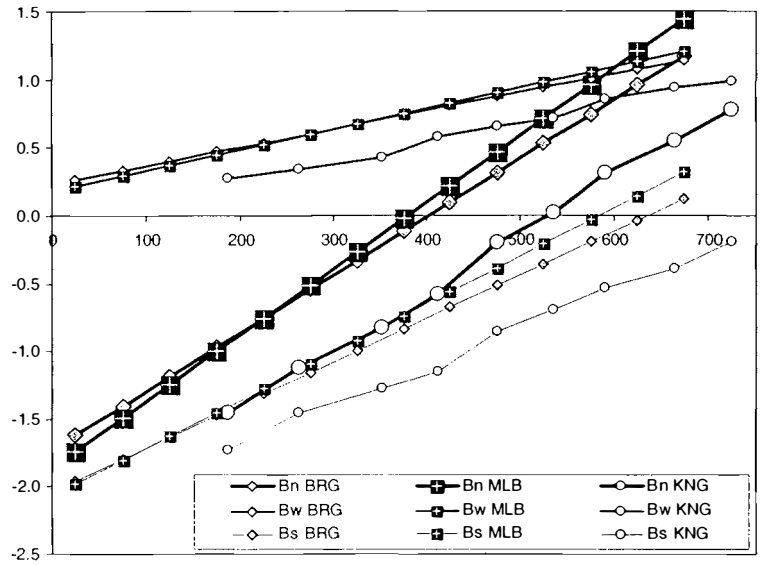

Figure 3 ***Reconstructed winter, net, and summer balances as a function of elevation for BRG, MLB, and those measured for KNG.***

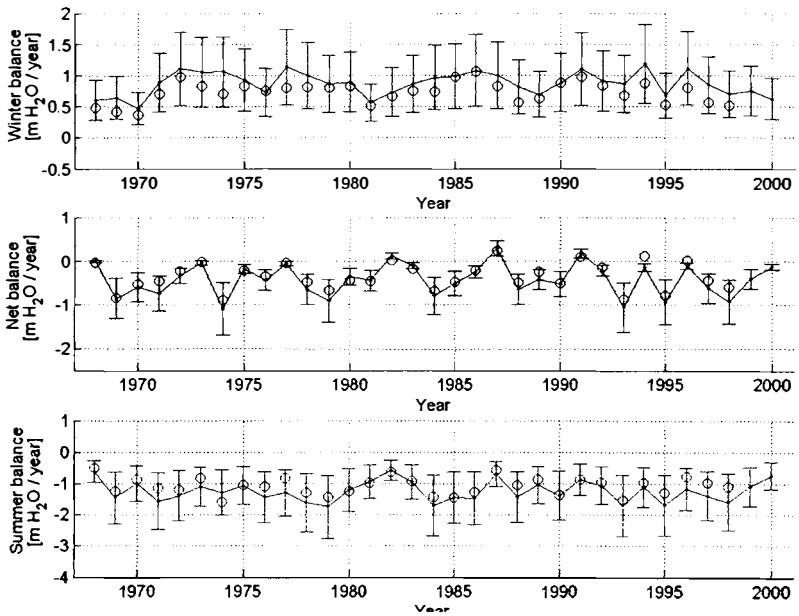

Figure 4 ***Reconstructed winter, net, and summer balances for Midre Lovénbreen (dots and line), and estimated errors, compared with those previously reported (open circles).***

Proglacial Surface Sediment Characteristics: Spatial Variation at Midre Lovénbreen, Svalbard

Richard Hodgkins
Susan Adair
Margaret Onwu
Adrian Palmer

Department of Geography, Royal Holloway, University of London, Egham, Surrey TW20 0EX, U.K. E-mail: r.hodgkins@rhul.ac.uk, phone +44 1784 443563

Simon Carr
Department of Geography, Oxford Brookes University, Headington Campus, Oxford OX3 0BP, U.K. E-mail s.j.carr@brookes.ac.uk, phone +44 1865 484333

Introduction

The sediments deposited by retreating glaciers supply abundant material for meltwater transport. Models of the delivery of sediment from mountain watersheds to fjords must take account of the routing and storage of sedimentary material, but sediment sources and sinks in glacierised catchments remain poorly defined and quantified. This study involves a search for statistical tools to discriminate sediment sources in proglacial systems, using the Midre Lovénbreen catchment near Ny-Ålesund on the southern margin of Kongsfjorden in the Svalbard archipelago as an example.

It has been suggested that proglacial river systems provide the key link between glacial processes and the wider environment (Warburton, 1999). The majority of research has so far concentrated on proglacial rivers in mid-latitude, high-altitude, glacierised catchments, while relatively little work has been conducted on high-latitude proglacial systems. Information on sediment dynamics in a wide range of glacial catchments is required to test hypotheses about the relative influence of glacial and non-glacial processes (Harbor and Warburton, 1993), and to develop useful models describing sediment transfer pathways and sediment storage, plus variation in these features with climate.

Methods

The catchment of Midre Lovénbreen (78° 53′ N, 12° 04′ E; 5.95 km^2) is well-constrained between a steep mountain watershed at high elevations and a pronounced end moraine at low elevations on the coastal plain (Figure 1). The area is lithologically diverse, with Lower Palaeozoic to Tertiary sediments, igneous and metamorphic units outcropping (Hjelle, 1993). Meltwater drains from the glacier at its east and west margins. A subglacial stream normally emerges during the melt season, sometimes under pressure in the glacier forefield, and usually flows to a confluence with the east-margin meltwater after a short distance. Approximately the middle third of the west stream flows through a low-gradient alluvial basin. Both east and west margin meltwaters form relatively straight, braided stream systems which penetrate the prominent end moraine before distributing widely across the coastal plain and entering Kongsfjorden (Figure 1). During the 2000 melt season, 117 0.05–0.10 kg proglacial surface sediment samples were collected from the margins of active streams, and subsequently returned to the U.K. to be analysed for particle size distribution by sieving and Sedigraph, and geochemical composition by Atomic Absorption Spectrophotometry (23 individual chemical species).

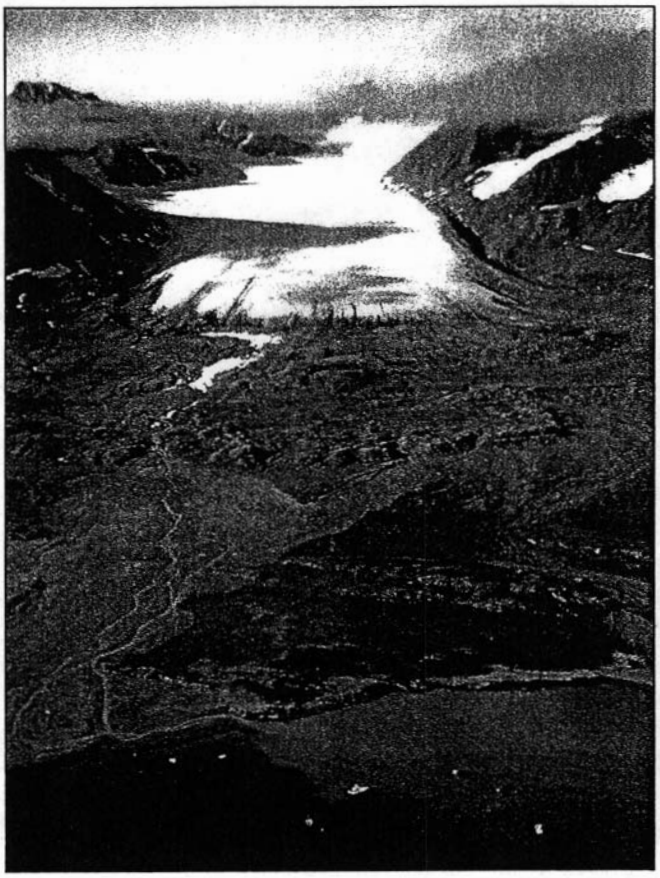

Figure 1. Oblique aerial view of the Midre Lovénbreen catchment from coast to watershed, looking approximately south-west. The proglacial area is confined between the prominent arcuate end moraine and the current glacier terminus; the distance between these is just under 1 km. The turbid nature of the meltwater discharging to Kongsfjorden is apparent in the lower right of the figure.

Results and Discussion

Particle Size Distribution

There is a general, lithology-independent trend towards downstream fining of sediments in the Midre Lovénbreen proglacial area, evident in plots of percentage weight of sample against phi-size category (Figure 2). Fractal geometry can be used to quantify this effect. Hooke and Iverson (1995) hypothesized that the crushing of grains was an important mechanism of deformation in subglacial tills, and that the particle-size distribution of such tills would be fractal, by analogy to the development of fault gouge material. In a self-similar material, the number, N, of particles of diameter d is $2m$ the number of diameter $2d$, where m is the fractal dimension. A log-log plot of number of particles against particle diameter yields a straight line of slope $-m$:

$$N(d) = N_0\left(\frac{d}{d_0}\right)^{-m}$$

where N_0 is the number of particles of reference diameter d_0. The ideal value of m for a fractal size distribution is 2.58. There is a systematic increase in the fractal dimension of the sample particle-size distribution (over five orders of particle-size magnitude) from 2.46 at the glacier terminus to 2.95 on the coastal plain, some 1.1 km downstream. These changes can be interpreted in terms of both glacial and fluvial processes. Fractal dimensions greater than 2.58 indicate an excess of fines, and a transition from particle production by crushing to particle production by abrasion; the former is likely to characterise high effective-pressure subglacial environments, the latter sub-aerial environments. The relatively low proximal fractal dimensions found in this case may be attributed to: (1) the generation of particles mainly by crushing, indicating low rates of subglacial sediment deformation; (2) eluviation of fine particles by meltwater.

Downstream fining has been described as a natural dynamic adjustment to variable water, sediment and energy inputs in fluvial systems (Gasparini et al., 1999). There are rapid changes in these parameters over short distances in the Midre Lovénbreen catchment, from the glacier margins, to the coastal plain. Though there is an indication of declining fractal dimensions in the most distal samples, eluviation of fines does not appear to have a strong effect in distal locations, as the fining is relatively progressive from the glacier terminus towards the coast: re-

deposition from low-energy meltwater on the low-energy coastal plain may play an important factor.

Particle Geochemistry

A rigorous, quantitative procedure was applied to the geochemical data in order to determine a composite, statistical 'fingerprint'. The non-parametric Mann-Whitney U-test was applied to common species from different drainage environments, to assess whether there were statistically-significant differences in concentration between them. Species which were significantly different were then entered into a multivariate discriminant function analysis, to identify the set of species best able in combination to discriminate different drainage environments (and therefore different sediment sources). 52 samples from the east drainage system of the glacier were first compared with 52 other samples from the west drainage system. 5 significant chemical species emerged and were entered into the discriminant analysis as predictors, and 66% of samples were assigned to their correct source; the squared distance between the groups was 0.71. 12 samples from the subglacial drainage system were then compared with 12 other samples from the east drainage system (these sources subsequently converge downstream). In this case, 14 significant chemical species emerged and were entered into the discriminant analysis as predictors, and 100% of samples were assigned to their correct source; the squared distance between the groups was 192.74. The composite fingerprint therefore appears to be a very effective tool for determining sediment provenance, and can be applied with confidence to glacial river systems.

Conclusions

Different physically- and chemically-based quantitative tools (fractal geometry, multivariate discriminant function analysis) are capable of discriminating surface sediments from a range of drainage environments in the proglacial area of Midre Lovénbreen. Such tools offer important ways forward in the broad task of finding spatial organisation in complex, rapidly-changing glacial hydrological systems (particularly as these systems are typically, strongly overprinted by environmental change effects). This in turn is a step towards the development of more physically-based and less deterministic models of sediment transfer and storage in glacierised environments. Fischer and Hubbard (1999), for example, suggest that it may be possible to incorporate quantitative, spatial information on sediment texture into glacial models, given that spatial patterns of both total sediment strain and fluvial eluviation may be approximated respectively from considerations of net flow distances and subglacial drainage patterns. The ability of the composite statistical fingerprint to discriminate sediment sources, on the basis of their geochemical composition, suggests that a multivariate mixing model, based on the chemistry of sediment suspended in meltwater, could be used to trace the seasonal evolution of fluvial sediment sources in glacial environments, in a way hitherto unattempted.

The Ny-Ålesund area is a very important location for studies of sediment transport systems under changing environmental conditions, as it possesses mountain watersheds and fjords in close spatial proximity, with a well-documented history of glacier retreat in the context of Twentieth-Century climate warming.

References

Fischer, U.H. & Hubbard, B. 1999: Subglacial sediment textures: character and evolution at Haut Glacier d'Arolla, Switzerland. *Annals of Glaciology 28*, 241–246.

Gasparini, N.M., Tucker, G.E. & Bras, R.L. 1999: Downstream fining through selective particle sorting in an equilibrium drainage network. *Geology 27*, 1079–1082.

Harbor, J. & Warburton, J. 1993: Relative rates of glacial and nonglacial erosion in alpine environments. *Arctic and Alpine Research 25*, 1–7.

Hjelle, A. 1993: Geology of Svalbard. *Norsk Polarinstitutt Handbook 7*.

Hooke, R.LeB. & Iverson, N.R. 1995: Grain-size distribution in deforming subglacial tills: role of grain fracture. *Geology 23*, 57–60.

Warburton, J. 1999: Environmental change and sediment yield from glacierised basins: the role of fluvial processes and sediment storage. *In* Brown, A.G., and Quine, T.A., *Fluvial Processes and Environmental Change. John Wiley and Sons Ltd*, 363–384.

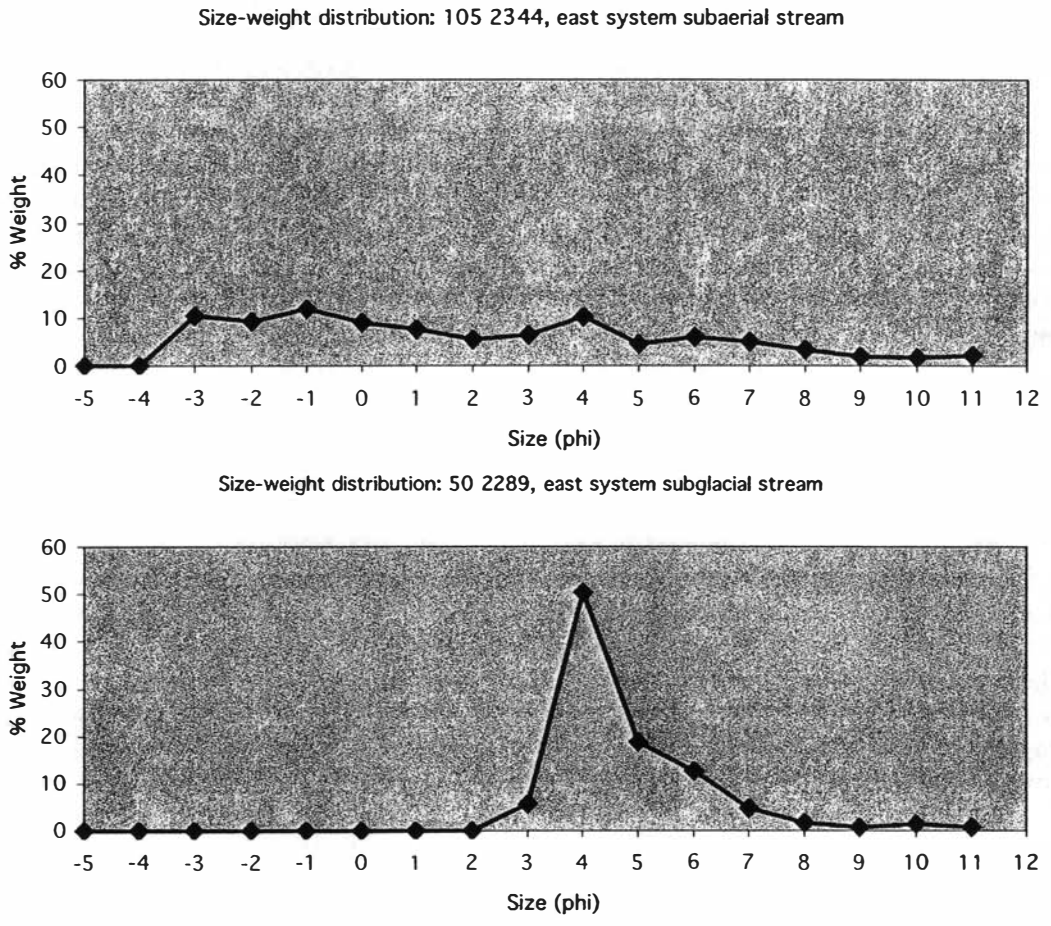

Figure 2. Particle size-weight distributions for two surface sediment samples (105-2344 and 50-2289) from the drainage system at the eastern margin of Midre Lovénbreen. Particle size changes from coarse to fine towards the right-hand side of the plots. The upper sample (m = 2.813, R^2 = 0.9989) is from the subaerial stream at the ice margin. The lower sample (m = 2.881, R^2 = 0.9005) is from the subglacial stream which emerges at the glacier terminus. Relative to the subaerial sample, the subglacial sample is distinctively depleted in coarse particles and augmented in fine particles.

Accuracy of GPS for glacier monitoring under special conditions in high arctic.

Manfred Stober *, Jacek Jania ♠, Zbigniew Perski ♦

* Hochschule für Technik Stuttgart (Stuttgart University of Applied Sciences), Department of Surveying and Geoinformatics, Stuttgart, Germany. Stober.fbv@fht-stuttgart.de ; phone + 49 711 121 2563

♠ University of Silesia, Department of Geomorphology, Sosnoviec, Poland . jjania@us.edu.pl ; phone + 48 32 291 7068

♦ University of Silesia, Department of Geological Mapping, Sosnoviec, Poland . perski@us.edu.pl ; phone + 48 32 291 83 81 e. 420

Introduction

GPS measurements in hight altitudes, especially if performed on glaciers, are differing from middle european continental measurements by many causes:

- generally bad geometry (GDOP) due to lack of satellites in zenith,
- large influences by ionospheric disturbances,
- multipath effects by surrounding mountains and glacier surface,
- large distance of rover from reference station due to logistical causes,
- high speed when used in kinematic mode for profiling during travelling with snow mobiles,
- no possibility of repeated measurements for accuracy augmentation in kinematic mode and even not in static mode because of glacier movement.
- transformation problems from WGS84 to local terrestrial geodetic coordinate system in order to compare results with old maps.

Most of the problems are common for GPS measurements in static and kinematic mode as well, but some are very special for kinematic profiling.

All these effects are studied as an example from the GPS measurements performed in the project „Calving intensity of tidewater glaciers in NW Spitsbergen and its importance for contemporary evolution of glacier system“ (GEOCALVEX-2001, supported by Ny-Aalesund-LSF grant NP 30/2001) on several glaciers arround the Ny-Aalesund area in spring 2001. Some measurements had been performed with Ashtech Z 12 receivers, but most of them with Leica instruments (system 300 and 500), all types with carrier phase and code measurements on 2 frequencies (L1, L2).

Assessment of accuracy

For assessment of accuracy, especially for the most interesting heights in kinematic GPS mode, several evaluation methods had been applied and compared:

- Ambiguity resolution success indicator and standard deviations given by Leica software processing (SkiPro) ,

- Standard deviation calculated from the short periodical height variations in kinematic profiling, comparing smoothed running average against to each original measurement,
- Differences in results from „repeated" measured points in a special test area (meandering course with crossing tracks),
- Correlation of standard deviations with ionospheric disturbances, calculated from the programme TEQC of UNAVCO,
- Correlation of standard deviations with multipath effects, calculated from the programme TEQC of UNAVCO.

Results

In this short abstract only some results are given without formulas.

Static measurements.

The static method was applied to some stakes in order to determine the glacier flow velocity . Measuring time was about 50 minutes with baseline lenght up to 20 km. Not all ambiguities could be solved. In average an accuracy of 0,021 m was achieved.

Kinematic measurements:

In 4 weeks of field work most of measurements had been performed as kinematic profiling from snow mobiles with measured epochs all 5 seconds. For shortening the baseline length a glacier reference was established as near as possible to the glacier. Comparisons with long and short baselines show the big advantage in solving ambiguities with glacier reference (figure 1). If the moving points are calculated from the camp as reference stations (distance up to 33 km), only about 50 % of ambiguities are solved compared against using the closer glacier reference (distance up to 20 km), although even these glacier references often are too far away from surveyed glacier areas.

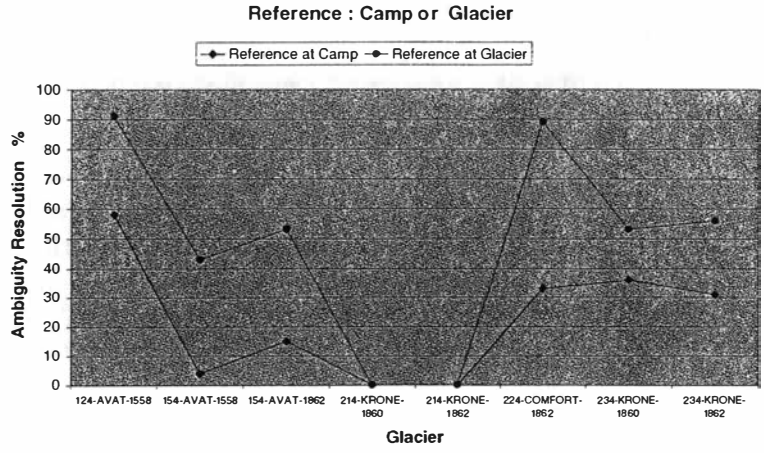

Figure 1: Dependence of ambiguity resolution on baseline lenght

The standard deviation of kinematic measured points (height component) is varying from 0,1 to 4,0 m, depending on ambiguity resolution (figure 2). Together with figure 1 we understand that baselines shorter than 10 km are neccessary for good results.

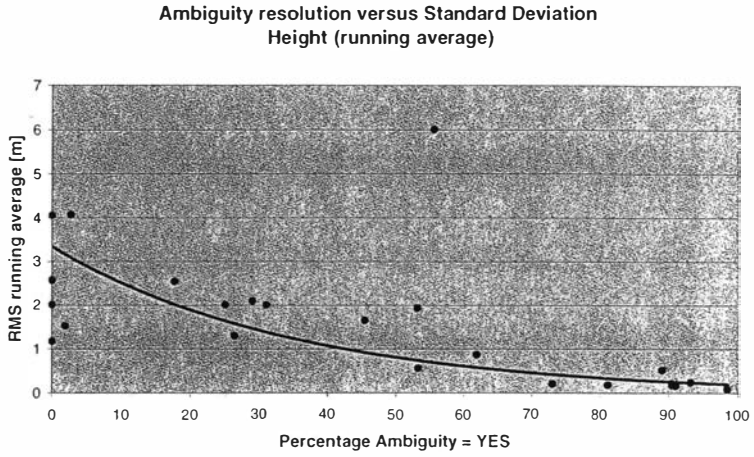

Figure 2: Dependence of standard deviation (height) on ambiguity resolution

Ionospheric effects

It is well known that ionospheric effects may disturb GPS phase measurements, especially in high latitudes (WANNINGER 1994). This effect is depending on sun spot activity which became nearly maximum in the year 2001 of our GPS observations. Our measuring area is situated in 80 ° North in high Arctic. In figure 3 we show an example of ionospheric influences calculated by the software toolkit for data quality checking TEQC (UCAR UNAVCO). The example is suitable for a reference point with permanent measurements all day (21.04.2001). In the upper part we see the total ionospheric delay in an order up to about 15 m , which should be eliminated by two frequencies L1 and L2. More problematic are the short periodic disturbances effecting the phase measurements as scintillations, with an amount up to ± 2-3 m. It is not possible for any GPS software to smooth these effects in kinematic GPS with positioning for every single epoch, so no better results as in the order of meters can be expected. Compared to middle european GPS measurements these effects are much greater and reduce the possible accuracy of kinematic measurements.

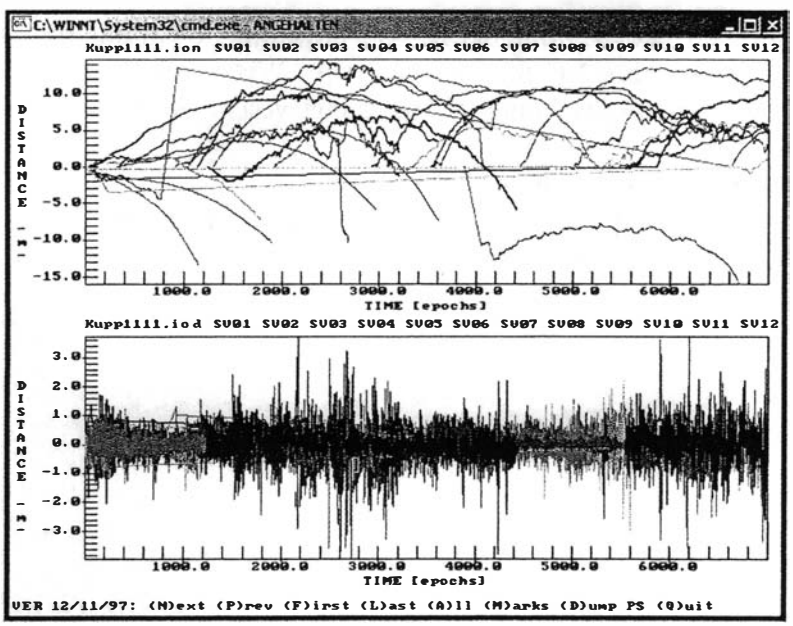

Figure 3: Example of ionospheric effects (21.04.2001, reference Kuppel-NP):
total effect (above), short periodic distance change (below).

Transformation of GPS results into a local coordinate system

The results of GEOCALVEX-2001 are referred to a fix point (KAIA) in Ny-Aalesund, given in the International Reference Frame (ITRF) and referred to ellipsoid GRS80, which for practical use is identical with WGS84. In order to compare the recent results with old maps we have to transform the coordinates in the old coordinate system (European Datum 1950 / ED50, International Ellipsoid Hayford, projection UTM 33N). Due to lack of identical points for determination of a 7-parameter set we used informations from Norwegian Mapping Authority Hoenefoss (NMA). The discrepances of transformed points are within an order of 2 m, which is sufficiant for our purpose.

Conclusion

The accuracy of kinematic GPS in Spitzbergen 2001 was much worse than in areas with lower latitudes. In spite of using glacier reference, the baselines often have been too long . Ionospheric influences are causing the very bad signal quality. Due to obstructions (mountains) and low satellite elevations in high arctic the geometry usually was bad and multipath effects are common. Often ambiguities could not be solved. Better results can be expected, if the snow mobile would run slower (not exceeding 20 km/h).

The transformation from WGS84 respectivly GRS80 into the local coordinate system (UTM, ED 50, International ellipsoid) was due to only few identical points not better than ca. 2 m, which is accurate enough for comparisons with old maps.

References

Wanninger, Lambert: Der Einfluß der Ionosphäre auf die Positionierung mit GPS. Heft Nr. 201, Schriftenreihe Wissenschaftliche Arbeiten der Fachrichtung Vermessungswesen, Universität Hannover, 1994.

UCAR UNAVCO Facility Boulder, Colorado: http:// www.unavco.ucar.edu, Data Quality Check software.

Changes of geometry and dynamics of NW Spitsbergen glaciers based on the ground GPS survey and remote sensing

Jacek Jania*, Zbigniew Perski# and Manfred Stober⊕

* University of Silesia, Faculty of Earth Sciences, Department of Geomorphology, Sosnowiec, Poland
jjania@us.edu.pl ; phone + 48 32 291 7068

University of Silesia, Faculty of Earth Sciences, Department of Geological Mapping, Sosnowiec, Poland
perski@us.edu.pl ; phone + 48 32 291 83 81 ext. 420

⊕ Hochschule für Technik Stuttgart (Stuttgart University of Applied Sciences), Department of Surveying and Geoinformatics, Stuttgart, Germany.
Stober.fbv@fht-stuttgart.de ; phone + 49 711 121 2563

Introduction

Svalbard glaciers are receding rapidly. Mass balance studies and survey of extent and thickness of glaciers are usually based on small, land-based types and little is known about such properties in the case of the larger, tidewater forms. Neither the mass loss due to calving of tidewater glaciers is fully understood. An overview of contemporary deglaciation of Spitsbergen will be incomplete until the processes which drive the geometry changes of its tidewater glaciers are much better studied.

The paper presents results of field studies done on five large glaciers in NW Spitsbergen (Åvatsmakbreen, Dahlbreen, Comfortlessbreen, Kronebreen and Kongsvegen) during the GEOCALVEX-2001 Expedition in April 2001, combined with the remote sensing data. Changes in glacier geometry and dynamics reflect current tendencies in evolution of larger glaciers of this area.

Methods

The kinematic DGPS method was widely used for determination of the actual topography of glaciers. Most of survey profiling from snow mobiles were done using four „Leica" instruments (System 300 and 500) and some of them had been performed with two „Ashtech Z-surveyor" receivers, but all types with carrier phase and code measurements on 2 frequencies (L1, L2). One or two reference stations were employed during surveying of particular glaciers. Details of methodology and the assessment of accuracy are presented by Stober et. al. (this volume). The topographic data from these surveys were compared with that of the Norwegian Polar Institute maps showing state of glaciers in 1936 and also with the surface profiles established by an airborne laser altimeter (ALA) survey from a NASA aircraft on 23rd May 1996. The glacier front (ice-cliff) positions were determined using remote sensing data (Landsat, ERS/SAR, Terra/ASTER) and old maps.

In order to measure the surface flow velocity, repetitive static surveys of several marker-stakes were carried out on Åvatsmarkbreen (two points) and Comfortlessbreen (three points) during a three-week period in April 2001. These ground velocity data were compared with interferometric analysis of ERS/SAR images from March 1994 and April 1996. Interferograms from the tandem mission ERS-1/ERS-2 with the 24 h temporal baseline (11th –12th April 1996) and from three images of the ERS-1 taken on 17th, 20th and 29th March 1994 were analysed. InSAR processing of the data from 1994 have been performed on 3 and 12 days data couples. Both configurations are characterized by very similar perpendicular baselines. The 3-days interferogram have been used to remove topographic effect from 12-

days interferogram based on assumptions that the flow velocity is not changing significantly over short time periods. This interferometric approach called 3-pass differential processing (Massonnet, Feigl 1998) is one of the best methods to eliminate topographic effects. During the processing of tandem data from April 1996 application of the external DEM (kindly provided by the Norsk Polarinstitutt - NPI) was tested. As the result of the InSAR processing the interferogram with corrected effect of topography but with some noisy parts due to temporal decoherence has been obtained. The velocity field calculations have been performed using ascending data only applying 3-pass interferometric approach (cf. Coren et al., 2000). However, reconstruction of the 3D velocity vectors was impossible due to high error of descending data.

Some results

The GPS kinematic survey data superimposed on the NPI DEM show a pronounced lowering of the ablation zones of the glaciers since 1936. The greatest decrease in ice thickness (80-90 m) evidently taking place at lower altitudes of glaciers (Fig. 1).

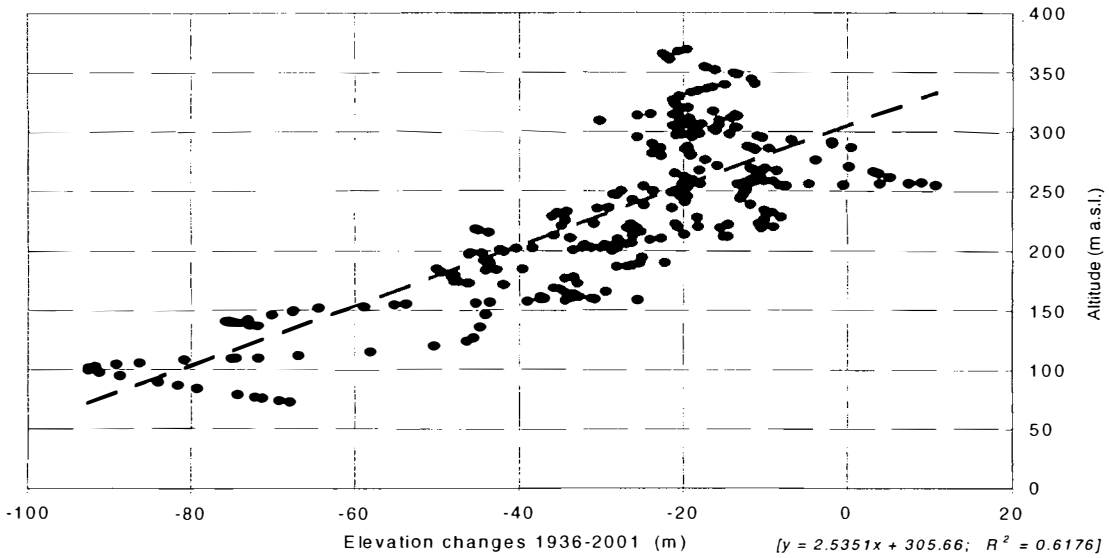

Fig. 1. Elevation changes along GPS kinematic trajectories on the ablation zone of Åvatsmarkbreen as function of altitude. A result of comparison of the GPS survey in April 2001 and the digital form of the NPI map 1:100 000 with the glacier topography from 1936.

Elevations from the ALA profile (1996) along the lower part of the Kongsvegen surface have been compared with the 2001 GPS kinematic profiling along the same track. Results show that thinning of the lower reach of the glacier is faster recently (>1.5 m/yr in period 1996-2001) than before i.e. 1936-1996 (ca. 1.2 m/yr).

Although the studied glaciers are usually thinning below the ELA, in the upper parts of the accumulation zones (above 500-600 m a.s.l.), the ice thickness has increased by 20-60 m, since 1936. It is well visible in results from Holtedahlfonna and the Lovenskiøldfonna-Dahlbreen transition area. However, there is no direct relationship between altitude and the rate of ice thickening in the accumulation zones.

Specifically, in respect to Comfortlessbreen, there is an increase of ice thickness both in the accumulation fields (by c. 80-100 m) and also the upper part of the ablation zone in this period. This may be the result of a build-up of the ice mass during a quiescent phase, a process which will be reversed when the next surge event takes place.

The retreat (or advance) of glacier fronts are a result of activity of opposite processes: glacier flow and calving intensity. Their proportions are different in case of each glacier and

also at different times and it is clear that this is not due to any single factor. Whereas the ice cliffs of Kronebreen, Kongsvegen and Comfortlessbreen retreated only slowly since 1987, in the same period the recession of Åvatsmarbreen and Dahlbreen ice fronts was considerable (50-60 m/yr). In general, the glaciers studied are both shorter and steeper than they were in 1936.

Ice flow velocities of glaciers varied in time and space. In April 2001, the surface velocities near the fronts of both glaciers were higher than they were in April 1996 and in March 1994. For two stakes in the frontal zone of Åvatsmarbreen flow rate of 0.042 and 0.025 m/d were noted in the period of 11-30 April 2001, while in the same area velocities were in order of 0.091-0.136 m/day between 6th and 22nd July 2000. Interferometric data from March 1994 (Fig. 2) show acceleration of glacier flow towards termini of tidewater glaciers. Higher surface velocities are also visible in upper parts of Åvatsmarbreen and Comfortlessbreen. Very sharp shearing zone between slow Kongsvegen and fast-flowing Kronebreen is noticeable.

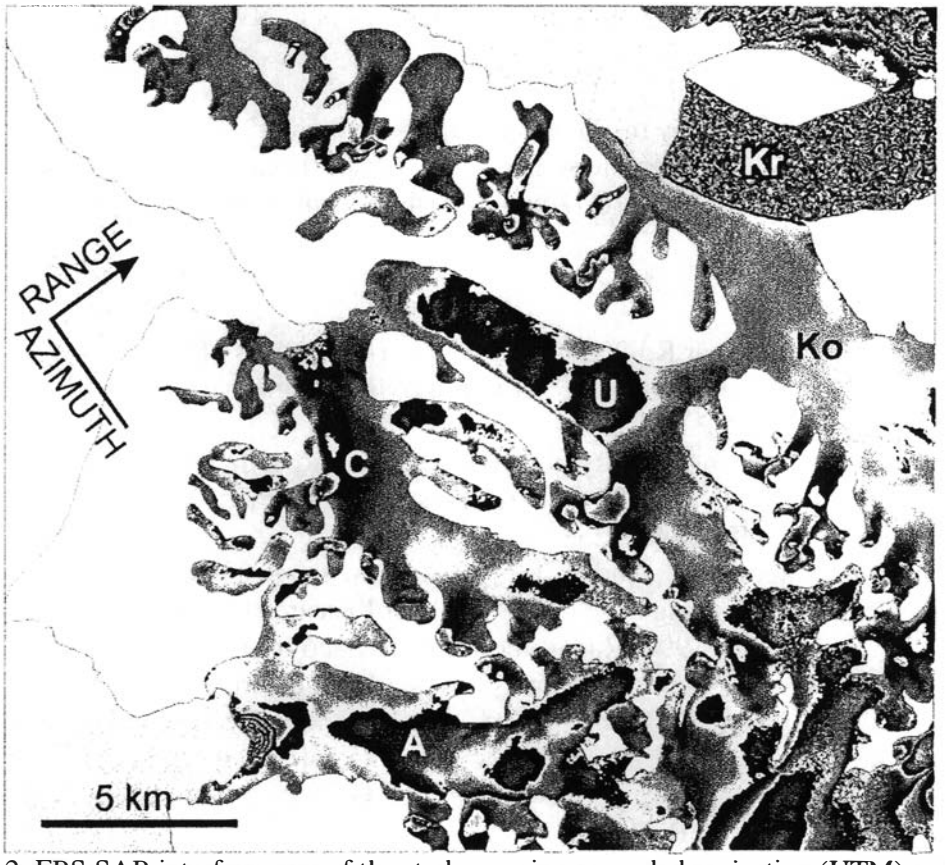

Fig.2. ERS SAR interferogram of the study area in geococded projection (UTM) and with corrected topographic effect, 17-20 March 1994 (II-nd Ice Phase data). Non-glaciated areas of land are masked out (white); uniform grey – sea; A – Åvatsmarkbreen, C – Comfortlessbreen, U - Uversbreen, Ko – Kongsvegen, Kr - Kronebreen.

Conclusions

No mass balance data are available for Åvatsmarkbreen and Comfortlessbreen. Assuming that the mass balance gradient is similar to the average for Kongsvegen and Austre Brøggerbreen, it would seem that the flow velocity of Åvatsmarkbreen and Comfortlessbreen is slower than the balance flux. This may be an indication of unstable flow regime and surge-type behaviour of both of them.

Very little is known about the seasonal changes in the velocity field near to the fronts of the Svalbard tidewater glaciers. The only available data, those for Kongsvegen (Voigt, 1979) and Hansbreen (Jania, 1988; Vieli et. al., 2002), show that velocities measured in April are only about half those of the active calving season (July-September). In respect of Åvatsmerkbreen and Comfortlessbreen, the data presented here and a knowledge of the approximate height of the ice cliffs where calving takes place, make it possible to estimate their calving flux. Mass loss due to calving amounts to c. 6-12% and c. 3-7% of the summer balance of these two glaciers. This proportion is appreciably smaller than that calculated for Hansbreen (c. 25 %) and the relatively small losses may be explained by the relatively slow ice flow during an inter-surge quiescent phase. As observed at the Kronebreen ice front, massive calving is typical of the fast flowing active surge phase (cf. Lefauconnier et al., 1994).

Noted retreat and decrease of ice thickness in lower parts of glaciers, when their higher accumulation areas are thickening, support conclusion that an unstable mass transfer is a characteristic feature of all the large polythermal glaciers in NW Spitsbergen.

Acknowledgements

Field survey was supported by the "Ny Aalesund – LSF grant" NP.-31/2001 and special grant of the University of Silesia. Remote sensing studies have been supported by the European Space Agency grant No. C1P-1076. Authors wish to thank Marek Grześ for his assistance in field works.

References

Coren F., Sterzai P., Vidmar R., 2000: Interferometric Analysis of David Glacier (East Antarctica). Proceedings of ERS-Envisat Symposium16-20 Oct-2000, Gothenburg, ESA publication SP-461

Jania, J., 1988: Dynamiczne procesy glacjalne na południowym Spitsbergenie [Dynamic glacial processes in South Spitsbergen – summary].Prace Naukowe Uniwersytetu Slaskiego, 955, Katowice, 258 pp.

Lefauconnier, B., Hagen, J.O., Rudant J.P., 1994: Flow speed and calving rate of Kongsbreen glacier, Svalbard, using SPOT images. Polar Research, 13 (1), 59-65.

Massonnet D., Feigl K. L. 1998: Radar interferometry and its application to the changes in the Earth's surface. Reviews of Geophysics 36 (4), 441-500.

Vieli, A., Jania, J., Blatter, H., Funk, M., 2002: Short-term velocity variations on Hansbreen, a tidewater glacier in Spitsbergen. Journal of Glaciology (submitted), 26 pp.

Voigt, U., 1989: Zur Blockbewegung der Gletscher. Geodatische und Geophysikalishe Veroffentlichungen, R. III, 44, 128 pp.

Glacier Monitoring and Detection of Superimposed Ice on Kongsvegen, Svalbard, using SAR Satellite Imagery

Max König[1], Jan-Gunnar Winther[1], Jemma Wadham[2], and Jack Kohler[1]

[1]Norwegian Polar Institute, Polar Environmental Centre, N-9296 Tromsø, Norway.
E-mail: max.koenig@npolar.no, phone: +47 77 75 05 61
E-mail: winther@npolar.no, phone: +47 77 75 05 31
E-mail: kohler@npolar.no, phone: +47 77 75 06 55

[2]Bristol Glaciology Centre, University of Bristol, Great Britain.
E-mail: J.L.Wadham@bristol.ac.uk, phone: +44 (0) 117 9289069

Introduction

One of the principle aims of using satellite imagery for glacier studies is the identification of various surface types on the glacier surface and to monitor their extent and variations of several years. Changes in the mass balance of a particular glacier will result in changes in extent of those surface types. We are using synthetic aperture radar (SAR) images from ESA's ERS satellites for our studies. In contrast to optical images, the radar signal in the microwave region (5.3 GHz) allows observations during cloudcover and night-time conditions. It is also unaffected by the dry winter snow cover, detecting the end-of-summer surface during the entire winter in Svalbard.

Study area and data acquisition

Kongsvegen glacier is located in the Kongsfjorden area in Svalbard (Figure 1). In April 1999 and 2000 we collected shallow ice cores (ca. 50 cm), besides conducting regular mass balance measurements. From structural analysis we determined if a particular ice core consisted of glacier ice, superimposed ice or firn. In addition, we acquired ERS SAR images for every winter between 1991 and 2002. The SAR images were calibrated, geocoded and terraincorrected as described in König et al. (2002).

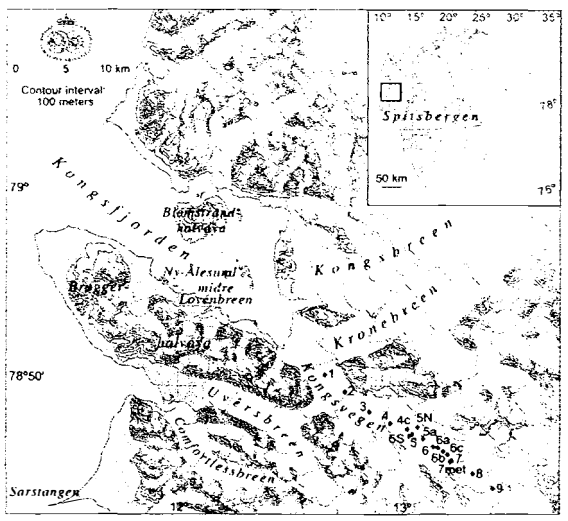

Figure 1: The study area. Core locations are marked on Kongsvegen.

Analysis and Discussion

The Kongsvegen SAR images for 1999 and 2000 can be seen in Figure 2. All our winter images show three distinct zones on the glacier surface. From earlier studies we can infer that the high backscatter zone corresponds to firn, while the low backscatter area corresponds to glacier ice. The nature of the medium backscatter zone on Kongsvegen, however, is not obvious at first. Figure 2 indicates the locations were ice cores were taken on Kongsvegen. The symbol at each location marks the type of glacier surface we encountered. Comparing the results from the

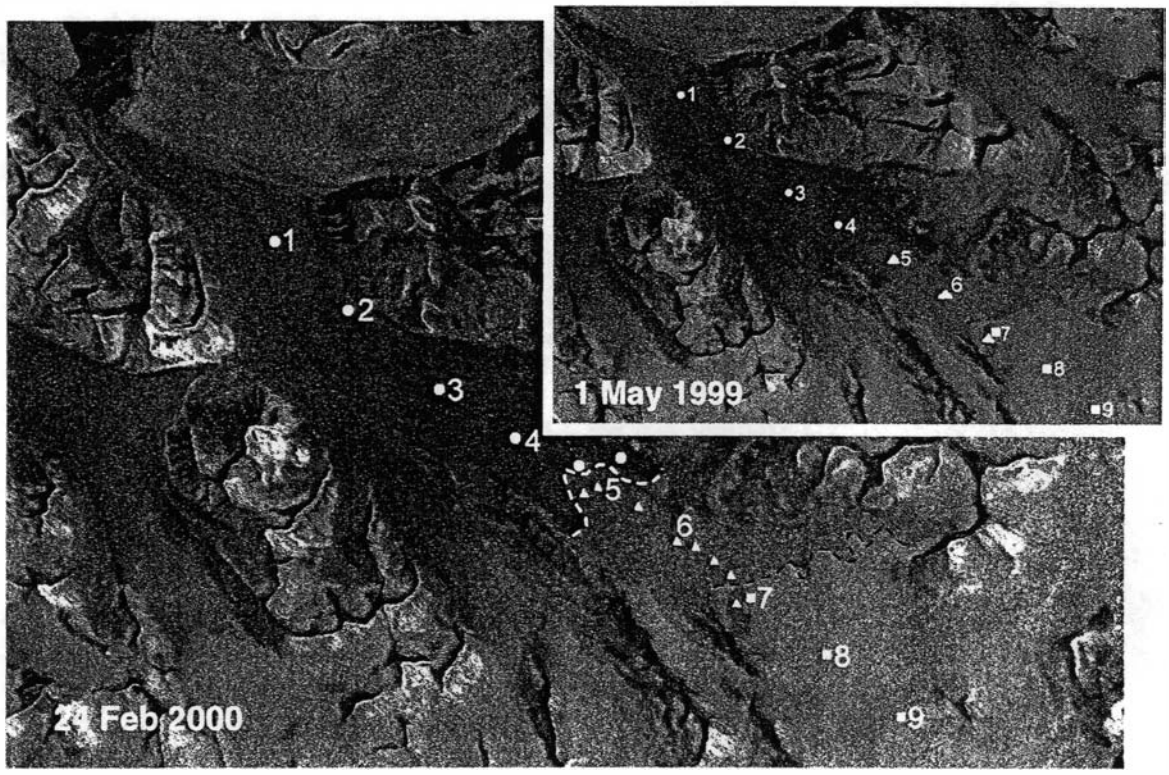

Figure 2: ERS-2 SAR images from Kongsvegen from from May 1st, 1999, and February 24th, 2000. Sites, where ice core analysis indicated presence of glacier ice (marked with a circle) coincide with an area of comparably low backscatter. Superimposed-ice core sites (marked by a triangle) coincide with an area of medium backscatter, and firn core-sites (marked by a square) coincide with an area of high backscatter. Note the highly crevassed tongue of the fast-flowing Kronebreen (upper left corner) giving high backscatter. See Figure 1 for geographic information and complete labelling of each core site. The SAR image data was provided by the European Space Agency (© ESA 2000).

core analysis with the SAR images, we find a striking correlation:

1) Areas with high backscatter correspond to the firn area. This confirms the results by Engeset et al. (2002), who concluded the same comparing SAR images from Kongsvegen with ground radar data.
2) Areas with low backscatter correspond to the glacier ice area.
3) Areas with medium backscatter, finally, correspond to the superimposed ice area.

The question arises why these three surface types each have their own distinct backscatter. Figure 3 shows a core from each area, showing the distinct structure of each surface type. The various crystals in the firn will reflect much of the incoming SAR signal back to the sensor, thus resulting in a high backscatter. The glacier ice is very clear and will not reflect very much of the SAR signal, thus resulting in low

Firn: average σ_0 = -0.6± 0.6 dB
1999 Core Sites on Kongvegen: 7, 8, 9
2000 Core Sites on Kongvegen: 7, 8, 9

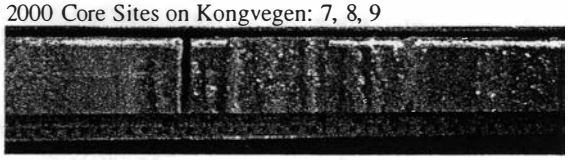

Superimposed Ice: average σ_0 = -6.2± 1.6 dB
1999 Core Sites on Kongvegen: 5, 6, 7met
2000 Core Sites on Kongvegen: 5,5S,5a, 6, 6a, 6b, 6c, 7met

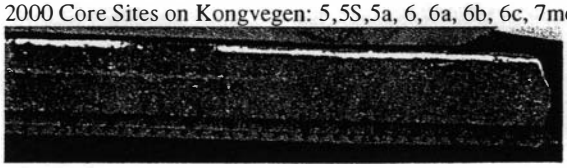

Glacier Ice: average σ_0 = -12.1± 1.1 dB
1999 Core Sites on Kongvegen: 1,2,3,4
2000 Core Sites on Kongvegen: 1,2,3,4, 4c, 5N

Figure 3: Photographs of representative ice cores from the firn area, superimposed ice area, and the glacier ice area on Kongsvegen. The average backscatter and corresponding core sites are listed.

backscatter. The superimposed ice core has layers consisting of very large air bubbles, as well as layers with many small air bubbles. We believe that it is the air bubble content in superimposed ice that results in a higher backscatter compared to glacier ice. A more detailed discussion on this can be found in König et al. (2002).

Backscatter Analysis

We have now identified the three zones visible on SAR images. As a next step we analyze the backscatter characteristics of each zone, which eventually will allow us to classify and monitor these zones over several years. This work is in progress and below we present the first results of our analysis.

For the backscatter analysis, we examine the SAR backscatter along the centreline of the glacier, following the core locations marked in the 1999 image in Figure 2. Results from an analysis of variance (ANOVA) show that the three zones can clearly be distinguished. However, even though each of the zones has a distinct range of backscatter values (see Figure 3), an ANOVA further shows that the backscatter distribution for a particular zone is not the same for different years. This means that the backscatter value for each zone needs to be determined newly each year.

Figure 4 analyses the separability of the three backscatter zone. Histograms from 1997 to 2002 show the backscatter falling into three distinct classes. Between 1992 and 1996, the boundaries are not so clear. Applying a simple filter (Davis, 1986) to the centreline backscatter, however, detects the boundary between zones in all years (see the peaks in the graphs to the left in Figure 4). For the glacier ice/superimposed ice boundary in Figure 4, the peak is sharper for 2000, while the broader peak for 1995 indicates a comparably more transitional boundary.

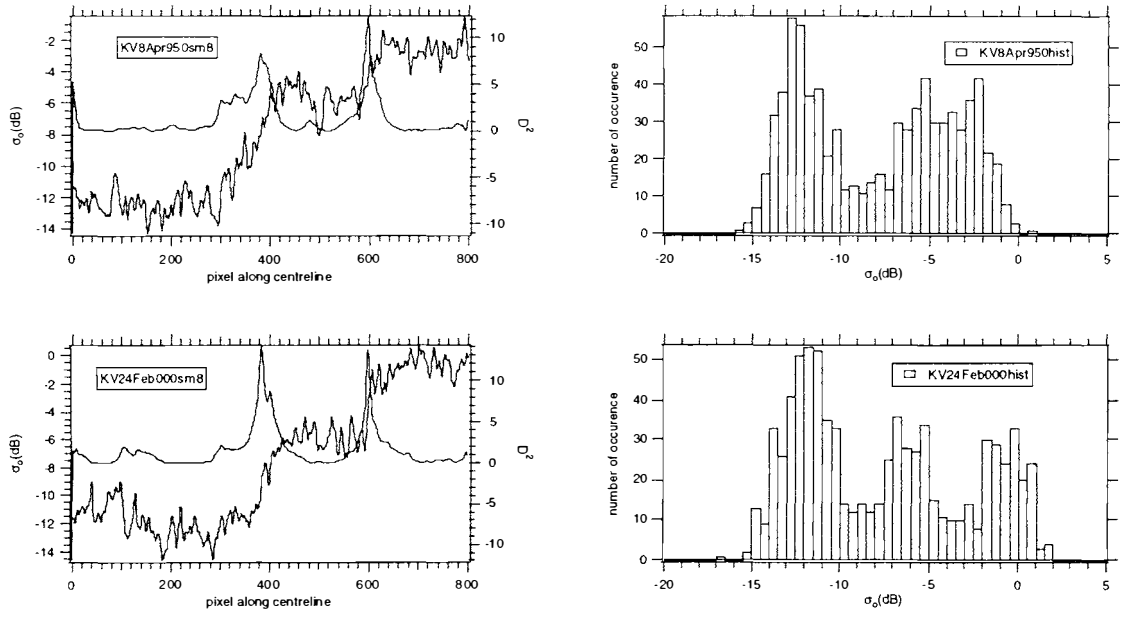

Figure 4: The graphs to the left show the SAR backscatter along the centreline of Kongsvegen. Peaks along the second, horizontal line indicate boundaries detected by a simple filter. The histograms to the right show three peaks for each of the three zones in 2000, while in 1995 two of the zones (superimposed ice and firn) do not separate so clearly.

Future plans and conclusions

We were able to show that SAR detects glacier ice, superimposed ice and firn as three distinct zones. Superimposed ice appears distinct in the SAR images due to its differing air bubble content. SAR backscatter is significantly different for the three zones, which can be separated clearly on the SAR images. This will allow image classification and monitoring of these three zones for assessing glacier mass balance from space. We plan to continue the backscatter analysis in more detail and then proceed to image classification over larger areas. Figure 5 indicates how such a classified image may look like. Having yearly images as in Figure 5 will show trends and changes within the last 10 years. This will enable us to tell, if any of these changes are related to changes in mass balance as observed in the field.

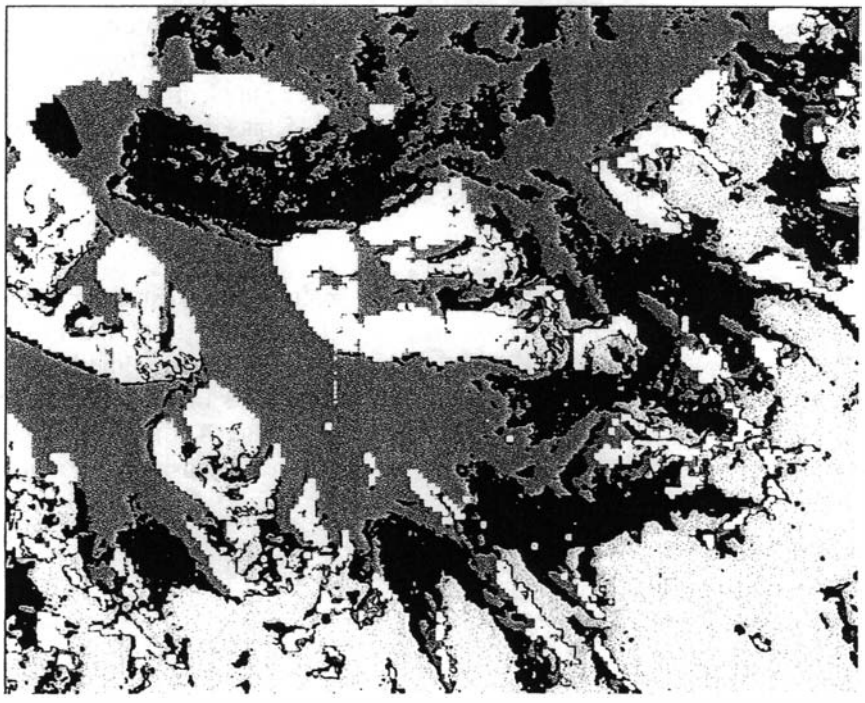

Figure 5: A test image, showing an initial classification attempt. White areas indicate non-glaciated areas and ocean, light-grey areas firn, black areas superimposed ice and the darker grey areas glacier ice. Note that this is a test image, containing several areas with incorrect assignment of classes.

References

Davis, J. C. 1986: *Statistics and Data Analysis in Geology.* New York: John Wiley and Sons.

Engeset, R. V., Kohler, J., Melvold, K., Lundén, B. 2002: Change detection and monitoring of glacier mass balance and facies using ERS SAR winter images over Svalbard. *Int. J. Rem. Sens. 23,* 2023-2050.

König, M., Wadham, J., Winther, J-G., Kohler, J., Nuttall, A-M. 2002: Detection of superimposed ice on the glaciers Kongsvegen and midre Lovénbreen, Svalbard, using SAR satellite imagery. *Ann. Glaciol. 34,* 335-342.

Regional patterns of meteorological variables in the Kongsfjorden area, Svalbard

Friedrich Obleitner & Jack Kohler
Institute of Meteorology and Geophysics, Innsbruck University, A-6020 Innsbruck, Innrain 52, Austria.
Norwegian Polar Institute, Polar Environmental Centre, N-9296, Tromso, Norway.

1. Introduction

Glacio-meteorological measurements have been performed on the glacier Kongsvegen, Svalbard since 2000. This work was done within the ICEMASS project, whose focus was on the mass balance of Arctic glaciers, and in close cooperation with the Norwegian Polar Institute. Knowledge of the regional distribution of the meteorological parameters is a basic issue in mass balance modelling, besides being of interest for other disciplines as well. Corresponding data are essentially useful for the parameterisation of atmospheric and glaciological models as well as for the validation of their output. Related aspects concerning glaciers in the Kongsfjorden area have been addressed by Lefauconnier et al. (1999) and Jania et al (1996). The interpretation of ice cores and satellite data is another issue in this context (König et al., 2001).

However, the remoteness of the high arctic interior and the harsh measurement conditions often means that there are seldom suitable data, apart from a few coastal synoptic weather stations (Forland et al., 1997). Interpolation of observational data from these stations is often used instead, but it is well known that the success of this method is limited due to effects of the complex topography of Svalbard and the associated modifications of the large-scale meteorological fields (Skeie and Gronas, 2000). The varying surface conditions (sea, tundra, snow/ice) induce specific boundary layer processes as additionally complicating factors. Combining our meteorological data from permanent automatic weather stations at the Kongsvegen glacier with Ny-Ålesund routine meteorological data contributes some new aspects to the above topics.

2. The data

The measurements started in April 2000, and have been gradually extended since then. By now, the measurement network comprises four automatic weather stations (AWS) that are located along the flow line of the Kongsvegen glacier (Figure 1). At this writing, AWS4 and AWS9 have not yet been downloaded since their installation in April 2002, so the current analysis is restricted to a sub-period with consistent data at stations AWS1 and AWS6.

AWS6 is designed as a full energy budget station measuring temperature, humidity, wind speed, wind direction at a nominal height of 2.5m above the surface, as well as the short- and longwave radiation components, snow height and snow temperatures. This allows for in-depth investigations of the seasonal evolution of the mass and energy budget of the local snow pack, which will not be considered here. AWS6 is located at about the elevation of the equilibrium line of the Kongsvegen glacier. The remaining AWSs measure temperature, wind speed and wind direction, and thus will yield information on the temperature and wind conditions at different elevations along the glacier. Their locations cover a height range of 173 m a.s.l. (at the tongue of the glacier) up to 865 m a.s.l. (at Kongspasset, the highest point of the glacier). All sensors were calibrated before fieldwork; the data are stored at one-hourly intervals and downloaded during maintenance of the stations once or twice a year. The stations performed remarkably well in view of the difficult measurement conditions, e.g. with respect to the formation of rime that is often experienced in these areas. However, there are a few gaps in the records, which were mainly due to failure in power supply. In addition, the quality of some data is suffering from the known constraints on unattended measurements (e.g. non-ventilated temperature sensors or changing height above ground).

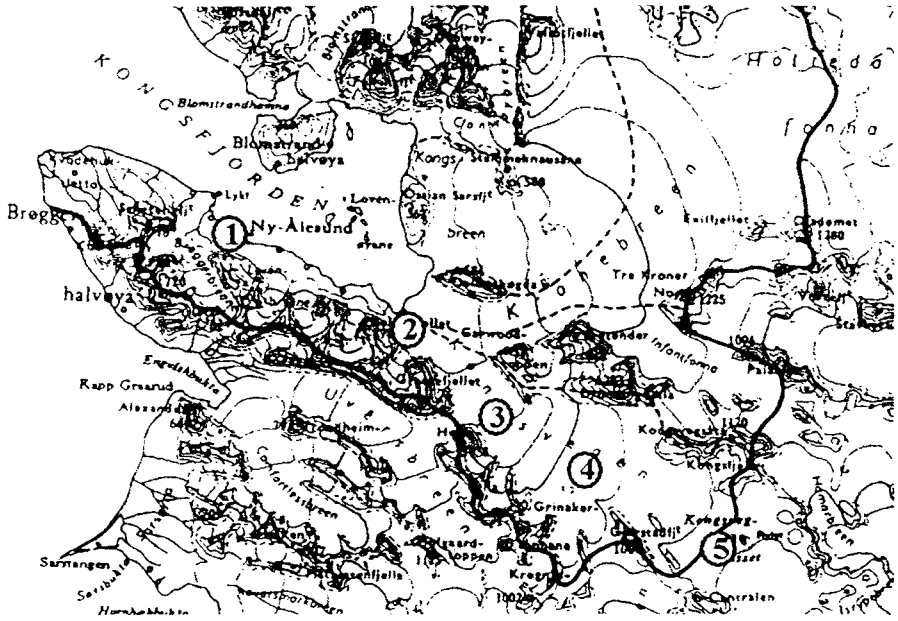

Figure 1 ***Topographic map of the Kongsfjorden area and the position of the automatic weather stations at Kongsvegen glacier. 1) Ny-Ålesund,(11m) 2) AWS1(171m) 3) AWS4(420m) 4) AWS6(543m) 5) AWS9(865m a.s.l.)***

3. A AWS6 year-round climatology

Table 1 is a compilation of year-round meteorological data as measured by AWS6 (April 2000 through September 2001, 543 m a.s.l.). In a glaciological context, AWS6 is of special interest for representing the conditions at the average elevation of the equilibrium line on Kongsvegen. This site is characterised by almost balanced net radiation and an overall humid regime, which can be attributed to the relative proximity of the glacier to the sea. The average wind speeds are on order 5 m s^{-1}, though hourly gusts in excess of 15 m s^{-1} have been recorded during the frequent storms. Annual air temperature is –10.5°C, with fairly constant summer temperatures around 0°C and a more variable winter temperature regime which can include large day-to-day changes, varying as much as 35°C in some cases. The former can be attributed to the stabilising influence of the melting ice surface; the latter is due to the vital synoptic disturbances enforcing a periodic break up of the otherwise persistent radiation inversions.

month 2000/2001	air temperature °C	relative humidity %	wind speed m/s	net radiation Wm^{-2}
4	-18.5	73	4.2	-10.2
5	-9.7	81	4.6	11.8
6	-3.4	83	3.3	27.0
7	-0.3	90	3.5	35.0
8	-1.9	89	3.5	14.3
9	-4.8	-	4.4	-1.6
10	-4.2	-	5.2	-7.6
11	-10.1	-	4.6	-1.5
12	-18.2	-	5.9	-16.1
1	-15.2	-	6.1	-16.0
2	-16.0	-	5.5	-16.3
3	-23.1	-	4.7	-10.9
4	-18.8	-	4.2	-5.4
5	-9.6	83	4.5	13.1
6	-2.6	86	3.8	49.0
7	-0.2	89	2.8	55.9
8	-0.6	90	3.9	27.9
9	-1.7	94	5.6	9.3
annual (5-4)	-10.5	86.0	4.6	1.1

Table 1: ***Mean monthly values of temperature, humidity, wind speed and net radiation at the location of AWS6, Kongsvegen glacier. The annual values refer to transition between dark and sunlight season (May 2000- April 2001).***

Figure 2a shows histograms of the measured wind directions at AWS6. Their annual distribution is characterised by two pronounced peaks following the overall orientation of the glacier (Figure 1). This pattern shows almost no seasonal differentiation throughout the year. The most frequent south-easterly directions reflect a prevalence of down-sloping, i.e. locally induced, glacier winds, which during winter especially are certainly modified by synoptic winds flowing over the Kongspasset gap. This is supported by comparison with data that are simultaneously measured by the Ny-Ålesund radiosondes at the same elevation as AWS6 (925 hPa, Figure 2b). The second peak with up-sloping northwesterly winds may be associated with synoptic winds from that direction, where topographically induced channelling effects might play a role too. Similarly, the minor peaks from the northeast and southwest are probably due to cross-winds flowing through topographic gaps in the upper Kongsvegen area. As a further comment on the regional (vertical) wind direction pattern, a general shift from near-surface easterly to upper-air westerly winds may be noted, which is accompanied by increasingly flatter distributions (Figure 2d). The latter gives another indication of distinct topographic influences on the regional wind regime.

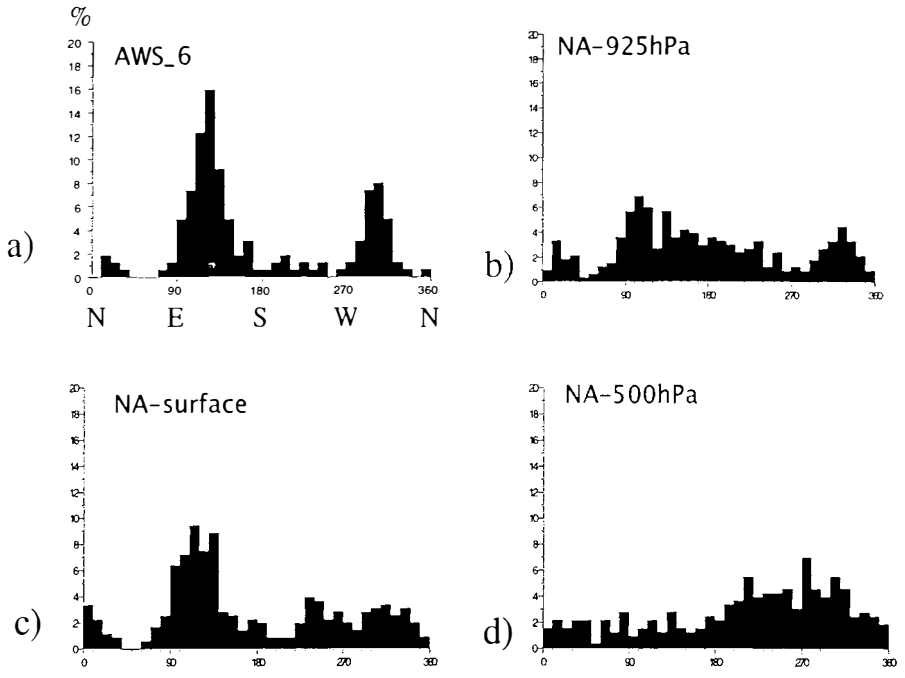

Figure 2 Mean annual relative wind direction frequencies (May 2000-April 2001) for: a) AWS 6; b) Ny-Ålesund 925hPa; c) Ny-Ålesund surface; d) Ny-Ålesund 500hPa (radiosondes, 12UTC).

4. On the regional temperature gradients

Knowledge about the air temperature at glacier sites is of basic interest in ablation modelling or in relationship to ice temperature profiles. For example, Jania et al. (1996) modelled the formation of superimposed ice at Svalbard glaciers by comparing measured ice temperatures with estimated annual air temperatures, while Lefauconnier et al. (1999) used positive degree days from meteorological data obtained at Ny-Ålesund to estimate ablation for several glaciers in the area.

In this context too, our data are useful for checking or improving the inherent assumptions on the height-dependence of temperature. Combining consistent data from two glacier sites and from Ny-Ålesund, Table 2 is a compilation of the mean monthly vertical temperature gradients

during summer 2001. As to be expected, the resulting values bracket the moist and dry adiabatic temperature gradients, with the larger values along the coastal section (NA-AWS) and the smaller ones along the glacier section (AWS6-AWS1). In interpreting the gradients, it is important to remember that they do not resemble free atmosphere (vertical) gradients; rather, they are of a composite nature (horizontal and vertical), and depend on the horizontal distances and correspondingly changing surface conditions. Thus, the large temperature difference between Ny-Ålesund and AWS1 must be largely attributed to specific boundary-layer effects due to the respective location of these stations at the open sea and on the glacier. Naturally, this effect is most pronounced in the central summer months. Following the slope along the ice surface of Kongsvegen at the other hand (AWS 6 –AWS 1), the temperature differences are less pronounced and less variable. This can be attributed to the moderating effect of the underlying ice that is almost continuously melting at both sites. Accordingly, these gradients tend to increase towards spring and autumn, times for which melt at the upper station is less probable than at the tongue of the glacier. The Ny-Ålesund-AWS6 temperature gradients approach the dry adiabatic value (-0.9°C/100m), which is quite different from the true free atmosphere temperature gradients that were simultaneously measured by the Ny-Ålesund radiosondes (-0.53 °C/100m). Former studies on the temperature regime of Kongsvegen assumed validity of -0.6°C/100m (Jania et al., 1996), whereas our data do not confirm the validity of using such gradients in a glacial setting.

	NA-AWS1	Na-AWS6	AWS 6-1	
May	-0.68	-0.93	-1.03	°C / 100m
June	-0.60	-0.74	-0.80	°C / 100m
July	-2.23	-1.04	-0.51	°C / 100m
Aug	-1.75	-0.91	-0.54	°C / 100m
Sept	-0.93	-0.90	-0.89	°C / 100m
summer 2000	**-1.24**	**-0.90**	**-0.75**	°C / 100m

Table 2 ***Mean monthly temperature gradients along various transects in the Kongsfjorden/Kongsvegen area.***

5. Further perspectives

Future studies will also include data from two additional weather stations that are have been operating since Spring 2002. This will expand current knowledge on the regional and temporal variability of the basic meteorological parameters (including solar and long-wave radiation), and will also allow for more detailed, process-oriented studies on for, example, the interaction of synoptic winds with topography or other wind systems. New effort should probably be put into achieving better information on regional precipitation patterns, which are not very well known, especially during summer, and yet are of equal importance for the various glaciological applications.

6. References

Førland E.J., I. Hanssen-Bauer and P.O. Nordli. 1997. Climate statistics and long-term series of temperature and precipitation at Svalbard and Jan Mayen, *DNMI_Rapport* No. 21/97, Norwegian Meteorological Institute, Oslo, 72 p.

Jania, J., D. Mochnacki and B. Gadek, 1996. The thermal structure of Hansbreen, a tidewater glacier in southern Spitsbergen, Svalbard. *Polar Research* **15**(1), 53-66.

Skeie P. and S. Grønås. 2000. Strongly stratified easterly flows across Spitsbergen. *Tellus* **52A**(5), 473-487.

Lefauconnier B., J.O. Hagen, J.B. Ørbæk, K. Melvold and E. Isaksson. 1999. Glacier balance trends in the Kongsfjorden area, western Spitsbergen, Svalbard, in relation to the climate. *Polar Research* **18**(2), 307-313.

König M., J.-G. Winther, and E. Isaksson. 2001. Measuring snow and glacier properties from satellite. *Rev. Geophys.*, **39**(1) 1-29.

Runoff in Svalbard

Lars-Evan Pettersson

Norwegian Water Resources and Energy Directorate (NVE), P.O. Box 5091 Majorstua, 0301 Oslo, Norway. E-mail: lep@nve.no, phone +47 22 95 92 35

Introduction

The Hydrology department at the Norwegian water resources and energy directorate (NVE) is the national institute for hydrology in Norway. NVE is operating hydrometric stations for mapping and supervising the water resources in the country. For any user of fresh water, e.g. for energy producers, water suppliers and so on, the knowledge of the availability and quantity of fresh water and its distribution in time and space is essential. Long term observations of discharge forms the basis for evaluations of runoff fluctuations and trends. In addition, the rivers are feeding fjords and sea with fresh water and they are the carriers of material like suspended load, chemical solutions, humus, debris, pollutions and so on. Since most measurements of river transported material is done by taking samples of the concentration of the material in the river, estimates of the total volume of suspended and diluted material is dependent on runoff data.

NVE and its predecessors have been responsible for operating water stage / water discharge stations in mainland Norway for more than 150 years. Also, the Directorate maintains the Norwegian hydrologic database, including data from stations operated by other institutes, by regulators, energy producers and others.

Hydrometric stations in Svalbard

In 1989 NVE included stations in Svalbard in the hydrometric station net work. In this year the station at Bayelva nearby Ny-Ålesund was established. Since then other stations were established, four near Longyearbyen, and two more in the Ny-Ålesund area, see table 1.

Table 1. NVEs stations for water stage / water discharge

Station	Drainage area, km^2	Glacier area, %	Number of years with complete discharge data	Additional parameters
Ny-Ålesund area				
400.1 Bayelva	30.9	55	12	Sediment transport, bed load, water temperature
400.3 Tvillingvatnet	0.36	0	4	Water extraction, water temperature
400.4 Londonelva	0.70	0	6	Sediment transport, water temperature
Longyearbyen area				
400.5 De Geerdalen	79.1	10	11	Sediment transport, water temperature
400.2 Isdammen	34.4	17	3	Sediment transport
400.6 Steintippdalen	3.8	0	7	Water temperature
400.7 Endalselva	28.8	20	6	Sediment transport, water temperature

A hydrometric station normally monitors water stage at a site where there is a fixed and persistent relationship between water stage and water discharge. The observation interval varies from 15 minutes, or shorter, in small catchments up to one hour in large catchments. Data are stored as water stage, both with a fine time resolution and as daily means. By using a rating curve for the station, the water stages can be transformed to discharge in m^3/s. These data can then be transformed further on to water volumes, e.g. m^3 in a day or in a month, or to specific runoff, e.g. l/s km^2, that is discharge per unit area. In water balance studies, the runoff is usually expressed as millimeter per time unit.

Some of NVEs hydrometric stations are established for short term studies, while the purpose for other stations are long term observations. Of the hydrometric stations in Svalbard, the stations in Bayelva and De Geerdalen are reference stations, where the observations are supposed to continue for long time.

The Bayelva station near Ny-Ålesund has a large part of the catchment covered by glaciers. The Bayelva river is quite typical for most rivers in the area. Tvillingvatnet, that is located in a small tributary to Bayelva, forms the water reservoir for the Ny-Ålesund community. The observations include water stage, discharge and the amount of water extracted for water supply. The station in Londonelva on the Blomstrand island across the fjord from Ny-Ålesund is of special interest since the catchment is small and without glaciers.

Runoff in Bayelva

The runoff in Bayelva is illustrated in figure 1.

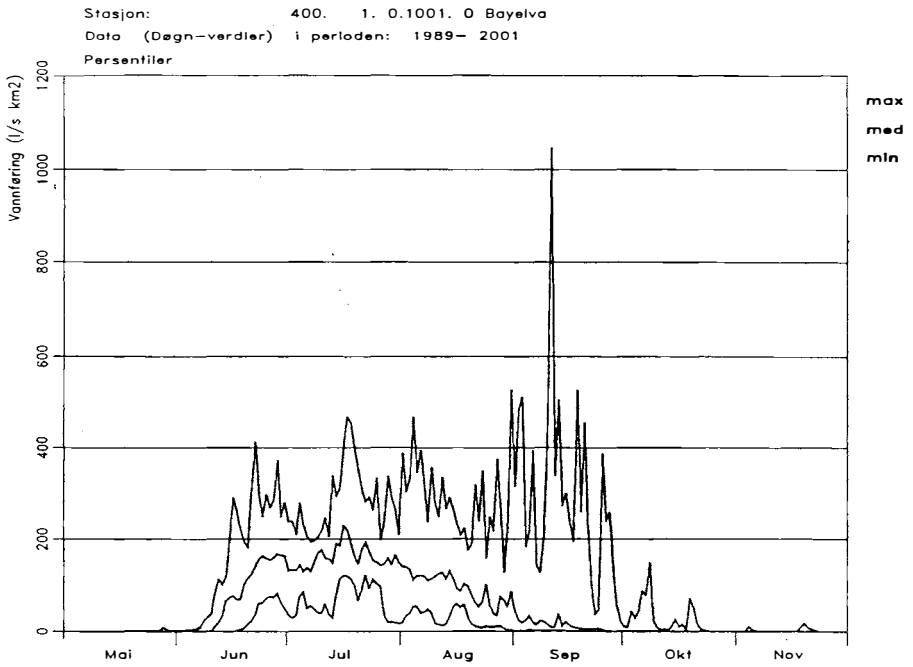

Figure 1. Characteristic specific runoff, l/s km^2, in Bayelva in the period 1989-2001. The figure shows maximum and minimum observed runoff each day during the year, and the median runoff, that is there are as many observations greater as less than this value.

Normally, the runoff in Svalbard takes place from early June to late September, but some years, runoff can occur already in May and as late as in October-November, see figure 1. The snowmelt in the glacier free areas is quite fast and intense. The main part of the snowmelt in these areas is completed by mid-July. Then the runoff is dominated by meltwater from the glaciers and rainfall events.

The snowmelt floods occur annually in early summer. However, the highest floods observed are caused by rainfall in the autumn. As seen in figure 1, the highest flood in Bayelva, in September 1990, was about twice as high as the second highest. The specific runoff as daily mean, was 1047 l/s km^2, or 32.4 m^3/s as discharge. The peak flood is normally much higher than the daily mean. In September 1990, the peak flood was 44 m^3/s or 1424 l/s km^2.

Table 2 presents the mean monthly and annual values for the runoff in Bayelva in the period 1990-2001.

Table 2. Mean monthly and annual data for Bayelva, 1990-2001.

	Discharge	Specific runoff	Runoff	Total runoff	Portion of annual runoff
	m^3/s	l/s km^2	mm	million m^3	%
May	0.00	0	0	0.0	0
June	2.35	76	197	6.1	18
July	5.08	164	440	13.6	40
August	3.59	116	311	9.6	28
September	1.64	53	137	4.2	13
October	0.07	2	6	0.2	1
November	0.01	0	1	0.0	0
Year	1.07	35	1092	33.7	100

In the period 1990-2001, the mean annual precipitation at the meteorological station in Ny-Ålesund was only 443 mm, while the mean annual runoff in Bayelva was 1092 mm. This low value for mean annual precipitation is due to the catch deficiencies that all precipitation gauges suffers from. In addition, Ny-Ålesund has probably less precipitation than any areas in the Bayelva catchment, since normally the precipitation increases with raising elevation. The discrepancies between runoff data in Bayelva and precipitation data in Ny-Ålesund can partly be explained by the fact that the measurements are underestimating the precipitation. But in addition the mass balance on the glaciers are influencing the runoff. The glaciers are supplying extra water to the river in years with a negative net mass balance.

Figure 2 illustrates the annual runoff fluctuations 1990-2001. The total annual runoff differs through the period with maximum 20 % from the mean. There are no significant trends, neither in annual runoff nor in monthly runoff. In June, both the two wettest years and the two driest years have occurred during the last four years. Therefore, there is no tendency to e.g. a change to earlier snowmelt or greater amounts of snow as a whole in the last years. September, in the last couple of years, have been quite wet, perhaps indicating a more humid climate in autumn, but on the contrary, the wettest September was in 1990, in the beginning of the period, with heavy rainfall floods. So far, the annual fluctuations in the runoff in Bayelva, can not be considered as anything else but normal.

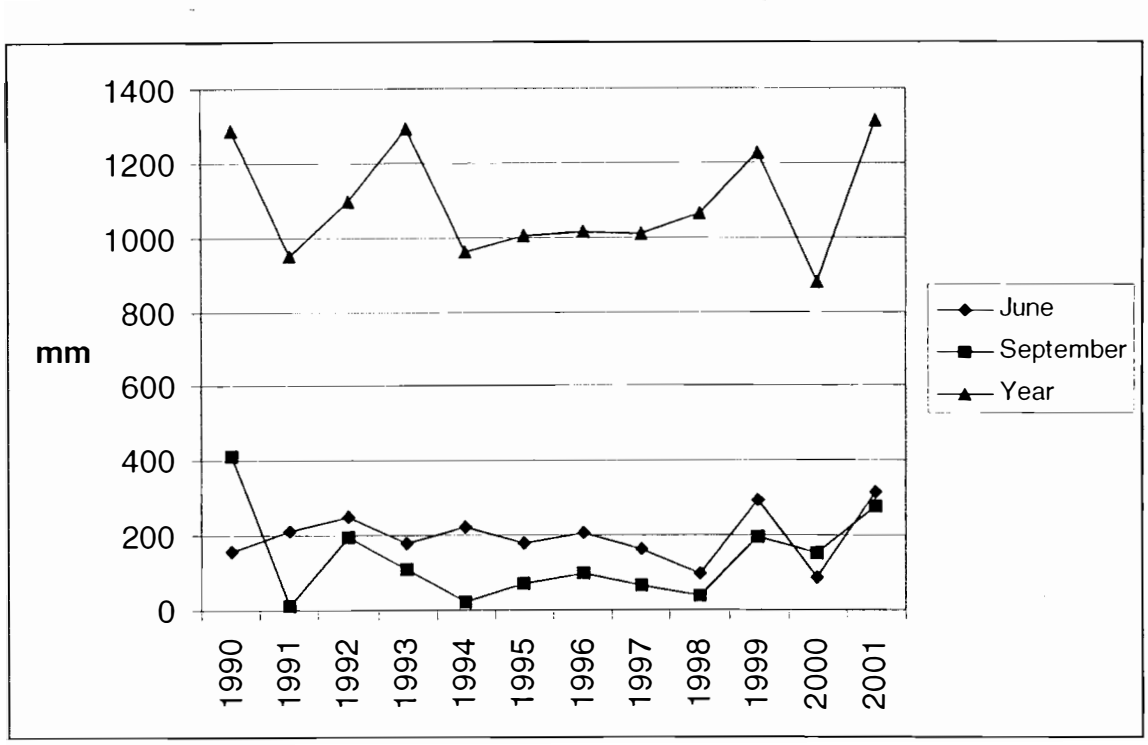

Figure 2. Annual and monthly runoff in Bayelva, 1990-2001.

This season, data from Bayelva has been transmitted in real time to NVEs head office in Oslo. Data for 2002 is shown in figure 3, based on observations with intervals of 30 minutes.

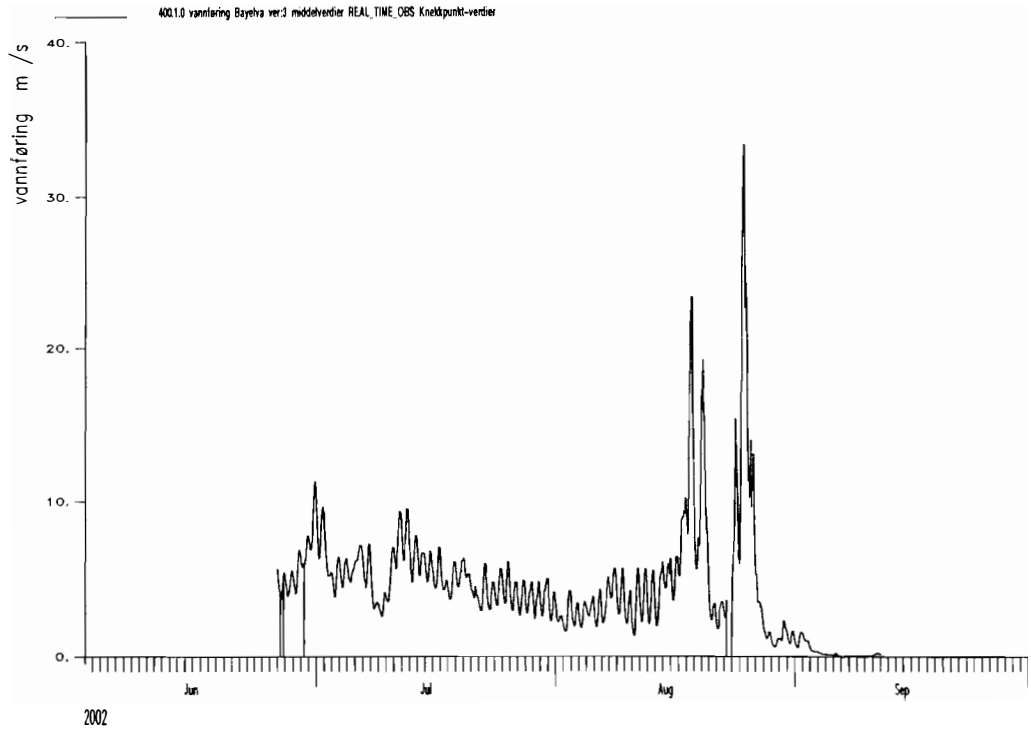

Figure 3. Discharge, m^3/s, in Bayelva, 2002

Chemical Denudation Rates in the Bayelva Catchment (Svalbard) in September-October of 2000

Wiesława Ewa Krawczyk, Bernard Lefauconnier & Lars-Evan Pettersson

Faculty of Earth Sciences, University of Silesia, 41-200 Sosnowiec, Będzińska 60, Poland, E-mail: wkraw@us.edu.pl, phone +48 32 2918901

ADREA, Le Mollard, F 38700 Le Sapey en Chartreuse, France, E-mail: b.lefauconnier@wanadoo.fr, phone +33 4 38864109

Norwegian Water Resources and Energy Directorate, P.O. Box 5091 Majorstua, N-0301 Oslo, Norway, E-mail: lep@nve.no, phone +47 22 959235

Introduction

Chemical dissolution of rocks by flowing water is a major agency transforming the Earth's relief and lowering its surface. Global climate modelling to estimate future increases of atmospheric CO_2 requires data on chemical rock weathering rates and CO_2 sequestration in glacier-covered regions. A review of chemical denudation research presented by Hodson et al. (2000) shows that most field monitoring in west Spitsbergen basins has been limited to July-August. The only basins with data on solute fluxes in September are Scottbreen (Bartoszewski 1994) and Werenskioldbreen (Pulina et al. 1984, Krawczyk 1994).

A trend to increasing precipitation totals during polar summers of 1990-2000 and rise of September mean monthly air temperatures above 0°C calls for conducting denudation research in this period, earlier considered to be the end of the ablation period, with only small outputs as dissolved loads.

Research was undertaken in the Bayelva basin, which has an area of 31 km^2 and includes two glaciers, Austre Brøggerbreen and Vestre Brøggerbreen. Earlier chemical denudation rates were obtained by Repp (1979, 1988) for the period 1974 -1978 and Hodson et al. (2000) for 1991 and 1992.

Methods

Discharge was recorded at the NVE station (BAYELVA – 400.1) situated near Ny-Ålesund. Water samples were taken by CISCO automatic sampler every 8 hours (at 00:00, 8:00 and 16:00) in the period August 26 – September 10. The first set of 24 samples was taken to the laboratory on September 2 and filtered immediately using pre-rinsed filter units and 0.45 µm membrane filters. In the filtered samples specific electric conductivity (CC-317 conductivity meter) and pH (JENCO pH meter) were measured. Sub-samples were collected in pre-rinsed 100 ml polyethene bottles and stored in the dark at c. 4°C. Chemical analyses were made in the earth science laboratories at the University of Silesia, Sosnowiec. Hydrogencarbonate concentrations were determined by titration with HCl and a mixed indicator. Concentrations of chlorides, sulphates and nitrates were determined by ion chromatography, using a Metrohm IC 761, with Dual-anion column, Na_2CO_3 + $NaHCO_3$ eluent. The concentrations of Ca^{2+}, Mg^{2+}, Na^+ and K^+ were determined by atomic adsorption spectroscopy (AAS) with a Solaar M6 instrument. Before cation analysis samples were acidified with HNO_3. Concentrations of dissolved silica were determined by spectrometry using the method of reduction to molybdenum-blue (Krawczyk 1996).

Charge balance errors of analyses were in the range –1.6% to 2.5%.

Meteorology

The polar summer season (i.e. the period with mean daily air temperature above 0°C) in 2000 was the longest one (147 days) recorded in Hornsund during the last 20 years (Krawczyk et al. 2002). In Ny-Ålesund polar summer started on June 12 and continued until October 25, a duration of 136 days.

The second part of this period (September-October) was warm and rainy (Figure 1). September was marked by mean monthly air temperature t_a=1.0°C and precipitation total P=127.8 mm; the highest rainfall occurred on September 14 (29.2 mm). In October mean monthly air temperature was 0.7°C, and the precipitation total was even higher than in September (136.4 mm).

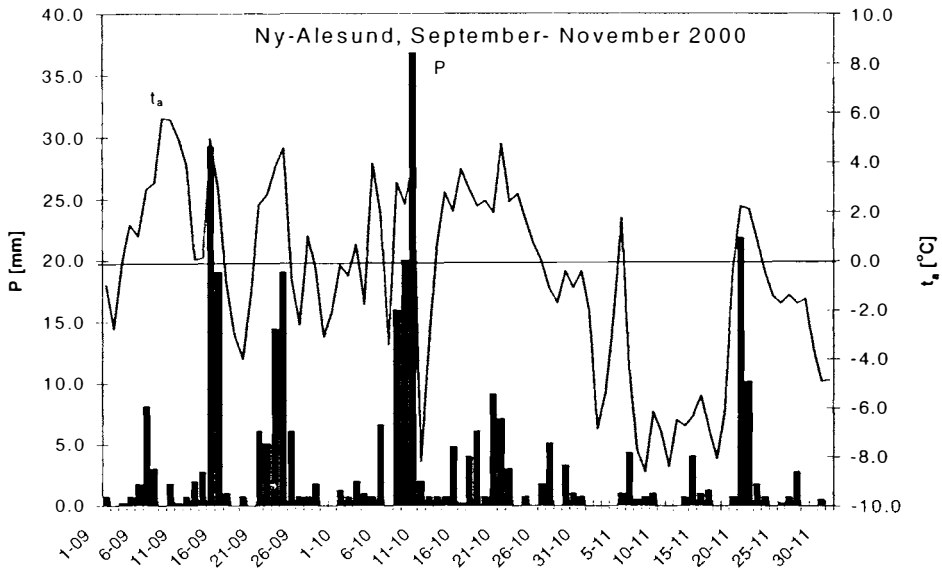

Figure 1. Mean daily air temperature and precipitation totals in Ny-Ålesund in September – November 2000. Data source: National Climatic Data Centre, NOAA, WMO Resolution 40, USA

Hydrology

In 2000 outflow from the Bayelva catchment commenced on June 12. Discharges were ceasing at the end of October but even in November, due to increase of air temperature and rainfall, two small discharge events were recorded ($0.15*10^6$ m^3). The highest daily discharge was recorded on September 14 (15.7 m^3/s). The volume of water discharged in Bayelva in September was only $0.5*10^6$ m^3 less than in August and comparison of distribution of monthly discharges in total yearly discharge shows that September water volumes were only 2% less than in August (Table 1).

Table 1. Distribution of Bayelva discharges during the polar summer (as % of total discharge)

	May	June	July	August	September	October	November
mean 1974-1978	1	17	46	34	2	0	0
mean 1990-2001	0	18	40	28	13	1	0
2000	0	10	47	**19**	**17**	**6**	1

The total volume of water discharged in Bayelva was $27.16*10^6$ m^3 (Figure 2). Distribution of discharges in 2000, in comparison with the mean from 1974-1978 (Repp 1988) and mean from the 1990-2001 (Pettersson 2002) shows that the hydrologically active period in the Bayelva catchment became longer. The volume of water discharged in July and August was only 66% of the total for he season, less then 80% recorded in the 70s.

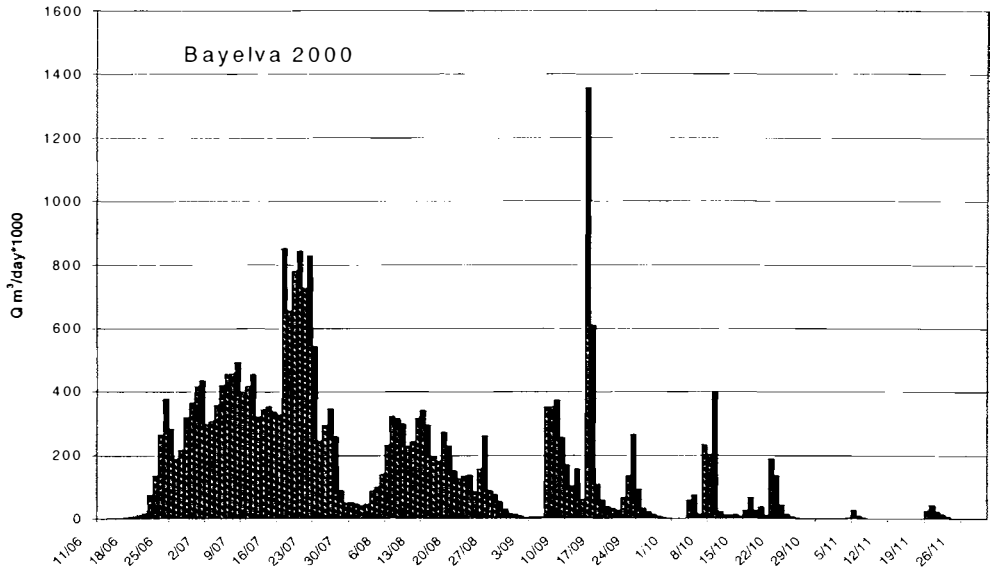

Figure 2. Water volumes discharged in Bayelva in 2000.

Water chemistry

Bayelva water samples (42) provide chemical composition in the period August 26 - September 10. Specific conductivity was in the range 84.0-188.5 µS/cm, pH in between 7.68 and 8.24; ranges of ion concentrations were wide in the case of Cl^- and SO_4^{2-} (Table 2).

To extrapolate these data for the full September-October period the discharge weighted mean ion concentrations were calculated for the sampling period. The assumption was made that the sample collected is representative of the eight hour sampling interval and total discharge was calculated for the period four hours before and four hours after the sampling time. Mean ion concentrations in September 2000 were higher by 1.6 times (Ca^{2+}, HCO_3^-) or even by 3.2 times (SO_4^{2-}) than means obtained by Hodson et al. (2000) and Hodson et al. (2002) in the summers of 1991 and 1992. These higher concentrations of sulphate are most probably of atmospheric origin, mean (v/w) sulphate concentration in Hornsund rainfall in 2000 was 1.0 mg/l and nss-sulphate has reached 0.43 mg/l due to dominating S+SW directions of atmospheric circulation (Głowacki, Krawczyk 2002).

Table 2. Range of ion concentrations in Bayelva (in mg/l)

	TDS	Ca^{2+}	Mg^{2+}	Na^+	K^+	HCO_3^-	SO_4^{2-}	Cl^-	NO_3^-	SiO_2
min	63.5	11.63	1.99	1.24	0.61	43.9	2.96	0.83	0	0.32
max	144.0	23.20	5.63	8.88	1.17	79.3	19.29	8.79	0.55	0.78

Chemical denudation rates - conclusions

Partitioning of Bayelva aqueous solutes was done for crustal, marine and atmospheric components, assuming that all chlorides are of marine origin, similarly as in the model proposed by Hodson et al. (2000). In September and October 2000 around $6.31*10^6$ m^3 of water

discharged from the Bayelva basin. The total crustal load amounted 369.1 tonnes, the dominating ions being hydrogencarbonate and calcium (Figure 3). The marine load was 16.3 tonnes and ions of atmospheric origin (HCO_3^-, SO_4^{2-}, NO_3^-) totalled 121.7 tonnes. Mean sulphate concentration in Hornsund rainfall in the polar summer of 2000 was used as a proxy for the atmospheric sulphate load. Contributions of crustal, marine and atmospheric components in total solute load were 72.8%, 3.2 and 24.0%.

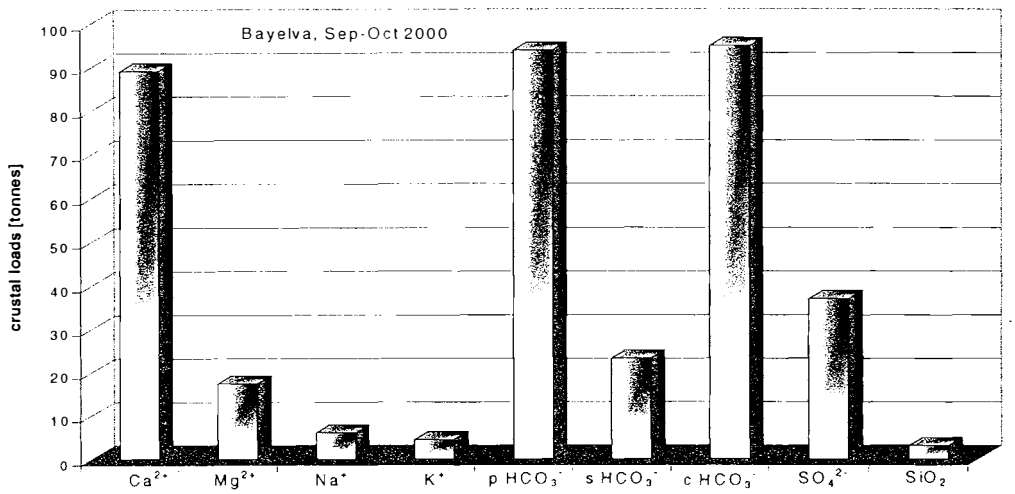

Figure 3. Bayelva crustally derived ion loads in September – October 2000. Partition of HCO_3^- load was made for pyrite (p), silicate (s) and carbonate origin of hydrogencarbonate ion.

The chemical denudation rate in Bayelva in September and October 2000, (the period normally not included in Svalbard chemical denudation research) was 4.8 m^3/km^2 or 202 Σ^+ meq/m^2. This is 48% of denudation rate estimated by Hodson et al. (2000) for 1991 and 1992. The estimated withdrawal of CO_2 from the environment in September-October 2000 was 749 kgC/km^2, less than the values of 2600 – 3000 kgC/km^2 a^{-1} reported by Hodson et al. (2000) in 1991 and 1992.

Acknowledgements
This work was supported by European Community - Access to Research Infrastructure, Action of the Improving Human Potential Programme.

References

Bartoszewski, S. 1994. Mechanical and chemical denudation in the Scott Glacier basin (West Spitsbergen). XXI Polar Symposium, Warszawa, 189-198

Hodson, A., Tranter, M. & Vatne, G. 2000. Contemporary rates of chemical denudation and atmospheric CO_2 sequestration in glacier basins: an Arctic perspective. *Earth Surf. Process. & Landforms 25*, 1447-71

Hodson, A., Tranter, M., Gurnell, A., Clark, M. & Hagen, J.O. 2002. The hydrochemistry of Bayelva, a high Arctic proglacial stream in Svalbard. *Journal of Hydrology*, 91-114.

Killingtveit, A., Pettersson, L.E. & Sand, K. 1991: Water balance studies at Spitsbergen, Svalbard. In Y.Gjessing, J.O.Hagen, K.A.Hassel, K.Sand & B.Wald (eds.) *Arctic Hydrology. Present and Future Tasks. Norwegian Committeee for Hydrology Report*, 23, 77-94

Krawczyk, W.E. 1994. Denudacja chemiczna w wybranych zlewniach SW Spitsbergenu, *PhD thesis, University of Silesia,* Sosnowiec, 233 pp.

Krawczyk, W.E. 1996: Manual for karst water analysis. *International Journal of Speleology, Handbook 1, Physical Speleology,* Bologna, 51 pp.

Repp, K. 1979: Breerosjon, glasio-hydrologi og materialtransport i et hoyarktisk miljo Broggerbreene, Vest Spitsbergen. Thesis, Hovdfagsopgave i naturgeografi, Universitetet i Oslo, 136 pp

Repp, K. 1988: The hydrology of Bayelva, Spitsbergen. *Nordic Hydrology*, 19, 259-268

Sea ice surface reflectance and under-ice irradiance in Kongsfjorden, Svalbard

by
Jan-Gunnar Winther, Norwegian Polar Institute, Polar Environmental Centre, N-9296 Tromsø
Kåre Edvardsen, Norwegian Institute for Air Research, Polar Environmental Centre, N-9296 Tromsø
Sebastian Gerland, Norwegian Radiation Protection Authorities, Polar Environmental Centre, N-9296 Tromsø
Børge Hamre, Department of Physics, University of Bergen, Allégaten 55, N-5007 Bergen

Abstract
Initial results from a field experiment on first-year fast ice in Kongsfjorden, Svalbard, in March 2002 is presented. We measured surface reflectance and under-ice irradiance covering the ultraviolet (UV) and visible (VIS) wavelength regions. Additionally, we present model results of wavelength-dependent transmittance of radiation in sea ice for various snow cover thickness on top of the sea ice.

Introduction

Optical properties of sea ice have interested researchers for several decades (e.g. Langleben, 1968; Perovich, 1994). The crucial role that Svalbard's seasonally ice-covered fjords play in the biological productivity dynamics has also been discussed (e.g. Mehlum, 1991). For example, sea ice algae survival depends on radiation penetrating the sea ice and the physical and chemical properties of the water below the sea ice and within brine drainage channels (Horner, 1985; Gerland et al., 1999). In this study we present data on surface reflectance and under-ice irradiation acquired during a field campaign in Kongsfjorden in March 2002. Also, some results from a coupled Atmosphere Snow-Ice-Ocean model is shown. Measurements were collected in the inner part of Kongsfjorden at the west coast of Svalbard at about 79°N.

Methods

The optical field measurements were performed using a spectroradiometer (FieldSpec, Analytical Spectral Devices Inc., Boulder, USA) that measures irradiance in the 350 to 2500 nm wavelength region. The instrument consists of three built-in separate spectrometers. In performing the reflectance measurements an 18° field-of-view adapter was used on the sensor that was mounted on a tripod. The surface reflectance (or albedo) is defined as the ratio between reflected and incident radiation (in Wm^{-2}). This relationship was determined by means of calibration measurements using a halon-target reference plate. More precisely, the incident radiation was obtained using the reference plate with known reflectance signature combined with reflected radiation measured of the natural snow (or sea ice) surface (Winther et al., 1999).

For the under-ice measurements a waterproof extension fibre was connected to a cosine receptor, mounted on a swing arm, which could be operated through a hole drilled through the sea-ice cover. After lowering the sensor into the drilled hole the arm was swung up 90°such that the sensor was positioned a few cm below the sea ice and about one meter horizontally away from the drill hole. Consecutive measurements above and below the sea ice with not more than approximately 10 seconds difference and selection of measurements during stable sky conditions leads us to neglect influence of radiation variations due to changing cloud conditions. Additionally, we used a six-channels radiometer ("NILU-UV") with 5 UV

channels and one PAR channel (400-750 nm) for under-ice measurements down to depths of about 7.5 metres. The UV centre wavelengths are 305, 312, 320, 340 and 380 nm.

Model experiments were performed using the CASIO-DISORT model that treats shortwave radiation in the **C**oupled **A**tmosphere **S**now-**I**ce-**O**cean (CASIO) system based on the **DIS**crete-**O**rdinate **R**adiative-**T**ransfer (DISORT) method. A detailed description of radiative transfer in the CASIO system, including the treatment of the interface conditions, is reported by Jin and Stamnes (1994). Model simulations using 1998 field data from Kongsfjorden (Gerland et al., 1999) for validation can be found in Hamre et al. (submitted).

Results

Figure 1 shows i) the average surface reflectance of repetitive measurements on March 15, 2002 (flat curve) and ii) the amount of irradiance at 1-meter depth relative to that at the sea ice-water interface (i.e. at 0-meter depth). Clearly, the absorption in the near infrared (NIR) part of the spectrum over the upper 1-meter of the seawater is relatively small compared to at wavelengths corresponding to the Photosynthetic Active Region (PAR) region (400-700 nm).

Figure 2 illustrates the vertical distribution of UV radiation over the upper 7.5 metres of the seawater (i.e., under-ice radiation).

In Figure 3 we illustrate how a snow cover on top of the sea ice affects the transmittance of radiation through the sea ice. Two things stand out; first, even a very thin snow layer blocks out most of the solar radiation. For example, a 5 cm thick snow layer reduces the transmittance with a factor of approximately 10. Second, Figure 3 clearly shows that more of the PAR radiation is transmitted through the snow-sea ice system than at shorter or longer wavelengths, especially for snow depths exceeding 10 cm.

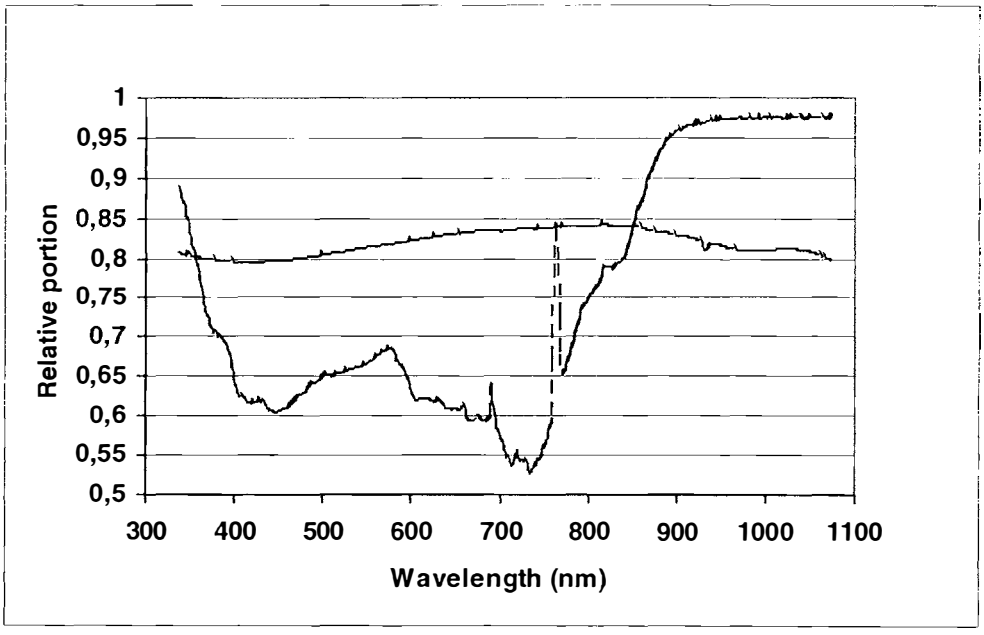

Figure 1. The plots show average surface sea ice reflectance on March 15 (flat curve) and the relative portion of irradiance between under-ice radiance measurements at a depth of 1 meter compared to those taken directly under the sea ice, i.e. at 0 meter depth (see text for more details).

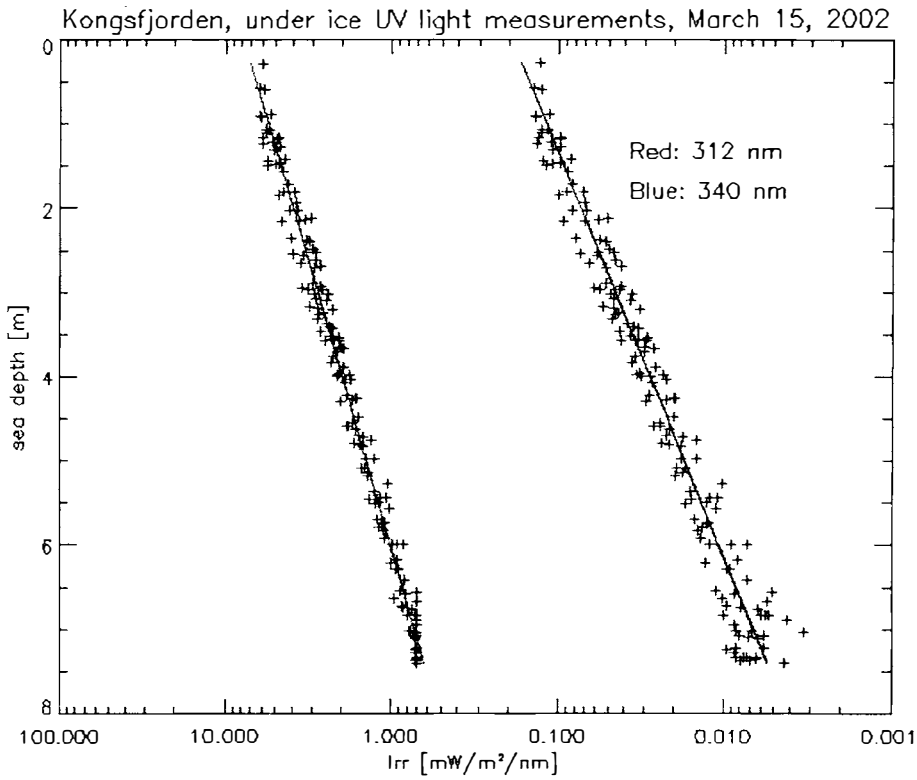

Figure 2. The NILU-UV is a six-channels radiometer with 5 UV channels and one PAR channel (400-750 nm). The UV centre wavelengths are 305, 312, 320, 340 and 380 nm. The curve to the left (340 nm) and the curve to the right (312 nm) are curve fits of the actual data (crosses) assuming the light absorption to follow the equation: $Irr(z) = Irr(0) \cdot \exp(-k \cdot z)$, where **z** is sea depth and **k** is attenuation coefficient. Measurements were done under snow-free, 28 cm thick sea ice, with the sun only 15 degrees over the horizon behind a mountain.

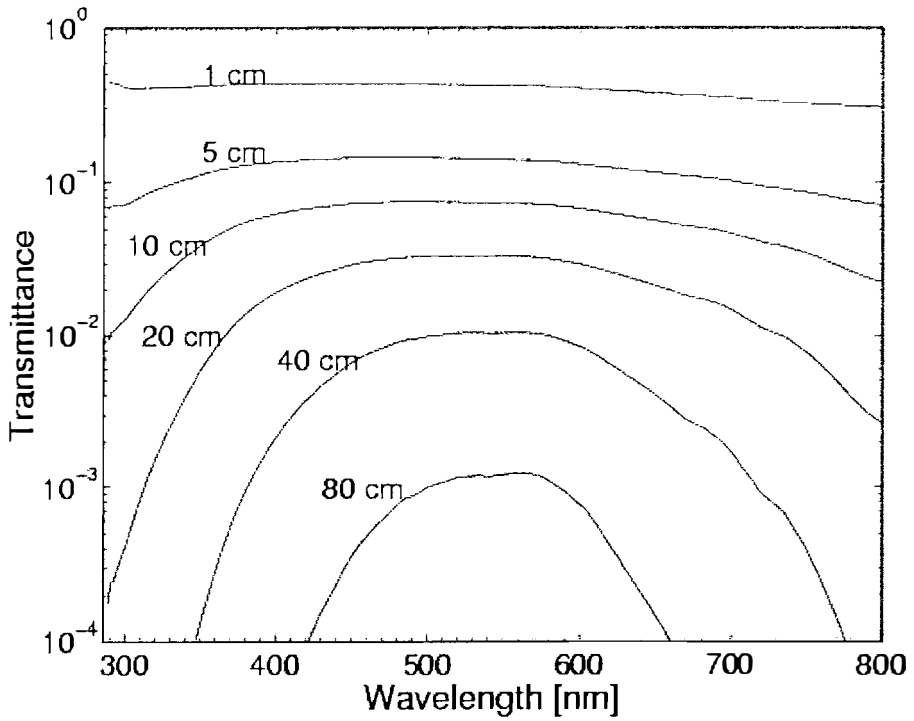

Figure 3. Modelled transmittance vs. wavelength for snow depths ranging 1 to 80 cm.

The latter effect is further exemplified in Figure 4 where transmittance of radiation versus snow thickness is separated for PAR, UVA and UVB radiation, respectively. For a snow cover of 20 cm roughly $10^{-3.0}$ (i.e. 1/1000), $10^{-2.0}$ (i.e. 1/100) and $10^{-1.8}$ (i.e. 1/63) of the radiation is transmitted through the snow-sea ice system in the UVB (280-320 nm), UVA (320-400 nm) and PAR wavelength region, respectively.

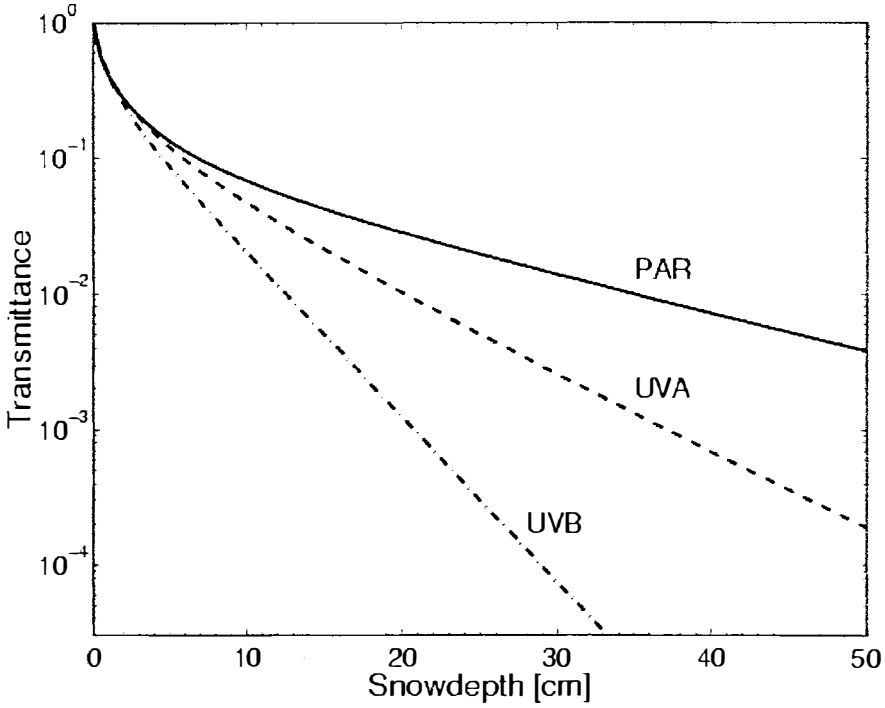

Figure 4. Modelled transmittance of PAR, UVA and UVB radiation vs. snow depth.

References

Gerland, S., Winther, J-G., Ørbæk, J.B. and Ivanov, B.V., 1999: Physical properties, spectral reflectance and thickness development of first year fast ice in Kongsfjorden, Svalbard. *Pol. Res.* **18**, 275-282.

Hamre, B., Winther, J-G., Gerland, S., Stamnes, J.J. and Stamnes, K., submitted: Modeled and measured optical transmittance of snow covered first-year sea ice in Kongsfjorden, Svalbard. *JGR-Atmos.*

Horner, R.A. (ed.), 1985: *Sea ice biota.* Boca Raton, FL (USA): CRC Press, 215 pp.

Jin, Z. and Stamnes, K., 1994: Radiative transfer in nonuniformly refracting layered media: atmosphere-ocean system. *Appl. Opt.* **33**, 421-442.

Langleben, M.P., 1968: Albedo measurements of an Arctic ice cover from high towers. *J. Glaciol.* **7**(50), 289-297.

Mehlum, F., 1991: Breeding population size of the common eider *Somateria mollissima* in Kongsfjorden, Svalbard, 1981-1987. *Nor. Polarinst. Skr. 195*, 21-29.

Perovich, D.K., 1994: Light reflection from sea ice during the onset of melt. *J. Geophys. Res.* **99**(C2), 3351-3359.

Winther, J-G., Gerland, S., Ørbæk, J.B., Ivanov, B., Blanco, A., and Boike, J., 1999. Spectral reflectance of melting snow in a high Arctic watershed on Svalbard: Some implications for optical satellite remote sensing studies. *Hydrol. Proc.* **13** (12-13): 2033-2049.

Observations of superimposed ice formation at melt-onset on fast ice on Kongsfjorden, Svalbard

Marcel Nicolaus, Christian Haas and Jörg Bareiss

Alfred – Wegener – Institut, D-27570 Bremerhaven, Germany,
E-mail: mnicolaus@awi-bremerhaven.de, phone: +49 471 4831 1753,
E-mail: chaas@awi-bremerhaven.de, phone: +49 471 4831 1128

University of Trier, D-54286 Trier, Germany,
E-mail: bareiss@uni-trier.de, phone: +49 651 201 4621

Abstract
Measurements of superimposed ice formation and snow properties as a function of the surface energy balance during melt-onset are presented. They were performed on Kongsfjorden between May 20 and June 03 2002. Rapid snow melt occured within 5 days and the snow cover initially 0.23 m thick transformed into 0.05 m to 0.06 m of superimposed ice. Melt-onset was characterized by rapid changes in the total energy balance, which became positive throughout the whole day after May 27. The increased energy fluxes were mainly caused by increases in incoming long-wave radiation due to overcast conditions.

Introduction
Sea ice and snow properties change dramatically during the spring/summer transition in response to a changing energy balance. This is most obviously reflected by the reversal of temperature gradients within the snow and ice. Before warming and melting results in decreasing ice thickness significantly, metamorphism and internal melting within the snow cover take place. This leads to increasing snow wetness until melt water percolates down towards the snow/ice interface, where it refreezes on the surface of the colder sea ice. This newly formed ice is called 'superimposed ice'. In the Antarctic superimposed ice can form layers of a few decimeters in thickness. As it contributes positively to the sea ice mass balance, it extends the Southern Ocean ice season and delays the overall albedo decrease. Further it influences the evolution of biological communities in and under the ice. In the Arctic superimposed ice is less important, because usually melt is much stronger and the newly formed ice decays quickly before the sea ice underneath also starts to melt.
Here we summarize various measurements quantifying superimposed ice formation, snow properties and time series of meteorological conditions like radiation and temperatures. The aim was to investigate the atmospheric boundary conditions leading to superimposed ice formation, the results will be used to parameterize superimposed ice formation in numerical models.

Measurements
Measurements were performed on fast ice 0.78 m thick covering Kongsfjorden on the western coast of Gerdøya (78.96 N, 12.26 E). Snow properties like snow height, density, wetness and temperature profiles, as well as spectral albedo, were measured several times during daily visits of the site. Additionally ice cores were drilled to measure sea ice thickness and salinity. The ice cores were also used to determine the thickness of superimposed ice.
Global and reflected short-wave radiation, incoming and outgoing long-wave radiation were measured to compute a radiation balance. Turbulent heat fluxes were derived from wind velocities, measured at the site, using the aerodynamic approach. Air temperature and air humidity were registered and additionally air temperatures form Koldewey Station (Ny Ålesund) were used, because the temperature measurements on the ice were significantly biased by radiation effects.

Results

The observation period was characterized by two distinct meteorological phases with clear sky before day 147 (May 27) and overcast conditions thereafter. The change is mainly represented by a drastic increase of incoming long-wave radiation of 70 W/m^2 on day 147 (Figure 1a). Afterwards the energy balance remained positive even at low sun elevation (Figure 1b) and the partially molten snow did not refreeze again. Hence day 147 demarcates melt-onset. As a consequence snow thickness started to decrease. Within 4 days (Figure 1d) the initial snow thickness of 0.23 m had reduced to 0.02 m.

During the first two days after melt onset snow wetness increased from a mean of 3.3 % to 7.3 %. Simultaneously the temperature at the snow/ice interface rapidly approached 0 °C as shown in Figure 1c). The mean density increased with decreasing snow height from 268±40 kg/m^3 before day 145 to 366±40 kg/m^3 on day 150. Snow grain size increased from <1 mm in the initially dry snow to 2 mm to 3 mm on day 150, shortly before the snow vanished completely.

Increasing snow wetness lead to the formation of superimposed ice and one day after melt onset (day 148) 0.025 m of superimposed ice were observed for the first time. The layer of superimposed ice grew up to 0.05 m to 0.06 m until day 152 before it began to deteriorate due to continued warming. The deteriorated superimposed ice consisted of polygonal grains of 5 mm to 15 mm diameter forming a snow-like surface cover.

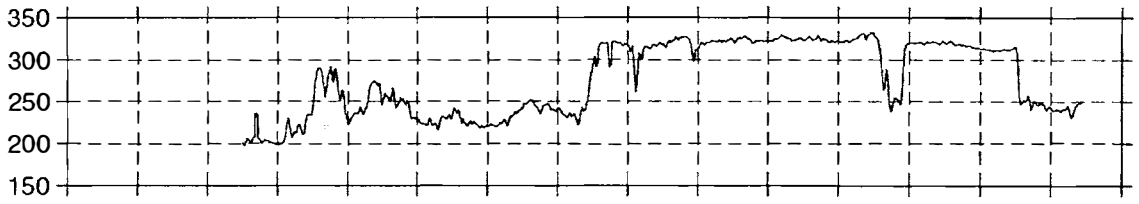

Figure 1: Time series of incoming and outgoing long-wave radiation (a), total energy balance (b), air temperature (2 m above snow surface) and snow temperature at the snow/ice interface (c) and thickness of snow cover and superimposed ice (d) as observed on Kongsfjorden fast ice.

Figure 2 shows how warming to the melting point progressed downward through the snow pack towards the underlying snow/ice interface (z=0 m). At pre-melt conditions before day 147 the whole snow cover was still frozen and temperature profiles show a pronounced diurnal cycle (Figure 2a). After melt-onset the negative temperature gradient has reversed and the topmost snow layers reach their melting point leading to a decrease in snow height (Figure 1d and 2b). At day 151 the melting front reached the ice surface. The isothermal snow melted rapidly, while sea ice thickness increased to 0.84 m due to upward growth of superimposed ice. Minimum temperatures within the ice remained at -1.8 °C at a depth of 0.5 m until the end of the observations. This negative temperature gradient provided the required conditions for superimposed ice formation at the surface.

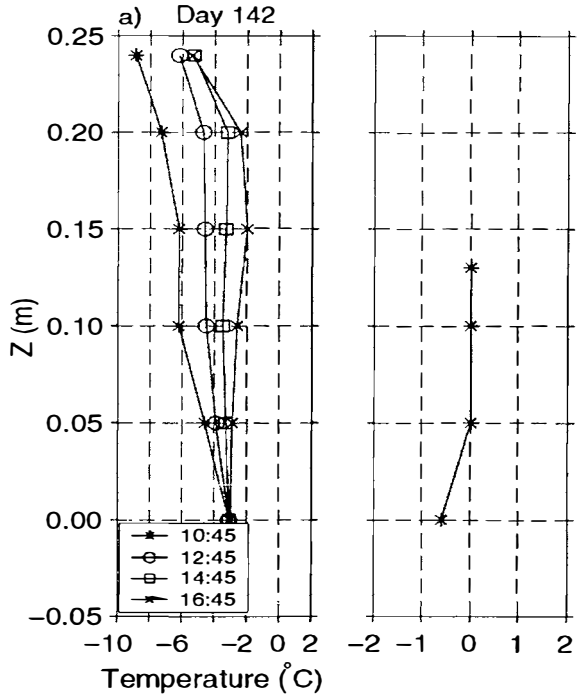

Figure 2: Vertical snow and uppermost ice temperature profiles for typical late winter (a), melt-onset (b) and melt conditions (c). Z=0 m refers to snow/ice interface and the topmost data point is at snow surface.

Wetting and deterioration of the snow are reflected in changes of spectral albedo (Figure 3). Initially the spectral albedo was high for all wavelengths and amounted to 0.9 until day 147. The increased wetness on day 149 lead to reduction of the near-infrared (>900 nm) albedo to 0.55. This shows that the onset of superimposed ice formation could be identified by spectral analysis of visible and infrared remote sensing data. The albedo of the snow-free, deteriorated surface was below 0.5 for all wavelengths.

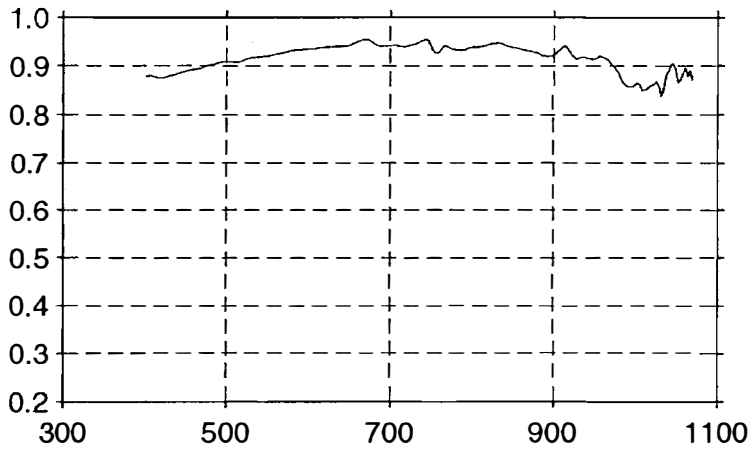

Figure 3: Spectral albedo for typical late winter (day 142), melt onset (day 149) and melt conditions (day 151).

The thick-section taken from an ice core drilled on day 150 (Figure 4) illustrates the typical layering of metamorphic snow over newly formed superimposed ice and the underlying sea ice (here the upper 0.055 m of 0.78 m are shown). In the photograph the 35 mm of superimposed ice can be recognized from characteristic air bubbles within the transparent ice. These bubbles appear partly white, because they were filled by snow during thick-section creation.

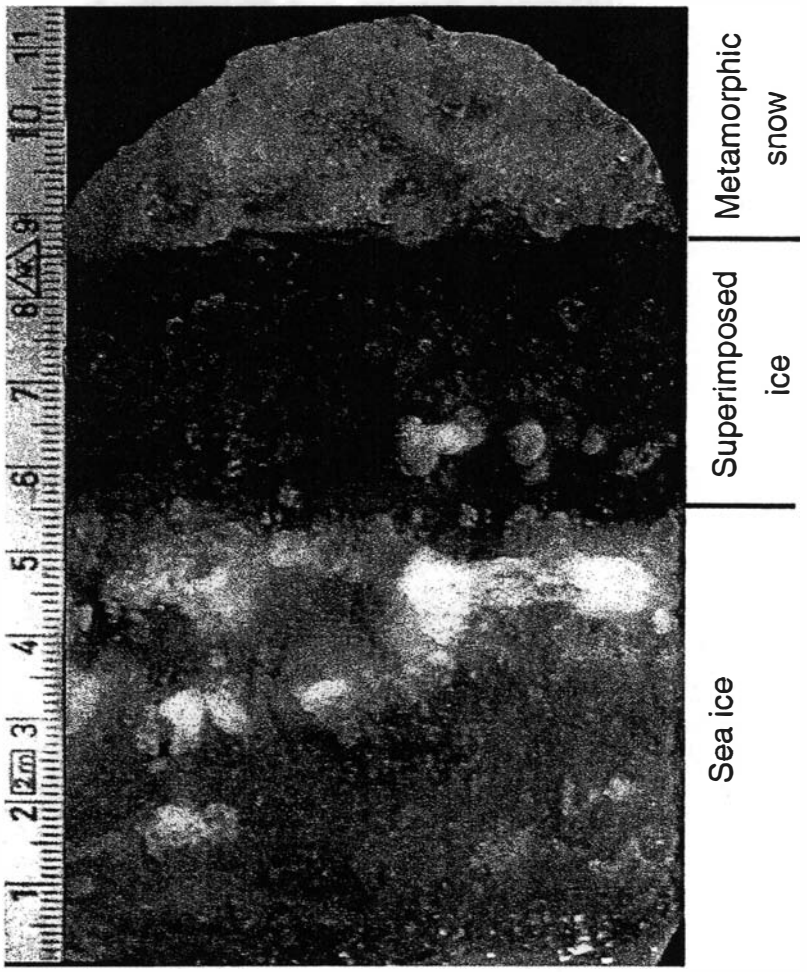

Figure 4: Photograph of a vertical thick-section (day 150) showing the typical sequence of metamorphic snow, superimposed ice and sea ice. The scale is in cm.

Discussion and conclusions

Melt-onset was initiated by increases of long-wave radiation due to overcast weather conditions, which lead to a positive radiation balance. As the melt water reaches the sea ice surface, being colder than the freezing point of fresh water, it refreezes. As a consequence we observed that 0.23 m of snow transformed into 0.05 m to 0.06 m of superimposed ice within 5 days. This transformation process seems to be typical if snow begins to melt on sea ice, because melt water always percolates downwards to the ice surface where it refreezes if it cannot drain. As mass conservation will apply, the final superimposed ice thickness corresponds to the initial snow thickness weighted by the density difference between snow and superimposed ice.

After superimposed ice has formed above the sea ice, two alternative scenarios can occur in the further development, depending on the heat flux from the water underneath. At our measurement site, which was characterized by its bay-like location, the positive atmospheric

energy balance dominated the energy flux into the ice body and forced a rapid deterioration of the newly formed superimposed ice. On the open fjord, sea ice underneath the superimposed ice melted quicker than the superimposed ice due to warmer water masses and resulting higher ocean heat fluxes. Therefore wide areas of the fjord were covered by superimposed ice with no or only rotten sea ice underneath. This shows how superimposed ice formation extends the ice season for some days.

Perspectives

We plan to perform more measurements in the following years to observe different melt progresses under alternative meteorological conditions. This will allow to generalize the above statements and to parameterize superimposed ice formation in numerical snow/sea ice models. With these parameterization and with the usage of remote sensing data the role of superimposed ice in the climate system can finally be investigated.

Acknowledgments

We are very grateful to the personal of the Sverdrup and Koldewey Stations as well as the Norsk Polar Institutt for their support on different levels. This study was performed under EC-LSF grant NP-9/2001 and by additional financial support through the Alfred Wegener Institut.

Detection of spatial, temporal, and spectral surface changes in the Ny-Ålesund area 79° N, Svalbard, using a low cost multispectral camera in combination with spectroradiometer measurements.

Jørgen Hinkler, Jon Børre Ørbæk & Birger Ulf Hansen

Institute of Geography, University of Copenhagen, Øster Voldgade 10, 1350 Copenhagen K, Denmark. E-mail: jh@geogr.ku.dk, phone +45 35 32 41 68

Norwegian Polar Institute, postbox 505, N-9171 Longyearbyen, Svalbard, Norway
E-mail: jonbo@npolar.no, phone: +47 79 02 26 00 (26 21 direct)

Institute of Geography, University of Copenhagen, Øster Voldgade 10, 1350 Copenhagen K, Denmark. E-mail: buh@geogr.ku.dk, phone +45 35 32 25 19

Introduction

This work is a pilot study on using a low cost "3 filter channel" spectral digital camera for monitoring spatiotemporal changes in surface reflectance during the melting season in the Ny-Ålesund area 79° N, Svalbard. The study is based on images taken at regular time intervals, radiation data obtained by a Fieldspec FR spectroradiometer, and solar radiation data measured at the Sverdrup Station in Ny-Ålesund.

The Study

During the period 23/5 2002 – 30/8 2002 a Tetracam multispectral digital camera was installed 474 metres above sea level at the Zeppelin Mountain Research Station, approximately 2 km from the Ny-Ålesund settlement. The camera has been taking an image automatically every day at noon (and at 10-minute intervals on a single day), making up a time series of spectral imagery at high resolution – in both space and time. The aim of the study is to use these images for surface classification and change detection. These results can then be used for further modelling in connection with surface energy balance studies. In order to make this possible a comprehensive work of calibration experiments are being performed.

Data to be used for the experiments have been collected during two field campaigns – one in mid May before extensive snowmelt began, and one at the end of June/beginning of July, where large vegetated areas and bare-soil areas were free of snow. The first campaign was initiated as a testing phase, where the camera was set up and adjusted to the prevailing light conditions and the first measurements of spectral reflectance for snow/ice, and gravel were performed. Additionally, a number of geographical positions were measured at different locations throughout the terrain, using GPS. These data are going to be used for orthographic rectification of the images (Hinkler et al. 2002). An orthographic image has the same scale throughout the whole image, which ensures correct estimations of the size of the different surface types. During the second campaign, the spectral properties of additional surface types (vegetation, dark organic matter, and water) were measured. Furthermore, surface reflectance was tested for different view angles using both the spectroradiometer and the camera.

At the time of writing, image data have been compared to incoming global radiation, solar azimuth angle and measurements of spectral reflection for snow (Winther et al. 1999).

Figure 1 is an example of a spectral image of the Ny-Ålesund area, and it is created as a false colour composite from the red(B), green(G) and near infrared(R) channels of the camera – similar to e.g. Landsat TM ch. 2, 3, and 4. The brightness of a given image - or Digital Numbers

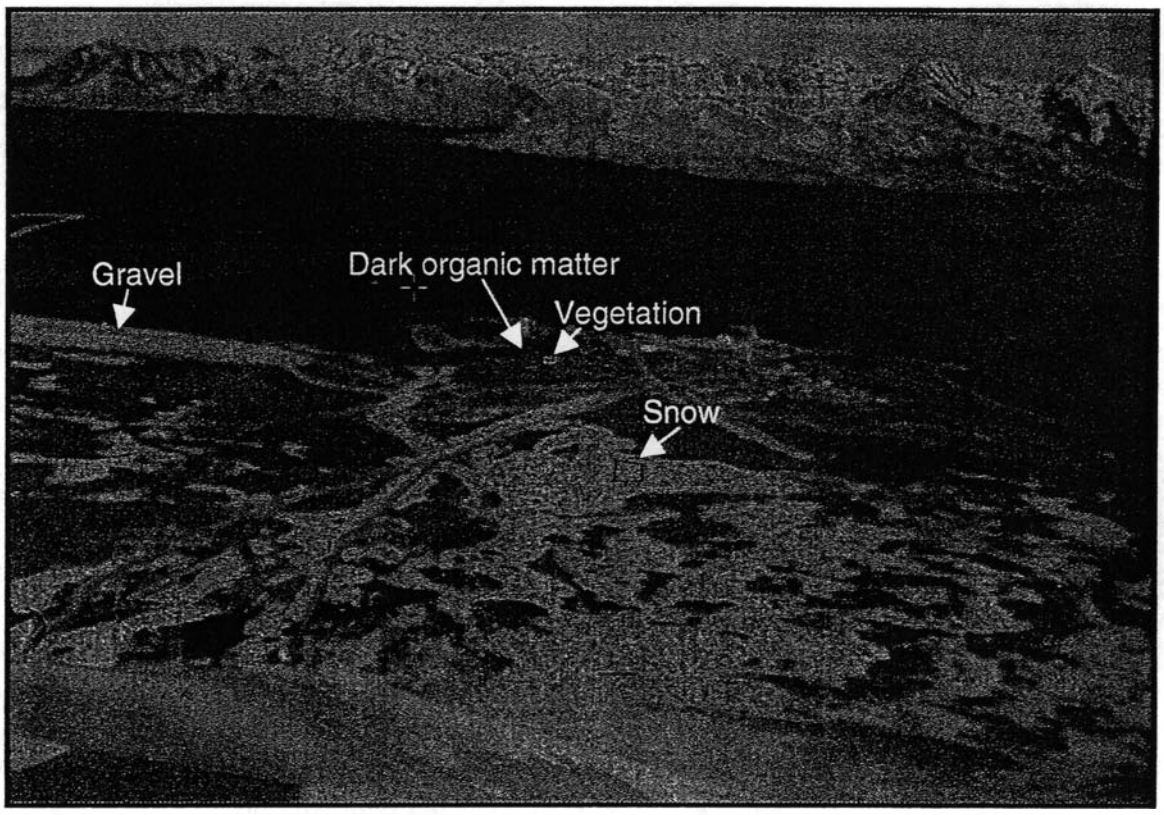

Figure 0. False colour composite of the Ny-Ålesund area obtained from the automatic spectral digital camera. Distinct surface types that have been spectrally investigated are indicated in the image.

(DN) are very sensitive to the amount of incoming solar radiation as well as the angular direction to the Sun (solar azimuth). These relationships are illustrated for red and near infrared in figures 2(a,b). The figures show the average DN's for snow and vegetation at 10 minute time intervals during a period of 26 hours (28/6 – 29/6). The figures reveal that image brightness is correlated to the global radiation and that the correlation is most significant at visible wavelengths. The cameras orientation is almost directly to the north. Consequently, when sunlight comes from northern directions during the night, image data become unusable for calculation of values related to the physical properties of the different surface types. This is due to strays of light reflected directly into the camera lens. Therefore it is important to emphasize that the cameras orientation must be in the direction away from the Sun at capture time. In figures 2(c,d) the relation between global solar radiation, red, and near infrared DN's, respectively is shown (due to azimuth problems, data obtained during the time around midnight have been excluded). Figures 2(c,d) also illustrates that the cameras response is very sensitive to the adjustment of the cameras diaphragm according to the present light conditions. During this study it has been attempted to adjust the diaphragm to cover light conditions varying from bright clear skies to overcast conditions. To avoid saturation on clear days, the diaphragm has been set at a relatively high level. Thus, on days with limited amounts of sunlight, images will be relatively dark, which reduces the dynamic range of the given image significantly. From the figures, it can be observed that at the current diaphragm-settings requires minimum 300-400 wm^{-2} global radiation in order to be able to obtain different calibrations for different surface types (fitted data range: 400 wm^{-2} and up).

In Figure 3 daily values (20/5 – 30/6) of the cameras red channel for the snow region are plotted against global radiation measured at the recording time. A visual examination of the images

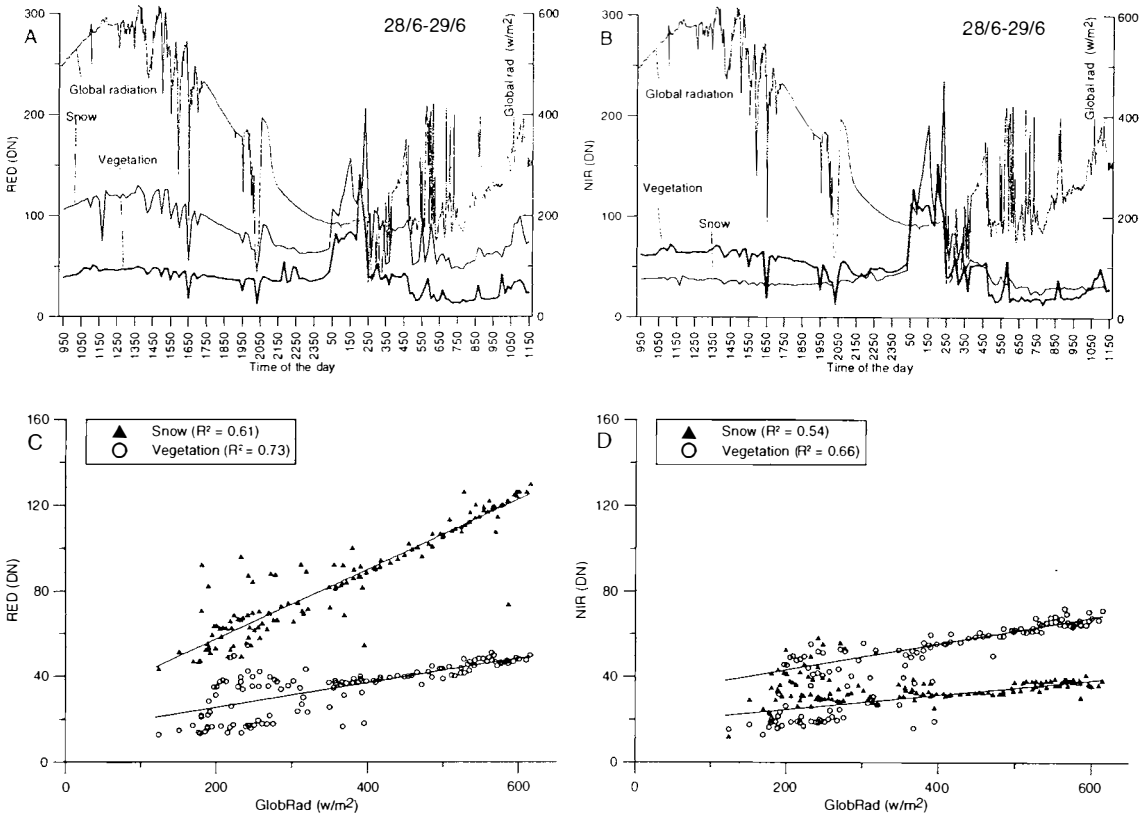

Figure 1. Image DN's for different surface types in relation to global radiation.

shows that at low levels of incident solar radiation it is possible to distinguish clouds from snow and at higher levels it is possible to separate new and old snow.

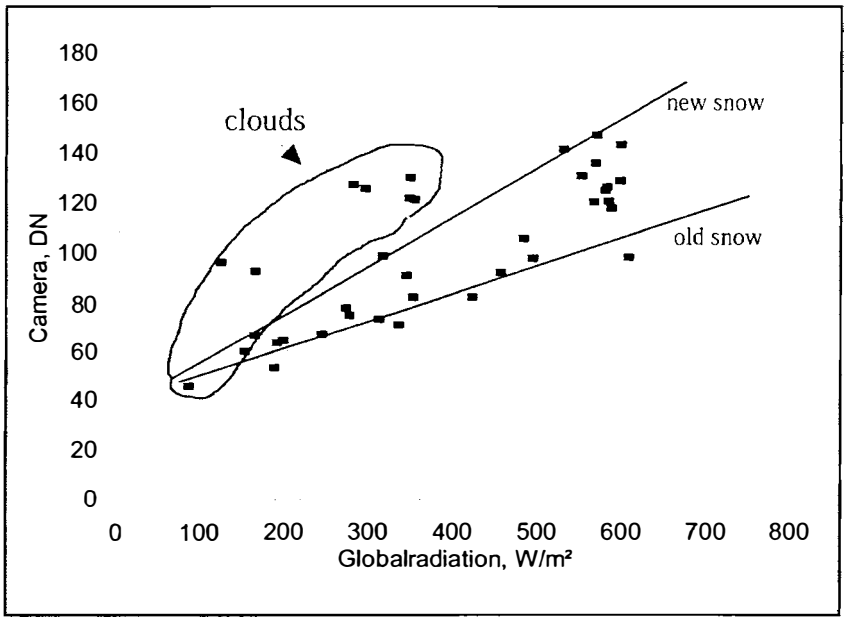

Figure 1. Camera DN's (red channel, snow region) plotted against global radiation, based on daily images captured during the period 20/5 – 30/6.

A classification test including four different surface types was performed. The test is based on red and near infrared DN's selected from a time span (28/6, 10:00-16:00) with relatively uniform radiative conditions. Figure 4 shows that for this time span the different surface types can be easily separated, however if data are obtained under more varying conditions the picture gets more complicated. To solve this task further work must be put in the development

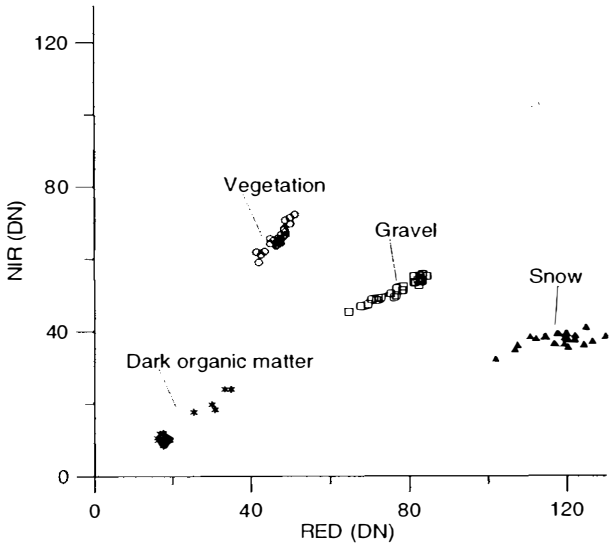

Figure 1. Nearinfrared and red channels plotted against each other for different surface types.

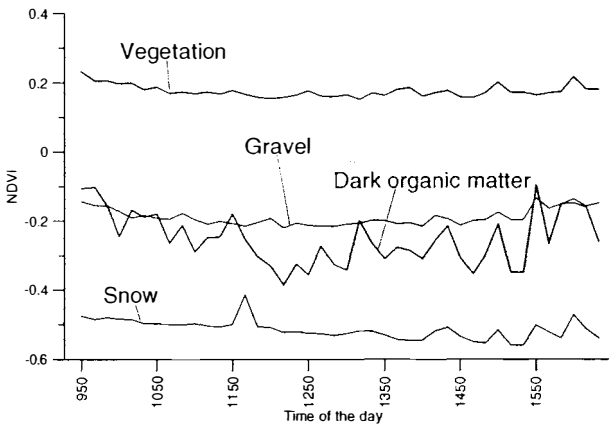

Figure 2. NDVI-index for different surface types, derived from image data obtained 28/6 -2002.

of the necessary calibration routine.

The Normalized Difference Vegetation Index (NDVI) is the most commonly used remote sensing-based index for detection of the greenness of vegetation (amount of chlorophyll and development of cell-structure in plants). The index is defined:

$$NDVI = \frac{NIR - RED}{NIR + RED}$$

The values of the index range between -1 and 1. Values above approximately 0.1 usually indicate that a certain amount of chlorophyll is present. Snow has a weaker reflectance at nearinfrared wavelengths than at visible wavelengths. Therefore snow-NDVI usually is well below zero. Figure 5 indicates that data have the potential for monitoring greenness during the growing season, and that snow and vegetation can be easily separated from gravel and dark organic matter, using this index.

Gravel and dark organic matter have NDVI values of the same order of magnitude and can difficult to separate using the NDVI. To solve this other methods based on absolute DN-values must be introduced.

Final Remarks

The Tetracam spectral digital camera offers the possibility to monitor spectral surface changes at high temporal and spatial resolution, however some technical difficulties regarding the adjustment of the cameras diaphragm and automatic exposure time have to be solved. Further work must be put into developing calibration routines based on solar radiation data; and a comprehensive analysis of spectral image data versus spectroradiometer data still needs to be performed.

References

Hinkler, J., Pedersen, S.B., Rasch, M. & Hansen, B.U. in press: Automatic snow cover monitoring at high temporal and spatial resolution, using images taken by a standard digital camera. *International Journal of Remote Sensing.*

Winther, J.-G., Gerland, S., Ørbæk, J.B., Ivanov, B., Blanco, A. & Boike, J. 1999: Spectral reflectance of melting snow in a high Arctic watershed on Svalbard: *Some implications for optical satellite remote sensing. Hydrological processes 13*, 2033.

Radiation and physical characteristics of tundra and landfast ice snow cover by the example of Barentsburg region and Greenfjord

B.V. Ivanov, O.M. Andreev, A.M. Bezgreshnov.
(Arctic and Antarctic Research Institute, Bering-38, 199397, Saint-Petersburg, Russia, b_ivanov@aari.nw.ru)

The heat exchange governed by radiation of the atmosphere and the underlying surface (ocean, sea ice, snow cover on land and glaciers) is an important component of the Arctic climate system. In Earth's polar regions, the change of the radiation characteristics of the atmosphere and the underlying surface influences the climatic conditions more than in any other place of the globe. This is primarily due to significant seasonal albedo changes of the aforementioned surfaces. The development of large-scale motions in the atmosphere also depends on the energy exchange intensity including the radiation exchange with the underlying surface. The short-wave solar radiation unlike the incoming long-wave radiation is not fully absorbed by the surface penetrating to the lower lying snow and ice layers. Its penetrating action determines the change in thermal physical, radiation and physical-mechanical properties of these media. Data on the radiation-thermal physical properties of snow are necessary to improve parameterization of the snow-ice cover melting processes in modern thermal-dynamic models of sea ice and land glacial covers. A number of Russian studies carried out on West Spitsbergen in recent years were devoted to this problem, including the studies of snow cover and permafrost interaction under the conditions of the archipelago (Krass and Merzlikin, 1987, Osokin and Jidkov, 1999). However, in the aforementioned studies there is no assessment of the consistency between the proposed models and the real meteorological conditions. Such an assessment is necessary both to check the performance of each specific model and for comparison of the possibilities of different models.

During the AARI expedition in the vicinity of Barentsburg settlement (West Spitsbergen) in May 2002, a complex of observations of the radiation thermal-physical characteristics of the snow cover and the related meteorological parameters of the surface layer was undertaken. Air temperature and relative humidity, wind speed and direction and atmospheric pressure were measured. Cloudiness, weather conditions and the state of the snow cover surface were estimated visually. Simultaneously, observations of the snow cover characteristics were conducted. The snow cover thickness, structure and density were estimated and vertical profiles of solar radiation penetrating the snow strata (descending and ascending fluxes) and snow temperature were measured. In addition, observations of the conductive heat fluxes in the snow strata and snow surface albedo were carried out.

Based on the experimental data obtained, a mathematical model of the snow cover thermal state evolved at the AARI was tested (Andreev and Ivanov, 2001). The model allows us to calculate the temperature profile in the snow cover given the real variability of the ambient meteorological parameters and the radiation-thermal physical characteristics of the snow cover.

The model is formalized in the form:

$$c\rho\frac{\partial T}{\partial t} = \lambda\frac{\partial^2 T}{\partial z^2} + \frac{\partial Iz}{\partial z};\quad 0 \le z \le h$$

(1)

with boundary conditions:

$$z = 0 \qquad \lambda\frac{\partial T}{\partial z} = \Phi \quad ,$$

(2)

$$z = h \qquad T(t,h) = T_z \quad ,$$

(3)

where **t** - time; **z** - a vertical coordinate; **h** – snow thickness; $\mathbf{I_z}$ - snow penetrating solar radiation; **T** - snow temperature; $\mathbf{T_z}$ - temperature at the lower snow boundary; **c** – heat capacity, ρ - density and **c** - snow heat conductivity.

The total heat balance of the snow surface **Φ** is represented in the form:

$$\Phi = F + H + LE + R$$

(4)

where **F** and **R** – short- and long-wave surface radiation balances; **H** and **LE** – vertical turbulent fluxes of sensible and latent heat.

The short-wave surface radiation balance and snow penetrating solar radiation are described by the following equations:

$$F = F_0(1 - A)(1 - i_0),$$

(5)

$$I_0 = F_0(1 - A)i_0,$$

(6)

$$\mathbf{I_z = I_o e^{-kz}} \quad ,$$

(7)

where: $\mathbf{F_o}$ - total incoming short-wave radiation; **A** – surface albedo; $\mathbf{I_o}$ – short-wave radiation penetrating through snow surface; $\mathbf{i_o}$ - transmission coefficient characterizing part of short-wave radiation passing through the surface or a thin layer identified with the surface itself (Andreev and Ivanov, 2001), **k** - coefficient of solar radiation attenuation in the snow cover .

To determine the vertical turbulent heat and moisture fluxes, the integral aerodynamic formulas with heat and moisture exchange coefficients depending on atmospheric stratification in the surface air layer were used (Makshtas, 1991). The long-wave radiation balance was calculated by the method specifically developed for the conditions of the Spitsbergen archipelago (Konig-Langlo and Augstein, 1994).

For calculation of heat conductivity and heat capacity of snow, we have used the expressions proposed in (Ebert and Curry, 1993). The snow heat capacity is presented in the form of a linear temperature function:

$$c = 92.88 + 7.364T$$

(7)

The snow heat conductivity depends on the snow density and intensity of its evaporation:

$$\lambda = 2.845 \cdot 10^{-6} \rho^2 + 2.7 \cdot 10^{-4} \cdot 2^{\frac{(T-233)}{5}} \quad (8)$$

The results of model calculations and data of full-scale measurements reveal that the model adequately simulates the vertical thermal structure of the snow cover determined by the impact of ambient meteorological conditions (Fig.1):

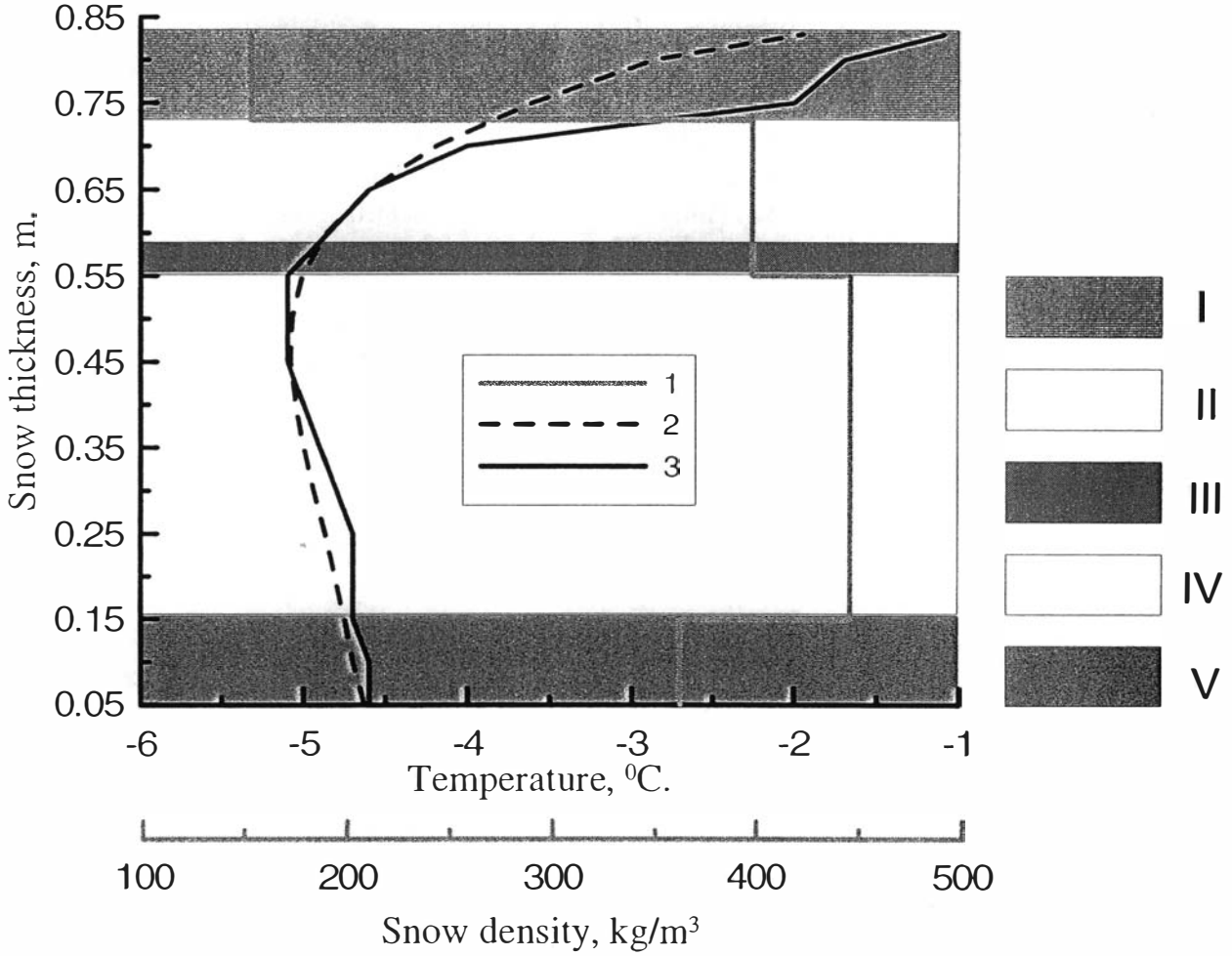

where: 1 – vertical distribution of snow density (field data); 2 – temperature distribution (model); 3 – temperature distribution (field data).

I – fresh snow (grain size1 mm)
II – crumbly snow (2-3 mm)
III – ice crust
IV – crumbly snow (0.4-0.5 mm)
V – firn (3-4 mm).

The described snow cover model is an integral part of a one-dimensional thermodynamic model of the snow-ice cover developed at the AARI (Andreev and Ivanov, 2001). Hence, based on good agreement of experimental and calculated data, it can be used both to estimate freezing of small rivers and streams typical of the West Spitsbergen area and the state of landfast and drifting ice in fjords.

Reference.

1. Krass M., Merzlikin V. 1987. The radiative thermophysics of snow and ice. Leningrad, Hydrology and Meteorology published house. 260.
2. Osokin N., Jidkov V. 1999. Interaction of snow cover and frozen soil in Spitsbergen conditions. In book: "Complex investigation of Spitsbergen nature". 131-145.
3. Andreev O., Ivanov B., 2001. Parameterization of radiation processes in the ice cover model. J. of Meteorology and Hydrology. 2, 81-88.
4. Andreev O., Ivanov B., 2001. The solution of problem about penetration of solar radiation in the snow cover. 2001. J. of Meteorology and Hydrology. 12, 65-69.
5. Makshtas A. 1991. The heat budget of Arctic sea ice in the winter. International Glaciological Society, Cambridge. 77.
6. Konig-Langlo G., Augstein E. 1994. Parameterization of the downward long-wave radiation at the Earth's surface in polar region. J. of Meteorology. 3, 343-347.
7. Ebert E., Curry J. 1993. An intermediate one0dimensional thermodynamic sea ice model for investigating ice-atmosphere interaction. J. Geophysical Research. 98, 10085-10109.

STUDY OF THE RIVER AND GLACIER HYDROLOGY OF THE WESTERN SPITSBERGEN

E. Chevnina

Arctic and Antarctic research institute, Saint-Petersburg, Russia.

The climate changes of the polar region have an effect for the quantitative and quality characteristics of the ice cover, annual and monthly freshwater flows. The data on current conditions of environmental system are necessary to use in models describing the future conditions of hydrological system, besides the forecasts distribution of temperature and precipitations fields, which can be received proceeding from the various scripts of climate change. In this sense Arctic and Antarctic Research Institute investigations are directed on study of hydrology of the Western Spitsbergen rivers and glaciers near Barentsburg, first of all, on the description of the present hydrological regime at the current climatic conditions.

The investigations of the rivers and glaciers of the Western Spitsbergen area were started in 2001. Two basic objects of research were chosen as result of this works. Fist of them is Grendalen river catchments area. The flow of Grendalen is formed on the rather large drainage area (95 km^2), mostly by rainfall and melting and characterizes a flow mode of the basic rivers. The second object is Aldegonda river catchments area, with the small drainage area and concentrated feed at the expense of melting of the glacier Aldegonda. The field works were carry out at spring of 2002 on the Grendalen and Aldegonda river basins to define the maximal snow storage, water equivalent (water quantity, which is concentrated in a snow cover) on the moment of active melting period beginning. These characteristics are the main factors, which form the spring flood. The snow data show that the maximal water equivalent change from 12,7 up to 44,1 g/sm^2, on the average 21,1 g/sm^2. Some elements of mass balance Aldegonda glacier were measured during the spring expedition.

The field program of hydrological works has been planned for the summer (July-September) period of 2002. It includes the observations on the water level, water discharge in various hydrological phases, solid matters and chemical flows. Grendalen and Aldegonda river basins will be the main objects of the research.

Sixth Ny-Ålesund International Scientific Seminar
"The Changing Physical Environment"
Polar Environmental Centre, Tromsø, Norway,
8-10 October 2002

Session: Solid Earth & Marine Environment

Tracy **Shimmield** et al.: Kongsfjord geochemistry: Initial Results.

R. **Delfanti** et al.: Oceanographic processes in the inner Kongsfjord (Svalbard): multidisciplinary results from 2000-2001 campaigns.

Christoph **Steinforth** et al.: Stability of VLBI and GPS reference points at Ny-Ålesund.

H-J. **Kümpel** and Marcus Fabian: Micro-movements on permafrost ground with regard to stability of geodetic reference points.

M. **Negusini** et al.: Results from the 2000 GPS campaign for the measurement of the reference point for the VLBI antenna in Ny-Ålesund.

Franco **De Santis** et al.: Validation and use of a new diffusive sampler for ozone monitoring in polar troposphere.

Kongsfjord Geochemistry: Initial Results

by
Tracy Shimmield, Eric Breuer, Graham Shimmield and Kenny Black
Scottish Association For Marine Science, DML, Oban, Argyll, Scotland

The combined effects of net residual current flow from the UK coastal waters (particularly the Irish Sea) to the northern seas off Norway and the Arctic has resulted in the transportation of artificial radionuclides, persistent organic pollutants and certain heavy metals such as Pb, Zn, Cu and Cd. Such marine pathways have been augmented by the atmospheric Hadley cell circulation resulting in concentration of airborne pollutants at high latitudes. Identifying the pathways and loadings of such vectors remains a key challenge in northern latitude impact studies.

By analysing sediment cores from Svalbard fresh water lakes and a Svalbard fjord it will be possible to identify which pathways, marine or atmospheric, are dominant for key contaminants.

Sediment cores from Kongsfjord have been collected during a Norwegian Polar Insitute hosted EU funded Large Scale Facility (LSF) field trip in April 2002 and again during a Scottish Association For Marine Science (SAMS) cruise which took place in June 2002 aboard the James Clark Ross. The cores were collected using both Sholkovitz and multi- coring. In conjunction to solid phase samples, pore waters have been extracted from the June samples for nutrient and trace element analysis. In addition marine transported anthropogenic contaminants, such as gasoline derived lead will be compared with samples collected in lakes near Ny-Alesund, which are believed to record primarily atmospheric transport processes.

Along with the sediment coring SAMS benthic lander was deployed within the fjord. The benthic lander enables *in-situ* measurements of dissolved oxygen in sediment pore water, which allows the calculation of oxygen supply to the sediment from overlying water and the removal rate of oxygen by the sediment.

Initial results from the Kongsfjord will be presented at the conference and will include nutrient profiles within the water column of the fjord, down core profiles of heavy metal concentrations and stable Pb isotopes, pore water nutrient profiles and *in-situ* micro-electrode oxygen profiles including depth penetration of oxygen and oxygen removal rates.

Oceanographic processes in the inner Kongsfjord (Svalbard): multidisciplinary results from 2000-2001 campaigns.

R.Delfanti*, R.Meloni°, C.Papucci*, S.Aliani°, G.Bartholini*, F.Degl'Innocenti°, C.Galli°, E.Lazzoni°, R.Lorenzelli**, A.Malaguti°°, S.Salvi**, A.Zaborska*

* ENEA - Marine Environment Research Centre, La Spezia, Italy
° CNR - Institute of Physical Oceanography, La Spezia, Italy
** ENEA - Research Centre Brasimone, Bologna, Italy
°° ENEA - Research Centre "E.Clementel", Bologna, Italy

The present knowledge on the main physical and biological characteristics of the Kongsfjord ecosystem have been recently described in two review papers (Svendsen et al., 2002; Hop et al., 2002). Few data, till now, have been gathered on water mass distribution and circulation in the inner fjord and their relationship to particle dynamics and sedimentation/resuspension processes. Multidisciplinary investigations have then been carried out in September 2000 and 2001 in the inner part of the Kongsfjord (Svalbard), at the glacier-sea interfaces (Fig. 1), eastward to 12° E.

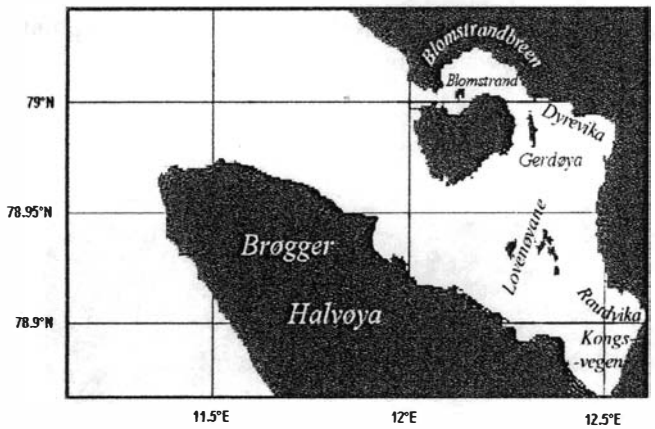

Fig. 1 – Study area

The aims were to investigate:

1. the extent of the main oceanographic processes occurring in this peculiar environment, and

2. the possible importance of "recent" passage opened between Blomstrand and Blomstrandbreen in influencing the hydrographic, sedimentary, and biological processes in the inner fjord.

Special focus was given to small-scale interactions of water masses with different characteristics, from the ice fronts to the outer fjord. About fifty CTD casts were performed both in 2000 and 2001 in the inner Kongsfjord, including Blomstrand passage.

In late summer the intrusion of the salty (>33psu) and warm (4.5°C) water into the inner fjord was visible all along the Southern coast as far as Kongsvegen (Fig. 2). The core was at about 25 m depth. Flowing anticlockwise along the glaciers front, the water became progressively colder and less saline: a layer of very cold fresh water produced by ice melting (5-10 m from the surface) was observed, and its northward outflow was visible out of the passage between Blomstrand and Blomstrandbreen (Fig. 3). This surface layer was not present in the outer areas. Lenses of dense water occupied the deep inter-moraine depressions. This hydrological pattern is possibly the result of the "recent" (early eighties) opening of the passage between Blomstrand and Blomstrandbreen, which activated a novel circulation regime, and likely influenced also sedimentation and biological processes in the inner part of Kongsfjorden.

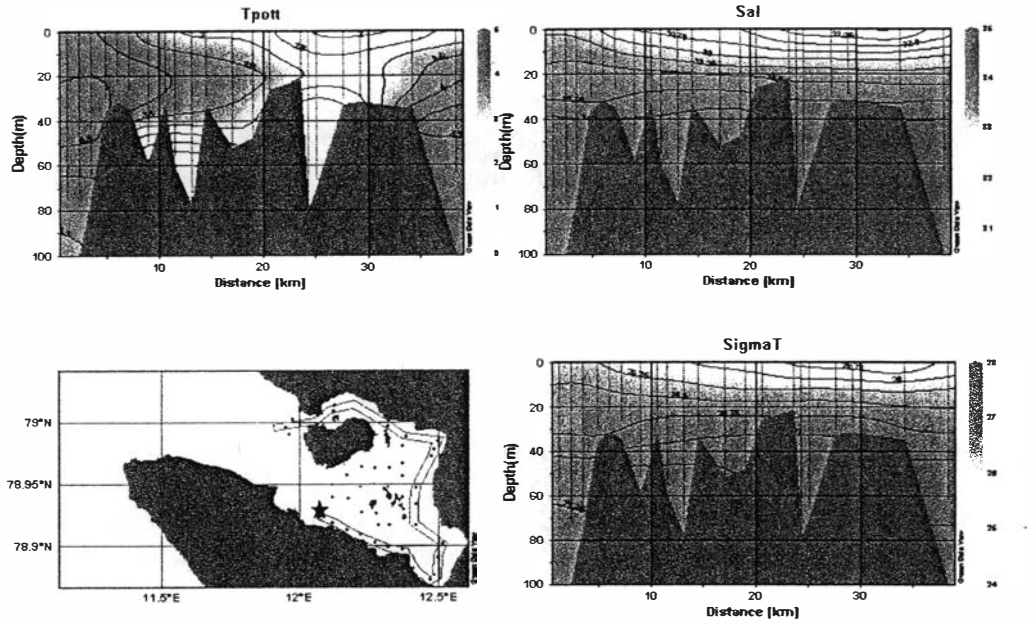

Fig. 2 - Potential temperature, salinity and density along the showed path (Star = starting point). Salty water intrusion is at about 20 m depth and fresh water lens are close to glaciers.

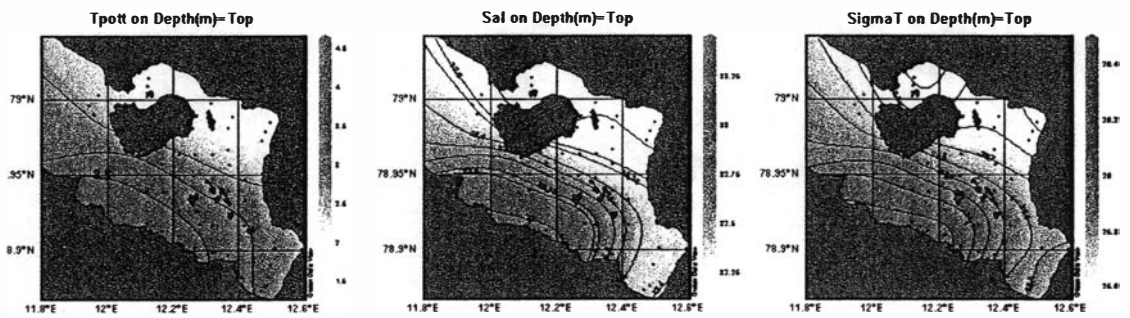

Fig. 3 - Distribution of surface waters. Salty waters enter from south and fresh waters exit northward.

In selected stations of the inner fjord and in a reference area in the outer fjord (Fig.4) euphotic depths, total suspended solids (TSS), chlorophyll and phaeopigments have been determined.
The southern part of the fjord (Stations KO2 and KO1) is mainly influenced by oceanic water (low TSS, high values of PAR penetration and chlorophyll *a*), but contributions from land are also evident: the presence of chlorophyll *b* and *c,* and of a lens of freshwater (evidenced by CTD profiles) suggest inputs from Brøgger Halvøya. In the inner part of the fjord, the melted glacier water is also marked by specific indexes characterising inputs of terrigenous origin: i) chlorophyll *b* and *c*, which are common in fresh water, ii) high values of suspended solids and, consequently, iii) strong attenuation of PAR penetration in the first few meters of the water column. The euphotic depth ranges from 10 to 2 meters.

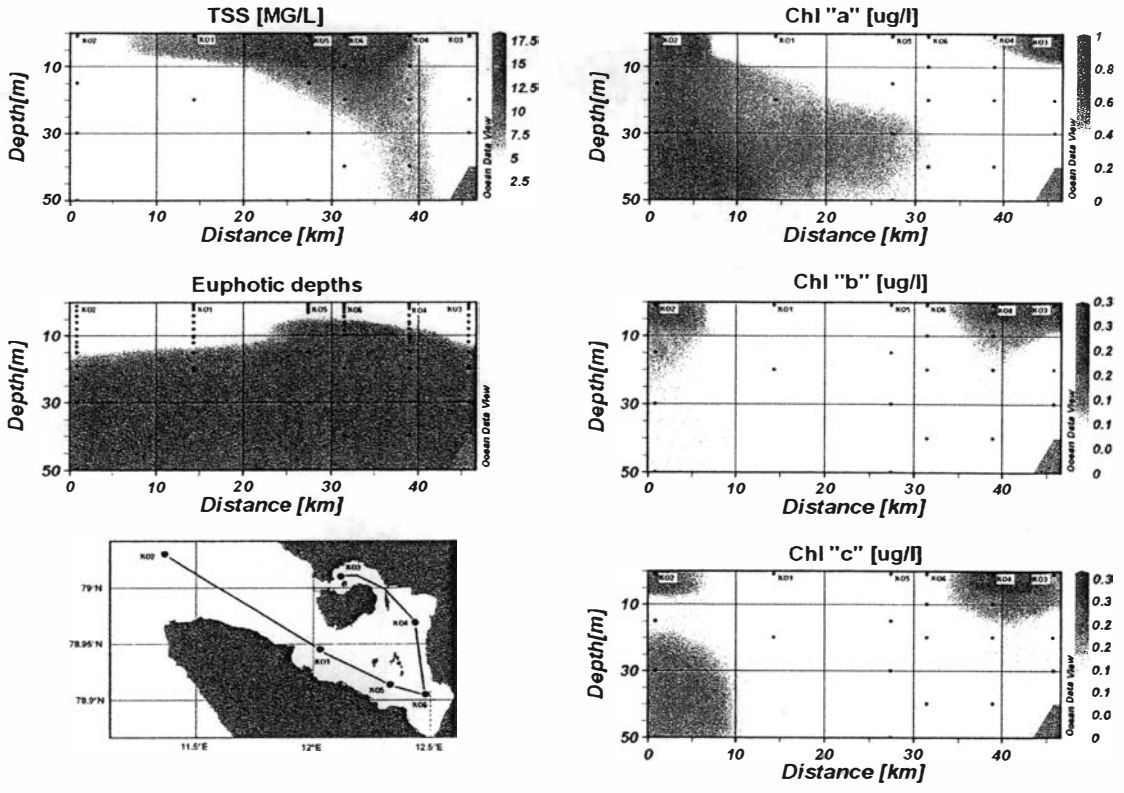

Fig.4 – Total suspended solids (TSS), euphotic depths (1% surface Photosinthetically Active Radiation – PAR 400-700 nm), chlorophyll *a*, *b* and *c* concentrations, along the path showed in the map.

The highest concentrations of total suspended solids (up to 100 mg dm^{-3}) were found near Rundvika and Kongsvegen, while they significantly decreased in the Blomstrand passage. Data derived from the disequilibrium $^{238}U/^{234}Th$ indicated, in these areas, particle fluxes in the range 5 to 8 g m^{-2} d^{-1} and very short particle residence times in the water column (around 5 days), suggesting fast sedimentation regime when approaching the glacier-sea interface. In contrast, the outer fjord was characterised by lower particle fluxes (2-4 g m^{-2} d^{-1}) and longer residence times (12-30 days). In the sediments of the inner fjord, the low POC/PON ratios (5 to 9) evidenced the input of fresh organic matter probably deriving from zooplankton that dies by osmotic shock in the contact with freshwater from the glacier outflow. They were also characterised by low concentrations of organic matter, due to its dilution into huge amounts of inorganic particles. The sill connecting Gerdøya to Lovenøyane seems to act as a trap for fine-grained particles that are aggregating and settling close to the glacier-sea interfaces, leading to preferential accumulation of sediments in the inter-moraine depression.

The sediment accumulation rates have been estimated by the analysis of the vertical profiles of $^{210}Pb_{ex}$ in sediment cores (Fig. 5). The sedimentation rate is highest close to the Southern part of Kongsvegen (exceeding 1.8 g cm^{-2} y^{-1}), and it is one order of magnitude higher than in the trough between Ny Ålesund and Blomstrand (0.2 - 0.4 g cm^{-2} y^{-1}), and two orders of magnitude that found (< 0.02 g cm^{-2} y^{-1}) in the outer fjord and on the continental shelf.

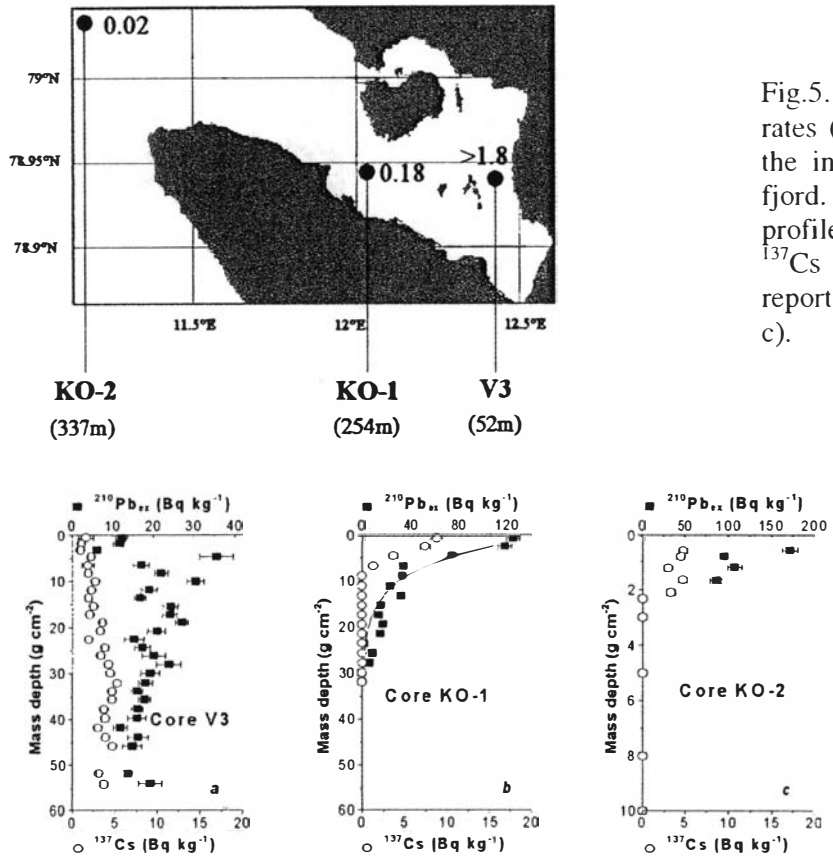

Fig.5. Sedimentation rates (g cm^{-2} y^{-1}) from the inner to the outer fjord. The vertical profiles of $^{210}Pb_{ex}$ and ^{137}Cs in sediments are reported in a), b) and c).

The main marine features of the late-summer situation in the inner Kongsfjord, at the glaciers-sea interface, have been preliminary delineated. Further investigations are needed to define the seasonal variability, and to assess the consequences of the Blomstrand passage on the inner Kongsfjord ecosystem.

References.

- Svendsen, H., Beszczynska-Møller A., Hagen J.O., Lefauconnier B., Tverberg V., Gerland S., Ørbæk J.B., Bischof K., Papucci C., Zajaczkowski M., Azzolini A., Bruland O., Wiencke C.,Winther J-G, & Dallmann W. 2002: The physical environment of Kongsfjorden-Krossfjorden, an Arctic fiord system in Svalbard. Polar Research 21 (1), 133-166.
- Hop H., Pearson T., Nøst Hegseth E., Kovacs K.M., Wiencke C., Kwasniewski S., Eiane K., Mehlum F., Gulliksen B., Wlodarska-Kowalczuk M., Lydersen C., Weslawski J.M., Cochrane S., Gabrielsen G.W., Leakey R.J.G., Lønne O.J., Zajaczkowsky M., Falk-Petersen S., Kendall M., Wängberg S-Å, Bishof K., Voronkof A.Y., Kovaltchouk N.A., Wiktor J., Poltermann M., di Prisco G., Papucci C. & Gerland S., 2002: The marine ecosystem of Kongsfjorden, Svalbard. Polar Research 21 (1), 167-208.

Acknowledgments.
This work was carried out with a substantial contributions of Ny Ålesund-LSF, Bergen Marine-LSF, the CNR-POLARNET "Progetto Strategico Artico", the EU-funded programmes "ARMARA" and "REMOTRANS", and the Italian Station "Dirigibile Italia".

Stability of VLBI and GPS reference points at Ny-Ålesund

Christoph Steinforth[1], Axel Nothnagel[1], Rüdiger Haas[2], Martin Lidberg[2]

[1]Geodetic Institute of the University of Bonn, Nußallee 17, D-53115 Bonn, Germany. E-mail: steinforth@uni-bonn.de, phone +49 228 732623

[2]Onsala Space Observatory, Chalmers University of Technology, SE-43992 Onsala, Sweden. E-mail: haas@oso.chalmers.se, phone +46 31 7725530

Due to its extreme northern location the Ny-Ålesund Geodetic Observatory plays an important role in global geodetic and geodynamical research. In close vicinity two permanent GPS units and a VLBI telescope are operated routinely in global monitoring programs by the Norwegian Mapping Authority. The VLBI telescope regularly participates in observing sessions of the International VLBI Service for Geodesy and Astrometry (IVS) (IVS 1999) for Earth rotation studies and crustal motion investigations. The GPS units submit their data daily to the International GPS Service (IGS) for similar purposes and for precise orbit determination (IGS 2000). Both geodetic measurement platforms also provide crucial data for the establishment and maintenance of the International Terrestrial Reference Frame (ITRF) (Altamimi et al. 2001).

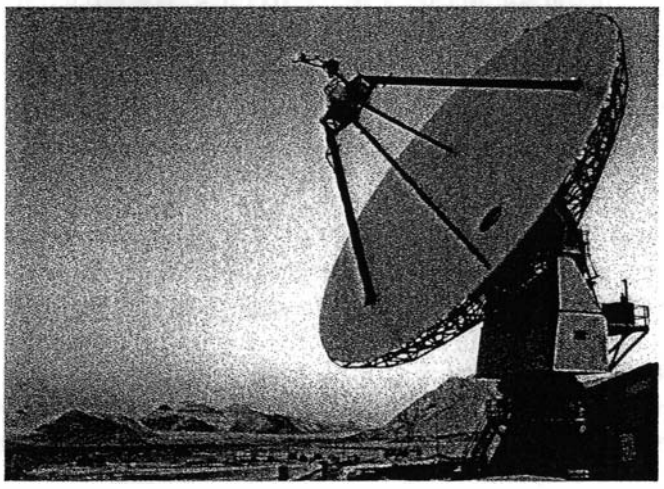

Fig. 1: Ny-Ålesund VLBI telescope

Two general requirements have to be fulfilled for successful investigations in the areas mentioned above. For maintenance of the terrestrial reference frame the excentricities, i.e. the 3D vectors between the observing instruments, have to be determined and monitored regularly at sites with multiple observing platforms in order to establish accurate links between the different observing techniques on a global scale. For global geodynamical studies the stability of the observing platforms has to be monitored with high accuracy in order to discern local effects from global phenomena like crustal dynamics, e.g. plate tectonics or crustal deformation. Both aims can only be reached by repeated precise local surveying. In order to carry out local measurements for the purposes mentioned above two surveying campaigns have been carried out in August 2000 and 2002.

While both, VLBI and GPS, are geodetic techniques which use microwave radiation, the dimensions of the GPS antenna and the VLBI telescope which is just a directional antenna are quite different. The positions of GPS antennas are referred to the respective phase centers located centrically for the horizontal components and at a defined height for the vertical

component. Local measurements can, therefore, rely on a more or less direct accessibility of the reference point.

For a VLBI telescope the situation is quite different. In geodetic VLBI the coordinates of a telescope are referred to the so-called VLBI reference point. Normally, this is the point where the azimuth and the elevation axis of the telescope intersect. However, in the case of the Ny-Ålesund telescope they do not intersect and the reference point is the point of the azimuth axis where the distance to the elevation axis is minimal (e.g. Nothnagel et al., 1995). This point should be invariant to any antenna movements performed in the course of the observations.

At the time of the erection of the telescope in 1995 a network of survey pillars had been installed in the vicinity of the telescope with emphasis on high stability aspects, e.g. thermal insulation and foundation on bed rock. One of the tasks within the local survey and stability control project consisted of determining the coordinates of the VLBI reference point within the system of the pillars. In addition, the pillar network is being used to do the same with the GPS antennas (the analysis of this data is still underway at the time of this publication).

In August 2000 the first epoch coordinates of both the pillar control network and the VLBI as well as the GPS reference points were determined (Nothnagel et al. 2002). A second epoch which permits a direct comparison of the results under stability aspects was observed in August 2002 using the same equipment and surveying principles. The ground network was determined predominantly by triangulation with Wild T2 theodolites and forced centering together with Mekometer distance measurements in 2000 plus precise levelling in both years. The analysis of the observations did not reveal any deformations of the pillar network between 2000 and 2002.

Due to the fact that the VLBI reference point cannot be materialized directly a more complicated survey setup had to be chosen in order to determine its coordinates in the frame of the surrounding pillars. When rotating the telescope in azimuth each end point of the elevation axis ideally describes a circle about the VLBI reference point. The average height of the two end points represents the height of the VLBI reference point. In order to determine the reference point at Ny-Ålesund the end points of the elevation axis were materialized by small pop rivets which were placed in the centric bores of the elevation bearings. Determining the 3D positions of these markers at different positions subsequently permits the computation of the VLBI reference point as the center of the circles. In order to provide sufficient redundancy the antenna was rotated in azimuth angle increments of about 20° measuring each position by forward intersects. For full visibility coverage of the targets at the antenna end points three auxiliary temporary survey points on tripods (#F1001, #F1002 and #F1003) were established augmenting the existing survey monuments. The analysis of the observations was carried out with the least squares adjustment program PANDA (GeoTec 1998) (cf. table 1 and figure 2).

Point	East [m]	σ [m]	North [m]	σ [m]	Height [m]	σ [m]
F91	432911,0120	-	8763837,3288	-	77,0250	-
F93	432843,6420	-	8763296,2180	-	78,2580	-
F95	432931,2995	-	8763873,0857	-	76,6890	-
F98	432936,3844	-	8763843,5153	-	77,1030	-
F1001	432901,9816	±0,0004	8763870,6070	±0,0003	77,9406	±0,0005
F1002	432942,9181	±0,0010	8763883,8841	±0,0010	72,0746	±0,0005
F1003	432959,7395	±0,0006	8763836,9782	±0,0003	76,5306	±0,0005

Tab. 1: Topocentric Coordinates of pillars and tripods

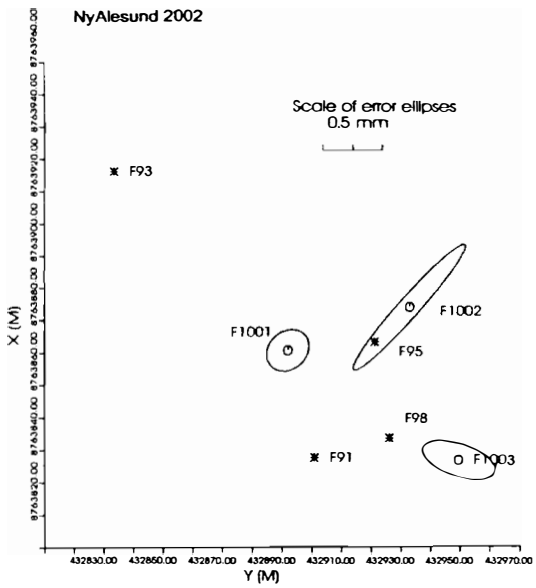

Fig. 2: Layout of Ny-Alesund control network

On the ground, pillars #F91 and #F98 together with the temporary points #F1001, #F1002 and #F1003 were occupied pairwise with two Wild T2 theodolites for trigonometric intersection and levelling. In 18 positions for each marker, horizontal directions and zenith distances were observed with both theodolites together with reference directions relative to one or two points in the network depending on the distance from the current instrument position. All measurements were carried out in double-sighting in order to eliminate collimation errors and errors of the transverse axes of the theodolites.

In the analysis the trigonometric intersects provided horizontal coordinates in the frame of the local coordinate system. The accuracy of the points were computed with the error propagation law resulting in errors in the horizontal coordinate components of the axis end points of < 1 mm RMS (Fig. 3). The height was transferred to the tripods by trigonometric levelling with ~1 mm (RMS) accuracy.

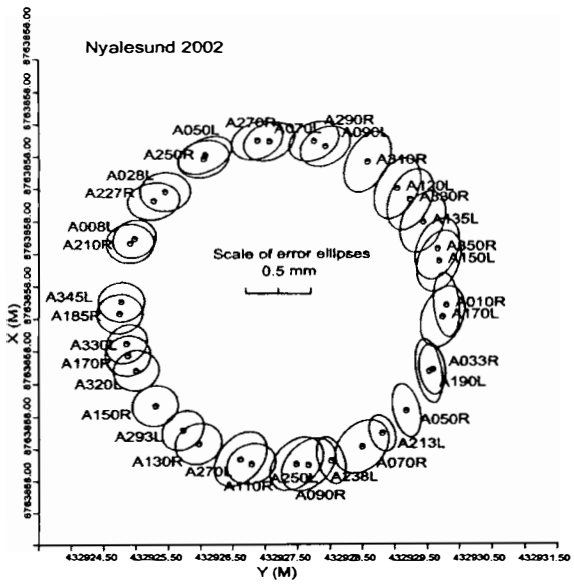

Fig. 3: Error ellipses of targets in different positions

Under the assumption that the telescope rotates around a central azimuth axis, the end points of the elevation axis should describe circles around this axis. The radii of these circles need not necessarily be identical since they depend on the location where the target markers were mounted.

Taking the coordinates of the end points at different azimuth positions as inputs, two least squares adjustments can be performed solving for the coordinates of the centers and the radii of the circles. Table 2 lists the coordinates and radii of the targets at the left (TL) and at the right end of the elevation axis (TR). The weighted averages of the two materializations are taken as the final coordinates of the VLBI reference point in the local system. In addition, for each of the horizontal positions the trigonometric levelling yielded height values. Averages of these were formed to determine the average heights of the target marks. The heights of target TL and target TR may differ slightly due to inaccuracies of the construction of the telescope but are still at the sub-millimeter level.

Target	East [m]	σ [m]	North [m]	σ [m]	Radius[m]	σ [m]	Height [m]	σ [m]
TL	432927,7701	±0,0004	8763860,7517	±0,0005	2,4903	±0,0003	87,2932	±0,0002
TR	432927,7713	±0,0007	8763860,7523	±0,0007	2,5261	±0,0005	87,2930	±0,0003
ref. point	432927,7704	±0,0006	8763860,7519	±0,0003			87,2931	±0,0001

Tab. 2: Parameters of the circles fitted to the series of positions with their formal errors and the final coordinates in the topocentric system (2002 only)

Looking at the standard deviations of the individual points at different azimuth angles it can be stated that the measurements were carried out with extreme precision and no significant displacements of the VLBI telescope were detected over the two years (table 3). The least squares fits of the circles on the one hand and of the average of the individual height determinations on the other hand also provide external quality checks.

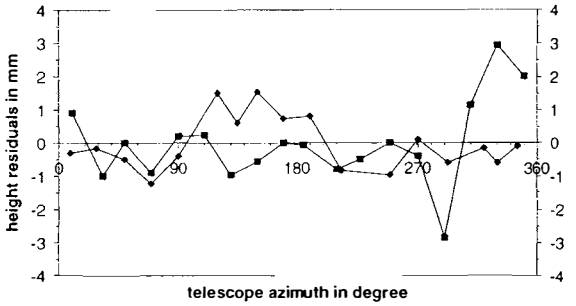

Fig. 4: Residuals of height components

Owing to the minimal scatter and the 18 individual positions contributing to the final results the errors of the resulting parameters (center coordinates in 3D and radii) become even smaller. Since the coordinates of each antenna position are often determined from different pairs of ground positions the resulting formal errors are also a good indicator of the absolute accuracy of the network and the stability of the telescope and its close surroundings.

Target	Δ East [mm]	Δ North [mm]	Δ Radius [mm]	Δ Height [mm]
TL	-0,3	-1,0	-1,2	-0,4
TR	0,9	-0,2	-1,6	0,0
ref. point	0,0	-0,7		-0,2

Tab. 3: Comparison of the results obtained in 2000 and 2002 (Delta = 2002 - 2000)

Acknowledgements

The research carried out at Ny-Ålesund Geodetic Observatory was funded by the European Community (EC) - Access to Research Infrastructure - Improving Human Potential Programme and the Large Scale Facility Programme (LSF) under grants NMA-22/2000 and NMA- 76/2001. We are particularly thankful to Helge Digre, Tom Pettersen, David Holland and Sune Elshaug of the Norwegian Mapping Authority and to the staff of Kings Bay AS who supported us in every aspect creating the basis for the success of this project.

References

Altamimi et al. (2001): EOS Transactions, AGU, Vol. 82, No. 25, 278-279

Geotec (1998) Panda für Windows, Version 2.12, Systemhandbuch, GeoTec GmbH, Laatzen

IGS (2000): IGS Annual Report

IVS (1999): IVS Annual Report, NASA/TP-1999-209243, Greenbelt MD, USA

Nothnagel A., M. Pilhatsch, R. Haas (1995): Proceedings of the Tenth Working Meeting on European VLBI for Geodesy and Astrometry, Matera, Italy; 121 – 13

Nothnagel A., B. Binnenbruck, Ch. Steinforth (2002): Measurements of Vertical Crustal Motion in Europe by VLBI, TMR Networks, European Commission, 78-82

Micro-Movements on Permafrost Ground with Regard to Stability of Geodetic Reference Points

Hans-Joachim Kümpel & Marcus Fabian

Leibniz Institute for Applied Geosciences (GGA), Stilleweg 2, D-30655 Hannover, Germany. E-mail: kuempel@gga-hannover.de, phone +49 511 643 3496

Geological Institute, Section Applied Geophysics, University of Bonn, Nussallee 8, D-53115 Bonn, Germany. E-mail: fabian@geo.uni-bonn.de, phone +49 228 73 9308

Purpose of the Project

The Norwegian Mapping Authority (NMA) is operating a space-geodetic observatory at Ny-Ålesund at the west coast of Svalbard. Several international parties take part in scientific studies being conducted at this high latitude station (78.93° N). The site is a cornerstone in the global geodetic network.

Among other projects, Very Long Baseline Interferometry (VLBI) and quasi-continuous Global Positioning System (GPS) surveys are being carried out to monitor crustal motion. Significant discrepancies in vertical station velocities have been reported from comparison of the VLBI data and the GPS data (Plag, 1999). The reason for the discrepancies is unknown, but has been speculated to result from relative sinking of the VLBI antenna or slow uplift of the GPS monument in the permafrost. Quasi-continuous monitoring of movements of the mountings could help to find out the reason for the differential motion (Plag, 1999). Detection of any irregular motions would also be useful for ongoing high precision gravity recordings that are currently conducted on the GPS monument at the observatory (Sato et al., 2001; R. Falk, pers. communication).

Assuming that any ground motion is not purely vertical, the requested control can effectively be obtained by means of quasi-continuous tilt measurements e.g., on the surface of the antenna basements. Based on our long year experience in operating tiltmeters and analysing tilt records (Kümpel et al., 2001) we have brought three tiltmeters of resolution 0.1 microradian (20 mesca) to the place to monitor micro-movements of both the VLBI and GPS antenna basements and thus to assess their stability over a period of about one year (one borehole tiltmeter, installed in a vertical cylindrical steel tube, and two platform tiltmeters; Applied Geomechanics Inc., 1991). Beyond the specific insights that will be gained for the Ny-Ålesund site, more general aspects like estimates of the magnitude and variability of micro-movements of monuments founded in permafrost ground are expected to result from the studies (Ny-Ålesund LSF- project NMA-57/2001, 9th call).

Instrumental Set-up

During our first visit (August 2001), a number of experiments were conducted prior to the final installation of the three tiltmeters, that is before the long term monitoring program was started on August 25, 2001. The tiltmeter tests were helpful to identify the site-conditions for the installation. One example for the type of encountered noise is given in Fig.1. On-site inspection of the data series recorded during the tests has revealed the following:

- The borehole instrument is the one that could best be installed on the VLBI antenna basement inside the antenna support frame (fixed in a steel cylindrical housing). The place is not temperature controlled.

- Micro-movements of the VLBI basement can effectively be monitored through tiltmeters of the type used here. Consistent tilt signals of order 5 microradian (= 1 seca) are observed when the VLBI antenna is moved to and operated in various elevations and/or orientations (at negligible wind speed!). The major part of the induced signal can be attributed to internal bending of the concrete basement block rather than to its inclination in whole. Extrapolated to the total diameter of 5 m of the antenna support frame on the VLBI basement, differential vertical movements appear to amount to only several micrometers (approxim. 5 μm) due to such operations (Fig. 1).

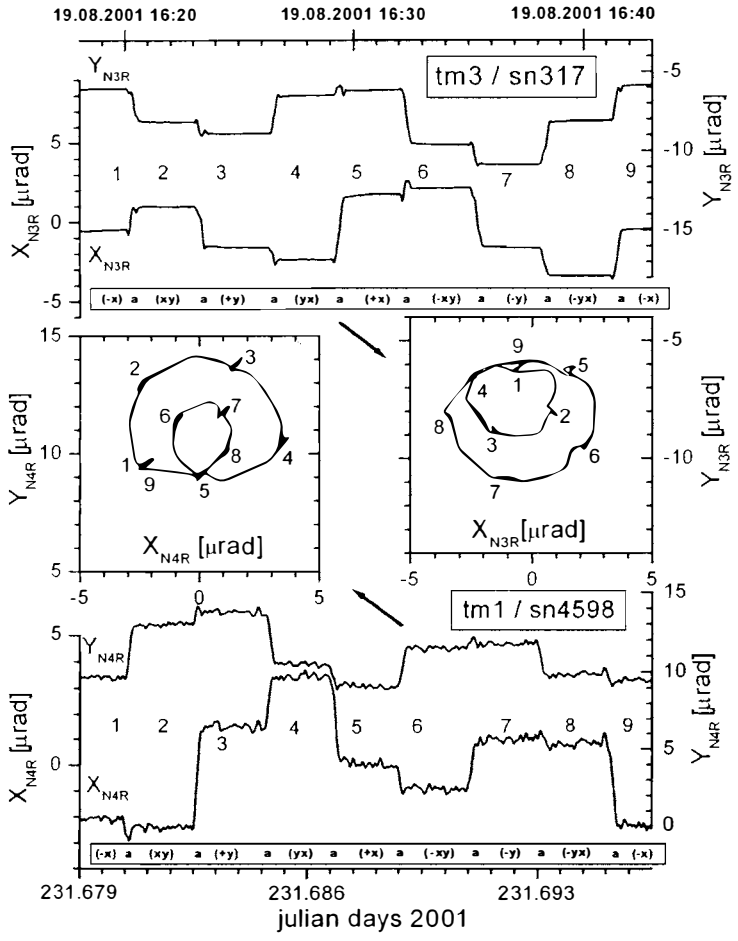

Figure 1: Recordings of tiltmeters tm1 (bottom and centre left) and tm3 (top and centre right) during test installations on basement of VLBI antenna on Aug. 19, 2001. Tilt signals in X- and Y-components, respectively, are induced by changing the azimuth of the VLBI antenna at elevation 45° above horizon and reflect deformation of the antenna basement. Numbers 1 to 9 denote different positions of the antenna which was moved clockwise 45° every 3 minutes (so that 1 and 9 are in fact identical positions). The tiltmeters were installed equidistant from and opposite of the centre of the basement. sn4598 and sn317 denote serial numbers of tiltmeters (Applied Geomechanics Inc., 1991).

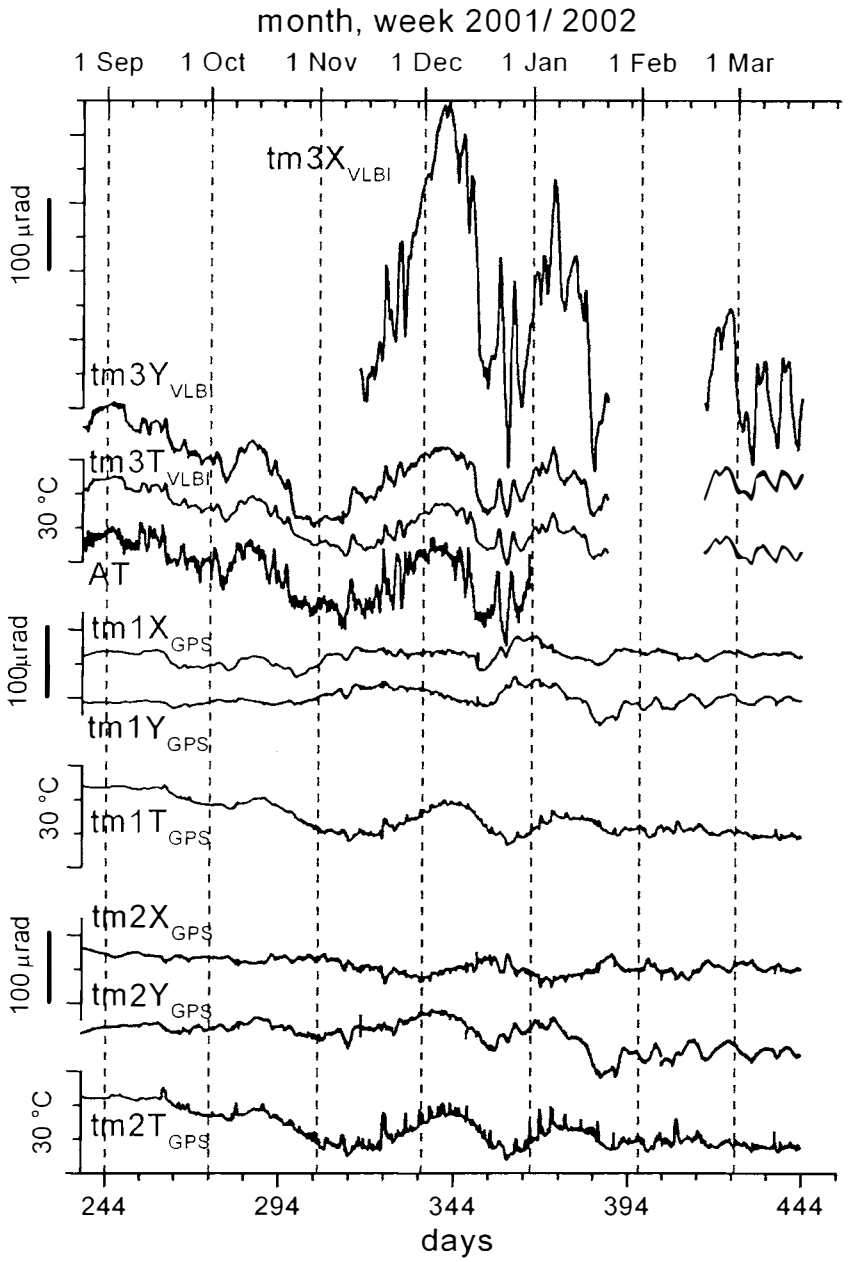

Figure 2: Data set of long term tilt monitoring on floor of basement of GPS antenna (centre and bottom, tm1 and tm2, respectively) and on floor of basement of VLBI antenna (top, tm3). Sampling rate of tiltmeter recordings is 5 minutes. Gaps in data set of tm3 are due to malfunctioning of X-component of tm3 (till mid Nov. 2001) and failure of recorder (Jan./Feb. 2002). AT is outside temperature as recorded from Alfred-Wegener-Institute, Ny Ålesund.

- A suitable place for installation of the two platform tiltmeters was found in the moderately temperature controlled room beneath the GPS antenna. The instruments were finally set up on the concrete basement and covered with insulation material.

- A major problem of the tilt measurements conducted at the Ny-Ålesund Geodetic Observatory is poor thermal stability of the available installation points. Tiltmeters, due to their high mechanical sensitivity, do critically respond to changes in temperature. To some extent this effect can be corrected, since temperature variations of the instruments are also recorded. Thermal insulation is another way to reduce thermal effects on the tiltmeters, at least for short term variations in temperature.

During the second visit (February 2002, M. Fabian), instrument performance was thoroughly checked and improved. The tiltmeter installed on the basement of the VLBI antenna was malfunctioning in one component till mid November 2001 (which was not obvious from the tests in August 2001); also, its recording system was interrupted for a few weeks in January/February 2002. A connector that was suspected to lead to erroneous readings in one of the tiltmeters was replaced. The way of fixing the borehole tiltmeter in the cylindrical steel tube was changed to reduce temperature effects. The measures taken appear to have been successful.

Preliminary Results

Up to March 2002, continuous recordings of the two instruments installed on the GPS antenna basement were obtained (Fig. 2). Variations in tilt signal amplitude range within 50 microradian that is within a magnitude which is typical for borehole installations at a few meters depth, at quiet sites in non-permafrost regions. Part of these variations can be attributed to changes in room temperature. Changes in tilt amplitude of the instrument installed on the VLBI basement amount to several hundred microradian and are again partly due to temperature effects. The interruptions were possibly caused by the harsh climate conditions at this place.

Assessment of how permafrost might affect the stability of the antenna basements will be possible when data of a full year will have been processed. So far, absence of major drifts in the tilt recordings suggests that permafrost effects are not dominant. More recent data will be presented during the Seminar.

References

Applied Geomechanics Inc. 1991: *User's Manual No. B-91-1004-Model 722 Borehole Tiltmeter, AGI,* Santa Cruz.

Kümpel, H.-J., Lehmann, K., Fabian, M. & Mentes, G. 2001: Point stability at shallow depths – experience from tilt measurements in the Lower Rhine Embayment, Germany, and implications for high resolution GPS and gravity recordings. *Geophys. J. Int. 146*, 699-713.

Plag, H.-P. 1999: Measurement of vertical crustal motion in Europe by VLBI; station report for Ny-Ålesund. *Proc. 13th Working Meeting on European VLBI for Geodesy and Astronomy*, Viechtach, 65-77.

Sato, T., Asari, K., Tamura, Y., Plag, H.-P., Digre, H., Fukuda, Y., Hinderer, J., Kaminuma, K. & Hamano, Y. 2001: Continuous gravity observation at Ny-Alesund, Svalbard, Norway with a superconducting gravimeter CT#039. *J. Geodetic Soc. Japan 47*, 341-346.

Results from the 2000 GPS campaign for the measurement of the reference point of the VLBI antenna in Ny-Ålesund

M. Negusini, P. Sarti, P. Tomasi

Istituto di Radioastronomia del C.N.R., Sezione di Matera, Italy

Abstract. The precise link between different space geodesy techniques (e.g.: GPS, SLR, DORIS or VLBI) is a fundamental task at any location where more than one technique is available. In the case of a VLBI antenna this task is, in general, quite difficult due to the dimension of the antenna and the fact that the reference point is, in many cases, a "virtual" point coincident with the intersection of the azimuth and elevation axis. This task is even more important where, like in Ny-Ålesund, there are differences in the vertical rate determined by different techniques (in this case VLBI and GPS). It is, therefore, crucial, with increasing importance of IGGOS, to establish a reliable and accurate ex-centers surveying method. Nowadays, the most modern methodologies of classical geodesy are able to meet these requirements, but a pure GPS approach could be much faster and straightforward.

1. Introduction

In August 2000 a GPS campaign has been carried out at the Ny-Ålesund station, for measuring the VLBI antenna reference point and the possible thermal deformations due to the effect of the sun on the antenna structure. Two GPS receivers have been fixed on the border of the VLBI dish, in order to reduce the multipath from the VLBI antenna structure and also to maximize the sky visibility from the GPS antennas. The structure support for the GPS antenna was a sort of gimbal, in order to keep the GPS antenna pointing to the zenith. Moving the VLBI antenna in azimuth and in elevation, it was possible, with the GPS systems, to estimate the position of the reference point of the VLBI antenna. In fact, if the GPS phase center moves in agreement with the structure of the VLBI antenna, it will describe a number of arcs, with their centers aligned along the azimuth axis, during rotation in azimuth at fixed elevation. During its motion in elevation, the GPS antenna will describe arcs centered at the elevation axis. Elevation biases between the gimbal ring and GPS phase center, if present, introduce a systematic height difference, which can be easily removed once the GPS data have been analyzed. Height biases are not crucial in azimuth circles' center determination. Once these biases have been taken into account, the GPS phase center moves in accordance with any point of the VLBI antenna structure. Bending of the support might introduce errors that are more difficult to model, but we are confident that these kind of biases are much smaller.

2. 2000 GPS campaign

We have originally planned to use at least 6 GPS receivers, but three of them were lacking and, therefore, the experiment was carried out using three GPS systems. One of the available GPS antenna had been already set up, for a different GPS campaign, with a recording interval of 20 seconds, on ground pillar number 97 (P97), which belongs to the local network, measured in 1999 (Tomasi et al, 2001).

The remaining two GPS antennas have been mounted on the VLBI dish using devices that were capable to keep the GPS antennas pointing to the zenith at every elevation angle of the VLBI antenna. The positions of the two antennas were on the border of the dish, respectively at 22.5 and –22.5 degrees with respect to North. The devices have been bolted to the VLBI antenna structure assuring that the rotation axis of the GPS antennas remain parallel to the elevation axis of the VLBI radio-telescope.

We used rapid static observation strategy. The shortest session duration in every position was 30 minutes, with observations acquired every 20 seconds. We have used a set of Z-surveyor Ashtech receivers and choke ring antennas.
GPS observations started moving the VLBI antenna stepwise in azimuth with intervals of 22.5 degrees. This has been done for different elevation angles, and in particular 88.5 and 50.0 degrees. Two more elevations angles, 15.0 and 5.0 degrees, have been measured using azimuth steps of 45 degrees.
We have also used a second different set-up and fixed the two GPS antennas at the opposite border of the VLBI antenna (parallel to elevations axis), using two other (L-shaped) devices at 90.0 and –90.0 degrees. In this new configuration we have moved the VLBI antenna in elevation. Movements started at 88.5 degrees, the larger elevation possible for this antenna, then 80.0 and then down to 10 degrees in step of 10 degrees of elevation. This has been done at azimuth angle 0 and 180 degrees, therefore, obtaining four elevation arcs. With these L-shaped devices a new set of observations using azimuth steps of 22.5 degrees at fixed elevation (88.5) has been collected.

3. GPS data analysis

The GPS data have been analyzed by means of the Bernese GPS software Version 4.2 (Hugentobler et al., 2001). Together with the data collected during the campaign, the data of the two permanent IGS stations in Ny-Ålesund, NYA1 and NYAL, have been analyzed in order to strength the results within ITRF97 reference frame (Boucher et al.,1999). It should be outlined that, due to the different recording rate, only one epoch per minute could be used between movable GPS (20 sec) and reference stations (30 sec). That is why baselines between mobile and P97 GPS antennas have been formed, in order to maximize the number of observations, while the two permanent stations have been used as constrains. We have used the ITRF97 coordinates for the P97 station given in Nothnagel et al. (2001), while for the NYA1 and NYAL the official ITRF97 coordinates and velocities. When P97 data were not available the mobile GPS have been linked to NYA1. The precise IGS orbits, in the given reference system and for the relevant time frame, were used. The CODE pole coordinates and tropospheric models have been used together with the IGS phase eccentricity file (elevation-dependent phase center corrections) which has been adopted only for the ground stations. In the GPS data analysis, an elevation cut-off angle of 10° has been set, an ambiguity-fixed solution has been computed. L1 carrier frequency has been analyzed and, consequently, an ionosphere model has been previously computed using the available data. Geocentric coordinates of mobile antennas have been estimated for each observing session and they are shown in Figure 1. Squares represent the VLBI movements in elevations, while circles are the movements in azimuth.

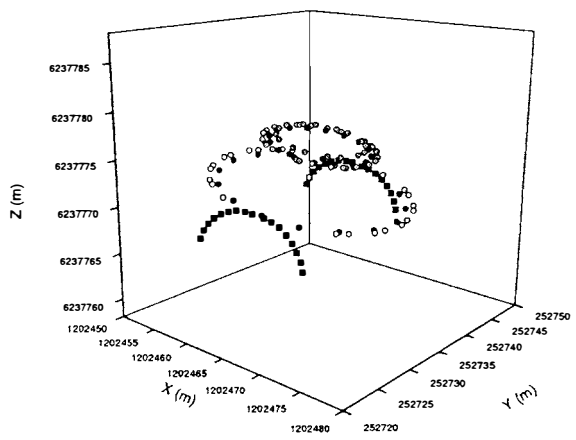

Figure 1: Estimated positions occupied by both mobile GPS antennas during the VLBI antenna movements.

4. Post-processing

In order to compute the VLBI reference point, GPS positions have been post-processed using a 3-D least-squares analytical geometry approach. Post-processing procedure is based on two Fortran77 programs that use a 3-D analytical geometry least squares approach for determining the best fit intersecting surfaces that, uniquely define the reference point. This is the approach that has been developed and used successfully in similar surveys (Sarti et al, 2000, Vittuari et al., 2001). VLBI antenna movements in azimuth (at fixed elevations) determine GPS antenna positions that ideally draw a circumference centered on the azimuth axis. In a similar manner, the centers of circumferences described by movements in elevation at fixed azimuth positions, belong to the elevation axis.

5. Results

Using the approach described above, it is possible to determine the reference point with a purely analytical computation. Once the centers' coordinates have been estimated, they have been transformed into a topocentric system, with origin in published ITRF97 VLBI reference point. Within this system, East and North components of azimuth circles' centers have been used to compute a weighted mean that represent East and North components of the invariant point. Similarly, Up component of the different elevation circles' centers have been combined to obtain the weighted mean estimate of the Up component of the reference VLBI point. These components and their wrms have been transformed back into ITRF97. Table 1 shows the resulting geocentric invariant point coordinates.

The final results are quite good with errors of the order of 1-2 mm for the X and Y components, and 11 mm for the Z component. Ny-Ålesund is located at a very high latitude and thus errors related to the sites' upper component are mainly transferred to the Z geocentric component along with their errors. It is well known that the upper component has larger error than the horizontal one.

Table 1: geocentric coordinates of the VLBI reference point at epoch 15/8/2000.

X (m)	Y (m)	Z (m)
1202462.705 ± 0.002	**252734.431 ± 0.001**	**6237766.039 ± 0.011**

6. Comparison

The invariant point has been estimated in two different terrestrial surveys, that have been performed in 1999 (Tomasi et al., 2001) and 2000 (Nothnagel et al., 2001), where total stations (angles and distances) and theodolites (angles only) have been used, respectively. This is a time consuming, though reliable and accurate, approach and requires an additional effort to put the measurements in a global reference frame. Using six common points measured by Tomasi et al. (2001) within a local reference system and by Nothnagel et al. (2001) within ITRF97, we have estimated the 7-parameters related to a 3-D Helmert transformation. These parameters have been used to transform the local invariant points into ITRF97, in order to compare the different estimates of the same VLBI reference point.

It is well-known that there are problems related with the realization of ITRF97 positions and velocities of Ny-Ålesund co-located GPS and VLBI. A better realization is the one associated with ITRF2000 (Altamimi et al., 2002). Results into ITRF97 have been transformed into the latter reference frame obtaining the results shown in Table 2, along with ITRF2000 invariant point. There is a general agreement between the official invariant point coordinates and the results obtained by Tomasi et al. (2001). GPS results do not statistically differ from the ITRF2000 value except for Y component. Results obtained by Tomasi et al. (2001) using terrestrial methods show a striking agreement and, compared to GPS, smaller uncertainties.

Table 2: Different estimates of the VLBI reference point transformed into ITRF2000.

ITRF2000	X (m)	Y (m)	Z (m)
2000 GPS campaign	1202462.697 ± 0.002	252734.427 ± 0.001	6237766.053 ± 0.011
1999 classical campaign (Tomasi et al., 2001)	1202462.700 ± 0.001	252734.424 ± 0.001	6237766.075 ± 0.002
2000 classical campaign (Nothnagel et al., 2001)	1202462.6970 ± 0.0003	252734.4240 ± 0.0003	6237766.0600 ± 0.0010
Official ITRF2000 at epoch 15/8/2000	1202462.702 ± 0.001	252734.423 ± 0.001	6237766.071 ± 0.004

7. Conclusion

We have investigated Rapid Static GPS survey as an alternative way to classical geodesy in estimating VLBI Reference Point. Although not completely satisfactory yet, results are very encouraging and suggest that, using an optimal distribution of the GPS observations in space and time, interesting results might be obtained.
Planimetric coordinates are accurately estimated, while the limiting factor of GPS is associated with the precision of the Up component: it is one order of magnitude lower then that determined using terrestrial methods and must therefore be improved to be usable for measuring the reference point of a VLBI antenna.
Moreover, the results are framed directly into the ITRF and this methodology might represent a way to determine the VLBI reference point with a simple and relatively fast method, applicable also to different VLBI antennas.

Acknowledgements: The research carried out at Ny-Ålesund Geodetic Observatory was funded by the European Community (E.C.) – Access to Research Infrastructure – Improving Human Potential Programme and Large Scale Facility Programme (LSF) under grant NMA - 13/2000.
We are thankful to the staff of the Ny-Ålesund Geodetic Observatory and in particular to Helge Digre for the invaluable help prior, during and after the GPS observing session.
The authors will also thank Maria Rioja for the great help during the observations at the site.

References

Altamimi Z., Sillard P., Boucher C. (2002): *"ITRF2000: A new release of the International Terrestrial Reference Frame for Earth Science Applications"*, J. Geophys. Res, in press.
Boucher C., Altamimi Z., Sillard P., (1999): *"The 1997 International Terrestrial Reference Frame (ITRF97)"*, Technical Note 27, Central Bureau of IERS, Observatoire de Paris, Paris
Hugentobler U., Schaer S., Fridez P. (Eds.) (2001): *"Bernese GPS Software Version 4.2"*, Astronomical Institute, University of Berne, p. 515
Nothnagel A., Steinforth C., Binnenbruck B., Brockmann L., Grimstveit L., (2001): *"Results of the 2000 Ny-Ålesund Local Survey"*, In: D. Behrend and A. Rius (Eds.): Proc. XV Working Meeting on European VLBI for Geodesy and Astrometry, Barcelona, Spain, pp. 168-176
Sarti P., Vittuari L., Tomasi P.; (2000): *"GPS and classical survey of the VLBI antenna in Medicina: invariant point determination"*, Proc. XIV Working Meeting on European VLBI for Geodesy and Astrometry, Castel S. Pietro Terme, pp. 67-72
Tomasi P., Sarti. P, Rioja M.; (2001): *"The determination of the reference point of the VLBI antenna in Ny-Ålesund"*. Memories of the National Institute of Polar Research, Special Issue 54, pp. 319-330
Vittuari L., Sarti P., Tomasi P., (2001): *"2001 GPS and classical survey at Medicina observatory: local tie and VLBI antenna's reference point determination"*, In: D. Behrend and A. Rius (Eds.): Proc. XV Working Meeting on European VLBI for Geodesy and Astrometry, Barcelona, Spain, pp. 161-167

Validation and Use of a New Diffusive Sampler for Ozone Monitoring in Polar Troposphere

Franco De Santis, Caterina Vazzana, Sabrina Menichelli & Ivo Allegrini

CNR – Institute on Atmospheric Pollution, Via Salaria Km 29.3, 00016 Monterotondo (Rome), Italy. E-mail: desantis@iia.mlib.cnr.it, phone + 39 (0)6 90 672 263

Introduction

Arctic troposphere plays an important role in environmental concerns for global change. Tropospheric ozone (O_3) is one of the most important atmospheric constituents both as a major greenhouse gas and as a species involved in photochemical processes through the production of hydroxyl radicals.

Conventional ozone measurement methods in the lower troposphere are typically based on (a) ultraviolet absorption, (b) a chemiluminescent reaction with ethylene gas. Simpler measurement techniques for assessing air quality may offer a cost effective alternative to conventional techniques for large-scale measurements carried out for mapping the air quality distribution.

During the past few years, diffusive sampling has been increasingly used for the assessment of environmental exposure to criteria pollutants (De Santis et al., 2002a and 2002b). Among the factors responsible for the increasing popularity of the method there is the low cost and the simplicity with which the sampling can be carried out.

Various designs of passive samplers have been developed for ozone. A diffusive measurement method based on the ozone reaction with indigo carmine has been described by Grosjean and Hisham (1992). The uptake rate of this device depends entirely on a calibration against a standard gas mixture in the laboratory, or on calibration in the field without any assurance of the constancy of the uptake rate whose variability is due largely to temperature and relative humidity changes. Other inaccuracies are associated with the dependence of the boundary layer thickness on wind conditions and on the constancy of the membrane thickness itself.

Koutrakis et al. (1993) developed a passive sampler based on the oxidation of nitrite to nitrate. Initial studies designed to test this device have shown its reliability but in subsequent use this sampler was found to be unacceptable during validation studies performed prior field operations. Inconsistent sampler response, due to apparent changes in effective sampling face velocity, was identified as a likely source of sampling bias. To overcome this limitations a battery operated controlled flow sampler was proposed.

In this paper we report on the development of the method of improving the determination of ozone by a diffusive technique, focusing, in particular, on measurements carried out in a polar region.

A simple, inexpensive sampler has been developed and tested in laboratory and then validated from June 2000 to May 2001 in arctic atmosphere near Ny- Ålesund, Svalbard Islands.

Experimental

The sampler used in this study is a modification of the open-tube design obtained by using a filter treated with appropriate reagents to trap ozone as recently modified by Bertoni et al. (2000) for the determination of BTX (benzene, toluene, xylenes). The body of the sampler is a cylindrical glass vial with a threaded cap at one end. O_3 is collected on a disc of impregnated microfiber filter. To avoid turbulent diffusion inside the vessel, the open end is protected using a fine stainless steel screen. Before and after sampling the screen is replaced with a polyethylene cap. The device is shown exploded in Fig. 1.

The microfibre filter (Marbaglass, Rome) was coated by using a solution of 1% sodium nitrite plus 2% glycerine in water and then dried in an oven at 70°C horizontally supported at the edges

on parallel glass rods glued to a glass plate. The absorbing surface is placed on a polyethylene disc having three small bulges held in position by a stainless steel ring. A second stainless steel ring is used to hold the disc. The absorbing pad faces the bottom of the device and air is sampled through the three small sectors.

The exposure chamber used in this study to examine the behaviour of the sampler in the laboratory is the same as previously reported in Scheeren et al. (1994), composed by a large glass vessel closed with a removable leak-proof cap, in which airflow, humidity, temperature and gas concentration could be controlled. The samplers were placed in the centre of the exposure channel and held in position so that the airflow was at right angle to the face of the samplers. The exposure chamber could hold up to six samplers.

Air streams containing known O_3 concentrations, generated by using an UV lamp (Mod. SOG-3, CA, USA), were diluted inside the chamber with clean air at controlled relative humidity (Humicon - D.A.S., Palombara Sabina, Italy). Ozone concentrations were measured by using an UV absorption analyser (API 400A, San Diego, USA).

Field measurements were carried out near Ny-Ålesund, Svalbard Islands (78°54'29" N, 11°52'53" E) from June 2000 to May 2001. The diffusive samplers were positioned, with their open ends down, under a stand at a height of about 2 m above the ground. Two additional samplers were deployed as field blanks during each exposure period. The stand is an aluminum semi-circular dome-shaped support with its downwards cavity closed with a grid to protect from excessive turbulence and to exclude dust and particulate matter interference.

After exposure, the filters were extracted in Dionex eluent (2.7 mM Na_2CO_3 and 0.3 mM $NaHCO_3$) and the concentration of the nitrate ion (product of the oxidation of nitrite by ozone) was determined using Ion Chromatography (Model 500, Dionex, USA equipped with a column IONPAC AS12A). The concentration of nitrate was calculated by referring to the calibration graph constructed by using the peak heights of nitrate standards.

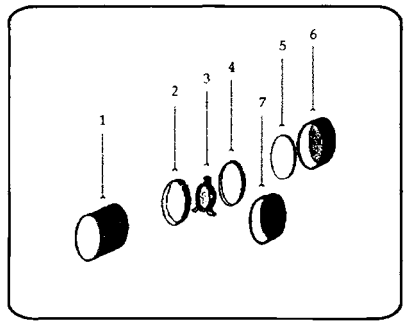

Figure 1 - Exploded scheme of the O_3 Diffusive Sampler: 1 – glass cylinder; 2 & 4 – ring; 3 – absorbent; 5 – septum; 6 – plastic cap; 7 –air barrier.

Results and Discussion

Linearity of response of the diffusive samplers (i.e. the extent to which response is directly proportional to input) was evaluated by exposure, in laboratory trials, to known concentrations of O_3 at 10, 50 and 80% relative humidity. In each trial, six samplers were exposed simultaneously in the glass chamber to O_3 levels up to about 700 ppb. Figure 2 shows the relationship between the hourly mean NO_3^- formation onto the filter of the diffusive sampler and O_3 mixing ratio measured with a UV analyser. This figure indicates that the sampler does exhibit very good linearity characteristics. The values lie on a straight line with a correlation coefficient of 0.99. The sampling rate calculated from the slope of the regression line was 5.7 cm^3/min.

A series of other laboratory experiments showed that the sampling range for O_3 varies between 230 ppb-hour and 72 ppm-hour. The lower limit (limit of detection, LOD) of the sampling rate is a function of the blank value (the LOD corresponds to three times the standard deviation of

nitrate blank values). The maximum limit represents the point at which the uptake is no longer a linear function of the concentration to which the sampler is exposed. In consideration of this upper limit value, an exposure time for O_3 as large as one month can be expected at an average concentration of 100 ppb.

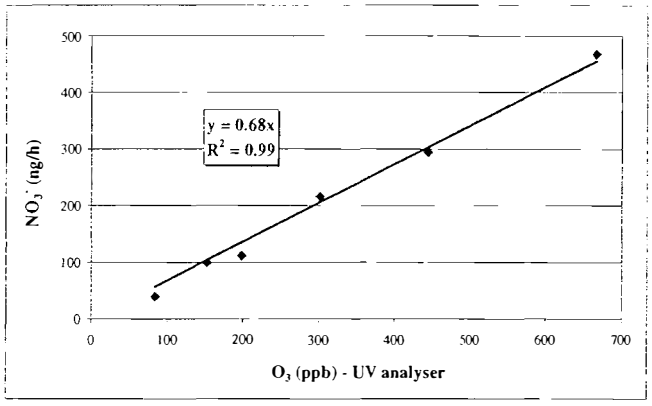

Figure 2 - Relationship between the hourly mean NO_3^- formation onto the diffusive sampler filter and O_3 mixing ratio determined by the UV analyser in laboratory experiments.

Field measurements in the Arctic troposphere were carried out in a location sited outside the research centre of Ny-Ålesund from June 2000 to May 2001. The values from the O3 diffusive sampler were compared with those of a co-located ultraviolet analyser of the Ny-Ålesund - LSF (Large Scale Facility). The O3 measurements made with the diffusive samplers were in a good agreement with the measurements from the automatic analyser, as shown in Fig. 3. Each data point was an average obtained from five samplers exposed simultaneously. The accuracy of the samplers was within ± 15% whereas the precision (relative standard deviation) was ± 3%. The slope of the linear regression line and the correlation coefficient are equal to 0.97 and 0.83, respectively.

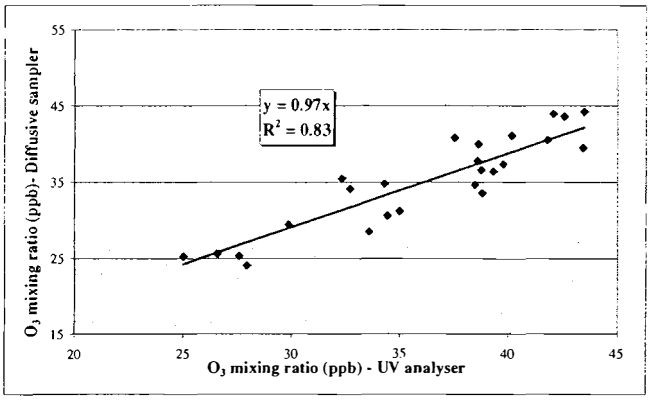

Figure 3 - Comparison between Diffusive Sampler and UV Analyser in Ny-Ålesund.

To determine whether a diffusive sampler can be used for monitoring in a polar site it is necessary to investigate whether samplers exposed for extended periods (weeks and months) give the same integrated response as a series of short-term samplers run side-by-side. The ratio of a 4-weeks average concentration computed from the sum of 2 subsequent 2-weeks samples to the monthly sample can be used to indicate the self-consistency of the method. Results obtained in 7 subsequent runs showed a very good agreement between the monthly and the sum of the fortnightly samples as can be noted from Fig. 4.

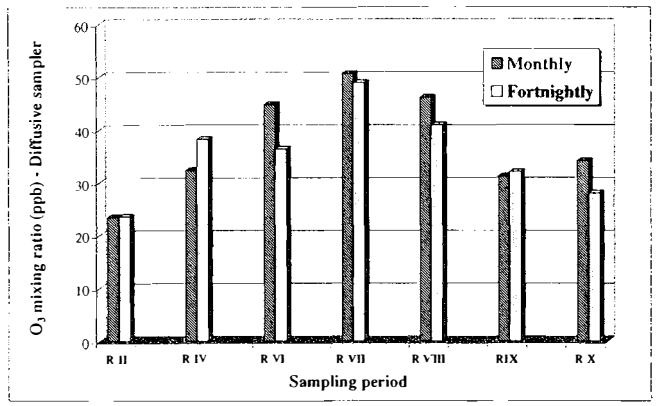

Figure 4 - Self-Consistency between monthly and fortnightly diffusive samplers exposed simultaneously in Ny-Ålesund.

Conclusions

The main advantage of this sampling device is that it is inexpensive and easy to use. Compared with the conventional pump-dependent active sampling procedures (i.e. diffusion denuders or automatic analysers), the main advantages of the method are cost effectiveness and simplicity. Furthermore the sampler can be stored at room temperature prior as well as after sampling and can therefore be used in remote areas. Another possible application of the sampler is the measurements aimed at the determination of the spatial distribution of O_3 over large areas where no data is available or the number of the existing automated monitors is not sufficient. They can also be used to check the representativeness of existing conventional sampling stations.
Results indicate that the accuracy of this device when compared to co-located continuous O_3 analysers is ±15% with precision of ± 3%.

Acknowledgements

Resources for this study were provided by Ny-Ålesund – LSF within the Project AWI-26/2000. We would like to thank Roberto Sparapani for the installation of the samplers stand and his assistance in Ny-Ålesund. The authors are grateful to the Ny-Ålesund Koldewey Station leaders Andrew Klaas and Mareile Wolff for their substantial support throughout the arctic campaign on changing the samplers batches. Finally the authors wish to thank Shinji Morimoto that provided the Ny-Ålesund UV analyser data.

References

Bertoni, G., Tappa, R. & Allegrini, I. 2000: Assessment of a new passive device for the monitoring of benzene and other volatile compounds in the atmosphere. *Annali Chimica* 90, 249-263.

De Santis, F., Vazzana, C., D'Angelo, B., Dogeroglu, T., Menichelli, S. & Allegrini I. 2002a: Validation and use of a new diffusive sampler for ozone assesment in the Lazio Region, Italy. In: Brebbia, C. A. & Martin-Duque, J. F. (eds.): Air Pollution X. WIT Press, 371-380.

De Santis, F., Dogeroglu, T., Fino, A., Menichelli, S., Vazzana, C. & Allegrini, I. 2002b: Laboratory development and field evaluation of a new diffusive sampler to collect nitrogen oxides in the ambient air. Analytical Bioanalytical Chemistry 373, 901-907; published on-line: 3rd July 2002.

Grosjean, D. & Hisham, M. J. 1992: A passive sampler for atmospheric ozone. J Air Waste Management Association 42, 169-173.

Koutrakis, P., Wolfson, J. M., Bunyaviroch, A., Froehlich, S. E., Hirano, K. & Mulik, J. D. 1993: Measurement of ambient ozone using a nitrite coated filter. Analytical Chemistry 65, 209-214.

Scheeren, B. A., De Santis, F., Allegrini, I. & Heeres, P. 1994: Monitoring SO2 with passive samplers: a laboratory evaluation of Na2CO3 and thriethanolamine as absorbing media. International J Environmental Analytical Chemistry 56, 73-85.

Sixth Ny-Ålesund International Scientific Seminar
"The Changing Physical Environment"
Polar Environmental Centre, Tromsø, Norway,
8-10 October 2002

Session: Changing Environment & Ecosystem Effects II

Nina **Gunde-Cimerman** et al.: Extremophilic fungi in coastal Arctic environment.

Josef **Elster** et al.: Diversity of cyanobacteria and eukaryotic micro-algae in subglacial soil (Ny-Ålesund, Svalbard).

Davey **Jones** et al.: Nitrogen in terrestrial arctic systems; Soil pools, plant growth, and environmental change.

Extremophilic fungi in coastal Arctic environment

N. Gunde – Cimerman[1], J. Frisvad[2], P. Zalar[1], S. Sonjak[1], A. Plemenitaš[3]
[1] University of Ljubljana, Biotechnical Faculty, Department of Biology, Večna pot 111, 1000 Ljubljana, Slovenia
[2] Department of Biotechnology, Technical University of Denmark, DTU - Building 221, 2800 Lyngby, Denmark
[3]University of Ljubljana, Medical Faculty, Institute of Biochemistry, Vrazov trg 2, 1000 Ljubljana, Slovenia

Key words: fungi, psychrophiles, black yeasts, *Penicillium*, Arctic, sea ice, glacier ice

Introduction

Microorganisms mainly sustain life in extreme environments. The Arctic and Antarctic regions have been investigated regarding the presence of psychrophilic bacteria, archaea and algae, but very rarely for fungi. The isolated species were mainly present in a dormant state and only occasionally, endemitic psychrophilic species were found. Low numbers of colony forming units (CFU) of fungi were detected on non-selective general media.
Frozen sea water and ice form a semisolid matrix, permeated by channels and pores, filled with brine including expelled salts as the ice crystals freeze together. Since changes in salinity are the dominant factors in external chemistry that can influence the internal biological assemblage, our efforts were concentrated on the isolation of xerotolerant/halotolerant fungi, able to grow on media with low water activities, due to high concentrations of salt or sugar. As temperatures in the environment drop, there is a gradual transition in microbial populations from the diverse mixed species inoculums originating in seawater, soil or air to psychrophilic species. Therefore the emphasis was given to isolation procedures and media, which gave selective advantage to fungi, with a combination of physiological properties, enabling life at low temperatures and/or water activities. These extremophilic fungi, potentially known also from other, stressful environments, could have a selective advantage over mesophilic mycobiota. They may be used as one of the very rare eukaryotic models for studying adaptations on the biochemical and genetic level to low water activity stress, due to high salt or sugar concentration or due to the binding of water as ice.
In this study quantitative data on the diversity and distribution of extremophilic fungi in seawater, sea ice and glacier ice are presented.

Materials and methods

Sampling, isolation and media
Seawater samples, sea ice and glacier ice, floating in seawater and chopped directly from the glacier in the end of Ny-Alesund fjord, were collected twice, in June and in August, during the season of 2001. The ice was aseptically molten. The presence of fungi in the seawater and sea ice and glacier ice water was determined by filtration immediately after sampling (Gunde-Cimerman et al. 2000).
The following solid agar media were used:
¤ *DRBC* (water activity a_w 1.0), a general-purpose enumeration medium. ¤ *DG-18* (a_w 0.946), a medium for enumeration of moderate xerophiles. ¤ *MYG* (a_w 0.941- 0.89), with 20/35/50% glucose and malt/yeast extract. ¤ *MEA+5/10/15/17/24/30% NaCl* (a_w 0.951 - 0.782), salt-based selective media. To all solid media chloramphenicol (50 mg/l) for prevention of bacterial growth was added.

For every sample five to eight parallel samples were filtered, incubated from 1-14 weeks at 15 and 22°C and the average number of colony forming units (CFU) per litre was calculated.

Taxonomy

Isolated melanized fungi were partially identified by morphology, physiology and by sequencing of ITS rDNA (Hoog et al.1999; Zalar et al. 1999a) to the genus and in some cases species level. Isolates of the genera *Penicillium, Aspergillus* and *Eurotium* have been identified by morphology, physiology and secondary metabolite profile, to the species level. Isolates of non- melanized yeasts were not yet identified.
All isolated strains are maintained in the EX-F Culture Collection of the Department of Biology, Biotechnical faculty, University of Ljubljana, Slovenia.

Determination of environmental parameters

In all water samples pH, temperature, salinity (areometer) and water activity (a_w) (CX-1 system, Campbell Scientific Ltd.) were determined.

Results

Population dynamics of isolated fungi: enumeration media

The combined number of CFU of non-melanized and melanized fungi was between 400 and 3000 CFU/l on DRBC (a general-purpose medium) and between 10 and 7000 CFU/l on DG-18 (a medium for xerophiles). The majority of CFU were nonmelanized yeasts, both in water and in ice samples.

The highest values (4000-7000 CFU/l) on DG-18 were detected in the sea and glacier ice and the lowest in sea water (10 CFU/l). CFU numbers obtained on DG-18 were always higher than on DRBC, as well as those obtained at 15oC in comparison to 22oC. The incubation time was shorter on DG18 medium than on DRBC and always shorter at 22oC, although approx. 20% of fungi did not appear at this temperature.

Population dynamics of fungi: selective sugar media

On selective media containing different sugar concentrations, the highest CFU values of fungi were obtained on the medium with 20% glucose (6000 CFU/l) and the lowest on 50 % glucose (3000 CFU/l). In almost all cases higher CFU values were obtained on the medium incubated at 15oC. The lowest fungal counts appeared in sea water and sea ice (20 CFU/l),while the highest (5000-6000 CFU/l) were obtained with glacier ice.
Melanized fungi appeared in sea water only occasionally, while they represented in glacier ice from 50-70% of the isolated mycobiota. The melanized fungi detected on sugar-based media were represented almost entirely by *Aureobasidum* sp. and to a lesser extent *Cladosporium sp.* Non-melanized yeasts were present only in the glacier ice samples on 20-35% glucose media, but none were detected on 50% glucose in any of the samples investigated. Thethird group of fungi was represented (30-40%) with the genus *Penicillium.* The prevailing species, found with the highest frequency in almost all samples was *P. crustosum.* Other isolated species were: *P. nordicum, P. arcticum, P. svalbardense, P. goenlandense, P. chrysogenum, P. nalgiovense, P. commune, P. lanosum, P. echinulatum, P. palitans, P. brevicompactum, P. olsonii and P. decumbens.*

Population dynamics of fungi: selective saline media

The highest fungal CFU/l (7000/l) were detected in the glacier ice sample on the medium with 5% NaCl. On selective saline media, the upper salinity range for the detection of fungi was 17% NaCl, at which the lowest CFU values of fungi appeared (up to 100 CFU/l). They were represented almost exclusively by g. *Penicillium* and only occasionally as well by melanized fungi At the lowest salinities (5%NaCl) non-melanized yeast represented approx. 75% of all fungi (up to 5000 CFU/l), but with an increase of salinity to 10%NaCl their numbers decreased to 2000 CFU/l and they represented approx. 60% of all isolated fungi. At even higher salinities they were almost completely replaced with melanized fungi and *Penicillium spp.* The most frequent *Penicillium* species was again *P. crustosum,* followed by *P. svalbardense, P. glabrum, P. thomii, P. arcticum, P. solitum, P. chrysogenum* and *P. polonicum.*

Discussion

It was generally assumed that the microbial communities in extreme environments are mainly composed of Archaea and Bacteria and a few eukaryotic species, but lately evidence of a higher diversity of eukaryotic microorganisms is becoming evident. It is not only represented with the primary producers, but also by saprotrophic fungi. An example of an extreme environment, where fungi have been isolated for the first time only recently, are man made solar salterns. Among the non-melanized fungi mainly different species of the known food-borne xerophilic genera were isolated, such as *Aspergillus, Penicillium* and *Eurotium,* while the melanized fungi were represented mainly by black, yeast-like hyphomycetes and the genus *Cladosporium.*

Fungi have been so far little investigated in natural, extremely cold environments. Sporadic reports described isolations from permafrost soils and plant litter and very rarely from ice or seawater. In all the cases, when classic microbiological techniques for the isolation of fungi were applied, the media used did not exert low water activity selective pressure and often not even low incubation temperatures. Recently, in some cases only molecular methods were used for the detection of fungi. Most fingerprinting methods rely on PCR, a technique that may alter the natural abundance of sequences and can be therefore biased. Other problems can be of technical nature, such as the presence of heteroduplexes, different sequences that might stop at the same position in a gradient gel or have the same restriction length and, finally, different bands, belonging to different operons of the same organism. Furthermore, some diverse populations can be lumped together or separated depending on the resolution of the methods. Another source of problems arises from from nucleic acid extraction procedures, which can be especially difficult in the case of fungi, due to resistant and varied cell walls. The influence of the sampling site has been poorly explored for most microorganisms, even in less »complicated« environments. Finally, the so called »universal« primers used for PCR amplification can overlook some of the potentially targeted microorganisms.

Therefore, in the initial stages of fungal isolations, adapted classical techniques can be the best way to initiate the isolation work, which can be continued later with more sophisticated approaches, complementing the initial results. The methods and media used for the isolations of fungi from cold sea water and ice, showed a a rich diversity of mycobiota, represented by melanized and non-melanized fungi. A surprisingly high fungal CFU per litre of water was detected, ranging from 30 – 100 in seawater, 200 – 2000 in sea ice and up to 10.000 in glacier ice. The majority of isolated fungi were initially hyaline and only eventually became pigmented. The main groups of isolated fungi were (i) different non-melanized yeasts, (ii) melanized fungi, being mainly represented by the oligotrophic melanized g. *Cladosporium* and a still unidentified species of *Aureobasidum* sp. and (iii) different species of g. *Penicillium.*

Black yeasts are polymorphic fungi able of yeast-like and mycelial growth and production of black pigment in their hyphae, yeast-like cells and conidia. Melanized filamentous fungi from the genus *Cladosporium* are taxonomically and phylogenetically closely related to black yeasts, both belonging to the order Dothideales Melanized fungi have been found on marble, limestone and granite in various extreme environments especially in arid or semi arid, hot and cold deserts and, most recently, hypersaline waters. They can endure harsh environmental conditions, due to polymorphic life cycles, formation of thick, melanized cell walls, meristematic growth, propagation by endoconidiation, adhesion, and production of extracellular polysaccharides.

Penicillium is a cosmopolitan genus of food-borne and soil fungi. Many species have a characteristic preference for growth at lower temperatures and can be often found in alpine soils and recently as well in tundra soil and permafrost layers. Their diversity and occurrence in glacier/sea ice, which has not yet been investigated, revealed a surprising richness and abundance. The prevailing species isolated almost in all samples was *P. crustosum*, a known food-borne species. The so far determined characteristics revealed significant metabolic differences within the species, that deserve further investigations. Among other isolated *Penicillium* species there were at least 4 new ones to science (*P. nordicum, P. arcticum, P. svalbardense and P. groenlandense)* and are currently being described.

Preliminary taxonomic analyses for some of the species, based on morphology, assimilation patterns, secondary metabolite profiles and molecular fingerprinting, show that there are differences from species isolated from other, non-extreme environments. Currently investigations are being made to discover if this is due to their geographic isolation or independent evolutionary origin.

In the ice shifts in salinities occur on a micro level and microareas of dry and wet alternate. The ice is low in nutrients most of the time, but then concentrations may occasionally reach quite high levels due to primary production within. Due to relatively high ion concentrations, the water availability is low under which conditions fungi grow optimally within the prevailing salinity ranges and are not much exposed to competition in their saprotrophic role. With high amounts of nutrients they can cope with the energetically demanding life at low temperatures and relatively low water activities. Due to their physiologic adaptations certain genera of fungi and yeasts in particular can well use the available water and come to full metabolic activity until the next period of suboptimal conditions starts. They are able to survive periods of environmental stress in a resting state, and respond to improved growth conditions immediately with increased metabolic activity and growth. Resistance to low temperatures and osmotically stressed conditions and life style probably enable these fungi to maintain a continuous colonization of the ice.

Acknowledgement:

The work in Ny-Alesund was funded by LSF fund from European Union. We would like to thank them for their financial help and Nick Cox, the manager of the British station for his humour and energy.

Diversity of cyanobacteria and eukaryotic microalgae in subglacial soil (Ny-Ålesund, Svalbard)

Josef Elster[1], Klara Kubeckova[1], Katerina Brynychova[2], Alena Lukesova[3], Marek Stibal[1] and Hiroshi Kanda[4]

Institute of Botany, Academy of Sciences of the Czech Republic, Trebon and Faculty of Biological Sciences, University of South Bohemia, Ceske Budejovice[1],
Faculty of Education, University of South Bohemia, Ceske Budejovice[2],
Institute of Soil Biology, Academy of Sciences of the Czech Republic, Ceske Budejovice[3] Czech Republic
National Institute of Polar Research, Tokyo, Japan[4]

Introduction

Study of the reinvasion and establishment of plant and animal life after ice retreat is one on the most important ecological problems. In the past, many Arctic and Antarctic research projects have dealt with primary succession processes and the effects of climate warming (Svoboda and Henry, 1987, Chapin et al. (eds.), 1992, Caulson et al., 1993, Lewis Smith, 1993, Levesque and Svoboda, 1999, etc.). Cyanobacteria and eukaryotic algae are the primary colonisers of areas, exposed for revegetation after the disappearance of ice cover. However, the initial stages in the process of recolonization have drawn little attention from researchers as reflected in the scant literature on this topic (Wynn-Williams, 1993, Elster and Svoboda, 1996, Elster et al., 1997, Elster et al., 1999), although higher plant invasion and subsequent plant community development depend on these early colonisers.

Cyanobacteria and eukaryotic algae are widespread in polar wetlands and soils and produce visible biomass, which represents a considerable global pool of fixed carbon. Together with associated microorganisms, they are involved in energy flow, mineral cycling, weathering processes and the biological development of the polar landscape. The polar terrestrial micro-flora is selected from a limited range of algae within the Cyanobacteria, Chlorophyta, Bacillariophyta and Xanthophyta (Akiyama, 1967, Novichkova-Ivanova, 1972, Engelskjon, 1981, Klavenes and Rueness, 1986, Ohtani et al., 1991, Broady, 1996, Elster et al., 1999, Elster, 2002, etc.).

Previous research

In 1997 and 1998, the species diversity of soil cyanobacteria and eukaryotic algae was studied along a 800m transect from the edge of the glacier across ground moraine of the East Brøgger glaciers, in vicinity of Ny-Ålesund, the north-western part of Svalbard. The East Brøgger moraine is approximately 2 km wide. 1997 and 1998 transects were in western part of the moraine. In 1999, three transects (A, B, C) across ground moraine were collected for cyanobacteria and eukaryotic cells

quantification. The localisation of the A treatment correspond to 1997 and 1998 transect. The B transect was localised in central part and the C in the eastern part of the moraine, respectively. Sampling sites were 25 m apart, along a gentle slope varying in: micro-topography, drainage, soil nutrients, organic matter content, substrate granular disintegration, and in composition and cover of bryophytes and vascular plants.

Several cultivation methods were used to cover whole spectrums of soil ecological conditions that can occur in the deglaciated soils. The following methods were used: direct microscopy of the wetted soil covered by microscope glasses, dilution plates methods with two selected media BG-11, BBM. In addition, the dilution plates were cultivated in three temperatures (8, 15 and 24 ^{o}C). No distant differences in species composition and abundance were recorded in these cultivation methods.

82 species of algae and cyanobacteria have been observed in 1997 and 1998 summer seasons. In total, 39 species of cyanobacteria and 43 species of eukaryotic algae (Chrysophyceae-1, Bacilariophyceae-7, Xanthophyceae-8, Chlorophyceae-21, Charophyceae-4, Conjugatophyceae-2) were found. However, about 60% of species were identified only to the genera level. In these species a detail morphological observation and life cycles study was performed.

Fluorescent microscopy (Olympus BX 60) was used for soil cyanobacteria and eukaryotic algae cells quantification. The number of cyanobacteria and algae cells per 1 gram of soil increased with distance from glacial front. In the first zone (glacial front to about 300m) the number of cell per 1 gram of soil fluctuated in values 10^3 to 10^6. In the second zone (300m to 1050 m) cells number fluctuated in range of 10^7 to 10^9. At the end of the B transect (about 1050m from glacial front) the number of cell per gram of soil slightly increased. Moreover, the cyanobacteria and eukaryotic algae were quantified separately. Cyanobacteria were more abundant in all studied sampling sites along deglaciated moraine. In addition, Cyanobacteria coccoid, filamentous and colony producing forms were quantified separately. Filamentous forms of Oscillatoriales and coccal Chroococcales were the most abundant in the first zone (from glacial from to about 400m). Later (in distances more than 400m from glacial front), Nostoc initial stages started to prevail. In eukaryotic algal group only diatoms and algae were quantified. Algae were more dominant in the transect B and C, and in contrary, the transect A was rich in diatoms.

Recent research

The processes primary succession by cyanobacteria and eukaryotic algae are influenced by many ecological factors. However, two of them (1) aerobiological and water inputs of viable cells and spores into deglaciated areas and, (2) ability to endure freeze-dry desiccation for long periods of time (perennial character) play a detrimental role in the processes of primary succession.

In summer season 2002, the diversity and abundance of cyanobacteria and eukaryotic microalgae will be studied in the vicinity of Ny-Ålesund, Southern part of Kongsfjorden, Svalbard, 79°N in the following habitats:

- subglacial soil (samples collected from below glacier ice)
- freshly deglaciated soil (close to glacial margins - up to 50m)
- glacial ice surface (cryoconite, streams flowing on ice surface, etc.)

- soils of habitats deglaciated many years ago (more than 50 years ago)

Cyanobacteria and eukaryotic algae diversity and abundance will be studied by similar methods as has been performed along East Brøgger deglaciated moraine. By synthesis of cyanobacteria and eukaryotic algae diversity and abundance results from above mentioned four habitats we will attempt to answer the crucial question: can prokaryotic cyanobacteria and eukaryotic algae survive extensive periods in frozen soil in glacial environments? Simultaneously, a second question is: do these "ancient" cells and spores play an important role in modern primary succession processes?

References

Akiyama, M. 1967: On some Antarctic terrestrial and subterranean algae from the Ongul Islands, Antarctica. Antarct. Rec. (Tokyo) 32: 71-77.

Broady, P. A. 1996: Diversity, distribution and dispersal of Antarctic algae. Biodiversity and Conservation 5: 1307-1335.

Caulson, S.; Hudkinson, I.D.; Strathdee, A.; Bale, J. S.; Block, W.; Worland, M. R. & Webb, N. R. 1993: Similated climate change: the interaction between vegetation type and microhabitat temperatures at Ny-Alesund, Svalbard. - Polar Biol. 13: 67-70.

Chapin, F. S., Jefferies, R. L., Reynolds, J. F., Shaver, G. R and Svoboda, J. (eds.), 1992: Arctic ecosystems in a changing climate. An ecophysiological perspectives. San Diego, New York, Boston, London, Sydney, Tokyo, Toronto: Academic Press, Inc.

Engelskjon, T. 1981: Terrestrial vegetation of Bouvetoya. Norsk Polarinst. Skrif. 175:17-28.

Elster, J. and Svoboda, J. 1996: Algal seasonality and abundance in, and along glacial stream, Sverdrup Pass 79 °N, Central Ellesmere Island, Canada. Mem. Natl Inst. Polar Res., Spec. Issue 51: 99-118.

Elster, J., Svoboda, J., Komárek, J., and Marvan, P. 1997: Algal and cyanoprocaryote communities in a glacial stream, Sverdrup Pass, 79 °N, Central Ellesmere Island, Canada. Arch. Hydrobiol./Suppl. Algolog. Stud. 85: 57-93.

Elster, J. 1999: Algal versatility in various extreme environments. In: J. Seckbach (ed.) Enigmatic Microorganisms and Life in Extreme Environments, p. 215-227, Kluver Academic Publishers.

Elster, J. 2002: Ecological classification of terrestrial algal communities of polar environment. In. GeoEcology of Terrestrial Oases L. Beyer and M. Boelter (eds.). Ecological Studies, Springer-Verlag, Berlin, Heidelberg, 303-319.

Levesque, E. & Svoboda, J. 1999: Vegetation re-establishment in "lichen-kill landscapes: a case study of the Little Ice age impact. - Polar Research 18(2): 221-228.

Klaveness, D. and Rueness, J. 1986: The supralittoral, freshwater and terrestrial algae vegetation of Bouvetoya. Norsk Polarinst. Skrif. 185: 65-69.

Novichkova-Ivanova, L. N. 1972: Soil and aerial algae of polar deserts and arctic tundra. In: I. B. P. Tundra Biome. Proceedings of the 4th International Meeting on the Biological Productivity of Tundra. (F. E. Wielgolaski and T. Rosswall, eds.) pp. 261-265. Stockholm: I.B.P. Tundra Steering Committee.

Ohtani, S., Akiyama, M. and Kanda, H. 1991: Analysis of Antarctic soil algae by the direct observation using the contact slide method. Antarc. Rec. (Tokyo) 35: 285-295.

Smith, R. I. 1993: The role of bryophyte propagule banks in primary succession: Case-Study of a Antarctic fellfield soil. In: Miles, J. and Walton, D. W. H. (eds.). Primary Succession on Land, p. 55-78, Blackwell Scientific Publications, Oxford.

Svoboda, J. and Henry, G. H. R. 1987: Succession in marginal arctic environments. Arctic and Alpine Research, Vol. 4: 373-384.

Wynn-Williams, D. D. 1993: Microbial processes and initial stabilisation of fellfield soil. In: Miles, J. and Walton, D. W. H. (eds.). Primary Succession on Land, p. 17-32, Blackwell Scientific Publications, Oxford.

Nitrogen in terrestrial arctic systems: soil pools, plant growth and environmental change

Davey Jones and John Farrar, University of Wales, Bangor
Bjørn Solheim and Christina Wegener, Univeristy of Tromsø

The cycling of carbon and nitrogen in arctic tundra soils is of considerable interest. First, we need to understand how low temperatures and a short season affect fluxes in these environments. Second, the potential impacts of climate change on these systems may be large, since warming is predicted to be greater than average in the north polar regions. Third, we need to know if there are likely to be any positive feedbacks as the climate changes – and there is one possibility of great significance in the tundra.

We are interested in both C and N fluxes in tundra systems. Since the cycling of the two is very closely interlinked, it is profitable to study them together. Here we will concentrate on nitrogen, but I will give a context in terms of carbon fluxes first.

Tundra is very carbon-rich, in spite of the small amount of living plant material. This is because the soils are rich in dead organic matter. This material has been accumulating steadily since the retreat of glaciers and ice-sheets, and is largely partly decomposed and modified plant material. Some of this stable organic matter is very old – ages of 200-2000 years are common. However the carbon fluxes through plant and soil are much higher than might be expected – a simplified carbon budget for these ecosystems suggests that plant material turns over with a half-time of about 5 years, and soil microbial populations with a half-time of weeks. The exchange of carbon with the atmosphere – by photosynthetic fixation of CO2 and respiratory release of CO2 by plants, soil microbes and animals – is very significant compared with the fluxes internal to the system, such as those from plants to microbes. The system is thus relatively open.

One possible effect of climate change is a consequence of warming. Soil microbial activity may rise due to warming, and then the rate at which the stable organic matter is remobilised may increase. Since the rates of deposition are so low, this might mean a net flux of CO2 out of the tundra. This will add to atmospheric CO2 concentration and thus provide a positive feedback to the process of climate change. Since the tundra C stores are large (280 Gt; Larcher) the global effect might be significant.

There are two distinct reasons why this positive feedback may not occur. One is based in carbon cycling, one in nitrogen cycling. It may be that soils (or rather their micro-organisms) acclimate to temperature. Higher plants acclimate – when moved to a higher temperature their rate of respiration rises, but metabolic adjustments cause the rate to fall over a period of about a week; it commonly returns to a rate nearly identical to that at its previous temperature. There is some suggestion that soils may do this, but we don't know why – so prediction is difficult.
The second reason lies in N cycling. The soil microbial populations may only be able to respond to increased temperature (and increased C input via photosynthesis) if

there is a sufficient supply of nitrogen. This is in doubt in many soils, and particularly in tundra. The key problem at low temperature is the formation and release of nitrate.

Nitrogen cycling is very different from C cycling. It is much more a closed system – inputs from the environment (as nitrate and ammonium in rain, as dinitrogen fixation) are relatively low, as are losses (as leaching in groundwater, or loss of nitrogen oxides and ammonium). Most N is recycled tightly within the ecosystem. The supply of nitrogen for new growth of plants and soil microbes comes from the decay of dead plants and micro-organisms; most of the N within them is in organic form and so when they decay, it is organic N that enters the soil. Rather as with C (because in many cases the same recalcitrant molecules contain both C and N) much of the soil N is relatively unavailable. Soluble organic N is a very small part of the total soil N. However it is this pool that is metabolised by specialised groups of microbes to ammonium and nitrate. These inorganic forms of N are competed for by plants and microbes, and the traditional view is that plants almost exclusively use nitrate and ammonium.

It is here that tundra may be special. At low temperatures, the rate at which soluble organic N is metabolised to ammonium and nitrate may be very low. If it is, it may be that both plant and microbial growth are limited by nitrogen even though the total amounts of N in the soil are high. If true, this would constrain response to climate change and reduce the positive feedback in the C cycle. However there is another possibility. Even if rates of ammonium and nitrate formation are low, both plants and microbes may be able to access the pool of soluble organic N directly. Then their growth would not be constrained by the low flux to ammonium and nitrate, and the positive feedback in the C cycle would be possible.

Accordingly we have studied the N fluxes in tundra soils. We ask: how abundant are ammonium, nitrate and organic N (particularly amino-acids)? what is the flux of amino-acids? can plants and microbes use amino-acids directly? does tundra respond to the addition of organic N (it responds by increased plant growth to the addition of inorganic N)?

We use two systems. We have made experimental additions of amino-acids. And we have examined areas of natural – but unusual – high N input. Svalbard has a number of cliffs where large numbers of birds nest. Below these cliffs, the vegetation is visibly different and the inputs of organic and ammonium-N are higher. We show that (as in many other soils) the amino-acid pool has a half-time of only a few hours, and so the flux through it is potentially sufficient to support increased plant and microbial growth when N inputs, C inputs or temperature increase. We therefore predict that tundra may indeed be very sensitive to climate change and potentially able to provide positive feedback to global warming.

LIST OF PARTICIPANTS

Name		Institution	e-mail address
Aliani	Stefano	CNR IOF	aliani@iof.cnr.it
Chevnina	Elena	Arctic and Antarctic Research Institute	agua@aari.nw.ru
Dahlback	Arne	Dept. of Physics, University of Oslo	arne.dablback@fys.uio.no
De Santis	Franco	CNR Istituto Inquianmento Atmosferico	desantis@iia.mlib.cnr.no
Delbart	Franck	CNRS Ingeneer	fdelbart@ifrtp.ifremer.fr
Di Prisco	Guido	IBP, National Research Council	diprisco@dafne.ibpe.na.cnr.it
Diaz Pont	Joana	Catalan Institute of Technology	joana@ictonline.es
Dominé	Florent	CNRS	florent@lgge.obs.ujf-grenoble.fr
Dulac	Francois	LSCE	dulac@lsce.saclay.cea.fr
Elster	Josef	Institute of Botany, Academy of Sciences of the Czech Republic	jelster@butbn.cas.cz
Eneroth	Kristina	Dept. of Meteorology, Stockholm University	kristina.eneroth@misu.su.se
Farrar	John	Institute of Envionmental Sciences	j.f.farrar@bangor.ac.uk
Gabrielsen	Geir Wing	Norwegian Polar Institute	geir@npolar.no
Glowacki	Piotr	Institute of Geophysics Polar and Marine Research	glowacki@igf.edu.pl
Gunde-Cimerman	Nina	University of Ljubljana Biotechnical faculty	nina.gunde-cimerman@uni-lj.si
Hagen	Jon Ove	Dept. of Physical Geography, University of Oslo	j.o.m.hagen@geografi.uio.no
Hanssen-Bauer	Inger	Norwegian Meteorological Institute	i.hanssen-bauer@met.no
Hansen	Kjell Tore	Svalbard Science Forum	ssf@lby.npolar.no

Hansteen	Thomas	Research Council of Norway	th@rcn.no
Hinkler	Jørgen	Institute of Geography, University of Copenhagen	jh@geogr.ku.dk
Hodgkins	Richard	Royal Holloway, University of London	r.hodgkins@rhul.ac.uk
Holmén	Kim	Department of Meteorolgy, Arrheniuslaboratory	kim@misu.se.su
Ivanov	Boris	Arctic and Antarctic Research Institute	b_ivanov@aari.nw.ru
Jania	Jacek	University of Silesia, Faculty of Earth Sciences	jjania@us.edu.pl
Keiichiro	Hara	National Institute of Polar Research	harakei@pmg.nipr.ac.jp
Kohler	Jack	Norwegian Polar Institute	jack@npolar.no
Krawczyk	Wieslawa Ewa	University of Silesia, Faculty of Earth Sciences	wkraws@us.edu.pl
Kriews	Michael	Alfred Wegener Institute for Polar and Marine Research	mkriews@awi-bremerhaven.de
Kristensen Solås	Monica	Kings Bay AS	direktor@kingsbay.no
Kümpel	Hans-Joachim	Leibniz Institute for Applied Geosciences	kuempel@gga-hannover.de
König	Max	Norwegian Polar Institute	max.koenig@npolar.no
Lefauconnier	Bernard	IPEV/IFRTP	b.lefauconnier@wanadoo.fr
Lehmann	Ralph	Alfred Wegener Institute for Polar and Marine Research	rlehmann@awi-potsdam.de
Lunder	Chris	NILU Tromsø	crl@nilu.no
Negusini	Monia	CNR	negusini@itis.cnr.it
Neuber	Roland	Alfred Wegener Institute for Polar and Marine Research	neuber@awi-potsdam.de
Nicolaus	Marcel	Alfred Wegener Institute for Polar and Marine Research	mnicolaus@awi-bremerhaven.de
Nilsen	Lennart	University of Tromsø	lennart@ibg.uit.no
Orheim	Olav	Norwegian Polar Institute	orheim@npolar.no
Pedersen	Ine-Therese	NILU Tromsø	itp@nilu.no

Pettersson	Lars-Evan	Norwegian Water Resources and Energy Directorate	lep@nve.no
Plag	Hans-Peter	Norwegian Mapping Authority	plag@statkart.no
Paatero	Jussi	Finnish Meteorological Institute, Air Quality Reseach	jussi.paatero@fmi.no
Schimmield,	Graham	Scottish Association for Marine Science	gbs@dml.ac.uk
Schimmield	Tracy	Scottish Association for Marine Science	gbs@dml.ac.uk
Shiobara	Masataka	National Institute of Polar Research	shio@nipr.ac.jp
Sparapani	Roberto	Consiglio Nazionale delle Ricerche	rsparapani@yahoo.com
Steinforth	Christoph	Geodetic Institute of the University of Bonn	steinforth@uni-bonn.de
Stober	Manfred	Fachochschule Stuttgart (University of Applied Sciences)	strober.fbv@fht-stuttgard.de
Ström	Johan	Stockholm University, Inst. of Applied Environmental Research	johan@itm.su.se
Viisanen	Yrjö	Finnish Meteorological Institute	yrjo.viisanen@fmi.fi
Wada	Makoto	National Institute of Polar Research	wada@pmg.nipr.ac.jp
Wangensteen	Bjørn	Dept. of Physical Geography, University of Oslo	bjorn.wagensteen@geografi.uio.no
Wiencke	Christian	Alfred Wegener Institute for Polar and Marine Research	cwiencke@awi-bremerhaven.de
Winther	Jan-Gunnar	Norwegian Polar Institute	winther@npolar.no
Yamanouchi	Takashi	National Institute of Polar Research	yamanou@pmg.nipr.ac.jp
Ørbæk	Jon Børre	Norwegian Polar Institute	jonbo@npolar.no